This is to certify that the

dissertation entitled
Development of Microprocessor-Based Steering Control System For An Apple Harvester Utilizing Non-Contact Sensing

presented by

C. Bert McMahon

has been accepted towards fulfillment
of the requirements for

Ph.D. degree in Ag. Egr.

Thomas H Burkhardt
Major professor

Date 9/10/82

DEVELOPMENT OF A MICROPROCESSOR-BASED STEERING CONTROL SYSTEM FOR AN APPLE HARVESTER UTILIZING AN ULTRASONIC SENSING SYSTEM

By

C. Bert McMahon II

A DISSERTATION

Submitted to
Michigan State University
in partial fulfillment of the requirements
for the degree of

DOCTOR OF PHILOSOPHY

Department of Agricultural Engineering

1982

ABSTRACT

DEVELOPMENT OF MICROPROCESSED-BASED STEERING CONTROL SYSTEM
FOR AN APPLE HARVESTER UTILIZING AN ULTRASONIC SENSING SYSTEM

By

C. Bert McMahon II

An automatic steering control system is needed for the USDA over-the-row-apple harvester because the operator cannot accurately steer the apple harvester for long periods of time.

The objectives of this research were to develop a non-contact sensing system and an automatic steering control system for the USDA over-the-row apple harvester. The automatic steering control system was required to accurately steer the apple harvester's front wheels such that each tree stayed within the harvester's allowable zone. This allowable zone was 45 cm wide, 409 cm long and centered on the harvester's centerline. The tree row was required to be either straight or a smooth continuous curve.

A microprocessor-based steering control system and a non-contact sensing system were designed to control the steering of the harvester's front wheels. The non-contact sensing system consisted of five sonar units which utilized ultrasonic transducers and circuit boards which were made by the Polaroid Corporation. The sonar units were used to measure the distance from each sonar unit to the tree trunk as the harvester moved over the tree row. The steering control system used a

microprocessor to perform a proportional control algorithm where the wheels were turned to a steering angle which was proportional to the harvester's position error. This control system used the sonar measurement as the feedback signal.

A simulation model was developed to simulate the harvester's closed-loop steering control system. The model reasonably predicted the motion of the harvester for a curved tree row and for a row with a step change.

The steering control system with a non-contact sensing system was tested using a simulated tree row. The results of the tests showed that for a straight and curved row the steering control system was effective at keeping each tree within the harvester's allowable zone at a harvester ground speed of 0.8 km/h (0.5 mph). During these tests the maximum deviation of the harvester centerline from the tree row centerline was 8.9 cm for the curved row and 5 cm for the straight row.

Approved by:

Thomas H Burkhardt

Major Professor

Donald D. Edwards

Department Chairman

ACKNOWLEDGEMENTS

The author wishes to express his sincere gratitude and appreciation to the following:

Dr. Thomas H. Burkhardt, the author's co-major professor, for his help in developing the technical content of this dissertation and for his many hours of reviewing and commenting on this manuscript.

Dr. Bernard R. Tennes, the author's co-major professor, for his guidance, support, and encouragement given during the development of the steering control system for the USDA apple harvester.

Dr. Ajit K. Srivastava, who served on the author's guidance committee, for his assistance in the development of the simulation model and guidance with this research.

Dr. P. David Fisher, who served on the author's guidance committee, for his guidance and suggestions for this research and for the knowledge gained in digital electronics due to the courses taught by Dr. Fisher.

Dr. Clark J. Radcliffe, who served as the outside examiner of this dissertation, for his suggestions and comments.

Richard K. Byler, fellow Ph.D. candidate, for his assistance and encouragement during this research.

The author wishes to acknowledge that the following undergraduate students and technical staff who helped accomplish this research effort; Joe R. Clemens, Shaun F. Kelly, Mary E. Maley, Mary L. Heyn, William A. Heyn, Paul E. Speicher, Theresa L. VanSlyke and Richard J. Wolthuis.

The author wishes to express his gratitude to the United State Department of Agriculture for providing financial support for this research.

The author is also very thankful for this opportunity to earn this dotoral degree and for the support from his wife, Sally, and from his parents and grandparents.

TABLE OF CONTENTS

	Page
LIST OF TABLES	v
LIST OF FIGURES	vii
CHAPTER	
1.0 INTRODUCTION	1
1.1 The Need for Automatic Steering Systems	3
1.2 Comparison of Sensing Methods	6
1.2.1 Contact Sensing Systems	7
1.2.2 Non-Contact Sensing Systems	8
1.3 Objective	11
2.0 LITERATURE REVIEW	13
2.1 Automatic Steering Control Systems Using Mechanic Contact Type Sensors	13
2.2 Automatic Steering Control Using Optical Type Sensor	18
2.3 Automatic Steering Control System Using Buried Cable	22
2.4 Automatic Steering Control Using Spacial Position Sensing	23
2.5 Sonar Sensor - Ultrasonic Transducer	25
3.0 DESIGN REQUIREMENTS	29
3.1 Alignment	29
3.2 Tree Spacing and Row Curvature	30

CHAPTER Page

3.3 Operating Environment 30

3.4 Interface with Harvester Steering System and Design Constraints 33

4.0 CONCEPTS TO DETERMINE TREE POSITION FOR AN AUTOMATIC STEERING CONTROL SYSTEM 35

4.1 Method 1 - Two Sonars Used to Determine Tree Position by Triangulation 38

4.2 Method 2 - One Sonar and One Angle Measurement Used to Determine Tree Position by Triangulation 40

4.3 Method 3 - Two Sonars Used to Detect the Tree Presence Zones 43

4.4 Method 4 - Two Optical Sensors and Two Angle Measurements Used to Determine Tree Position by Triangulation 45

4.5 Method 5 - Two Optical Sensors Used to Detect Tree Presence in Zones 48

4.6 Method 6 - Multiple Sonars Used to Measure Tree Position 50

4.7 Final Selection of Tree Sensing Concept 54

5.0 APPLE HARVESTER STEERING CONTROL SYSTEM 55

5.1 Dynamic Considerations of the Automatic Steering Control System 63

6.0 SONAR SENSOR DEVELOPMENT 66

6.1 Sonar Sensing System 70

6.1.1 Description of Sonar Circuits 72

6.1.2 Description of Interface Circuit 78

6.2 Sonar System Testing and Results 83

6.2.1 Sonar System Accuracy Tests and Results . . 84

6.2.2 Sonar Beam Angle Tests and Results 94

CHAPTER Page

7.0 SIMULATION MODEL WITH INTERACTIVE COMPUTER GRAPHICS . . . 101

7.1 Model Requirements 102

7.2 Simulation of Steering Control System 105

7.2.1 Microprocessor Simulation Model 109

7.2.2 Harvester Motion Simulation Model 111

7.2.3 Model Verification and Validation 115

7.3 Simulation Results 124

8.0 CONTROL SYSTEM SOFTWARE 131

9.0 PERFORMANCE TESTS AND RESULTS 149

9.1 Configuration of the Steering Control System 149

9.2 Test Procedure 152

9.3 Results of Straight Row Tests 159

9.4 Results of the Curved Row Tests 163

9.5 Test Results - Row with Step-Change 173

9.5.1 Reliability Problems During Test 181

10.0 SUMMARY 185

11.0 CONCLUSIONS 196

12.0 SUGGESTIONS FOR FURTHER STUDY 198

APPENDICES

A. DATA FROM SONAR ACCURACY TESTS 201

B. COMPUTER PROGRAM FOR HARVESTER SIMULATION MODEL 212

CHAPTER Page

C. ANALYSIS OF THE HARVESTER'S INERTIAL EFFECTS DUE TO GROUND SPEED 223

D. COMPUTER PROGRAM FOR THE HARVESTER'S MICROPROCESSOR-BASED STEERING CONTROLLER 242

E. DATA FROM PERFORMANCE TESTS OF THE HARVESTER'S STEERING CONTROL SYSTEM 256

LIST OF REFERENCES 265

LIST OF TABLES

Table		Page
6.1	Data from accuracy test for sonar unit done at 25.5°C. . . .	86
6.2	Data from accuracy test for sonar unit one at -1.0°C	90
8.1	List of the Microprocessor I/O Ports	143
9.1	The X-Y Coordinate Position of Tree Stands for the Curved Row Tests	158
A.1	Sonar Distance Data from Accuracy Test for Sonar Unit-2 at Air Temperature of 25.5°C	202
A.2	Sonar Distance Data from Accuracy Test for Sonar Unit-3 at Air Temperature of 25.5°C	203
A.3	Sonar Distance Data from Accuracy Test for Sonar Unit-4 at Air Temperature of 25.5°C	204
A.4	Sonar Distance Data from Accuracy Test for Sonar Unit-5 at Air Temperature of 25.5°C	205
A.5	Sonar Distance Data from Accuracy Test for Sonar Unit-2 at Air Temperature of -1.0°C	206
C.1	Position Coordinates of CG from Dynamic Model for Vehicle of Weight 89,000 N and 22,200 N	239
E.1	Harvester's Position Data Collected for Three Performance Tests with a straight Row	258
E.2	Harvester's Position Data Collected for Three Performance Tests with a Row Containing an 8 cm Step Change	258
E.3	Harvester's Position Data Collected for Three Performance Tests with a Curved Row on a Campus Lawn	259
E.4	Harvester's Position Data Collected for Three Performance Tests with a Curved Row on a Concrete Driveway	260
E.5	Computed Position Coordinates of Front-Point A and Rear Point-B for Three Performance Tests with Straight Row	261

Table Page

E.6 Computed Position Coordinates of Front-Point A and Rear-Point B for Three Performance Tests with Curved Row on a Campus Lawn 262

E.7 Computed Position Coordinates of Front-Point A and Rear-Point B for Three Performance Tests with Curved Row on a Concrete Driveway 263

E.8 Computed Position Coordinates of Front-Point A and Rear-Point B for Three Performance Tests with Row Containing 8 cm Step Change 264

LIST OF FIGURES

Figure		Page
1.1	Perspective View of the USDA Over-The-Row Apple Harvester	2
1.2	Top View of the USDA Over-The-Row Apple Harvester	4
1.3	Front View of the USDA Over-The-Row Apple Harvester	5
3.1	Top View of Harvester Showing the Allowable Zone for Tree Trunks During the Harvesting Operation	31
3.2	Diagram of Tree Row Showing the Minimum Radius of Curvature	32
3.3	Schematic Diagram of the Apple Harvester's Hydraulic Circuitry for Front Wheel Steering	34
4.1	Method 1 - Tree Sensing Using Two Sonar Units to Determine Tree Position	39
4.2	Method 2 - Tree Sensing Using One Sonar and One Angle Measurement to Determine Tree Position	42
4.3	Method 3 - Tree Sensing Using Two Sonar Units to Detect the Tree Presence in Zones	44
4.4	Method 4 - Tree Sensing Using Two Optical Sensors and Two Angle Measurements Used to Determine Tree Position	47
4.5	Method 5 - Tree Sensing Usng Two Optical Sensors to Detect Tree Presence in Zones	49
4.6	Method 6 - Tree Sensing Using Multiple Sonar Units to Determine Tree Position (Top View)	51
4.7	Method 6 - Tree Sensing Using Multiple Sonar Units to Determine Tree Position (Front View)	52
5.1	Diagram of Major Components of the Automatic Steering Control System	56
5.2	Diagram of Tree Position Error	59

Figure Page

5.3 Block Diagram of the Apple Harvester Automatic Steering Control System 64

6.1 Polaroid Ultrasonic Circuit Board 67

6.2 Polaroid Ultrasonic Transducer 68

6.3 Timing Diagram of Ultrasonic Circuit Board 69

6.4 Diagram of Sonar Sensing System 71

6.5 Sonar Circuit Diagram for One Sonar Unit 73

6.6 Timing Diagram of Sonar Circuit for Objects for Range Less Than 240 cm 75

6.7 Timing Diagram of Sonar Circuit for Objects With Range Greater Than 240 cm 77

6.8 Interface Circuit Program 79

6.9 Timing Diagram for Interface Circuit 82

6.10 Distance Data for Sonar Number One at 25.5^{o}C 87

6.11 Distance Data for Sonar Number One at -1.0^{o}C 89

6.12 Plot of Sonar Data to Determine Transducer Beam Angle . . . 96

7.1 Mode 1 Graphical Output From The Simulation with K = 1.0 104

7.2 Mode 2 Graphical Output From the Simulation with K = 2.0 106

7.3 Flow Chart of the Harvester Steering Control System Simulation 107

7.4 Flow Chart of the Simulation Model for the Harvester's Microprocessor Functions 110

7.5 Diagram of the Harvester Steering Geometry 114

7.6 Diagram of the Harvester for Data Collection Test 116

7.7 Sonar Data and Wheel Position from System Test at 0.8 km/h Using a Continuous Wooden Fence 118

7.8 Flow Chart of Harvester Motion Simulation 123

Figure Page

7.9 Graphical Output of Simulation - Mode 2 with K = 0.5 126

7.10 Graphical Output of Simulation - Mode 1 with K = 0.5 127

7.11 Graphical Output of Simulation for Curved Row Mode 2 with K = 0.5 129

7.12 Graphical Output of Simulation for Curved Row Mode 1 with K = 0.5 130

8.1 Block Diagram of Steering Control System 132

8.2 Flow Chart of the Computer Subroutine Used to Turn the Harvester Front Wheels 134

8.3 Flow Chart of the Steering Control Program for the 1802 Microprocessor 137

9.1 Diagram of Simulated Tree Stand Used in Steering Control System Tests 150

9.2 Diagram of Linkage that Supports the Front Pen 153

9.3 Plan View of Harvester Showing Pen Locations for Performance Tests 154

9.4 Plan View of Test Configuration Used for Straight Row Test 156

9.5 Path of the Harvester for Straight-Row Test Number 1 . . . 160

9.6 Path of the Harvester for Straight-Row Test Number 2 . . . 161

9.7 Path of the Harvester for Straight-Row Test Number 3 . . . 162

9.8 Path of the Harvester for Curved Row Test Number 1 on a Concrete Driveway 164

9.9 Path of the Harvester for Curved Row Test Number 2 on a Concrete Driveway 165

9.10 Path of the Harvester for Curved Row Test Number 3 on a Concrete Driveway 166

9.11 Path of the Harvester for Curved Row Test Number 1 on a Campus Lawn 168

9.12 Path of the Harvester for Curved Row Test Number 2 on a Campus Lawn 169

Figure Page

9.13 Path of the Harvester for Curved Row Test Number 3 on a Campus Lawn 170

9.14 Path of the Harvester Predicted by the Simulation Model for Curved Row 172

9.15 Path of the Harvester for Row with Step-Change-- Test Number 3 174

9.16 Path of the Harvester Predicted by the Simulation Model for Row with Step-Change with Time Constant Equal to 2.0 seconds 177

9.17 Path of the Harvester Predicted by the Simulation Model for Row with Step-Change and Model Modified to Turn the Wheel 0.4^{o} for Each 2 cm of Tree Position Error 179

9.18 Path of the Harvester Predicted by the Simulation Model for Curved Row with Model Modified to Turn the Wheels 0.4^{o} for Each 2 cm of Tree Position Error 180

9.19 Path of the Harvester for Row with Step-Change-- Test Number 1 182

9.20 Path of the Harvester for Row with Step-Change-- Test Number 2 183

A.1 Distance Data from Sonar Unit-2 at Air Temperature of $25.5^{o}C$ 207

A.2 Distance Data from Sonar Unit-3 at Air Temperature of $25.5^{o}C$ 208

A.3 Distance Data from Sonar Unit-4 at Air Temperature of $25.5^{o}C$ 209

A.4 Distance Data from Sonar Unit-5 at Air Temperature of $25.5^{o}C$ 210

A.5 Distance Data from Sonar Unit-2 at Air Temperature of $-1.0^{o}C$ 211

B.1 Listing of the Program for the Harvester's Steering Control System Simulation Model 213

C.1 Diagram of Steering Angle and Block Diagram of Vehicle Model 224

C.2 Diagram of Tire Side Slip Angle 226

Figure Page

C.3 Typical Tire Characteristic of Side Force with Respect to Side Slip Angle 227

C.4 Dimensions for Vehicle 228

C.5 Body Centered Axes Model for Vehicle Equations of Motion 231

C.6 Basic Ackermann Steering Geometry 232

C.7 Free-Body Diagram of Forces for Steady State Turn with Allowable Tire Friction Force Equal to 2,200 N (500 lbf) 233

C.8 Plot of Steering Angle and Yaw Rate 236

C.9 Computer Program used to Compute the Vehicle Response Due to a Specified Steering Angle Input 238

D.1 Assembly Language and Object Code Listing of the Program Used by the Steering Controller's Microprocessor 243

1.0 INTRODUCTION

For several years, the United States Department of Agriculture (USDA) has been developing an over-the-row apple harvester. This harvester which is being developed by Tennes et al. (1976) is an experimental prototype harvester. They also are doing research and development work to design spraying and pruning equipment. By installing the appropriate equipment on to the harvester's main frame, this machine can be used for harvesting, spraying and pruning of apple trees. Figure 1.1 is an illustration of the USDA apple harvester.

The harvester is equipped with a hydrostatic drive system used to drive all four wheels and hydraulic cylinders are used to steer the front and rear wheels. The hydraulic system also supplies power for other auxillary equipment. Tennes and Brown (1981) have reported on the development of the shaker bar system and the basic dimensions of this system are shown in Figures 1.2 and 1.3. For the harvesting operation, the harvester is being designed to operate in a high density orchard which contains semi-dwarf trees that are spaced in either a straight or curved row at a minimum distance of 305 $\pm$5cm (120 $\pm$2 in) between the tree trunk centerlines along the row. These rows are to be spaced apart at a nominal distance of 487 cm (192 inches). During the harvesting operation, the harvester travels at a constant speed of 0.8 km/h (0.5 mph).

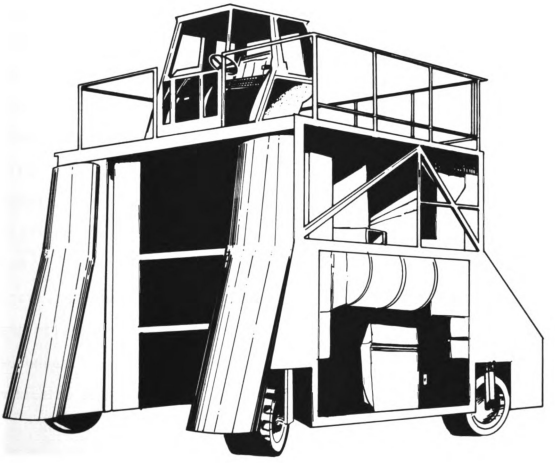

Figure 1.1 Perspective View of the USDA Over-The-Row Apple Harvester

1.1 The Need for Automatic Steering Systems

In order to harvest apples effectively, the USDA apple harvester should drive over the tree row so that the tree trunk centerline follows along the harvester's longitudinal centerline within an allowable tolerance. Tennes and Brown (1981) have reported that the harvester's shaker system performance may be improved if the harvester is centered over the tree row when the shaker bars are operating. During preliminary tests, they found that the harvester should be centered over the tree such that the harvester's centerline is within $\pm$22 cm (9 in) from the tree trunk centerline. Accurate steering may also prevent damage to the trees and the harvester due to inadvertent collisions with an apple tree. But, manual steering to keep the harvester centered on a tree is a difficult task. To accurately steer the harvester, it is necessary that the operator see the tree trunk, but due to the operator's position on top of the harvester, the field of view to the tree trunk is blocked by tree foliage. Therefore, since manual steering is difficult and since accurate centering of the harvester over the tree may improve the effectiveness of the harvester shaker system, there is a need for an automatic steering control system which will perform the task of automatically steering the harvester over the tree row.

An automatic steering control system may be able to solve other problems associated with steering agricultural vehicles. Busse et al. (1970) have reported that for a corn combine, operators appear to be

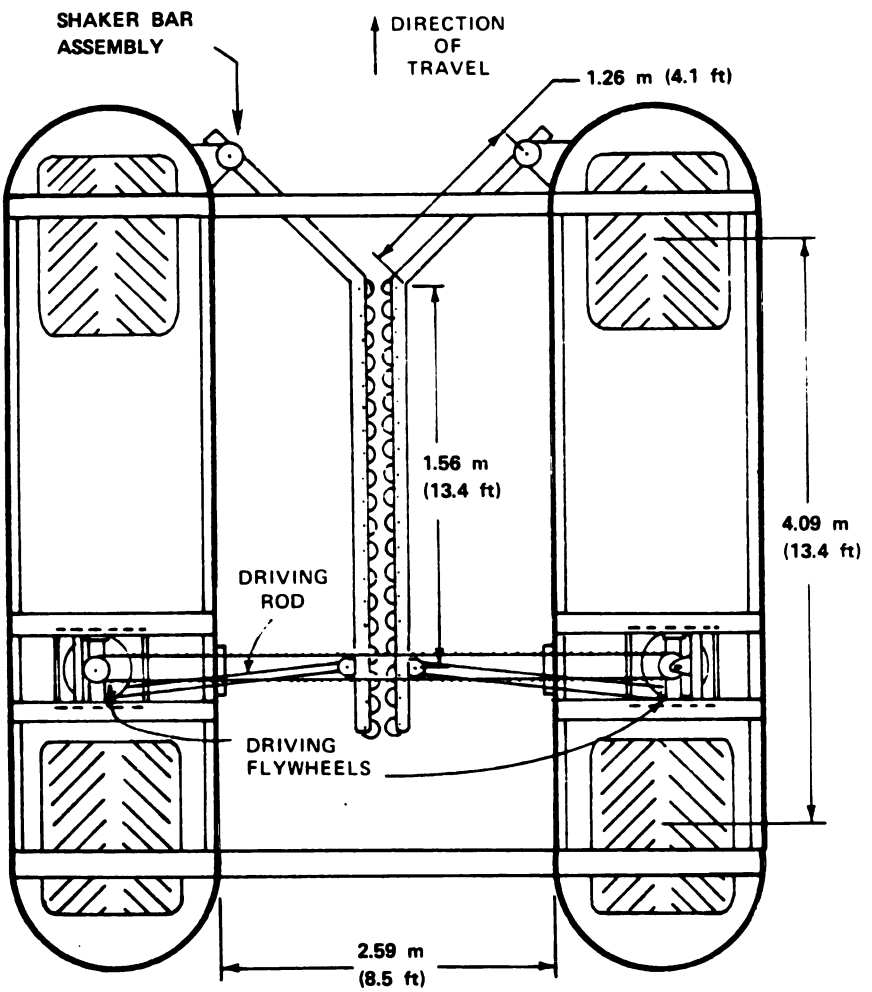

Figure 1.2. Top View of the USDA Over-The-Row Apple Harvester.

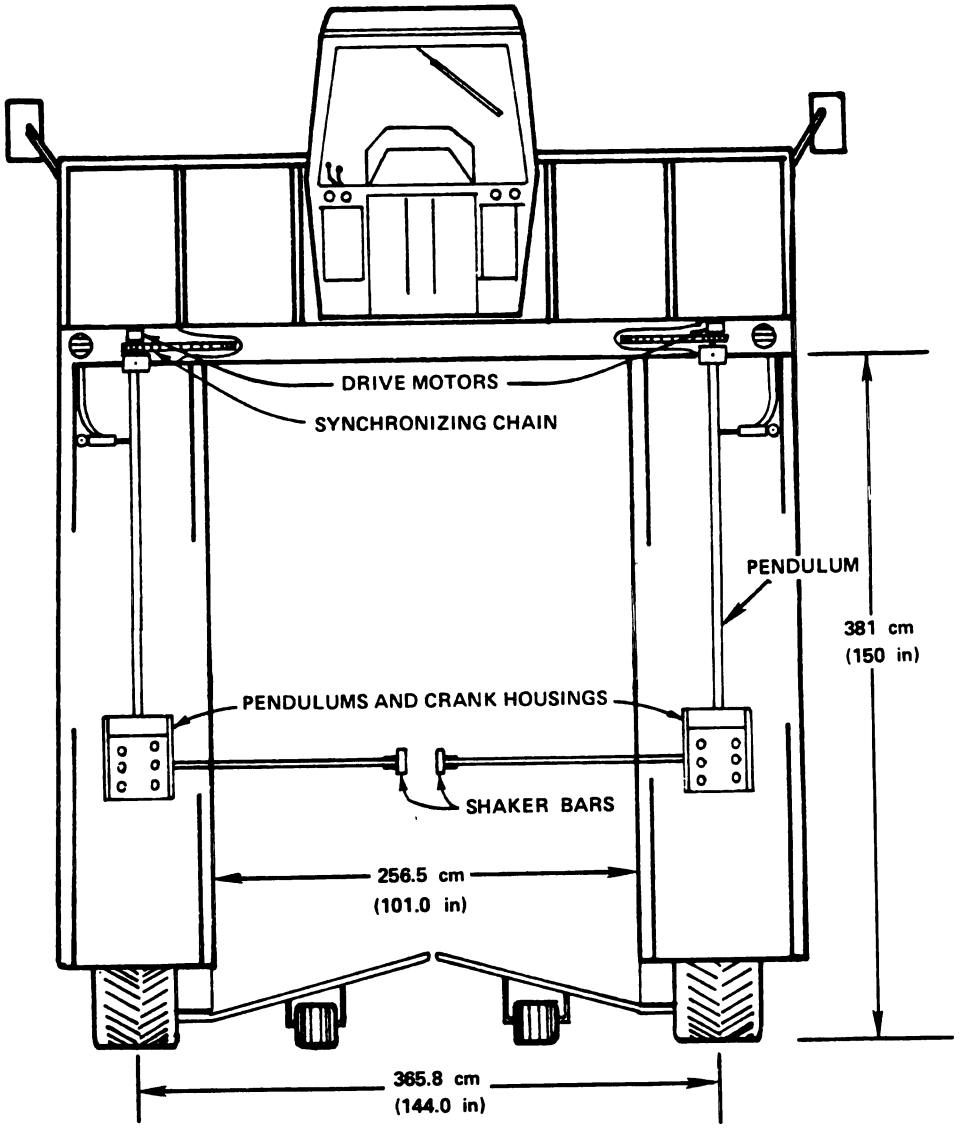

Figure 1.3. Front View of the USDA Over-The-Row Apple Harvester.

physically limited to operating at speeds of 5 to 6 km/h for long periods, yet the automatic steering system that was developed by Busse (1970) operates effectively at speeds of 8 to 9 km/h. Busse also reported that when an automatic steering system was used for a combine, the operator could put his full attention on regulating the forward speed as required by the crop conditions and thus the operator was able to increase the output of the harvester up to 15 percent. In addition to a limit on the forward speed with manual steering, the accuracy of manual steering may be affected by the complexity of the steering task and by operator fatigue. Kirk et al. (1975) reported that long hours of steering a self-propelled swather is very taxing and monotonous. The operator must continuously make steering corrections to accurately follow the edge of the standing grain. Also, due to the sensitive steering system of a swather, Kirk et al. have reported that even an experienced operator can have difficulty accurately steering to minimize the amount of overlap onto the previously cut swath. Therefore, it may be possible to use an automatic steering system on an agricultural vehicle to: (1) help reduce the fatigue due to long hours of steering, (2) increase the forward speed, (3) allow the operator time to control other machine functions which could improve the machine output, and (4) help reduce the overlap that sometimes results with manual steering.

1.2 Comparison of Sensing Methods

The development of an automatic steering control system can be divided into two major components, a controller and sensing system. The function of the controller is to: (1) receive signals from the sensing

system; (2) process these signals and; (3) transmit signals that will control a machine or system. Controllers may be divided into two types; (1) analog electronic controller which processes analog signals, and; (2) a digital electronic controller which processes digital signals and which may use a microprocessor. In order for a controller to perform well, a sensing system must be available to send a signal containing appropriate information to the controller. Sensing systems may also be divided into two categories; contact and non-contact sensing systems. Since the development of a control system requires the selection of a sensing system, these two types of sensing systems will be compared.

1.2.1 Contact Sensing Systems

There are generalized problems associated with use of a contact type sensing system and these problems result because the contact type sensor must make physical contact with the object that is being sensed. A typical example of a contact sensor is a mechanical feeler arm assembly that is used to sense the position of an object. The mechanical feeler arm assembly is usually held in a undeflected position during its operation. As the feeler arm moves to a position where it contacts the object that is being sensed, the object applies a force to the arm and this causes the arm to be deflected to a new position. The feeler arm can be connected to an electrical transducer which converts the deflection of the arm to a voltage signal that represents the position of the arm. The position of the arm also represents the position of the object that is being sensed. Because the contact type sensor contacts the sensed objects, several problems can occur.

One problem with contact sensing is damage of the sensing assembly. During the sensing operation, when the vehicle is traveling at high ground speeds, the sensing assembly can strike or impact the sensed object with enough force to damage the sensing assembly. Also, this impact with the sensed object can cause the sensing assembly to rebound or bounce off the sensed object and this rebounding can result in erroneous signals that are sent to a controller. Also, the sensed object can become damaged by the impact with the sensing assembly. Another problem is that a contact assembly can become fouled with debris. This usually results because the sensing assembly is placed in an area where it can sense an object and this is typically at a location where the sensing assembly is unprotected from fouling by debris. There is also a problem of sensing system failures that are due to excessive wear of moving parts. Contact type sensors typically have several moving parts such as bearings or gears and, thus, a sensing system can fail periodically due to the excessive wear of these moving parts. Busse et al. (1970) also have explained that there is a problem with sensing fragile objects. Busse et al. (1970) have reported that a contact type sensor has not been developed to effectively sense the position of stems of small grain plants because these stems are too weak to activate a contact type sensor.

1.2.2 Non-Contact Sensing Systems

To begin the discussion of how a non-contact sensing system may be advantageous when compared to a contact sensing system, we must first consider the definition and understand the general operation of a non-contact sensing system. Non-contact sensing is usually accomplished by transmitting a signal such as light, radio waves, or ultrasonic sound

pulses toward the object that is being sensed. The signal travels to the object and reflects from the object back to the sensing system. Generally, the reflected signal allows the sensor to detect the presence of an object in a specific sensing zone, although some sensing systems can sense more information about the object such as, color, shape, or range of the object from the sensor. The use of light, radio waves and sonar are only some of the ways that non-contact sensing can be accomplished. This subject of non-contact sensing (or sometimes called remote sensing) is a broad area that covers many different sensing systems. In order to give a description of how a non-contact sensing system operates, two examples of non-contact sensing systems will be briefy explained.

Two examples of non-contact sensing systems are radar and sonar (airborne). With a radar system, an object's distance from the radar unit can be measured. The radar transmits a pulse of electromagnetic waves (radio waves) toward an object and for some objects the electromagnetic waves are reflected back to the radar unit. The time is measured for the pulse of waves to travel out to the object and back to the radar unit. Then the distance to the object is computed using the measured time interval. In this computation, the total distance traveled by the pulse of waves is equal to the measured time interval multiplied by the velocity of the pulse. The pulse velocity is the speed of light. The airborne sonar system works in a similar manner as the radar system, altough the sonar system transmits a pulse of ultrasonic sound waves. This pulse of waves is also reflected from the surface of an object and returned to the sonar system. Then, like the radar system, the object's distance is determined by computation using

the time of travel of the pulse and the velocity of pulse. The pulse travels at the speed of sound.

When comparing a non-contact sensing system to contact sensing, the non-contact sensing system appears to e able to solve some of the problems associated with the contact systems. First, non-contact sensors are typically not damaged by the object that is sensed because the object does not contact the sensor. Also, since the object does not strike or impact the non-contact sensor, there is not a problem with the sensor's rebounding or bouncing from the surface of the object as it sometimes occurs with cntact sensors. Second, a non-contact sensing system can sometimes be positioned on a machine in a remote location where it can be protected and this protection usually prevents the non-contact sensing system from being fouled by debris. Third, a non-contact sensing system can generally be built with few moving parts, thus, there is a lower probability of failure due to the excessive wear of the moving parts. And, fourth, a non-contact system can be used to sense weak or fragile objects which is a problem for contact type sensors, because they must apply a force to the object.

Therefore, it appears that a non-contact system may be able to solve the problems associated with contact sensing systems. Since the non-contact sensing system has the potential of providing good performance without the problems of a contact sensing system, it is worthwhile to develop a non-contact sensing system that can be used on an automatic steering control system for an agricultural vehicle. The development of a non-contact sensing system and digital electronic controller was selected as the subject of this research.

1.3 Objective

The objectives are:

1. Design and test a non-contact sensing system which can measure the distance from the sensing system to a tree trunk.
2. Design a microprocessor-based automatic steering control system for the USDA apple harvester using a non-contact sensing system.
3. Design the steering control system to control the steering of the harvester's front wheels.
4. Design the steering control system to steer the harvester so that each tree passing through the inside space of the harvester stays within an allowable zone. The allowable zone is 45 cm wide, 409 cm long and is centered on the harvester centerline. This zone extends from the harvester's front wheels to the rear wheels (Figure 3.1).
5. Design the steering control system to satisfy the performance objective of item 4 above with the harvester traveling at a forward velocity of 0.8 km/h (0.5 mph) and with either a straight or curved tree row. A curved tree row shall have trees positioned on a smooth continuous curve with minimum radius of curvature of 121.9 m (400 ft).
6. Design the control system to interface with the existing USDA apple harvester steering system and to have a total cost of less than $2,000 for the electronic equipment used in the steering control system.

7. Test the steering control system using simulated conditions. These tests shall determine if the steering control system satisfies the control system performance objectives which are listed above.

These objectives were used to develop a set of design requirements which are shown in Chapter 3.

2.0 LITERATURE REVIEW

A review has been done of reseach work on automatic steering systems that are used in agriculture. The steering systems that were reviewed can be divided into four categories and the categories are automatic steering systems using: (1) contact type sensors, (2) optical type sensors, (3) buried cable technique and (4) special position sensing. Research work on the development of automatic steering systems has been published for many years. Grovum and Zoerb (1970) in their work to develop an automatic steering system have reviewed many different types of automatic guidance systems that were developed outside the field of agriculture. They concluded that sensing systems such as laser and radar have been used successfully in military applications for guidance control but are too expensive to be used on an agricultural field machine. Also, several references were reviewed on the subject of sonar sensing systems.

2.1 Automatic Steering Control Systems Using Mechanical Contact Type Sensors

Grovum and Zoerb (1970) have designed an automatic steering control system to steer a tractor during the plowing operation. A sensing system and an electronic analog controller were designed such that the tractor follows a furrow that has been previously plowed. This sensing system was a displacement sensor which consists of two mechanical feeler arms that contact both sides of the furrow in order to sense the position of the furrow. When the tractor is not accurately following

the furrow, one of these feeler arms will move away from a neutral position. The feeler arm is connected to variable resistors and when the feeler arm moves to a new position the variable resistor circuit produces an output voltage signal which is proportional to the amount of displacement of the feeler arms.

This steering control system by Grovum and Zoerb (1970), also included a directional gyroscope. The gyroscope was used in the control system for two purposes. First, the signal from the gyroscope was used to keep the tractor heading in a straight line on the first pass of the tractor through the field because on the first pass there was no furrow for the tractor to follow. Second, the gyroscope was used as a feedback signal in the control system so that this signal would attenate an error signal from the displacement sensor. This results in a damping effect and the tractor has a slower response to the error signal from the displacement sensor. The voltage signal from the gyroscope is proportional to the change in azimuth of the tractor's direction of travel.

Grovum and Zoerb (1970) also utilized an analog electronic controller in this steering control system. The controller processes the analog voltage signals from the directional gyroscope and the displacement sensor, and these signals are feedback signals in the closed loop automatic control system. Grovum's simulation model of the control system indicated that the system behaved like a linear second order system. The test results of the control system showed that the system was unstable with the displacement sensor mounted next to the rear of the tractor. With the displacement sensor mounted near the front wheels the control system provided effective control for speeds up

to 6.8 km/h (4.2 mph). The tests also showed that at speeds less than 6.8 km/h the signal from the direction gyroscope was not neded, but at speeds greater than 6.8 km/h the gyroscope signal was required to achieve stable control of the tractor.

Shukla et al. (1970) have reported on the analysis of a vehicle steering control system. In this analysis a model was developed that simulated the kinematic motion of a vehicle with front and rear wheel steering. The model was developed for an automatic steering control system that used an ideal proportional control algorithm. In this control algorithm, the controller sends out a signal to turn the wheels to an angular position corresponding to 1.0 radian per 30.4 cm (12.0 in) of error detected by a path detection sensor. This path detection sensor was tested at various locations in order to find the best sensor position. They also assumed that the wheels turn (for steering) at a high enough rate that negligible time is required for the wheels to arrive at the desired wheel position. The wheel turning rate is defined as the angular velocity of the wheel where the wheel rotates about its vertical centerline. The model was used to investigate effects on the tractor tracking error that was caused by changing the major dimensional parameters that define the vehicle steering system. To verify the model, a simplified tractor steering control system was used to determine if a good correlation existed between the path traveled by the experimental test vehicle and the path predicted by the computer model. The agreement between the predicted and measured results were so closely correlated that they concluded there were no gross errors in the simulation model. Some of the major conclusions from their study are: (1) the path detection sensor's optimum position is approximately 30.4 cm

(12.0 in) in front of the front wheels; (2) to achieve stable operation at least one path detection sensor must be near or in front of the front wheels, and (3) effective steering control can be achieved by using the error signal from a path detection sensor in front of the front wheels to control the steering of both the front and rear wheels. These conclusions were based on results of the computer simulation with the vehicle velocity set at 8.0 km/h (5.0 mph).

Another steering control system, reported by Busse et al. (1970), is the development of automatic steering control for a combine and forage harvester, which was done by the Claas Company. This machine when used to harvest corn, uses a pair of feeler arms to sense the position of corn stalks. When the harvester is not centered on the row, the corn stalks will contact the feeler arms and move the feeler arms from a normal positon to a displaced position. The feeler arm is connected to a variable resistor circuit which converts the position of the feeler arm to a voltage signal from the feeler arm circuit is sent to an electronic analog controller. When steering corrections are needed, the controller sends a voltage signal to a hydraulic valve and this causes the wheels to turn. An analog voltage signal is also received by the controller to determine the angular position of the wheels. Busse et al. have tested the steering control system and have reported that the harvester deviated from the row centerline 2.5 cm (1.0 in) at speeds less than or equal to 6.0 km/h (3.7 mph) and at speeds up to 9.7 km/h (6.0 mph) the deviation did not exceed 5.1 cm (2.0 in).

Upchurch et al. (1980) have reported on the design and development of an automatic steering control system for the USDA apple harvester.

The control system uses a sensor arm system which contacts the tree trunk to detect tree position. At the front of the apple harvester one sensor arm system is mounted on the left side of the apple harvester and one on the right side. The sensor arms are located near the harvester centerline so that if the harvester is not centered over the tree, then one of the sensor arms is pushed by the tree trunk. The sensor arm system is designed as a 4-bar linkage and is spring loaded to hold the arm in a neutral position. As the tree pushes on one of the sensor arms the sensor arm moves to a new position. A shaft encoder is mechanically connected to the sensor arm and the shaft on the shaft encoder turns as the sensor arm moves. The shaft encoder produces a 4 bit binary output number which is proportional to sensor arm position, and this binary number also represents tree position. The binary code from the shaft encoder is sent to the microprocessor based digital electronic controller and the controller sends signals to electrical relays which control the operation of solenoid operated hydraulic valves. These valves are used to steer the front and rear wheels. Shaft encoders are also used to determine the angular position or steering angle of the front and rear wheels.

Upchurch et al. have tested the steering control system and they reported that the control system kept the harvester centered on a curved path which had a minimum radius of curvature of 22 m (75 ft) within a tolerance of $\pm$7.6 cm (3.0 in) with a forward speed of 0.8 km/h (0.5 mph).

These automatic steering control systems that have been reviewed are significantly different from the objectives of this research project for the development of an apple harvester steering control system. Most

of the control systems that were reviewed had a position-error signal that was continuous, whereas the apple harvester may only have a noncontinuous error signal because the trees are 304 cm (120 in) apart in the row. The review of these control systems found that all but one system used an electronic analog controller whereas the apple harvester is being developed for a microprocessor based controller. The reviewed control system used contact sensors and the apple harvester is being developed for the non-contact sensors. A control system that was designed by Upchurch et al. (1980) was an effective steering control system for following a row of apple trees using contact sensors. But, the steering control system for this research should use a non-contact sensing system and will require the development of: (1) a non-contact sensing system; (2) computer control algorithm; (3) computer software, and (4) hardware to interface the sensing system with a controller.

2.2 Automatic Steering Control Using Optical Type Sensor

Kirk and Krause (1970) have designed a steering control system for a swather which uses an infrared proximity sensor to measure the distance from the sensor to the stems of small grain plants. This sensor measures the intensity of the reflected light and then converts it to a voltage signal. The voltage signal is processed by a linearizing circuit to produce an output voltage that is linearly proportional to the distance measured. The range of the sensor is 10 to 56 cm (4 to 22 in). An analog electronic controller receives the voltage signal from the sensing system and the controller sends signals to hydraulic valves to steer the wheels. The voltage signal is used by the controller to determine the error in position of the swather. The

wheels are then turned to a steering angle that is proportional to the position error.

Kirk and Krause have reported that on a single pass, the swather will follow the row within ± 12.2 cm (4.8 in) at speeds in the range of 3.2 to 12.1 km/h (2 to 7.5 mph). For the case where the swather made more than four passes, the edge of the crop which was cut by the swather developed an oscillating pattern with 30 cm (12 in) amplitude with wave length of 12.2 m (40.0 ft). For a larger number of passes, amplitudes greater than 30 cm were observed.

Ambler et al. (1980) have developed a prototype tractor which does not require a driver. This tractor uses optical sensing to follow a plowed furrow and an electronic distance measuring device to measure the distance to reference targets for controlling the turn that is required at the end of each furrow. This electronic distance measuring device can be described as an optical ranging system. The range measurement from the ranging system is used by a microprocessor based controller for locating the end of the furrow and controlling the turn-around of the tractor at the end of the furrow. This control system also requires a measurement of the bearing which is the direction of travel of the tractor. This bearing measurement is made by using the ranging system and a precision potentiometer. The ranging system rotates at a rate of one revolution per second and the potentiometer setting changes as the ranging system rotates. When the ranging system is pointing toward the pole or target at the end of the furrow a voltage measurement is taken from the potentiometer and this voltage signal is translated into an angle. This angle is the direction of travel of the tractor relative to the target. The targets are posts which are wrapped with reflective tape

and these posts are located near the end of furrows with a spacing between posts of 15 m. Note, that the steering control system for the USDA apple harvester is not being designed for an automatic turn around at the end of a tree row.

This optical ranging system that was developed by Ambel et al. measures the distance to the posts by processing a modulated infrared light signal that is transmitted to the post and reflected back to the ranging system. The infrared light beam is produced by energizing and de-energizing an infrared light emitting diode at a frequency of 5MHz. In order to make a distance measurement, the light beam is directed toward the target and the beam is reflected back to the ranging system. The ranging system then receives the reflected modulated light signal and measures the phase shift between: (1) the transmitted beam, and (2) the received (or reflected) beam. This measured phase shift is converted to the target's range. This distance measured by the ranging system is usually called electronic distance measurement. Smith (1980) reported on a similar ranging system developed by Hewelett Packard Corporation which is called an industrial distance meter (Model 80850 A).[1] This system is accurate to within ±5 mm plus 1 mm per kilometer of range and the reading rate is 9 measurements per second.

This steering control system that was developed by Ambler et al. (1980) used another optical sensor to determine if the tractor was

---

[1]Trade names are used in this paper solely to provide specific information. Mention of a product name does not constitute an endorsement of the product by the author to the exclusion of other products not mentioned.

accurately following the edge of the furrow. This system uses a light source that is directed downward at a furrow wall. The light reflected from the furrow goes through a lens that directs the light onto two arrays of photo cells. If each of the two arrays receive light covering equal area on the photocell arrays then the tractor sensor is centered on the furrow edge. Each photocell array produces an output voltage which is proportional to the number of photocells in the array which receive the reflected light. The voltage signal from each array is summed to produce a single voltage signal which is linearly proportional to the error of the tractor position. The polarity of the voltage corresponds to the direction of the error in tractor position. This error signal is sent to an analog controller circuit to execute the required steering of the tractor's front wheels.

After reviewing these references on steering control systems, it appears that these systems are not directly applicable to the apple harvester steering control system for the following reasons. All of these control systems used sensors to measure a continuous signal for vehicle position-error and these signals were processed by an analog controller which controlled the vehicle steering. However, the apple harvester steering control system will probably have to use a noncontinuous position-error signal due to the space between trees. Also the design of the apple harvester steering control system has the objective to utilize a microprocessor based controller. The electronic ranging system that was described, may be effective at measuring the range to apple trees, but this system is too expensive for the apple harvester control system. The optical sensor that was designed by Ambler et al. to follow the furrow is specially designed to sense the edge of a furrow

and it would not function as a sensor to detect apple trees. This concept of using an optical sensor appears feasible to sense the position of an apple tree trunk, but a new lens system and electronic circuit would be required. The infrared optical sensor that was developed by Kirk et al. may be applicable for apple tree trunk sensing for the apple harvester's non-contact ranging system, but there is the disadvantage that the sensor functions only within a small range. The sensor's maximum range is 56 cm (22 in).

2.3 Automatic Steering Control System Using Buried Cable

The buried cable technique is a concept that has been investigated for many years. Schafer and Young (1980) have developed a digital electronic controller for a tractor which utilizes the buried cable technique. The tractor's control system uses a pair of antennas which develop a signal that indicates if the tractor is either to the right or to the left of the cable. The steering control system uses this signal so that the tractor follows the buried cable. The buried cable transmits an electromagnetic wave due to low frequency (3 kHz) alternating current flowing in the cable. The antenna circuit develops a logic signal that corresponds to the tractor's position. This system has only two logic states which are: state (1), the tractor is off the course to the left of the buried cable, or state (2), off the course to the right of the buried cable. The controller for the steering control system uses a 8085 microprocessor which sends out an eight bit binary code number to control the direction of wheel turning (for steering) and the rate of wheel turning. Six bits of this number are used to control the rate of wheel turning. This is accomplished by sending the six bit

numbers to a digital-to-analog converter and then sending the analog voltage signal to a proportional control valve in the hydraulic circuit. The computer algorithm that is used to control the steering, increments the binary number for the turning rate at discrete time intervals during the time period when the error logic signal remains unchanged. At the time when the error logic signal changes to the other state, the binary code for the rate of turn is reset to zero and the binary code for the direction of turn is changed to the other direction. Then the control process repeats. Preliminary test results of the tractor's steering control system indicated that the tractor's deviation from the cable is within $\pm$7.0 cm at speeds up to 20 km/h (12 mph) for a straight line course without towing an implement.

The buried cable method is too expensive for use in an apple orchard and therefore this technique was not selected for development with the apple harvester's automatic steering system.

2.4 Automatic Steering Control Using Spacial Position Sensing

Smith et al. (1979) have investigated the feasibility of controlling the steering of a tractor using a technique called non-contact spacial position sensing. This technique requires that the coordinate position of two points on the tractor be measured relative to a fixed reference point. One method to accomplish this is to use two radar units which are at two fixed locations in a large field. The radar units could then measure the distance to two points on the tractor, and by using triangulation, the X and Y coordinate position of the two points on the tractor could be computed. The X-Y coordinate system is fixed to the field.

The work by Smith et al. investigated the feasibility of a computer algorithm to control the steering of a tractor so that a towed implement follows a specified path. The computer algorithm assumes that accurate tractor position coordinates are available. Smith et al. did not develop any sensing system to measure the tractor coordinate position. The computer control algorithm computes the front wheel steering angle for a discrete interval of time so that the towed implement would follow a specified path. In addition to this control algorithm, algorithms were written for the case of a rear-steer tractor with a front mounted implement and the case of an articulated tractor with a towed implement.

A computer simulation of the control algorithm was used to verify the feasibility of the algorithm. The simulation shows that for speeds up to 5.4 km/h (3.4 mph) the maximum error of the implement from the desired path for all three cases is $\pm$1.1 cm (0.4 in). Therefore, Smith et al. (1979) concluded that the use of the control algorithm was feasible. Smith et al. (1979) also reported on a verification test of the steering control algorithm using a computer controlled small scale model with a length scale factor of nine. The results of these texts with the scale model simulator show that the maximum error predicted for a full scale tractor is $\pm$4 cm of deviation of the implement from the specified straight line path.

This technique of using non-contact spacial position sensing requires a set of radar units or other non-contact distance measuring equipment to measure the coordinate position of two points on the tractor relative to a fixed reference point on the field. This type of

measuring equipment is too expensive to be utilized for the apple harvester steering control system.

2.5 Sonar Sensor - Ultrasonic Transducer

A sonar transducer which is a non-contact sensor, can be used to measure the distance from the sonar transducer to an object. To measure a distance or range to an object, first an ultrasonic sound pulse is sent out from the transducer. Then, the time is measured for the sound pulse to travel from the transducer to the object and reflect back to the transducer. The time measurement is converted to a distance by using the fact that a sound pulse in air travels at the speed of sound which is 331.0 m/s for dry air at zero degrees Celsius.

A reference was not found for an automatic steering system which utilizes an ultrasonic sensor, although Coad (1979) reported on the application of an ultrasonic sensing system on a sugar cane harvester to control the height of the cutter bar. An ultrasonic sensing system was developed and interfaced to an electronic controller which uses a 6800 microprocessor. The controller computed the average distance from the transducer to the ground and the average distance from the transducer to the top of the sugarcane stubble. The difference between these two measurements represents the height of the cut sugar cane stubble. This sonar distance data was recorded and it was noticed that the data contained many erroneous values. Therefore, an averaging technique was used to smooth the data. Three averaging techniques were investigated. Coad (1979) selected the weighted-running-average for development in the computer algorithm because it required less computer memory to

implement; it gives more weight to the most recent data sample and; it allowed for changing of the weighting factor. The weighting factor affects how fast the computed average of the distance corresponds to changes in the actual distance. Test results using a soil-bin-simulator show that the computer algorithm was effective in measuring the height of the sugar cane stubble. Further work was planned to develop this ultrasonic sensing system into a complete controller for controlling the cutter bar height on a sugar cane harvester.

A report by Gross (1978) explained that ultrasonic transducers are becoming more popular and are being utilized in control systems. It was reported that small electrostatic ultrasonic transducers are being used because they produce a beam that has sharper boundaries than other types of sonar transducers and because the beam angle of divergence can be as small as 5.5 degrees. A disadvantage of a sonar ranging system is that the sound pulse travels at the speed of sound which varies with the air temperature and this can cause difficulties in obtaining accurate sonar measurement if the sonar system is operated over a large temperature range.

Another reference was reviewed that described an ultrasonic transducer that is developed for an automatic focusing system for a camera manufactured by the Polaroid Corporation.[2] This transducer is small, about 3 cm in diameter, and is controlled by a small electronic circuit. The Polaroid Corporation began marketing in 1980 a sonar ranging system which consists of an electrostatic transducer and an electronic controller circuit. The costs of these components are $17.00

---

[2]Ultrasound in Focus, Ultrasonics, Sept. 1979, pp. 195

for the transducer and $25.00 for the controller circuit. The electronic controller circuit is made on a small printed circuit board which is approximately rectangular with dimensions of 10 cm (4 in) by 5 cm (2 in). The sonar controller circuit is designed to operate on a special 6 volt battery designed by the Polaroid Corporation. Electrical timing signals are produced by the controller circuit which can be used by an electronic interface circuit to determine the distance to an object. One timing signal indicates the moment when the ultrasonic pulse is sent and another timing signal indicates the moment when the reflected ultrasonic sound pulse has returned to the transducer. The transducer transmits and receives the ultrasonic sound pulse. The Polaroid Corporation also markets a demonstration-display-board for $125.00. This demonstration-board displays the distance measured by the sonar system on 3 digit, light emitting diode (LED) displays. The distance is displayed in dimensions of feet and the least significant digit is one tenth of a foot. The range of the display system is 27.4 cm (10.8 in) to 10.7 m (35 ft). The measurements are made at a rate of five per second.

Ciarcia (1980) also described the Polaroid sonar system and explained a circuit designed to interface the Polaroid demonstration-board with a microprocessor based computer. This design by Ciarcia (1980) is limited to the performance specifications of the Polaroid demonstration display board. The resolution of the measured distance is 3 cm (0.1 ft) and the maximum rate of measurement is five per second. For many control systems this rate may be too slow. Therefore, if these maximum performance requirements do not meet the design

requirements for a particular control system, then a new interface for the sonar controller circuit will be needed.

An ultrasonic sensing system (also called a sonar sensing system) has several desirable characteristics that make the ultrasonic system appear to be feasible for development in a steering control system. First, the cost of an ultrasonic sensor is low; second, the ultrasonic system is non-contact sensing system; and third, the ultrasonic sensors appear to have voltage signals available that allows interface with a digital electronic controller. However, there is a significant amount of development work required to develop an ultrasonic sensing system that can be utilized in the steering control system for the USDA apple harvester. Three major tasks for developing an ultrasonic sensing system are: (1) develop a feasible concept for using the ultrasonic sensing system to sense tree position; (2) develop digital electronic circuits to interface the ultrasonic sensing system with a digital electronc controller, and (3) develop the computer control algorithm and software that will effectively control the steering of the USDA apple harvester.

3.0 DESIGN REQUIREMENTS

The design objectives of section 1.3 were used as a basis to make a specific set of design requirements for the apple harvester automatic steering control system. These design requirements are primarily concerned with defining the allowable tolerance on the alignment of the harvester with the tree centerline during the harvesting operation and with defining the basic operating environment for the harvester. Also, since the harvester has already been built, the steering control system must be designed to interface with the harvester's existing steering system. The following sections specify the design requirements for the apple harvester's automatic steering control system.

3.1 Alignment

During the harvesting operation, the apple harvester's steering control system shall keep the harvester centered over the tree such that the tree trunk stays within an allowable zone as the harvester drives over the tree row with a ground speed of 0.8 $\pm$0.3 km/hr (0.5 $\pm$ 0.2 mph). This allowable zone is a rectangular area 45 cm (18 in) wide by 408 cm (161 in) long. The allowable zone is oriented so that the longitudinal centerline of the zone is overlayed onto the longitudinal centerline of the harvester and this is illustrated in Figure 3.1. This allowable zone extends from the front wheels of the harvester to the rear wheels. The steering control system shall keep the harvester centered according

to this alignment specification when operating within the specified operating environment.

3.2 Tree Spacing and Row Curvature

The apple harvester shall follow the tree row with an alignment on the trees as specified by Section 3.1 and with the trees spaced in the row according to the following specification. The trees shall be spaced in the row with a distance of 305 $\pm$5 cm (120 $\pm$2 in) between tree trunk centerlines. A tree row shall have trees positioned such that an arc which passes through any three adjacent trees has a minimum radius of curvature of 121.9 m (400.0 ft). Fig 3.2 illustrates that this minimum radius of curvature corresponds to a 7.6 cm (3.0 in) tree offset from a straight line that extends through the centerline of the nearest two trees in the row. This requirement for row curvature was selected because most of the apple trees planted in the future will probably be planted by a tree planter which is similar to planter developed by Tennes and Burton (1979). This planter operates with sufficient accuracy to meet the spacing tolerance of $\pm$5 cm along the tree row, and meet the requirement of minimum radius of curvature of 121.9 m.

3.3 Operating Environment

The apple harvester shall be capable of operating according to the performance criteria of Sections 3.1 and 3.2 with the following environmental conditions. The operating environment is defined as air temperature in the range of $0^{o}C$ ($32^{o}F$) to $32^{o}C$ ($90^{o}F$) and relative humidity in the range of zero to 100 percent. Rain or snow is not an acceptable operating environment, although, the steering control system shall be capable of exposure to rain or snow without being damaged.

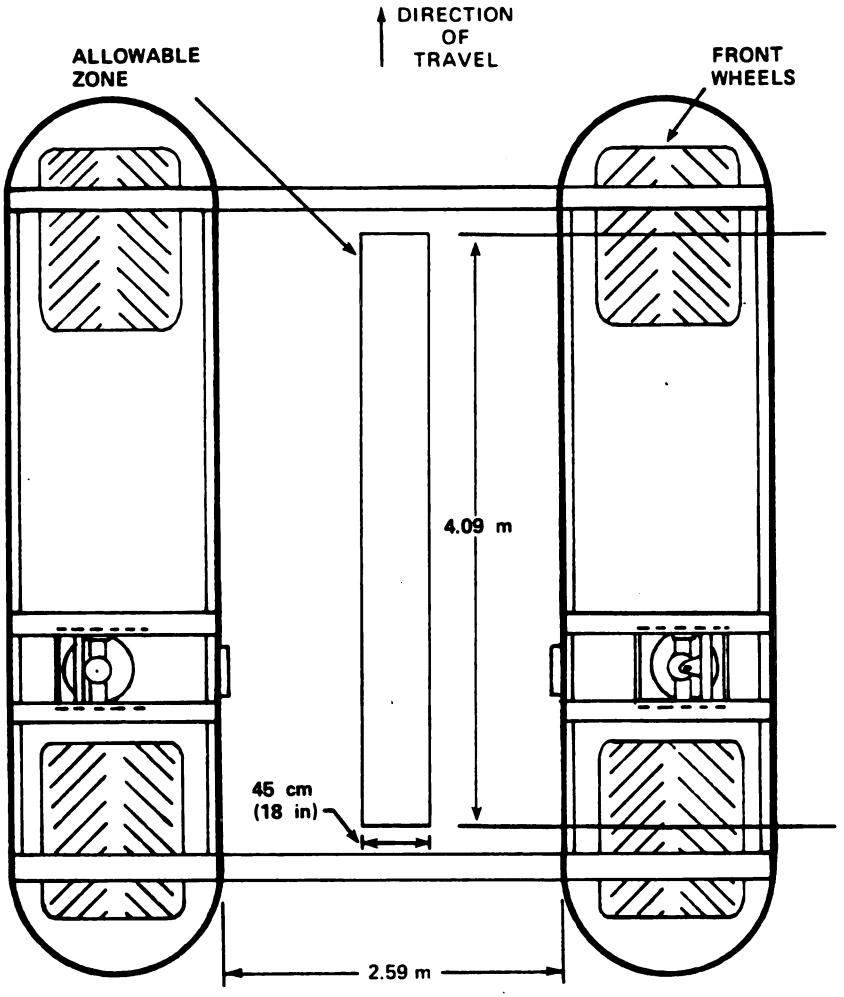

Figure 3.1 Top View of Harvester Showing the Allowable Zone for Tree Trunks During the Harvesting Operation.

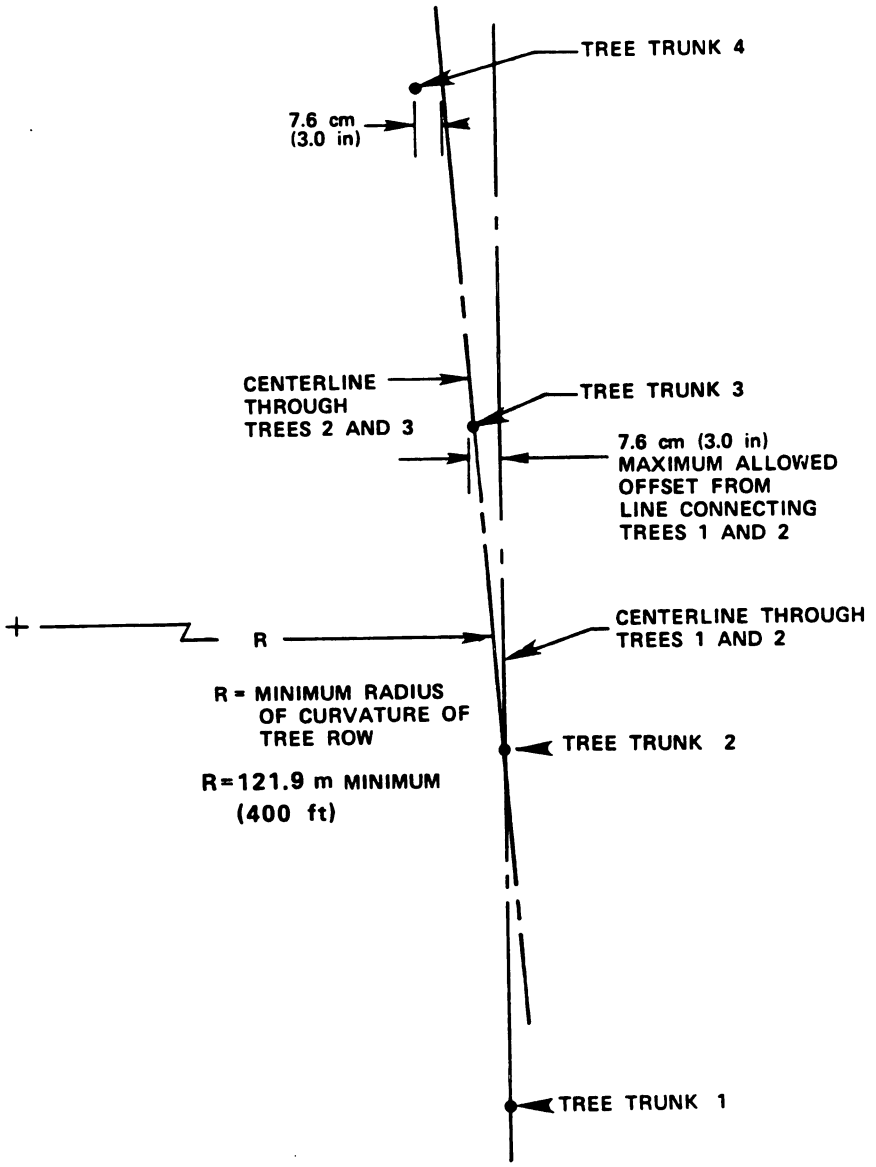

Figure 3.2 Diagram of Tree Row Showing the Minimum Radius of Curvature.

3.4 Interface With Harvester Steering System and Design Constraints

The steering control system shall interface with the existing steering system of the USDA over-the-row apple harvester and shall control the steering of the harvester's front wheels. This existing steering system includes hydraulic circuitry that controls hydraulic cylinders to steer the front wheels. Figure 3.3 is a schematic diagram of the steering system hydraulic circuitry.

The development of the steering control system must also consider constraints on the design of the control system. In order to keep the steering control system economically feasible, it is estimated that the cost to manufacture the hardware for the steering control system should not exceed $2,000. This estimate is based on an apple harvester that would have a cost in the range of $50,000 to $100,000. Thus, this constraint on cost was used as a design goal for the steering control system. Also, it is a design goal that the control system be designed for high reliability and have features that facilitate maintenance and repair. Further research is required to develop specific requirements for system cost, reliability and maintainability.

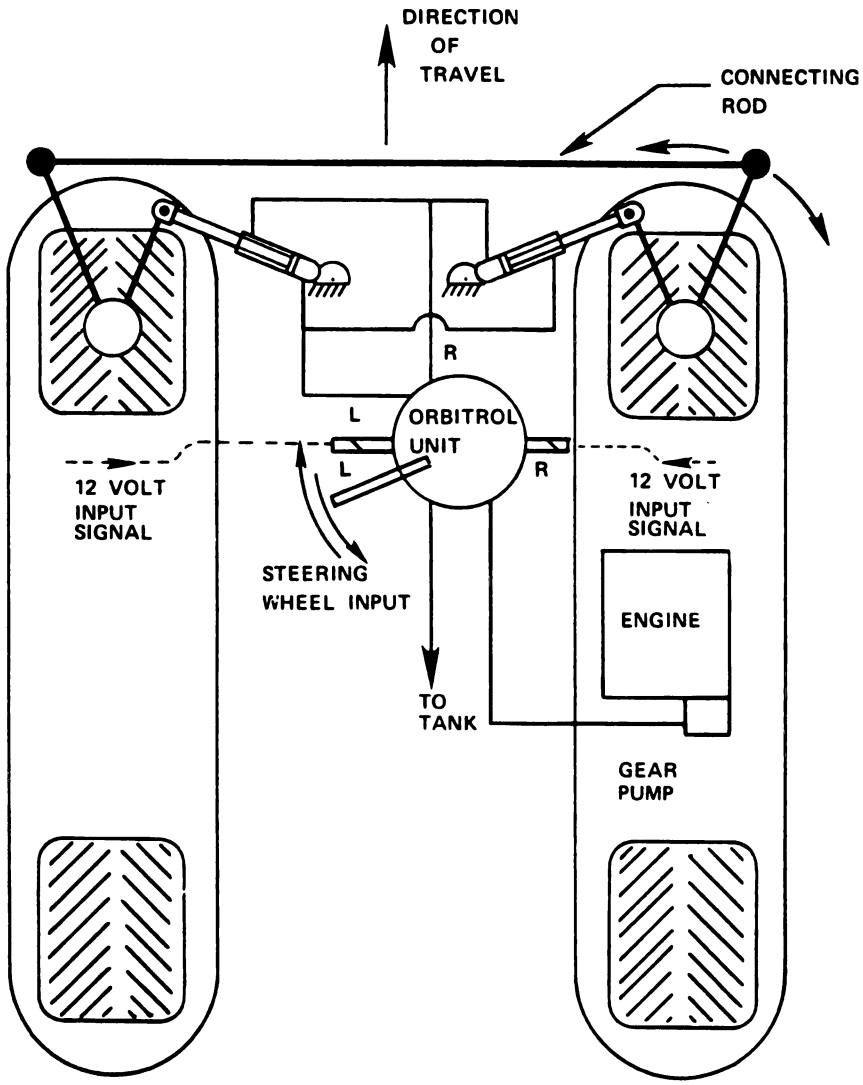

Figure 3.3 Schematic Diagram of the Apple Harvester's Hydraulic Circuitry for Front Wheel Steering.

4.0 CONCEPTS TO DETERMINE TREE POSITION FOR AN AUTOMATIC STEERING CONTROL SYSTEM

One of the essentials for an automatic control system is a sensing system which can produce a signal that represents information about the performance of the system. For the apple harvester, the steering control system needs a sensing system that can sense the position of the tree. The sensing system must sense the position of a tree which is ahead of the apple harvester. Next, the steering controller uses the information from the sensing system to determine if the harvester is correctly aligned with the tree. If the harvester is not aligned within the allowable tolerance, the steering controller must activate the steering system and steer the harvester to correct for this out-of-tolerance condition. The steering correction is then accomplished before the harvester gets to the tree. In the following sections several concepts have been developed for tree sensing systems. These concepts have been divided into six methods to sense the tree using non-contact sensors.

Two general types of sensors were considered for the sensing concept. The first sensing system is a sonar (airborne) system. A sonar system can either measure the range to a tree or it can detect if a tree is present in the sensing zone of the sonar. The second type of sensor that was considered was an optical sensor. An optical sensor can be used to detect the presence of a tree in the sensor's sensing zone. In order for this optical system to operate, a reflector is placed on the

tree trunk so that the sensor can detect the tree trunk. The optical sensor transmits a modulated infrared light beam toward the tree trunk. When the light beam shines on the tree trunk, the light beam is reflected back to the optical sensor where it is received by a receiver circuit. Note, that a retroreflective target should be used because the light will be reflected back toward the optical sensor instead of being reflected at a different angle which would normally occur with a mirror type reflective surface. An example of a retroreflective type reflector is the typical reflector that is used on bicycles. When the light is reflected back to a receiver circuit on the optical sensor, the receiver circuit produces an output logic signal that is at the TRUE state and the output is FALSE when the receiver does not receive the modulated infrared light beam. The optical sensor is not affected by sunlight which consists partially of infrared light, because the receiver is designed to detect only modulated infrared light. The transmitted light beam is modulated by energizing and deenergizing a light emitting diode (LED).

The optical sensor and sonar sensor were selected for the tree sensing concepts because those systems appear to be reliable and are commercially available at a low cost. Also, these types of sensors produce an electrical signal that can be used to interface the sensor with the controller of the harvester's steering control system. The fact that these sensors were commercially available was considered important because time would not be required to actually develop the sensor, and the low cost of these sensors would help keep the cost of the control system within the costs constraints as specified in Section 3.4.

Six concepts have been developed to sense the tree position for the harvester's steering control system. In these concepts it was assumed that the tree's position was in front of the harvester during operation of the sensing system in order to achieve stable and effective steering control. With sensing the tree that is ahead of the front wheels, the steering controller has time to make any necessary steering corrections before the harvester drives over the tree. This assumption that stable control can be achieved by sensing the tree in front of the front wheels is also supported by results from Grovum et al. (1970) and Shukla et al. (1970). These researchers concluded that sensing the positional error of the vehicle at a point ahead of the front wheels did result in achieving a stable automatic steering control system.

Some of these six concepts for tree sensing utilize a sensor that measures the tree position. Then, the steering controller can use this tree position information to compute the magnitude of the lateral offset of the tree from the harvester's centerline. This lateral offset of the tree is considered the tree position error and is used by the steering controller to make the steering corrections that are required to maintain the harvester's alignment on each tree as specified by the alignment design requirement (see Section 3.1).

Some of the other concepts that were developed for tree sensing, only detect if the tree is present in the sensor's sensing zone. With this type of sensing technique, a sensing zone is established on the left and right sides of the harvester and these zones extend forward from the front of the harvester. If a tree is detected in either one of these sensing zones, it means that the tree is too far offset from the harvester's centerline and a steering correction is necessary. When the

sensor detects a tree in a sensing zone, it sends a signal to the control circuit. The control circuit then activates the steering system to make a steering correction. This type of control system can be described as an ON-OFF type control system.

4.1 Method 1 - Two Sonars Used to Determine Tree Position by Triangulation

Method 1 is a steering system that uses two sonar units to determine the position of the tree which is in front of the harvester. Figure 4.1 is a diagram that shows the apple harvester with two sonar units that sweep from side to side to measure the distance to the tree. Each sonar unit scans the area ahead of the harvester and sends to the controller a distance measurement when a tree is in the sensing zone. These two distance measurements are used by the controller to compute the tree position or lateral offset of the tree from the harvester centerline. This computation is based on the technique of triangulation which allows computation of the tree's position by analyzing the dimensions of triangles. A triangle that specifies the tree position can be defined by using the two distances measured by the sonar units and the base dimension between the sonar units. Thus, a triangle is completely defined without an angle measurement. After the controller has computed the tree lateral offset, then the controller must make any needed steering corrections so that the harvester will be centered over the tree as the harvester drives over the tree.

One of the significant factors that affects the feasibility of Method 1 is the accuracy of computing the lateral offset of the tree from the harvester's centerline. This lateral offset is important because it represents the tree-position-error signal that will be used

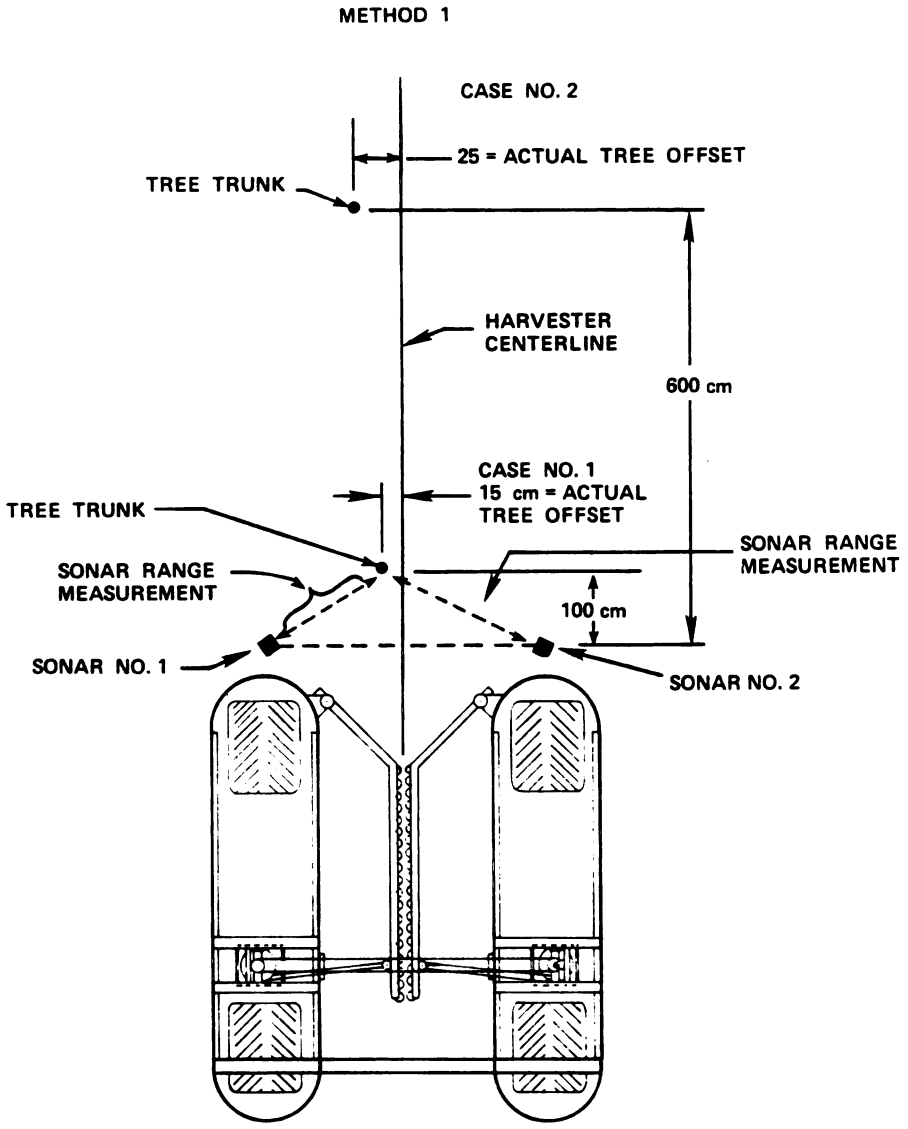

Figure 4.1 Method 1 - Tree Sensing Using Two Sonar Units to Determine Tree Position

by the steering controller. To check the accuracy of computing the tree lateral offset, the tree offset was computed using the maximum amount of tolerance for the sonar measured distance. The assumed accuracy tolerance for the sonar was ± 3 cm over the range of 30 to 600 cm. The computation of tree lateral offset was done for two cases of tree position. For the first case the tree was 100 cm in front of the harvester and the tree was actually offset 15 cm from the harvester centerline. For the second case the tree was 600 cm in front of the harvester and the offset was 25 cm. Figure 4.1 is a diagram that shows these tree positions. A computation of the tree offset was done to determine how much error would result using the worst allowed tolerance for the sonar measurement. The error is the difference between the actual tree offset from the harvester centerline and the computed tree offset. For the first case, the computed tree offset was 18 cm and for the second case the computed tree offset was 35 cm. These results show that the error in the computed offset is 3 cm when the tree was 100 cm ahead of the harvester and 10 cm when the tree was 600 cm ahead of the harvester. When using this technique to compute the tree position the error decreases as the tree range decreases. These values of error are not excessive and therefore, based on these preliminary results Method 1 is a feasible method to sense tree position.

4.2 Method 2 - One Sonar and One Angle Measurement Used to Determine Tree Position by Triangulation

Method 2 is a tree sensing concept similar to Method 1. With Method 2, a triangle which defines the tree position is determined by measuring the angle and distance to the tree relative to a point on the harvester. This angle and measurement represents the polar coordinates

of the tree. Then, after the tree position coordinates are measured, the lateral offset of the tree from the harvester centerline can be computed using triangulation. Figure 4.2 is a diagram that shows the tree position and shows the distance and angle that represents the tree position coordinates.

A sonar unit is used to measure the distance to the tree. In this concept, the sonar could be attached to a mechanical system so that the sonar can sweep from side to side to scan the area ahead of the harvester. A shaft encoder could be connected to this mechanical system and the encoder could be used to measure the angular position of the sonar. This angular position represents the direction that the sonar sound pulse will travel when it is transmitted. During the operation of the sonar system, the sonar unit would sweep from left to right. When the sonar has turned to a position such that an ultrasonic sound pulse reflects back from the tree, then at that moment, the angular position of the sonar is measured and the distance to the tree is measured. This angular position of the sonar unit also represents the angular position coordinate of the tree.

These measurements of tree position are used to compute tree lateral offset. The computations of tree offset were done using the worst tolerance for angular position and sonar measurement. The sonar is assumed to be accurate to ± 3 cm over the range of 30 to 600 cm and the tree angular position is assumed to be accurate to within ± 2 degrees. The tree offset was computed for case one where the tree was 100 cm ahead of the harvester and tree offset was 15 cm. Computations were also done for case two where the tree was 600 cm ahead of the harvester and tree offset was 25 cm. Figure 4.2 is a diagram that shows

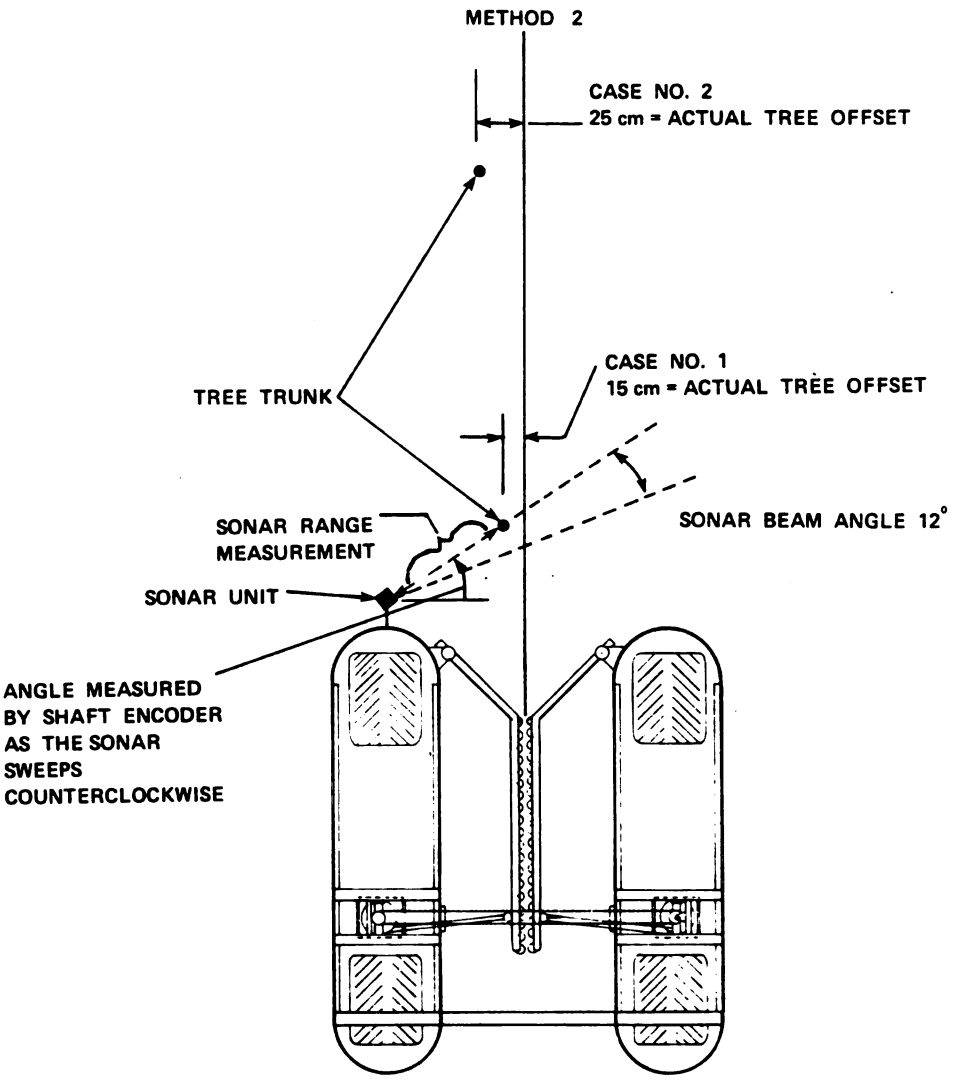

Figure 4.2 Method 2 - Tree Sensing Using One Sonar and One Angle Measurement to Detemine Tree Position

the location of these trees relative to the harvester. The computed offset was 21 cm for case one and 36 cm for case two. On comparing the actual tree offset with the computed tree offset, the computed tree offset can have an error of 6 cm and 11 cm for case one and two respectively. These errors in computed tree offset are not excessive; thus it appears that Method 2 is feasible. But, there is a high degree of uncertainty in the assumption that the tree angular position is accurate to within ± 2 degrees, and therefore more research is required to verify this assumption in order to complete the evaluation of the feasibility of Method 2.

4.3 Method 3 - Two Sonars Used to Detect the Tree Presence in Zones

Method 3 is a tree sensing concept that uses two sonar units to detect if a tree is present in one of two sensing zones. Figure 4.3 shows a diagram of these two sensing zones which are in front of the harvester. One of these sensing zones is on the left side of the harvester and the other is on the right side. If a tree is detected in one of these zones, then a steering correction is necessary because the tree is located at a position which is laterally offset an execessive amount from the harvester's centerline. If the tree is located between these two sensing zones then the harvester is properly aligned with the tree and a steering correction is not required. The sonar transducers that were developed by Polaroid have a beam angle which is approximately 12 degrees and this beam angle also represents the angle of the sensing zone which is shown in Figure 4.3. This sensing system cannot detect a tree which is too far to the left or to the right of the harvester

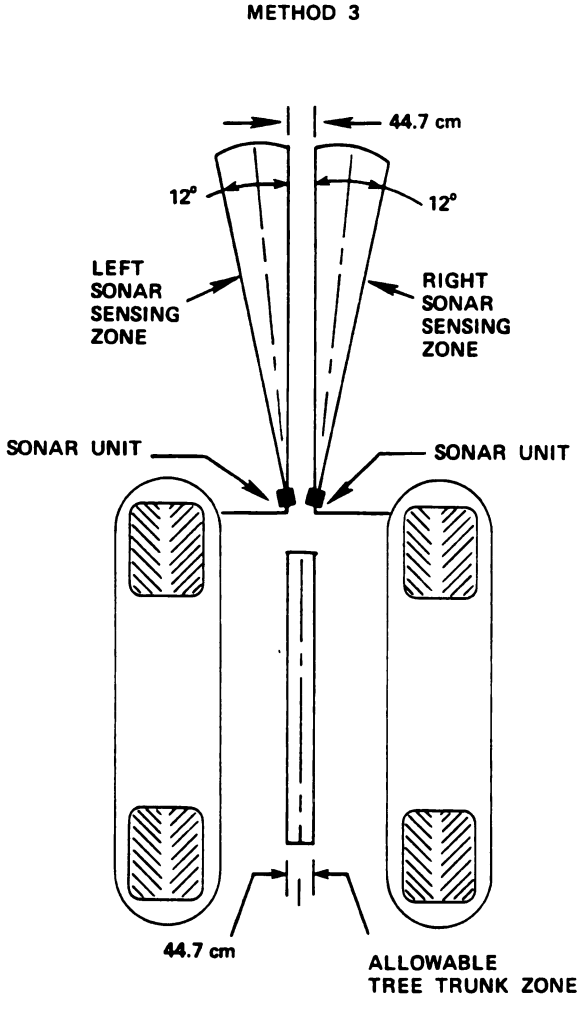

Figure 4.3 Method 3 - Tree Sensing Using Two Sonar Units to Detect the Tree Presence in Zones

centerline because the tree would not be in any of the sensing zones and if the tree is not detected in a sensing zone then a steering correction will not occur.

This method of tree sensing is infeasible for the following reasons. First, the sonar units must be located close to the harvester centerline where there is the potential that a tree will collide with one of the sonar units and damage the sonar system. A movable frame could be designed so that the sonar sensor would move out of the way of each tree but, a mechanism of this type could be complicated and expensive. Second, when the tree row is curved, there is the potential for the sonar unit to detect another tree in the curved row instead of the tree which is directly in front of the harvester. This could occur because the sonar sensing zone is 10.6 m long and thus if a wrong tree is detected then the steering controller would execute an erroneous steering correction.

4.4 Method 4 - Two Optical Sensors and Two Angle Measurements Used to Determine Tree Position by Triangulation

This tree sensing concept uses two optical sensors and two angle measurements to determine the tree position. The optical sensors are used to locate the tree and a shaft encoder is used to measure the bearing of azimuth of the sonar beam. This azimuth can also represent the angular position coordinate of the tree. During the operation of this sensing system the optical sensor sweeps from side to side to locate the tree which is ahead of the harvester. As the optical sensor is sweeping it sends out a modulated light beam. The tree has a retro-reflective target mounted on the tree trunk and when the optical sensor

is pointing toward the tree, the modulated light reflects back from the tree. At the moment when the optical sensor receives the reflected light beam an output signal goes to the TRUE state. The optical sensor can be mechanically connected to a shaft encoder and when the output signal from the optical sensor goes to TRUE, the angular position of the sonar unit is measured by the shaft encoder. This angular position represents the angular position coordinate of the tree. Figure 4.4 is a diagram that shows the harvester, the two optical sensors, and the two angle measurements that are needed to define the position of the tree. These two angle measurements define a triangle, and thus triangulation can be used to compute the tree lateral offset from the harvester centerline. An optical sensor was purchased and preliminary tests indicated the beam angle of this sensor was 4.0 degrees when a rectangular target was used.[3] This target has the dimensions of 1.8 cm (0.7 in) by 15.2 cm (60 in). This sensor operated effectively when the target was in the range of 0.0 m to 9.1 m.

The tree position can be computed using the distance between the two sonar units and the two angle measurements. To check the accuracy of this tree sensing method, the tree lateral offset was computed for a tree that is offset 50 cm from the harvester centerline and the tree is ahead of the harvester within a range of 100 to 450 cm. The computed lateral tree offset were in the range of 57 to 59 cm and thus the error between the actual tree lateral offset and computed offset is in the

---

[3]Photoelectric transducer was purchased from Banner Engineering Corp., 9714 10th Ave. No., Minneapolis, MN 55441; Model MULTIBEAM with internal components; scanner block SBLX; logic block LM 3; power block PBT and reflector No.2 BRT-L.

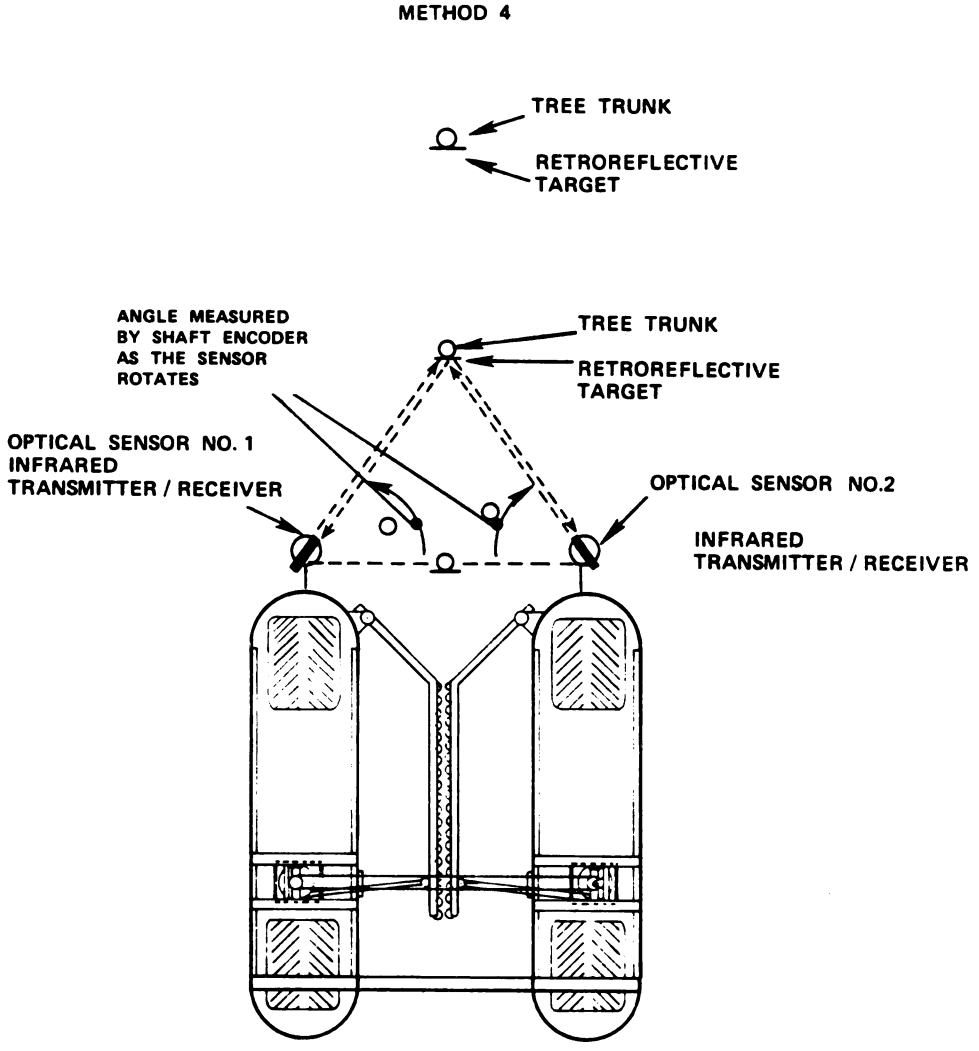

Figure 4.4. Method 4 - Tree Sensing Using Two Optical Sensors and Two Angle Measurements Used to Determine Tree Position

range of 7 to 9 cm. This error is acceptable, although there is a high degree of uncertainty in the assumption that the tree angular position can be measured within ± 1 degree. For this sensory system to operate, a reflector must be attached to each tree, thus there would be a large cost to purchase and attach these reflectors to the trees, and there would be an additional cost to replace those reflectors which are damaged by vandalism or inadvertent collisions with orchard machinery. Therefore a more detailed economic analysis must be done in order to complete the evaluation of the feasibility of this sensing method.

4.5 Method 5 -- Two Optical Sensors used to Detect Tree Presence in Zones

This sensing technique used two optical sensors to determine if a tree is present in one of the two sensing zones. Figure 4.5 is a diagram which illustrates the harvester with two optical sensors that are used to detect trees in one of two zones. These zones are on the left and right sides of the harvester's centerline. The zones extend into the area ahead of the harvester and are located close to the harvester centerline so that this sensing system can detect if a tree is offset an excessive distance from the harvester's centerline. For this tree sensing concept, if one of the optical sensors detects a tree in the sensing zone, then a steering correction is required so that the harvester will be aligned with the tree as it drives over the tree. Note, that this sensing system cannot detect a tree which is too far to the left or right of the harvester centerline because the tree would not be in any of the sensing zones and if the tree is not detected in a sensing zone then a steering correction will not occur.

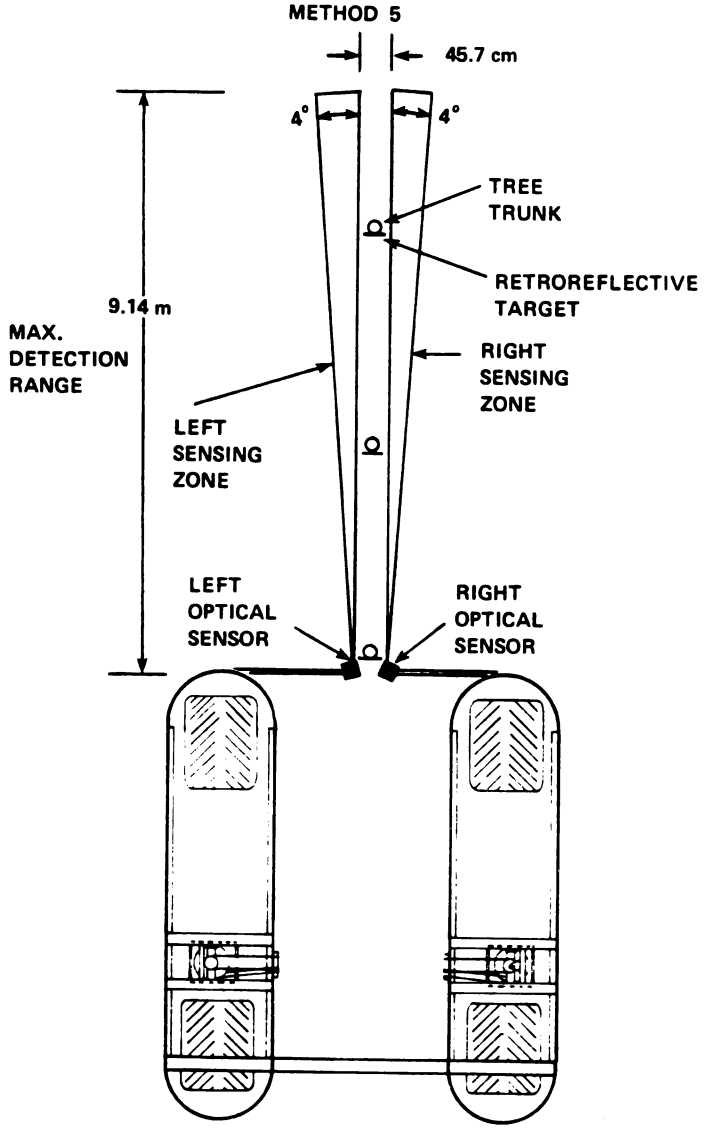

Figure 4.5. Method 5 - Tree Sensing Using Two Optical Sensors to Detect Tree Presence in Zones

This method of tree sensing is infeasible for the following reasons. First, these optical sensors are located 22 cm from the harvester's centerline which is a location where a tree may collide with the sensor and damage the sensor. Second, there is a potential that if the tree row is curved, then the optical sensor may detect another tree instead of the tree which is directly in front of the harvester. This could occur because the optical sensor which was described in the previous section has a sensing zone with a range of 9.1 m and if the tree row curves into one of the sensing zones, then a wrong tree may be detected. This would cause the steering controller to execute an erroneous steering correction.

4.6 Method 6 - Multiple Sonars Used to Measure Tree Position

Method 6 uses several sonar units to measure the position of the tree. Illustrated in Figures 4.6 and 4.7 is a tree sensing system which uses several sonar units that are mounted in an array in front of the left front wheel and these sonar units are pointed toward the harvester's centerline. These sonar units are positiooned such that the centerlines through the sensing zones of each sonar unit are perpendicular to the harvester centerline. As the harvester drives over the tree row, each sonar will move past each tree in the row. When the harvester moves forward to a position such that at a tree trunk is in one of the sonar unit sensing zones, then that sonar unit measures the distance to the tree trunk. This measurement of tree position can be used by a steering controller to compute the tree lateral offset from the harvester centerline. Then, the steering controller can execute a steering correction as needed if the tree offset is too large. The

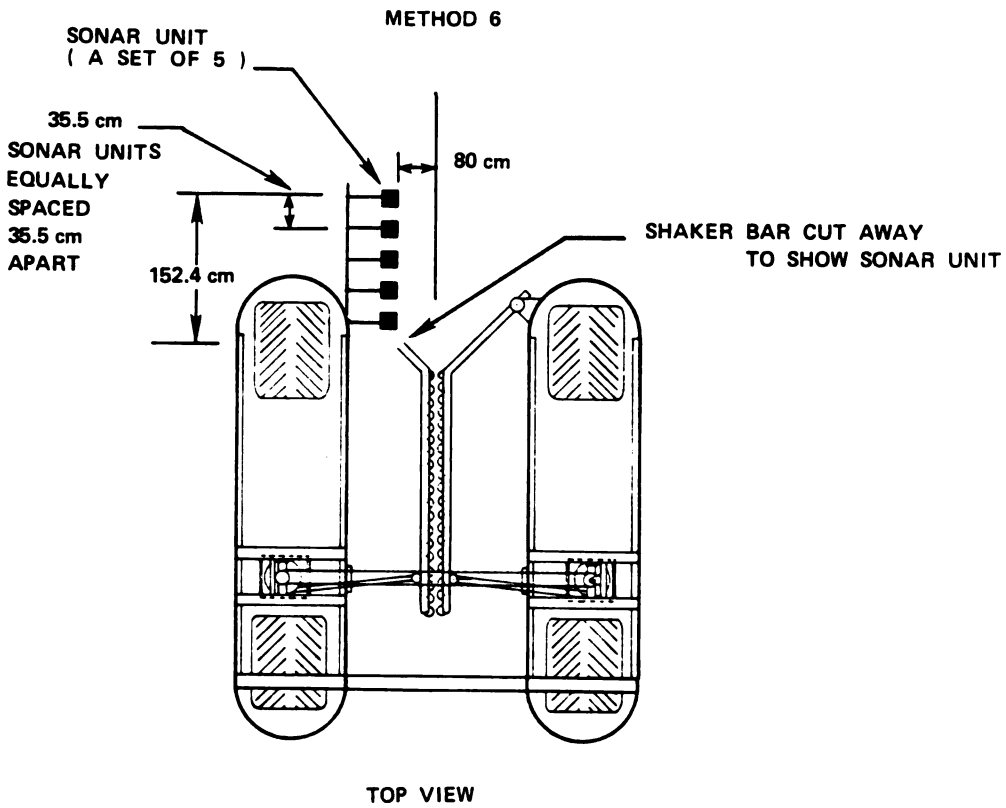

Figure 4.6. Method 6 - Tree Sensing Using Multiple Sonar Units to Determine Tree Position (Top View)

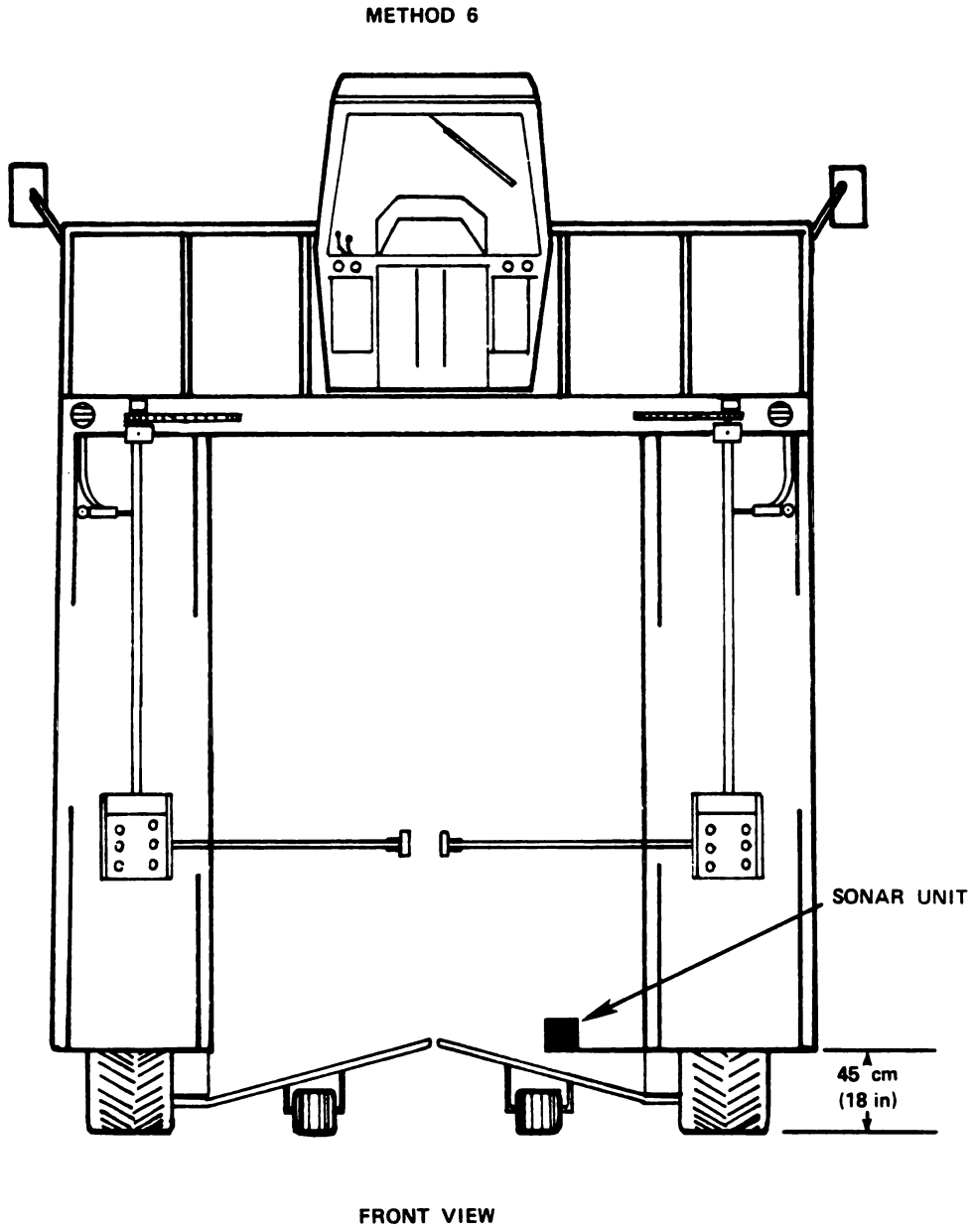

Figure 4.7. Method 6 - Tree Sensing Using Multiple Sonar Units to Determine Tree Position (Front View)

distance of tree offset from the harvester centerline can be computed by knowing the sonar's position from the harvester centerline and the sonar measurement of range from the sonar unit to the tree. To compute the tree offset, subtract the sonar measurement of tree range from the sonar's position (distance from harvester centerline). The accuracy of this computation can also be estimated. If the sonar measurement is accurate to within $\pm$3 cm and if the sonar's position is accurate to within $\pm$1 cm then the tree lateral offset could be computed with an accuracy of $\pm$4 cm. This amount of inaccuracy is not excessive and is not expected to cause any problem with development of an automatic steering control system for the USDA apple harvester.

As shown in Figure 4.6 this concept of tree sensing uses five sonar units. These sonar units are arranged so that the array of sonar units is 142.2 cm long and when operating at a ground speed of 0.8 km/h (0.5 mph) the tree will move past all five sonar units in 6.4 seconds. Thus, by using five sonar units there will be 6.4 seconds of time available to make any needed steering corrections to keep the harvester aligned with the tree. And, based on data reported by Upchurch et al. (1980), it is estimated that the harvester steering system and controller would have a short enough response time that any needed steering corrections can be made within the 6.4 second time span, using five discrete tree position measurements from the sonar sensing system. Thus, based on this preliminary evaluation, Method 6 is a feasible tree sensing system for the USDA apple harvester. To make a more complete study of the feasibility of this tree sensing method, a dynamic analysis of the complete steering control system is needed to verify that the

system response time is short enough to make any needed corrections within the available time of 6.4 seconds.

4.7 Final Selection of Tree Sensing Concept

After reviewing the description of each of the six tree sensing concepts, Method 6, the system which uses the array of five sonar units, was selected for development. This method was selected because based on a preliminary evaluation it is a feasible system. Also this sensing system does not have any moving parts which could fail due to excessive wear or due to the moving parts being fouled by debris. Another factor considered is that the sonar's position is 80 cm from the harvester centerline and this reduces the probability of the sonars being damaged by colliding into a tree. The electronic circuitry for the sonar sensing system is expected to have high reliability and adequate accuracy. When considering the computer software required to compute the tree position, the automatic steering controller needs to use the sonar's measurement of tree range and perform simple arithmetic operations. Thus, complex arithmetic algorithms or large table-look-up algorithms should not be required to compute tree position.

5.0 APPLE HARVESTER STEERING CONTROL SYSTEM

The automatic steering control system for the USDA apple harvester has been developed with the tree sensing system that was described as Method 6 (Section 4.6). This tree sensing system uses an array of five sonar units mounted on the front of the harvester. Figure 5.1 is a diagram which shows the major components of the steering control system. This control system is designed to operate according to the following description. The steering control process begins with one of five sonar units detecting a tree. The sonar unit then sends a timing signal to the interface circuitry. The interface circuit is designed to convert the timing signal from the sonar unit into an eight bit binary number that repesents the measured distance to the tree. This binary number is an input number for the controller. The controller uses the binary number to determine if the tree trunk which is ahead of the harvester is aligned on the harvester centerline within an allowed tolerance. Another component of the steering control sytem is an absolute shaft encoder, (Model 76-GC10-4-E-1, Litton Inc.) which uses a ten bit gray code output. This shaft encoder is used to measure the angular position or steering angle of the front wheels of the harvester. Only six bits of the ten bit binary code from the shaft encoder are used. The two least significant bits and the two most significant bits from the shaft encoder are not used. When using the six bits from the encoder, each output code represents 1.4 degrees of rotation of the encoder's shaft.

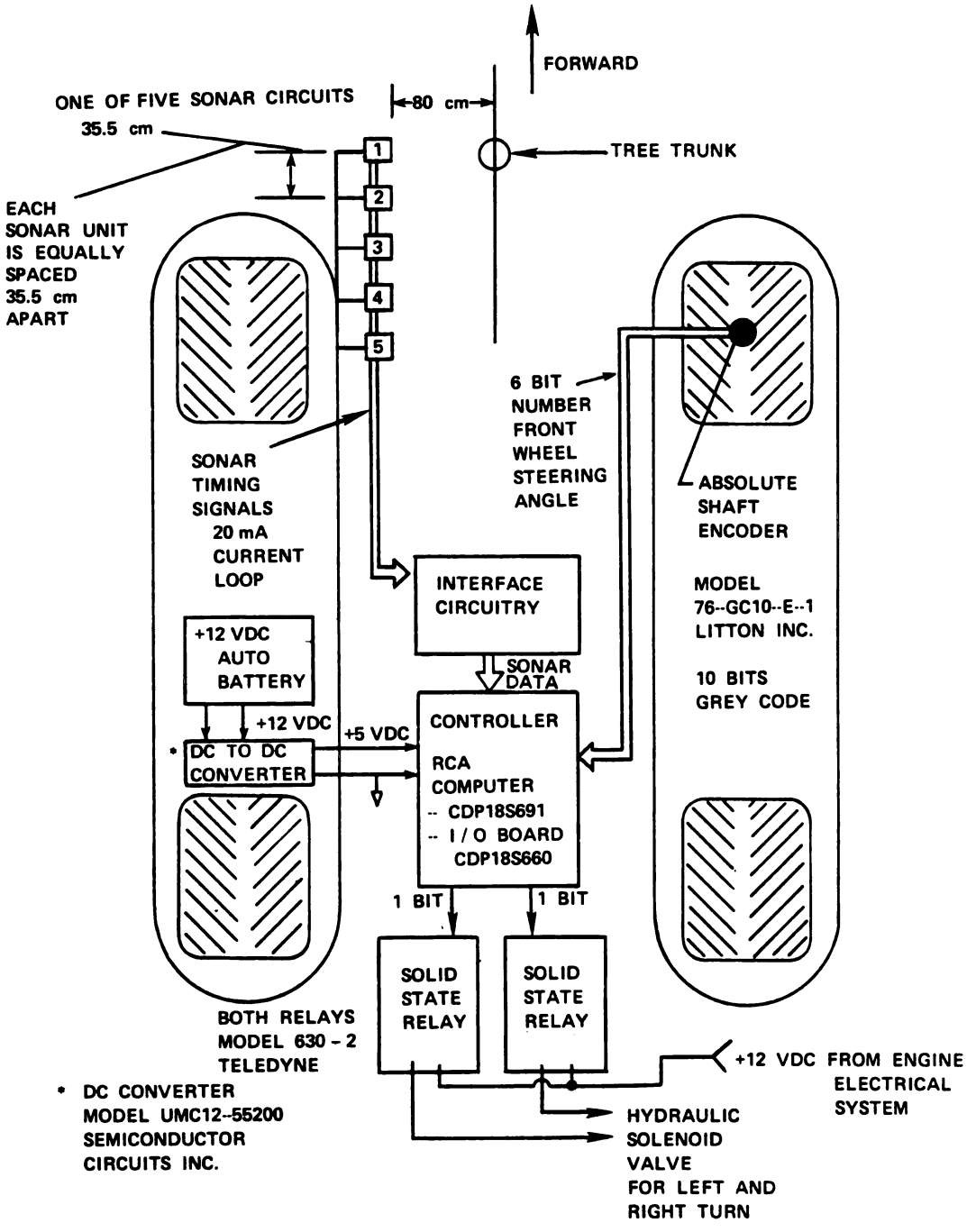

Figure 5.1. Diagram of Major Components of the Automatic Steering Control System.

In order for the shaft encoder to measure the front wheel steering angle, the encoder is attached to a vertical shaft which turns as the wheels are turned (or steered) to a new steering angle. Turning of a wheel refers to wheel rotation about the wheel's vertical centerline for the purpose of steering the apple harvester. The encoder is mechanically connected to a shaft on the harvester steering system such that for each degree of rotation of the harvester's front wheels, the encoder shaft rotates one degree. The shaft encoder is calibrated so that when the harvester's front wheels are pointing straight ahead, the shaft encoder output is a gray code binary number of magnitude equal to 32, and this represents a steering angle of zero degrees. Then, when the front wheels steer left the encoder output number increases and when the front wheels steer right the encoder output number decreases.

The next major component of steering control system is the controller. The controller is a microprocessor based computer (model CDP18S691 with I/O board no. CDP18S660, made by RCA). This is a CMOS type computer which uses less than 1 amp at +5 VDC and has high noise immunity. The computer is in a compact card case with dimensions of 13 cm by 4 cm by 10 cm. This computer also has a special switch that allows the computer to operate in a single-step mode and one of the computer cards contains six hexidecimial display digits for the computer address bus and data bus which are very helpful for debugging software and hardware.

During operation of the steering control system, the controller executes any needed steering correction. When a steering correction is needed the controller sends a CMOS level signal to one of two solid state relays (Model 630-2 made by Teledyne). One relay is used to steer

right and the other relay is used to steer left. When a solid state relay is ON, a +12 VDC signal is sent to one of two hydraulic solenoid valves which controls the position of two linear actuators. The motion of the linear actuators steer the harvester's front wheels. The hydraulic circuit diagram is shown in Figure 3.3.

A proportional control algorithm was selected for the automatic steering control system. Basically, this proportional control algorithm computes a tree position error and then directs the wheels to turn to a steering angle or wheel position that is proportional to the tree position error. The following is a more detailed description of how this control algorithm operates. First, a sonar unit measures the range to a tree trunk. The controller receives a binary number from the interface circuitry that represents the range or distance from the sonar unit to the tree. The controller then computes the distance from the tree to the harvester centerline. Figure 5.2 shows a diagram of a sonar unit and a tree trunk. This diagram shows that the sonar unit is positioned 80 cm from the harvester centerline. Also shown is a tree trunk with a diameter of 4 cm and if the tree trunk is centered on the harvester centerline then the left edge of the tree trunk is 78 cm from the sonar unit. This tree is labeled TREE A in Figure 5.2 and also shown in this Figure is TREE B which is not on the harvester centerline. Therefore, the position error or tree offset for TREE B (in Figure 5.2) can be computed by:

$$E = 78 - S \tag{5.1}$$

where E = tree position error (cm)

S = sonar mesurement (cm)

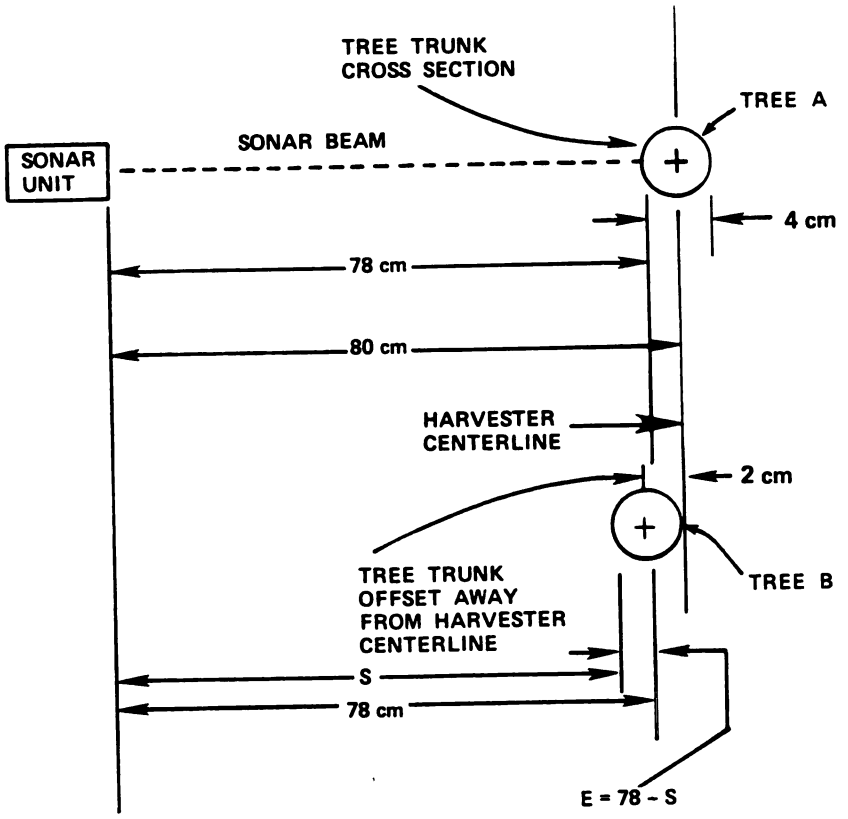

E = TREE POSITION ERROR (cm)

S = SONAR MEASUREMENT (cm)

Figure 5.2. Diagram of Tree Position Error.

Note that tree trunk diameters will vary between 4 cm and 14 cm and therefore an average value of 75 may be used in equation 5.1 to compute error for a production version control algorithm that could be used in orchards containing trees which have the full range of tree trunk diameters.

After the tree position error is computed, the control algorithm checks to see if the error is within an allowed range of tree position error. For example the allowable tree position error may be ± 2 cm although the best value must be determined by either a dynamic simulation of the control system or by experimental tests. If the tree position error exceeds the allowable tree position error, then the front wheels must be turned so that the error is reduced to a value that is within the allowed range of error. When the controller has determined that a steering correction is needed, the controller executes a turn so that the wheels turn to a position which is proportional to the tree position error. The wheels are turned in the direction which causes the harvester to move in the direction needed to reduce the tree position error. The controller continuously is checking the tree position error and as the tree position error decreases, the controller directs the wheels to turn to a position of smaller steering angle. Note that when the steering angle is zero, the wheels are pointed straight ahead and the shaft encoder code for the front wheel position is equal to 32.

Thus, a wheel position code for the new steering angle for the front wheels is computed by the controller using the equation:

$$D = K\ (78 - S) + 32 \qquad (5.2)$$

where D = Desired wheel position code

K = Proportional gain factor

S = Sonar measurement (cm)

The desired wheel position code, D, is a value that is scaled so that the controller can periodically compare the value of D directly with the value of the shaft encoder code to determine if the wheels are turned to the correct wheel position. The value for the gain factor, K, must be determined by analysis or tests.

The tree sensing system has five sonar units and the one controller will determine one valid tree position measurement for each sonar unit. Each time a valid sonar measurement is made, a new value for D is computed. As soon as D is computed the controller will direct the wheels to turn in the approprite direction until the wheel shaft encoder code equals the value of D. The wheels remain at this steering angle until the next value of D is computed. When the value for D is computed using the tree position measurement from sonar number five, a time delay routine is used because sonar number five is the last sonar in the array. And, the harvester must then travel about 152 cm before the next value for D can be computed using the tree position measurement from sonar unit number one. For this time delay routine, one second is allowed for the front wheels to turn to the wheel position equal to the value of D and the wheels are held at that position for the duration of

the time delay. Next, the wheels are turned back to the straight ahead position. The wheels stay in the straight ahead position until the next value of D is computed. The one second magnitude for the time delay was selected as an approximate value, because this value is close to the 1.5 second time duration required for a tree to move from one sonar unit to the next sonar in the sonar array as the harvester travels at 0.8 km/h (0.5 mph).

One objective of this research was to design the steering control system for a cost less than $2,000. The major components of the control system and their costs were: RCA computer ($850); I/O board ($375); wheel position shaft encoder ($350); two solid state relays for steering the front wheels ($60); five solid state relays for activating the sonar units ($70); interface circuit board ($100); five sonar units ($300); and DC to DC converter ($100). Note that each sonar unit includes a Polaroid transducer and Polaroid circuit board which have a cost of $17 and $25 respectively. The cost to manufacture one complete sonar unit is about $60. The interface circuit has discrete electronic components and integrated circuits which cost about $40 and the estimated total cost to manufacture one complete interface circuit is $100. Therefore the total cost of these components of the steering control system is $2,205. This is $205 over the cost objective of $2,000. Note, that the steering control system as described in Chapter 8 includes a video display monitor and keyboard and these components were not included in the cost of the control system because they were used only for the development of the control system. The cost of the video display monitor and keyboard were $200 and $360 respectively. Chapter 8 also explains why the five solid relays were used to activate the sonar units.

There are two ways to reduce the cost of the control system. First, the I/O board could be eliminated and a special circuit board could be designed to do all of the I/O functions. The cost to build such an I/O circuit would be about $75. Second, the computer could be replaced by one single board computer (DP18S601 by RCA) which has a cost of $325. Thus, if these two changes were made, the total cost of the control system would be $1,430. Therefore, this data indicates that the control system can be designed using electronic components which have a total cost less than $2,000.

5.1 Dynamic Considerations of the Automatic Steering Control System

The automatic steering control system for the apple harvester has three major components that affect the dynamic behavior of the control system and these are the kinematic motions of the apple harvester, the microprocessor based controller and the wheel steering motor (hydraulic linear actuator). This type of control system may be called a regulator because the reference signal is set at a constant value of 78. The reference signal of 78 was used because when the harvester's centerline is perfectly aligned with a straight tree row then the distance measured by the sonar unit is 78 cm. Thus, this control system controls the position of the harvester until the sonar measured value is 78 cm. Figure 5.3 shows a block diagram of the apple harvester's automatic steering control system. The controller used a proportional control element (Figure 5.3) where the harvester's wheels were turned to an angle which was proportional to the harvester's lateral position from a tree trunk. Note that the sonar sensing system was positioned ahead of the harvester's front wheels so that the harvester would be aligned on the tree trunk before the tree trunk passes through the inside space of

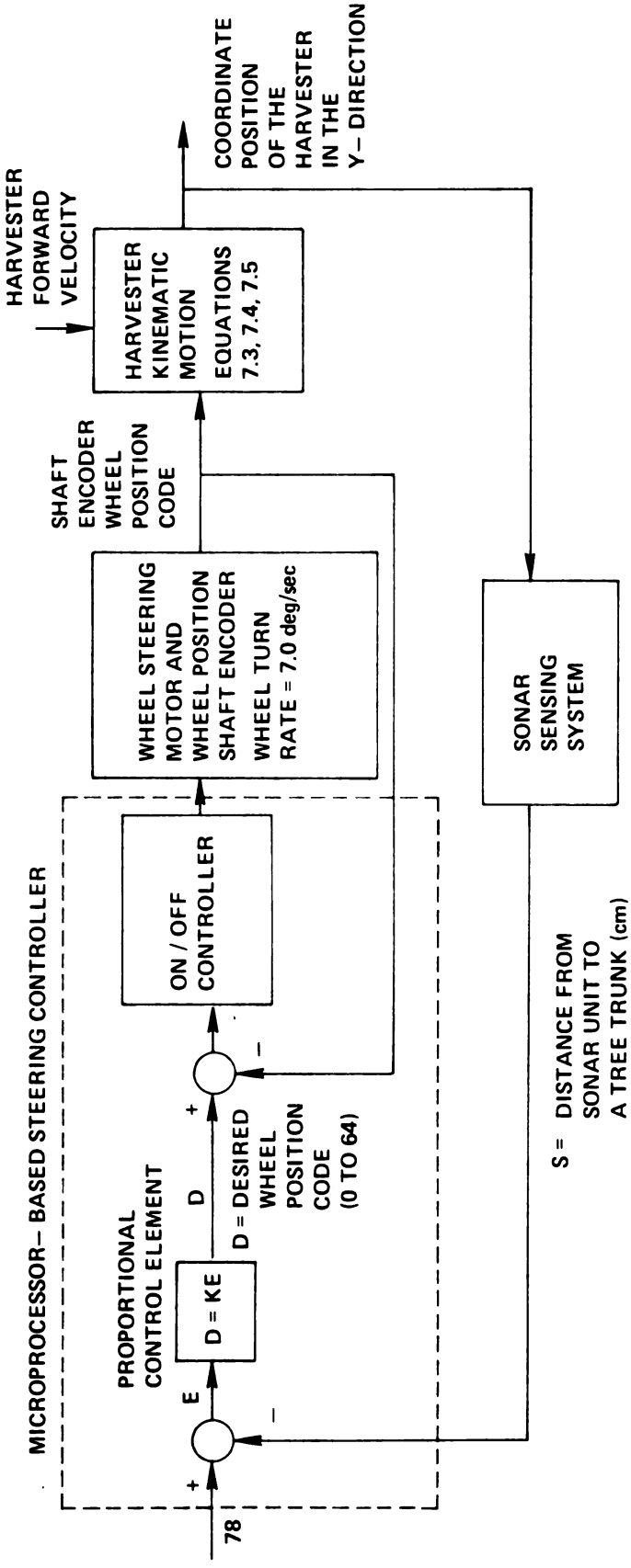

Figure 5.3 Block Diagram of the Apple Harvester Automatic Steering Control System

the harvester. The block diagram shows that the control system is a closed loop control system with a feed back signal of the harvester's position. The harvester's position is measured by the sonar sensing system.

Analysis of the response of this control system is difficult due to the fact that the sonar sensing system only provides sonar measurements when the tree is moving past one of the five sonar units. The sampling method used to determine a sonar measurement was designed such that only one valid sonar measurement was made for each sonar unit. Thus, there were about 1.5 seconds required for the tree to move from one sonar unit to the next sonar unit and during this time a sonar measurement was not available to be processed by the microprocessor. To analyze the response of the control system for a given value of proportionl gain (k) which was used by the microprocessor, a simulation model was developed. This model was designed to simulate the steering control system that is shown in Figure 5.3.

6.0 SONAR SENSOR DEVELOPMENT

In developing the sonar sensing system for the apple harvester, the ultrasonic transducer and circuit that are produced by the Polaroid Corporation were selected to be the major sensing components. Circuit diagrams and technical information on the Polaroid ultrasonic circuit and transducer were obtained from the Polaroid Corporation.[4] Figures 6.1 and 6.2 are illustrations that show the dimensions of the Polaroid ultrasonic circuit and transducer. Figure 6.1 also shows a required modification to the Polaroid circuit board which is needed for proper operation of the signals TRANS and ECHO. The specified voltage for this system is +6 VDC although it has been determined that the circuit board will work well with a +5 VDC power supply[5]. The ultrasonic circuit board requires 2.5A of current only during the time when the ultrasonic sound pulse is being transmitted. The sound pulse duration is one millisecond.

The basic control signals for the Polaroid ultrasonic circuit board are shown in Figure 6.1. Figure 6.3 shows the timing diagrams for these signals. Two of the major timing signals are TRANSMISSION (TRANS) and DETECTED ECHO (ECHO). When the signal TRANS goes to logic HIGH, it

---

[4]Information was from Ultrasonic Ranging System Manual, Polaroid Corporation, Ultrasonic Range Marketing, Cambridge, MA 02139.

[5]Personal communications with technical representative of the

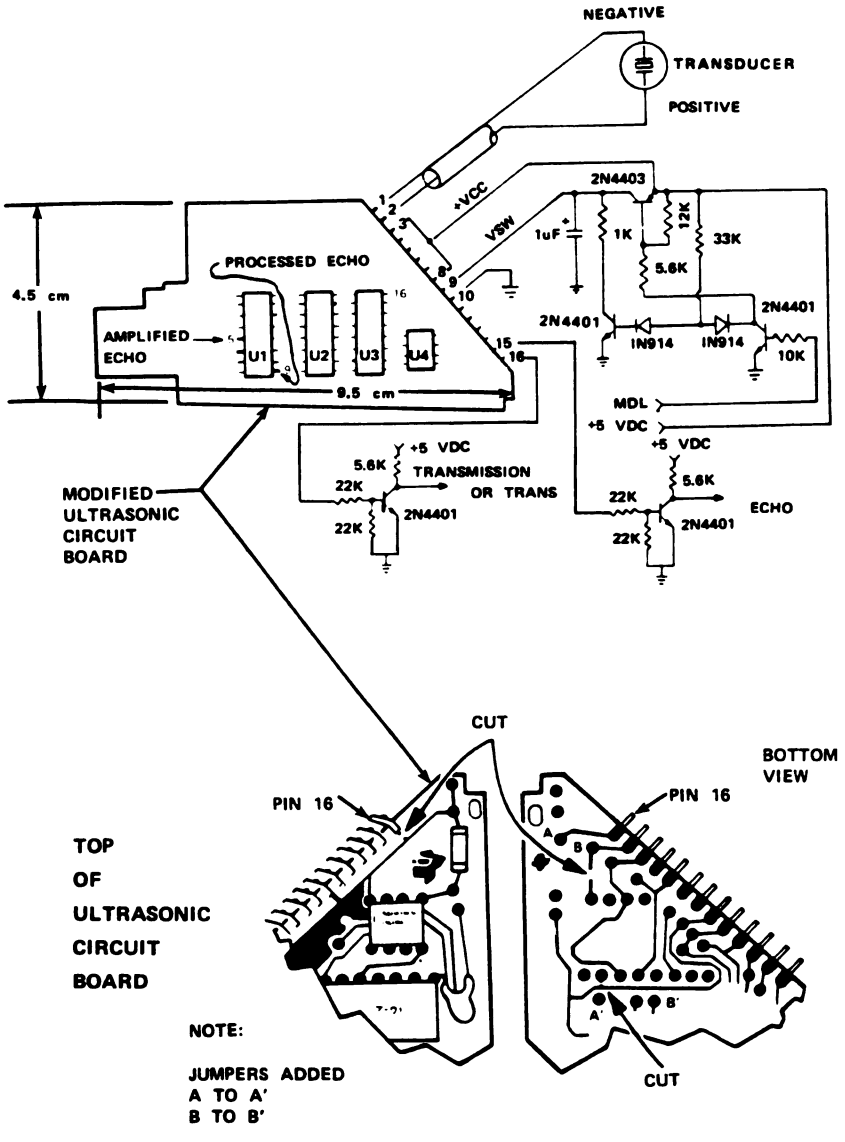

Figure 6.1. Polaroid Ultrasonic Circuit Board

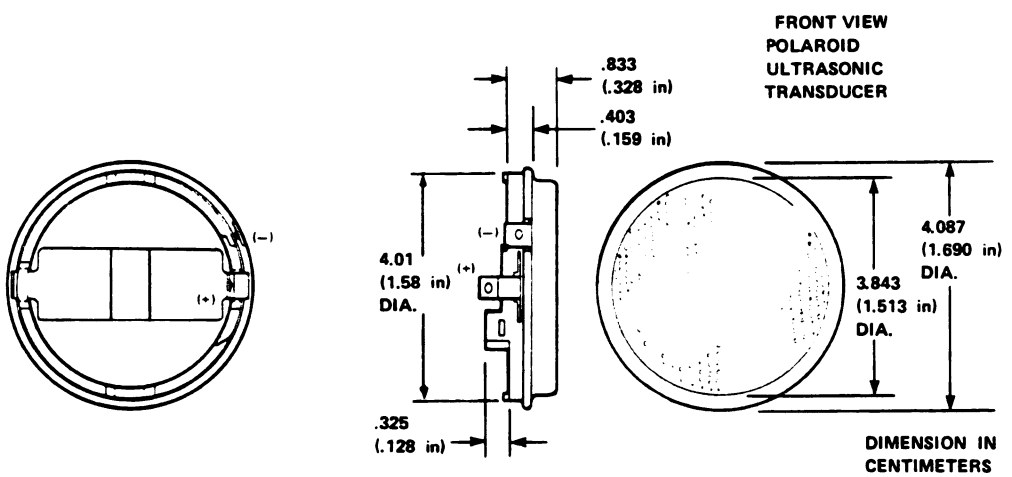

Figure 6.2. Polaroid Ultrasonic Transducer

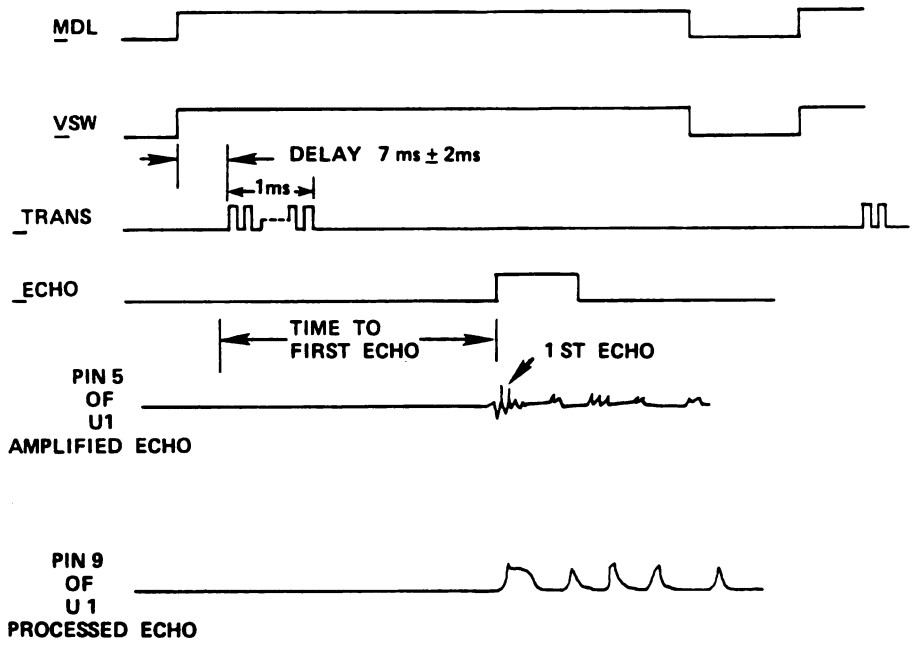

Figure 6.3. Timing Diagram of Ultrasonic Circuit Board.

indicates the start of transmission of the ultrasonic sound pulse, and when the ECHO signal goes to logic HIGH it indicates that the ultrasonic pulse echo has been received by the ultrasonic transducer.

Note also in Figures 6.1 and 6.3 that the ultrasonic circuit board uses a signal VSW to start a cycle. One cycle is represented by sending the sound pulse and receiving the sound pulse echo. For the VSW signal, the Polaroid specifications indicates that VSW be at logic LOW for 40 ms before the next cycle starts, although this 40 ms interval can be reduced if the distance to be measured is small. In order to obtain a valid distance measurement, the VSW signal must remain HIGH until ECHO goes to logic HIGH. The MDL signal (see Figure 6.1) is used to generate the VSW signal. Thus, the main signals that are used to interface with the ultrasonic circuit board are TRANS, ECHO, and MDL and these signals are compatible with CMOS logic levels when both the Polaroid ultrasonic circuit board and CMOS interfacing circuits use a +5 VDC power supply.

6.1 Sonar Sensing System

The sonar sensing system for the USDA apple harvester is shown in Figure 6.4. This figure shows an array of five sonar units which are positioned ahead of the harvester's front wheels. Each of the sonar units contains a sonar circuit. The sensing system consists of five sonar circuits and five interface circuits. A sonar circuit is designed to produce one timing signal that specifies the moment when the sonar sound pulse is transmitted and specifies the moment when the sound pulse is received by the ultrasonic transducer. A 20 mA current loop is used to send the timing signal from the sonar circuit to an interface circuit. The interface circuit is used to interface a sonar circuit

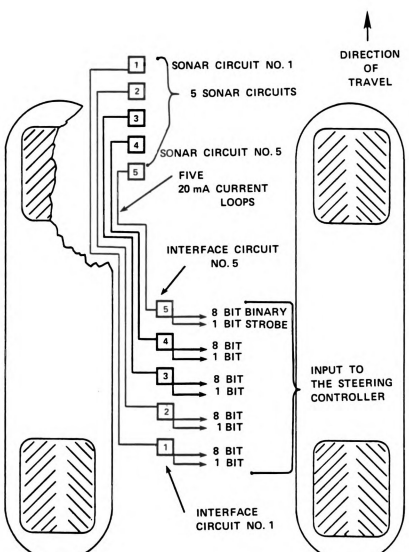

Figure 6.4. Diagram of Sonar Sensing System

with the microprocessor based steering controller, and the interface circuit is designed to convert the timing signal from a sonar circuit into an 8 bit binary number which represents the measured distance from the sonar unit to the apple tree trunk.

6.1.1 Description of Sonar Circuits

Each of the five sonar units contains a sonar circuit. A sonar circuit was designed using CMOS logic gates and the sonar circuit uses the Polaroid ultrasonic circuit board and transducer. A block diagram of a sonar circuit is shown in Figure 6.5. The sonar circuit has two main functions. First, the sonar circuit must control the ultrasonic circuit board so that ultrasonic sound pulses are sent out at a rate of 21.7 Hz. This allows range measurement to the tree trunk to be made at a 21.7 Hz rate. This rate was selected so that several sonar range measurements to the tree trunk could be made as a sonar unit on the harvester moves past a tree trunk. By using this 21.7 Hz rate of sonar measurements the steering controller can sample several sonar measurements to determine a single valid mesurement from a particular sonar unit. It is assumed that only one valid sonar measurement is needed for each sonar unit because the harvester's steering response is slow and only small harvester position changes could occur while a tree is in the sensing zone of a sonar unit. Note, that the sonar measurement rate was selected based on a maximum ground speed of 4.8 km/h (3.0 mph), and the sonar units operate at a high measurement rate to make at least four sonar measurements while a tree trunk is in the sensing zone of a given sonar unit. Also, the sonar circuit was designed to produce a timing signal called COUNT which is sent to the interface circuit.

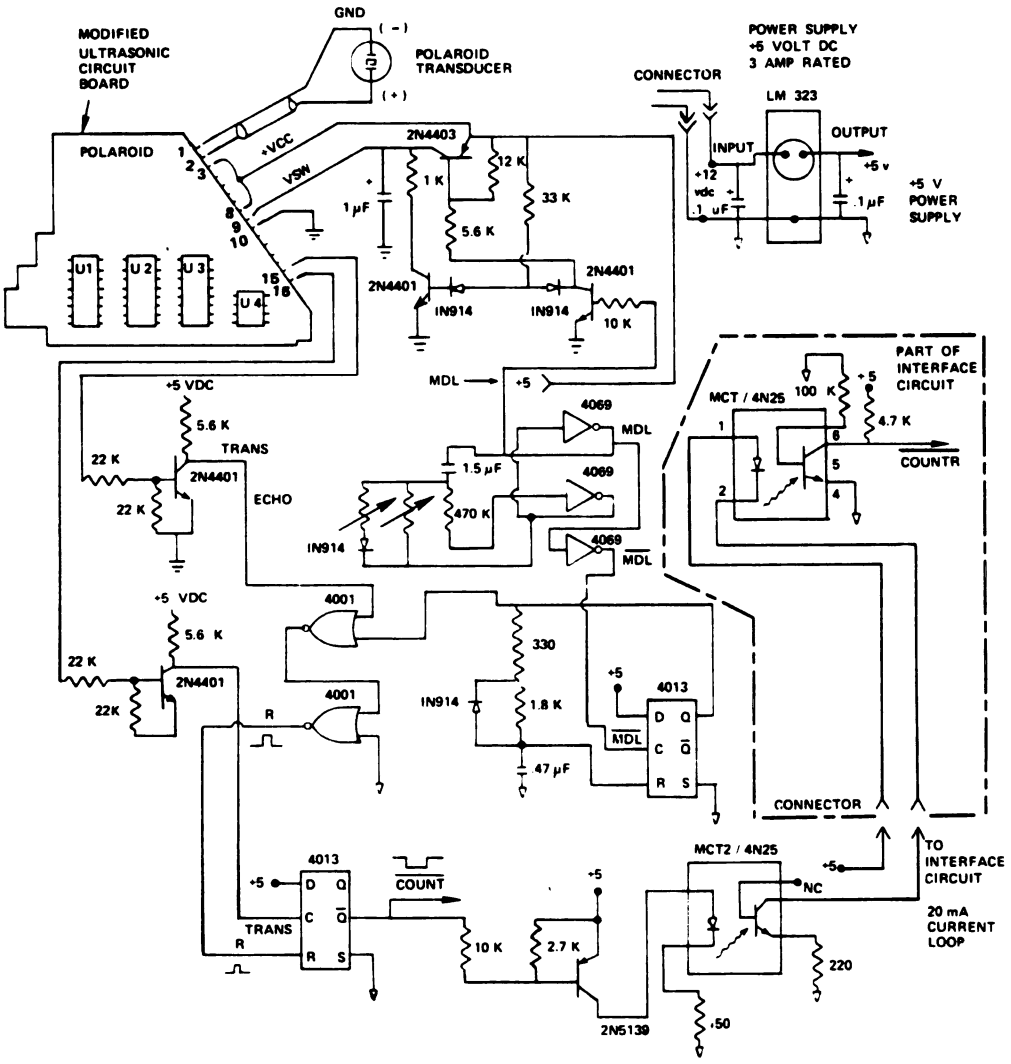

Figure 6.5. Circuit Diagram for One Sonar Unit

First, the sonar circuit was designed to control the rate of transmitting sound pulses. A sonar circuit transmits sound pulses at a rate of 21.7 Hz. This was accomplished by designing the wave form of the MDL signal so that it was at logic HIGH for 26 ms and at logic LOW for 20 ms and then this cycle repeated. With this wave form, the periodic wave form of MDL has a period of 46 ms and a frequency of 21.7 Hz. Note, that if the frequency of MDL is changed then the rate of sonar measurement is also changed. Since the period of MDL is short, the sonar circuit cannot measure the distance to objects which are further than 240 cm from the transducer because the echo returning from the sensed object will return to the transducer after the MDL signal has changed to logic LOW. And, the ECHO signal will not respond to an echo received when MDL is at logic LOW. These timing signals are shown in the timing diagram of Figure 6.6. Note that the sonar system for the apple harvester does not require range measurements greater than 240 cm, although longer distances can be measured with this circuit by increasing the period of the MDL signal.

The second function of the sonar circuit is to produce a timing signal called $\overline{\text{COUNT}}$. This signal was designed to be at logic LOW only during the time that the ultrasonic sound pulse was traveling from the transducer to the object being sensed and back to the transducer. This timing signal was used by the interface circuit to produce an 8 bit number that represents the range of the object. This timing signal, $\overline{\text{COUNT}}$, changes logic states according to the following sequence and this sequence is shown in the timing diagram in Figure 6.6. This sequence for one cycle begins with the TRANS signal at logic LOW. The TRANS

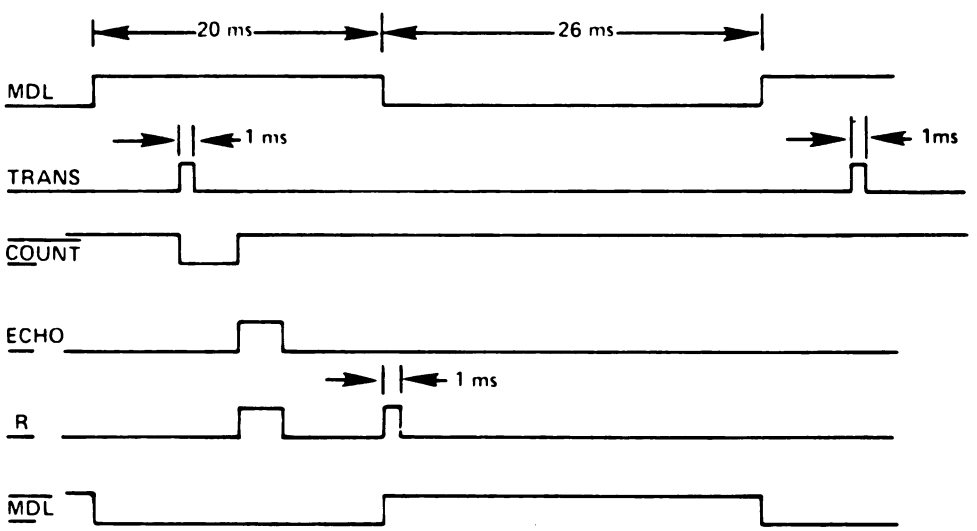

Figure 6.6. Timing Diagram of Sonar Circuit for Objects for Range Less Than 240 cm

signal goes to logic HIGH when the sound pulse is transmitted from the transducer. When the TRANS signal changes from LOW to HIGH, the $\overline{\text{COUNT}}$ signal changes from HIGH to LOW. Next, the sound pulse echo is received by the transducer and the ECHO signal changes from LOW to HIGH causing the R signal to change from LOW to HIGH. The change of the R signal causes $\overline{\text{COUNT}}$ to change from LOW to HIGH. This completes one cycle for the sonar unit for the case where the range to the object is less than 240 cm. If the object being sensed is more than 240 cm from the transducer, then a different sequence of timing events occurs. Figure 6.7 is a timing diagram for the case where the range to the object is greater than 240 cm. For this condition of measured distance greater than 240 cm, the only change in the timing sequence is in the way the $\overline{\text{COUNT}}$ signal changes state from LOW to HIGH. The signal $\overline{\text{MDL}}$ is used to reset COUNT back to logic HIGH if an echo has not been received. When $\overline{\text{MDL}}$ changes from LOW to HIGH, a monostable produces a one milisecond pulse. This pulse causes the signal R to produce a pulse and then $\overline{\text{COUNT}}$ changes from LOW to HIGH. By resetting the $\overline{\text{COUNT}}$ signal with this technique the interface circuit can only measure a maximum value of 240 cm. Therefore, for any sonar measurement which is less than 240 cm, the object is within the allowable range of the sonar. If the sonar measurement is greater than 240 cm, then this indicatees that the object is either not in the sonar sensing zone or the object is at a distance greater than 240 cm. Therefore, sonar values less than 240 cm were used as valid sonar measurements from the apple harvester sensing system and the sensing system for the apple harvester only requires maximum distance measurements of 150 cm.

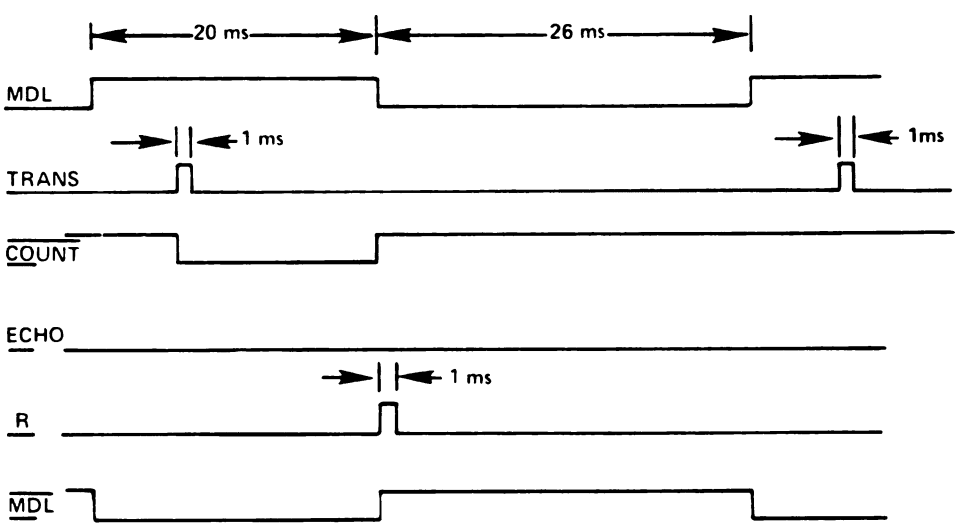

Figure 6.7. Timing Diagram of Sonar Circuit for Objects With Range Greater Than 240 cm

This $\overline{\text{COUNT}}$ signal is also used to control the 20 mA current loop. The current loop is a timing signal that transmits the $\overline{\text{COUNT}}$ signal of a sonar circuit to an interface circuit as shown in Figures 6.4 and 6.5. When $\overline{\text{COUNT}}$ is at logic LOW, the 20 mA of current is flowing in the current loop circuit and when $\overline{\text{COUNT}}$ is HIGH the current does not flow in the current loop. Figure 6.5 also shows that the 20 mA current loop connects to an optoisolator (MCT2 or 4N25). The output transistor of the optoisolator in the interface circuit produces the signal $\overline{\text{COUNTR}}$. This signal is approximately equivalent to the $\overline{\text{COUNT}}$ signal in the sonar circuit. The main differences between $\overline{\text{COUNT}}$ and $\overline{\text{COUNTR}}$ are switching delays and slow rise time caused by the two optoisolators that are used in the current loop circuit.

The sonar circuit uses the optoisolators so that noise from the ultrasonic circuit board is kept isolated from the interface circuit. A +5 volt (direct current) voltage regulator is used to supply the power for the sonar circuit. This voltage regulator and LM323 can supply up to 3A of current. The input voltage source for the voltage regulator is a large 12 volt automobile battery.

6.1.2 Description of Interface Circuit

An interface circuit was designed and is shown in Figure 6.8. Each of the five interface circuits uses a timing signal from a sonar circuit to produce an 8 bit binary number that represents the range from the sonar unit to the object that is being sensed. The interface circuit is basically a timer-counter circuit. The $\overline{\text{COUNTR}}$ signal in Figure 6.8 is the timing signal that is received from the sonar circuit. The $\overline{\text{COUNTR}}$ signal is at logic LOW from the moment the sound pulse is transmitted

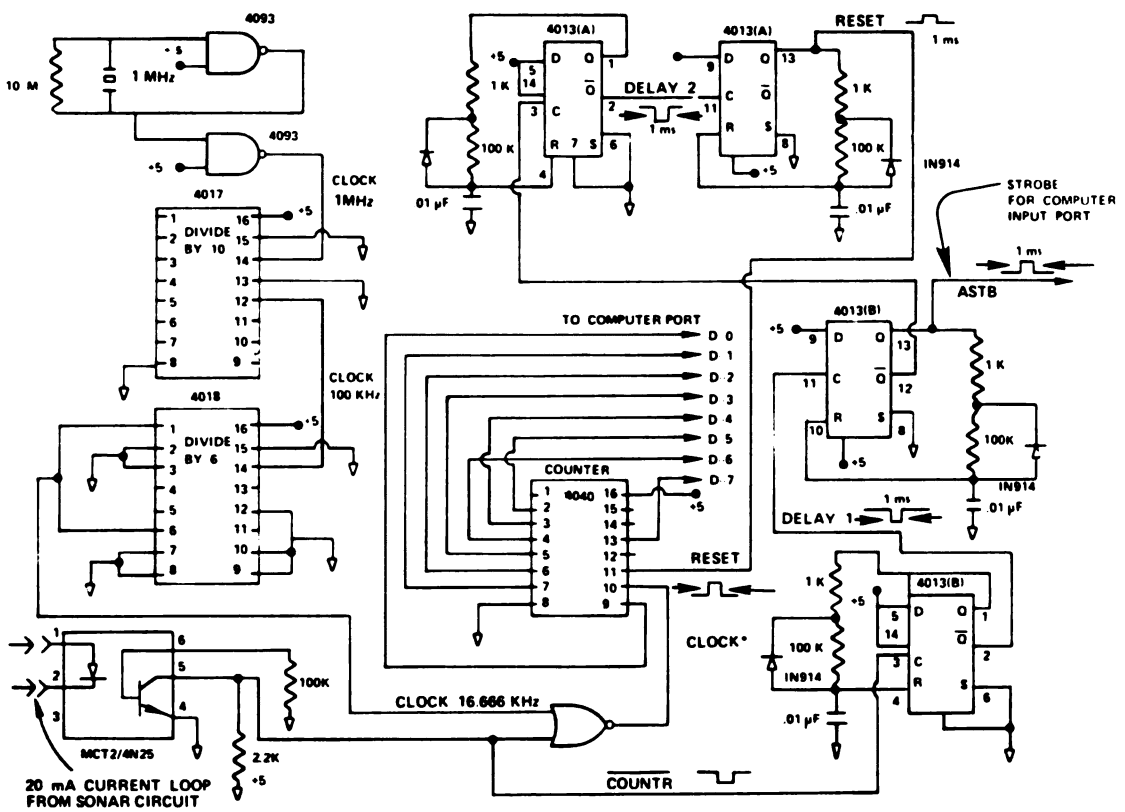

Figure 6.8. Interface Circuit Diagram

until the sound pulse echo is received by the sonar circuit. An interface circuit is designed to count clock pulses only during the time that $\overline{\text{COUNTR}}$ is at logic LOW. A clock frequency is then selected so that the clock signal produces one pulse during the time the ultrasonic sound pulse travels 2 cm. Since the sound pulse must travel out to the object and back to the transducer the sound pulse travels twice the magnitude of the distance to the object. Thus, for every centimeter of range to an object, the sound pulse must travel two centimeters. To determine the clock frequency the velocity of the speed of sound in air must be known. As explained by Gross (1978), the sound pulse travels at the speed of sound and is a function of air temperature according to the equation:

$$V = 331.5 + (0.607)\ T \quad \text{(m/sec)}$$

$$\text{where } T = \text{air temperature} \quad (^{o}C)$$

For air at a temperature of zero degrees Celsius, the velocity of an ultrasonic sound pulse is 331.4 m/sec. For the hypothetical case where the range from the sonar transducer to an object is 1 cm, the sound pulse must travel 2 cm and the time required for the sound pulse to travel 2 cm is 6.033×10^{-5}s. If a clock signal in an interface circuit is designed to produce one pulse every 6.033×10^{-5}s, then one clock pulse will occur for each centimeter of range to the object. Using 6.033×10^{-5}s as the period of the clock signal, the corresponding frequency is 16.575 kHz. The clock frequency selected for the interface was 16.67 kHz because it could be easily designed using a 1 MHz crystal to develop a 1MHz clock signal and then dividing this clock signal by six hundred. Using this frequency of 16.67 KHz should only cause an error in the sonar measurement of less

than 1% for sonar measurement less than 150 cm with air temperature of $0^{o}C$. A block diagram of this circuit to produce the clock signal is shown in Figure 6.8. In order to develop an 8 bit number that represents the distance to the object, the $\overline{\text{COUNTR}}$ signal is used to start and stop the sending of the clock signal to a binary counter. The interface circuit is designed such that when $\overline{\text{COUNTR}}$ is at logic LOW, the 16.67 kHz clock signal is sent to the counter. The clock signal is stopped from being sent to the counter when $\overline{\text{COUNTR}}$ is at logic HIGH. Refer to Figure 6.9 for the timing diagram of these signals in the interface circuit.

Four monostables or one-shots are used in the interface circuit to produce time delay pulses and control signal pulses. These pulses have a duration of one millisecond each. The time delays are used to control the timing of several signals in the interface circuit. The first delay occurs when $\overline{\text{COUNTR}}$ changes from LOW to HIGH. This gives the counter some time to settle because a ripple counter is used and it requires about five microseconds for the output of the counter to become valid. After the first delay, the signal ATB, is a one millisecond control signal pulse which is used to indicate that the 8 bit number on the counter is ready or valid. This ASTB signal is a control signal used to latch data into a steering controller input port. The ASTB pulse will latch an 8 bit number that represents the sonar measurement. After the ASTB signal pulse, another one millisecond delay pulse occurs. This second delay pulse is followed by a RESET signal pulse which is used to reset the counter. Note, that when five interface circuits are grouped together and built onto one circuit board then only one 16.66 kH clock signal is needed. This clock signal can be used by each of the five

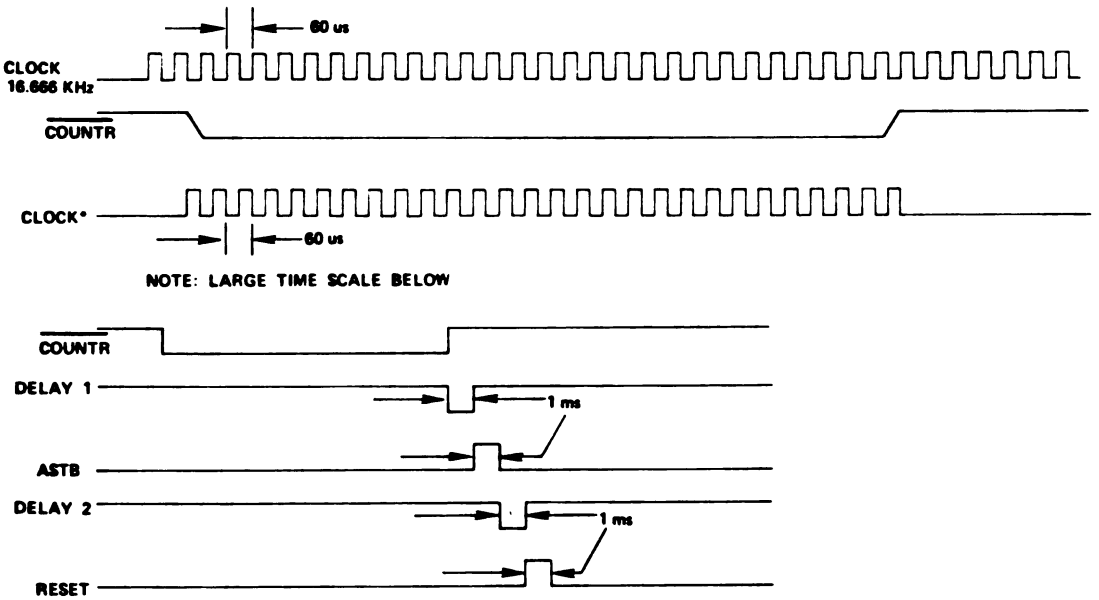

Figure 6.9. Timing Diagram for Interface Circuit

interface circuits. This technique of using one common clock signal was used to develop one large interface circuit board that sends five binary numbers to the steering controller.

6.2 Sonar System Testing and Results

A sonar system was built and tests were performed to evaluate the accuracy of the range measurements of the sonar system. Tests were done at 25.5^{o}C and -1.0^{o}C to check the effect that temperature has on the accuracy of the sonar measurements. Tests were also performed to check the approximate beam angle of the Polaroid ultrasonic transducer. The beam angle basically represents the sensing zone which is the area where an object can be detected by a given sonar unit.

The objectives of the accuracy tests were to determine the accuracy of a sonar unit within the temperature range of 0.0^{o}C and 32.2^{o}C because these are the limits of the operating temperatures for the sonar unit which are specified in the design requirements. Since a large temperature controlled chamber was not easily accessible, one test was performed outdoors where the outside air temperature was -1.0^{o}C which was close to the operating temperature limit of 0.0^{o}C. Another test was done indoors where the highest available air temperature was 25.5^{o}C. This temperature was close enough to the upper operating temperature limit of 32.2^{o}C that the sonar reading could be estimated using the assumption that the sonar measurement will change linearly with air temperature. The sonar reading should change linearly because the sound pulse that is transmitted by the sonar unit travels at the speed of sound and the speed of sound changes linearly with the change in air temperature. Also it is assumed that there are negligible temperature effects on the sonar measurements that are caused by changes in the

performance of the digital electronic circuitry. The manufacturer's operating temperature range for the integrated circuits used in the sonar system is -40^{o}C to 85^{o}C. The effect on the sonar accuracy due to the air relative humidity was not studied because a report by Gross (1978) indicated that the speed of sound changes less than 0.5% due to a change in the relative humidity from 0 to 100%.

6.2.1 Sonar System Accuracy Tests and Results

Five sonar circuits and one interface circuit were constructed according to the circuit diagrams in Figures 6.5 and 6.8. These circuits were then tested to determine the accuracy of the sonar distance measurements. The test procedure was performed as follows. First, a flat metal target was positioned such that the target was centered on the sonar beam centerline at a specific distance or range from the ultrasonic transducer. The target was a piece of sheet metal that had a square surface area with dimensions of 12.7 cm by 12.7 cm. The air temperature was 25.5^{o}C.

The size of the target was selected because it was assumed that the performance of the sonar system may be affected by the size of the surface area of the target, therefore this target size that was selected approximately represents the size of objects the sonar system may be used to detect. Preliminary tests have indicated that the sonar readings are more consistent at detecting an object with a large surface area. The target also has a hard flat surface and this type of surface was selected because it was assumed that this surface would be the best type surface for reflecting a sound pulse. Thus, this hard flat surface should result in sonar readings with the highest possible accuracy for a target of the same size and this accuracy should represent a base line

for the best accuracy for this sonar system. If other targets are used, the sonar accuracy may vary from the accuracy obtained in these tests.

In order to collect the sonar data for this test, the sonar system was connected to a computer (RCA Model CDP18S694) which uses an interpreted BASIC language and assembly language for the 1802 microprocessor. The computer was programmed to read four consecutive sonar measurements and store these measurements. These four measurements were for one specific position of the target. The computer program used assembly language subroutines so that the sonar data could be quickly read from the interface circuit and the values stored in the computer memory. The computer program also directed the sonar data to be printed onto a teletype and stored on cassette tape for further data analysis. Four sonar readings were collected for each position of the target and the range to the target was changed in 10 cm increments from a range of 30 cm to 150 cm. When the range to the target was between 75 cm and 85 cm the target was moved in 1 cm increments to obtain additional data points in this zone of target distances. Typical measurements by the apple harvester sonar sensing system will be in this range of 75 to 85 cm. The 150 cm upper limit on the target position was selected because this represents the maximum distance measurement required for the apple harvester sonar system. The lower limit of 30 cm for the target position was used because this was near the value of 28 cm which is the minimum reading that the sonar system is capable of making.

Preliminary tests on the sonar system also indicated that for a given target position the sonar reading would oscillate between two values. For example if the sonar reading was initially 30 cm, then

sometimes the sonar reading would change back and forth between the values 30 and 31. Therefore, to show this variability in the sonar readings, the test was done by taking four sonar readings at each target position.

The sonar data was plotted and Figure 6.10 shows this plot of sonar data versus the actual target range for sonar unit one. The data plots for the outer four sonar units are in Appendix A. The data for sonar unit one are in Table 6.1 and the data for the other four sonar units are in Tables in Appendix A.

Table 6.1. Data from Accuracy Test for Sonar Unit One at 25.5^{o}C.

Target Actual Range cm	Four Consecutive Sonar Measurements cm				Average Sonar Measurement cm
30	31	30	31	31	30.75
40	40	40	40	40	40.40
50	50	50	50	50	50.00
60	60	60	60	60	60.00
70	69	69	69	69	69.00
75	74	75	75	74	74.50
76	75	75	75	75	75.00
77	76	76	76	76	76.00
78	77	77	77	77	77.00
79	78	78	78	78	78.00
80	79	79	79	79	79.00
81	80	80	79	80	79.75
82	81	81	81	81	81.00
83	82	82	82	82	82.00
84	82	83	83	83	82.75
85	84	84	84	84	84.00
90	89	89	89	89	89.00
100	98	98	98	98	98.00
110	109	108	108	108	108.25
120	118	117	117	117	117.25
130	127	127	127	127	127.00
140	137	137	136	137	136.75
150	147	147	147	146	146.75

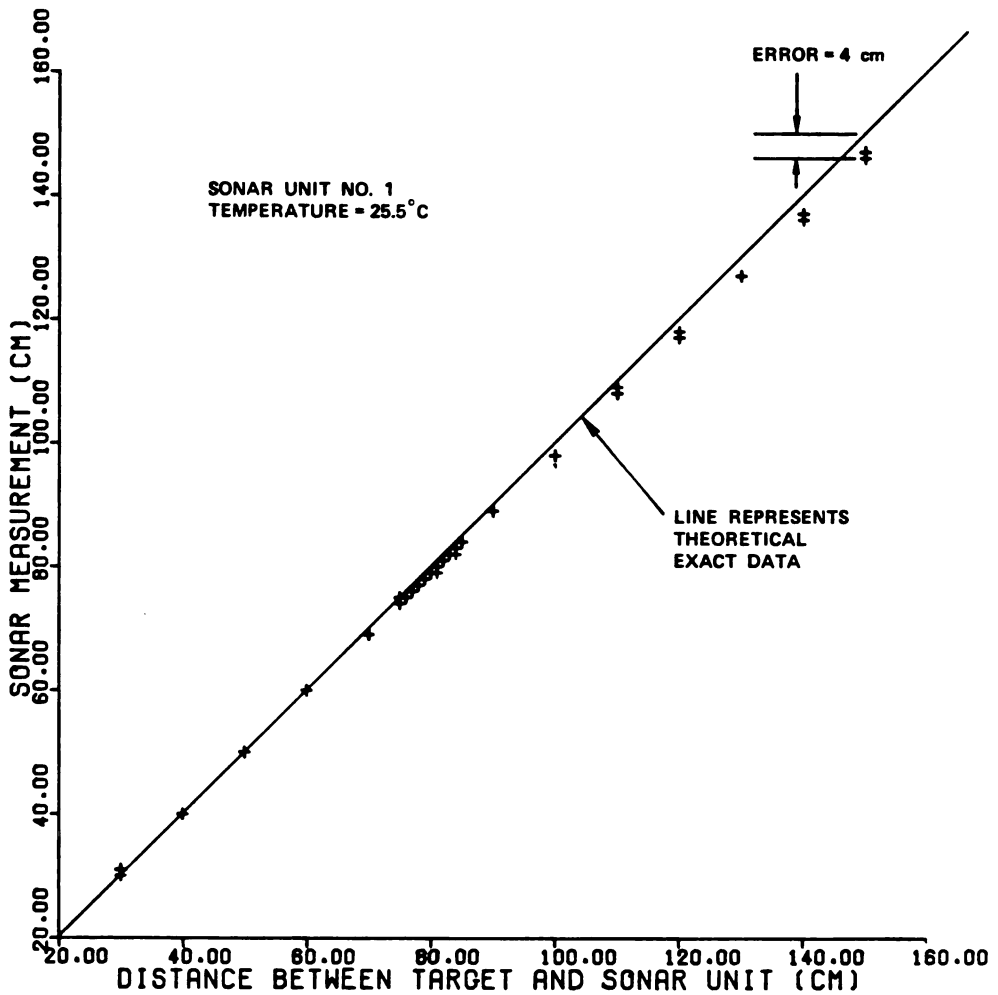

Figure 6.10. Distance Data for Sonar Number One Accuracy Test at 25.5°C.

The plot of the sonar data for sonar unit number one is typical of the plots for the other four sonar units. Also, each of the sonar data plots shows that the data points lay close to a straight line. Note, that in the data plot of Figure 6.10, at each target position the values of four sonar readings were plotted, therefore, when only one point is shown on the graph for a given target position, then that data point on the graph represents four sonar readings of equal value. For the case where two data points are shown on the graph for a given target position, then the four sonar readings are distributed between these two plotted sonar reading values. By inspection of Table 6.1 it can be determined how many sonar readings are represented by each plotted data point in Figure 6.10. Note that in Figure 6.10 the data show that the maximum sonar measurement error is 4 cm when the actual distance to the target was 150 cm.

A linear regression analysis was done for the data from each of the five sonar units. The form of the equation of the straight line that best fits the data is:

$$S = mx + b$$

where

S = predicted sonar reading (cm)

m = slope of the line

x = actual target range (cm)

b = intercept with S axis

The regression equations and correlations coefficient for each of the sonar units are:

for Sonar 1

$$S = (0.96521)X + 1.75116 \qquad (6.1)$$

$$R = 0.99992 = \text{correlation coefficient}$$

for Sonar 2

$$S = (0.96237)X + 2.13578 \qquad (6.2)$$

$$R = 0.99993$$

for Sonar 3

$$S = (0.96419)X + 1.86059 \qquad (6.3)$$

$$R = 0.99990$$

for Sonar 4

$$S = (0.96609)X + 1.67628 \qquad (6.4)$$

$$R = 0.99992$$

for Sonar 5

$$S = (0.96313)X + 2.09320 \qquad (6.5)$$

$$R = 0.99991.$$

This same test procedure to determine sonar range accuracy was also done for sonar unit number one and two at an air temperature of $-1.0 \pm 0.5^{o}C$. Table 6.2 shows the collected data for sonar unit one and Figure 6.11 shows a plot of this sonar distance data for sonar unit number one. See Appendix A for the data from sonar unit number 2.

Table 6.2 Data from accuracy test for sonar unit one at -1.0°C.

Target Actual Range cm	Four Consecutive Sonar Measurements cm				Average Sonar Measurement cm
30	32	32	32	32	32.00
40	42	42	42	42	42.00
50	52	53	53	53	52.75
60	63	63	63	63	63.00
70	73	73	73	73	73.00
75	78	78	78	78	78.00
76	79	79	79	78	78.75
77	80	80	80	80	80.00
79	82	82	82	82	82.00
80	83	83	84	83	83.25
81	85	84	85	85	84.75
82	85	85	85	85	85.00
83	86	86	86	86	86.00
84	87	87	87	87	87.00
85	88	89	88	88	88.25
90	94	93	93	94	93.50
100	104	103	104	104	103.75
110	113	114	114	114	113.75
120	124	124	124	124	124.00
130	134	133	134	133	133.50
140	144	143	144	143	143.50
150	154	154	154	154	154.00

A linear regression was also done on this sonar data and the straight line equations that best fit the data are:

Sonar 1

$$S = (1.0399)X + 1.98690 \qquad (6.6)$$

$$R = 0.99990$$

Sonar 2

$$S = (1.01567)X + 1.69050 \qquad (6.7)$$

$$R = 0.99993$$

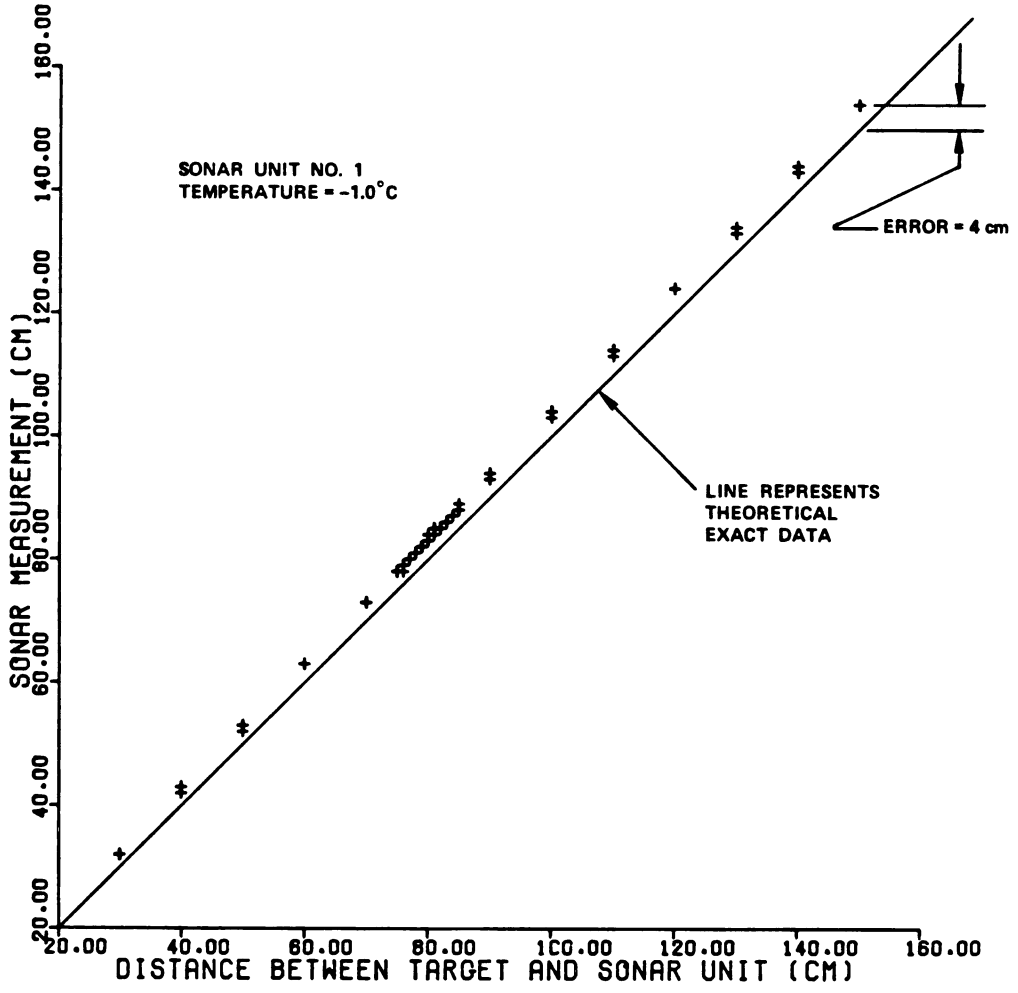

Figure 6.11. Distance Data for Sonar Number One Accuracy Test at -1.0°C.

The data of Figure 6.11 show that the maximum sonar measurement error was 4 cm although Table 6.2 shows that this maximum error occured at a target distance of 150 cm, and at several other target distances.

The inaccuracy of the sonar data can be seen qualitatively in Figures 6.10 and 6.11. By inspection of the graph of sonar data in Figure 6.10 where the air temperature was 25.5^{o}C, it can be seen that the data points form a line that has a greater slope than the line which represents the theoretical exact data. This line for theoretical exact data is the line which represents sonar distance measurements which are equal to the actual distance from the sonar unit to the target. Therefore, any sonar data points which are on the theoretical exact line shown in Figure 6.10 or 6.11 have zero error. Note, the regression line through the data was not drawn through the data points because the line would make it difficult to see the small variations between data points. Therefore, since the data points of Figure 6.10 diverge from the line for theoretical exact data, the error of the sonar data increases as the range increases. This increasing error results because the 16.67 kHz clock frequency in the interface circuit is not the optimum frequency for the air temperature of 25.5^{o}C. On inspection of the sonar data of Figure 6.11 where the test air temperature was -1^{o}C, it can be seen that the data points form a line that is nearly parallel to the line that represents the theoretical exact data. The sonar data is offset slightly from the theoretical line and this offset or error in the sonar data may be partially caused by using a clock frequency of 16.67 kHz instead of using a clock frequency of 16.55 kHz which would be the computed frequency for sonar measurement at -1^{o}C air temperature. This computation of clock frequency was explained in section 6.1.2. Another possibility for the

offset is signal delays in the electronic circuitry. Further research is required to determine the cause for this error in this sonar data.

On inspection of the data it is seen that the developed linear regression equations have a correlation coefficient almost equal to one, and therefore it can be concluded that the equations for the lines that were developed are good predictors of the sonar values for a given target position assuming the sonar readings were taken with the same conditions as used during this accuracy test. A value for R near one also indicates that most all of the data points lay near or on the regression line. It is also assumed that the accuracy for each of the five sonar units is equivalent. This is shown by equations 6.1 to 6.5 being nearly equal, and by inspection of the data which show that there are negligible deviations between each of the five sonar unit's readings at each target position. Since the sonar data for all five sonar units was very similar for air temperature of 25.5^{o}C, only two sonar units were used for accuracy tests at air temperature of -1^{o}C.

An important point about the data in Figure 6.10 and 6.11, which are the sonar data at air temperatures of 25.5^{o}C and 1.0^{o}C respectively, is that the maximum deviation of the sonar reading from the theoretical exact value is 4 cm. This deviation or error can be computed by:

$$E = S - T \tag{6.8}$$

where E = error (cm)

S = sonar reading (cm)

T = theoretical exact sonar reading (cm)

Therefore it can be concluded that the tests indicate that the sonar units are accurate between $\pm$4 cm for the target distances of 30 cm to

150 cm and for air temperatures between -1.0^{o} and 25.5^{o}C. Using linear extrapolation an error of 6 cm (error defined by equation 6.8) was computed for sonar measurements with air temperature of 32.2^{o}C. Therefore, the sonar system accuracy is expected to be within $\pm$6 cm for the temperatures between 0.0^{o}C and 32.2^{o}C, for sonar system readings in the range of 30 cm to 150 cm, and for the same conditions as used in this test.

This error or inaccuracy of the sonar system is acceptable for use in the apple harvester steering control system because it is believed that with this sonar inaccuracy the apple harvester steering control system will be effective at controlling the harvester so that each tree trunk stays within the defined allowable zone as specified by the design requirements. This allowable zone is 45.7 cm wide and if the maximum tree trunk diameter is 14 cm then there would still be 31.7 cm of width available in the allowable zone that the tree must stay within. Therefore, this $\pm$6 cm inaccuracy in the sonar reading is not expected to pose a serious problem for controlling the apple harvester steering. Note, also that this 6 cm error is the maximum expected error at 32.2^{o}C and at sonar readings of 150 cm and that the expected error is less at lower temperatures and at smaller sonar reading values.

6.2.2 Sonar Beam Angle Tests and Results

A test was done to check the beam angle of a sonar unit. This beam angle is important because it indicates the area in front of the sonar transducer where an object may be detected. Also, the test was done to determine if there is a large error in a sonar reading when the object is near the outer edge of the sonar beam. The test procedure for measuring the beam angle was made based on the assumption that two lines

extending from the sonar transducer approximately define the sonar beam angle. The beam angle defines an area where objects that are inside the beam angle are detected by the sonar unit and objects which are outside the sonar beam angle are not detected. A cylindrical tube was selected as a target for this test because it was assumed that this type of target would be the best for reflecting the sound pulse back in the direction of the transducer even when the target is offset from the sonar beam centerline. This assumption was based in preliminary tests which indicated that a flat surface can reflect a sound pulse in a direction away from the sonar transducer and then the object would not be detected beause the transducer did not receive a strong echo. Therefore, it was believed that a cylindrical shaped target would provide data that represent the largest beam angle of the transducer. The size of the target for this test was selected to approximately represent an apple tree trunk. The basic procedure of the test was to begin the test with the target initially at a position offset from the beam centerline so that the sonar did not detect the target. Then the target was moved toward the beam centerline until the sonar unit detected the target. This was done at several positions on each side of the sonar beam so that data could be collected to define two lines which describe the beam angle.

The test was performed as follows. A piece of steel tubing 3.8 cm in diameter and 61 cm long was used as a target. A guide line was positioned above the sonar transducer to be used as a reference line so that the position coordinates of the target could be measured from the reference line. The reference line was positioned so that it was approximately at the centerline of the transducer's beam. Figure 6.12

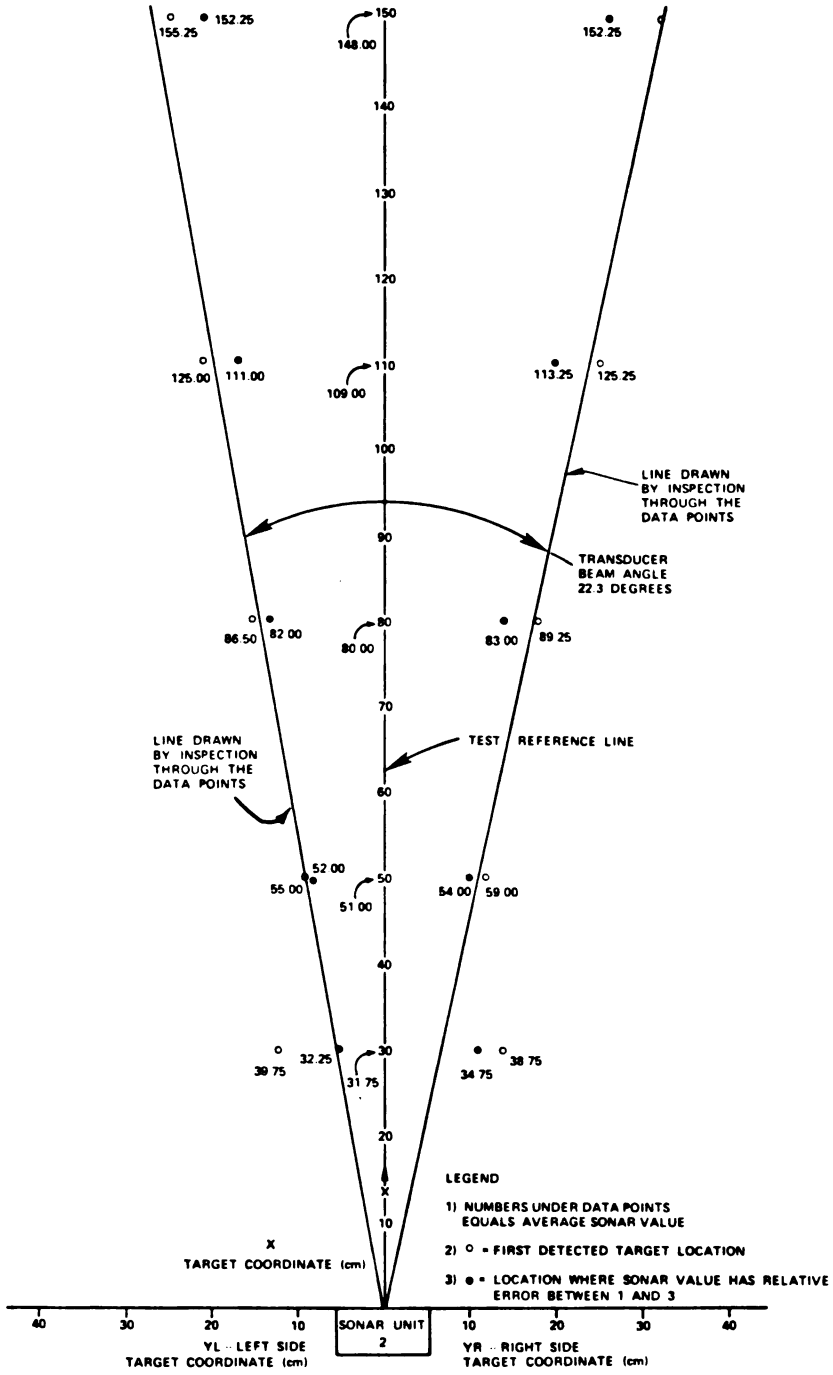

Figure 6.12. Plot of Sonar Data to Determine Transducer Beam Angle. Target used was a steel cylinder of 3.8 cm. diameter and 70 cm. long.

shows the sonar unit and in this figure the x-axis represents the reference line. The target was positioned with the long axis of the tube held vertically and the target was initially placed 30 cm ahead of the transducer. The target was offset to the right, perpendicular to the reference line. This 30 cm distance and the offset were designated as the X and YR coordinates of the target respectively. When the target was on the left side of the reference line, the target coordinates were X and YL. The coordinates were measured from the reference line to the target's vertical centerline that was scribed on the surface of the steel tube that was used as the target. The target was initially at a YR coordinate position that was out of the sonar beam angle, thus the target was undetected by the sonar unit. When the sonar did not detect an object in the beam angle (or sensing zone) the sonar reading value was between 213 and 215 cm. Next, the target's offset was decreased by moving the target toward the reference line in increments of one centimeter. These small increments were used to accurately locate the edge of the sonar beam. Then at each coordinate position of the target four consecutive sonar measurement values were read by a small computer that was connected to the interface circuit of the sonar system. This computer was the same one as described in section 6.2.1. The target was moved on this YR coordinate axis until the target was directly in front of the sonar transducer. The target was then moved to a new X coordinate position and the procedure was repeated. This test was done on both the right and left side of the reference line to determine the locations where the target would be detected by the sonar transducer. This procedure was performed for X coordinates of values of 30, 50, 80,

110, and 150 cm. These X coordinate values were selected to obtain data points through the full range of 30 to 150 cm which would define two lines that represents the boundaries of the sonar unit sensing zone. The sonar data was printed on a teletype and stored on cassette tape.

The purpose of performing the test was to determine the beam angle, or the zone of sensing, for the Polaroid ultrasonic transducer. This beam angle was determined by plotting the coordinate positions of the target where the target was first detected. A plot of this data is shown in Figure 6.12. These coordinate positions where the target was first detected indicate the outer edge of the beam angle. A line was drawn through these data points and the beam angle was determined graphically to be 22 degrees. Also, shown in this plot is the average of the four sonar values for each target coordinate position and the plot shows the average sonar value when the target is near the center of the zone. Notice that there is a major deviation between the average sonar value where the target was first detected and the average sonar value where the target was at the reference line. This indicates that there is additional error in the sonar readings when the target is at the outer edge of the sonar beam angle.

It was observed during this test that as the target was moved away from the sonar beam edge, toward the reference line, this additional error rapidly decreases. To illustrate how this additional error decreases as the target position was changed, another set of target positions were plotted and are shown in Figure 6.12. This set of target positions were those target locations where the average sonar value was greater than the sonar value near the reference line by 1 to 3 cm. On inspecting this plotted data, there are only a few centimeters

separating these target positions and the positions that represent the outer edge of the sonar beam angle. Notice, that at the target location at the outer edge of the sonar beam the measured sonar value is not very accurate and thus to obtain a more accurate sonar value, the target should be well inside the sensing zone.

Since these beam angle data indicate that the sonar readings are not accurate when the object being sensed is on the edge of the sonar beam angle, then some method must be used to compensate for this in order to achieve effective operation of the apple harvester steering control system. During the operation of the sonar sensing system the apple harvester will be moving down a tree row at a constant 0.8 km/h (0.5 mph) and an apple tree trunk will move across the sonar beam in a direction approximately perpendicular to the sonar beam centerline. This means that if the steering controller is continuously sampling the sonar readings from a particular sonar unit then the tree will be detected at the edge of the sonar beam and these may be erroneous sonar readings. One technique that may solve this problem is to delay using any sonar readings until the tree has moved into the sonar beam angle and away from the edge of the sonar beam angle. This may be accomplished by sampling the sonar readings until the sonar value is less than 150 cm. When this value is obtained it is assumed that the tree has entered the beam angle and the sonar is close to the edge of the sonar beam angle. After the tree is detected to be in the beam then the steering controller can execute a time delay by waiting until five sonar values have been sent to the steering controller and this would take 0.23 s because a sonar measurement is made every 0.046 s. Four of the five sonar values are not used because they may be erroneous. The

fifth sonar reading is assumed to be a valid sonar reading. Then once a valid sonar reading has been made, no further readings are made by that particular sonar unit and this would allow the tree to move out of the sonar beam angle without taking any sonar readings near the rear edge of the sonar beam angle where the sonar readings may also have a large error. This process repeats with the next sonar unit in the array of five sonar units. The next sonar unit waits until it detects the tree trunk entering the sonar beam angle and then this sensing process begins again.

7.0 SIMULATION MODEL WITH INTERACTIVE COMPUTER GRAPHICS

A simulation model with interactive computer graphics was applied to design an algorithm for the harvester's automatic steering control system. Computer facilities of the Case Center for Computer Aided Design at Michigan State University were used to simulate the harvester's motion.

A computer model was developed to simulate the motion of the apple harvester and the control tasks of a microprocessor based steering control system. The simulated motion of the harvester, as it traveled over a row of apple trees, was displayed on a graphics terminal. The use of computer graphics allowed the vehicle's response to be quickly displayed and analyzed. The influence of the system variables on the vehicle response was easily simulated and displayed. The most important design consideration for the performance of the steering control algorithm was the alignment of the harvester with respect to the apple tree trunks. Figure 3.1 is a diagram of the allowable zone which is 45 cm wide and extends from the front wheels to the rear wheels. A design requirement for the steering control system was that the tree trunk must stay within this allowable zone as the harvester passed over the tree.

---

[1]The Albert H. Case Center for Computer-Aided Design is a college wide facility. Dr. James Bernard, Professor of Mechanical Engineering, is the director. Software was developed at the Case Center by Mark Zykin, Case Center computer technician.

The computer facility used to develop the simulation model was the Case Center for Computer Aided Design which was established in the College of Engineering for research and teaching in the areas of Computer-Aided Design/Computer Aided Manufacturing (CAD/CAM). The CAD System is built around a PRIME 750 computer. The PRIME 750 computer has two 80 MB disk drives and services a color graphics terminal, a number of graphics and alphanumeric terminals, four dial-in lines, a digitizer and a Printronix printer.

The PRIME 750 had compilers for both Fortran IV and Fortran V. Fortran IV was used for the automatic steering control simulation. The main software packages that were used in the steering simulation were the PLOT 10, AGII, UTILV, and IMSLS. The PLOT 10 package (or TEKV Library), developed by the Tektronix Corporation, does the basic drawing of graphics data. The AGII program, also by Tektronix, calls PLOT 10, scales the graphics screen, draws the frame on the graphics screen and draws the labels. The program UTILV, which was developed at the Case Center, is a special program which allows other standard software library to run on the PRIME 750. The IMSLS software package, which was created by the IMSL Corporation, is a set of single precision mathematical subroutines. Subroutine DVERK, from the IMSLS package, was used for solving differential equations which were used to model the harvester motion.

7. 1 Model Requirements

A simulation model was needed to predict the motion of the harvester as it moved over a tree row with the front wheels steered by a microprocessor based steering control system. This simulation model was needed to reduce the time required to design the steering control

algorithm for the harvester's steering control system. This control algorithm was converted to a computer program for the harvester's microprocessor based steering controller. The design of the steering control algorithm is affected by many parameters, therefore, the following parameters were selected as variables in the simulation model. The selected variables were harvester velocity, number of trees, X - Y position coordinates of trees, geometry of steering system, wheel steering rate (angular velocity), parameters of the control algorithm, measurement rate (cycles per second) of tree sensing system and position of the sensors relative to the harvester.

To easily determine if the control system had satisfied the harvester's performance requirements, a graphical display of the harvester motion was needed. Therefore, two graphical display routines were selected for development. The first graphical display routine, called Mode 1, was designed to use the harvester's allowable zone (as defined by Figure 3.1) as a frame of reference. This display routine uses the allowable zone of the harvester as a moving frame of reference. As the harvester moved along the tree row, the graphical routine plotted the position of the tree trunks relative to the allowable zone. The scaling of the graphical output is the same in both the X and Y directions. Thus, there was no distortion due to unequal scaling and a Mode 1 output made it easy to determine if the tree was within the allowable zone as the harvester moved along a tree row. Figure 7.1 is an example of a Mode 1 output. The graphical output from the model was observed on a graphics terminal and a printer was used to make copies of the graphical output.

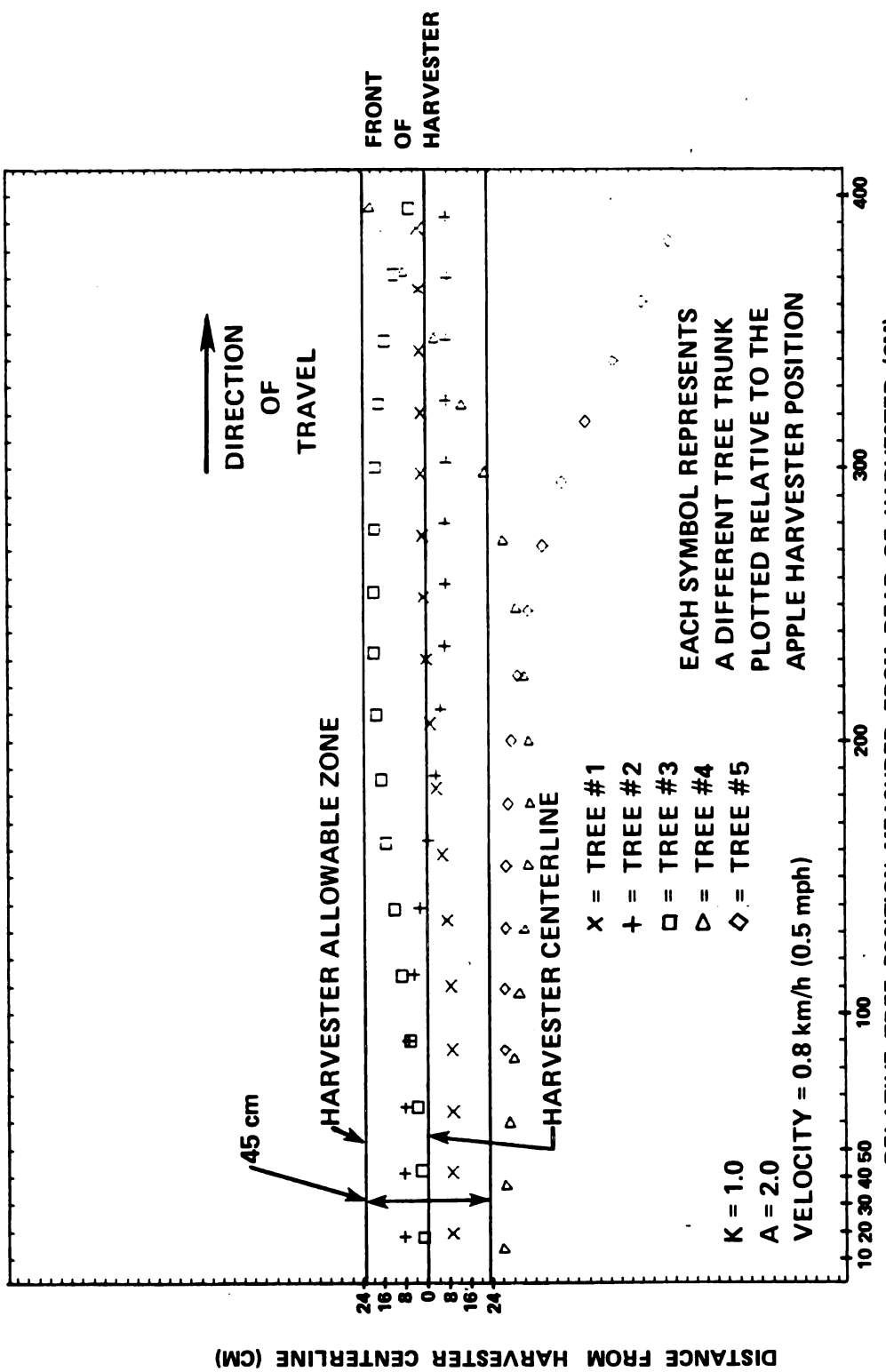

Figure 7.1 Mode 1 Graphical Output from the Simulation with K = 1.0

As a given symbol is repeated, a tree's position relative to the harvester is plotted as the tree passes from the front of the harvester to the rear of the harvester.

The simulation model also had a graphical display routine called Mode 2. This routine plotted at discrete times the position of the harvester's centerline relative to a fixed X and Y coordinate system. Also shown in this graphical output are positions of the tree trunks in the tree row. Figure 7.2 is an example of the Mode 2 graphical output from the simulation. A Mode 2 output was useful because it showed the path of the harvester as it moved along a tree row. The path of the vehicle provides information about the response of the steering control system.

Figures 7.1 and 7.2 are graphical outputs from the simulation model using the same values for system parameters. Therefore, in both of these figures the motion of the harvester is the same. The motion of the harvester as shown in Figures 7.1 and 7.2 indicated that the steering control algorithm was not effective. This version of the algorithm was not effective because as shown in Figure 7.1 two trees were not within the allowable zone. A more detailed explanation of this is given later. Note, that the scale factors for the X and Y directions are not equal for a Mode 2 output. This was done so that several trees could be plotted along the X-axis but still allow for easy reading of the harvester's displacement in the Y-direction.

7.2 Simulation Of Steering Control System

A simulation model was developed to show graphically the kinematic motion of the harvester as it traveled along a tree row with the steering controlled by a microprocessor based controller. Figure 7.3 shows a flow chart of the computer program for the simulation model. The graphical output of the simulation facilitated the interpretation of the harvester's response. On inspection of the flow chart (Figure 7.3)

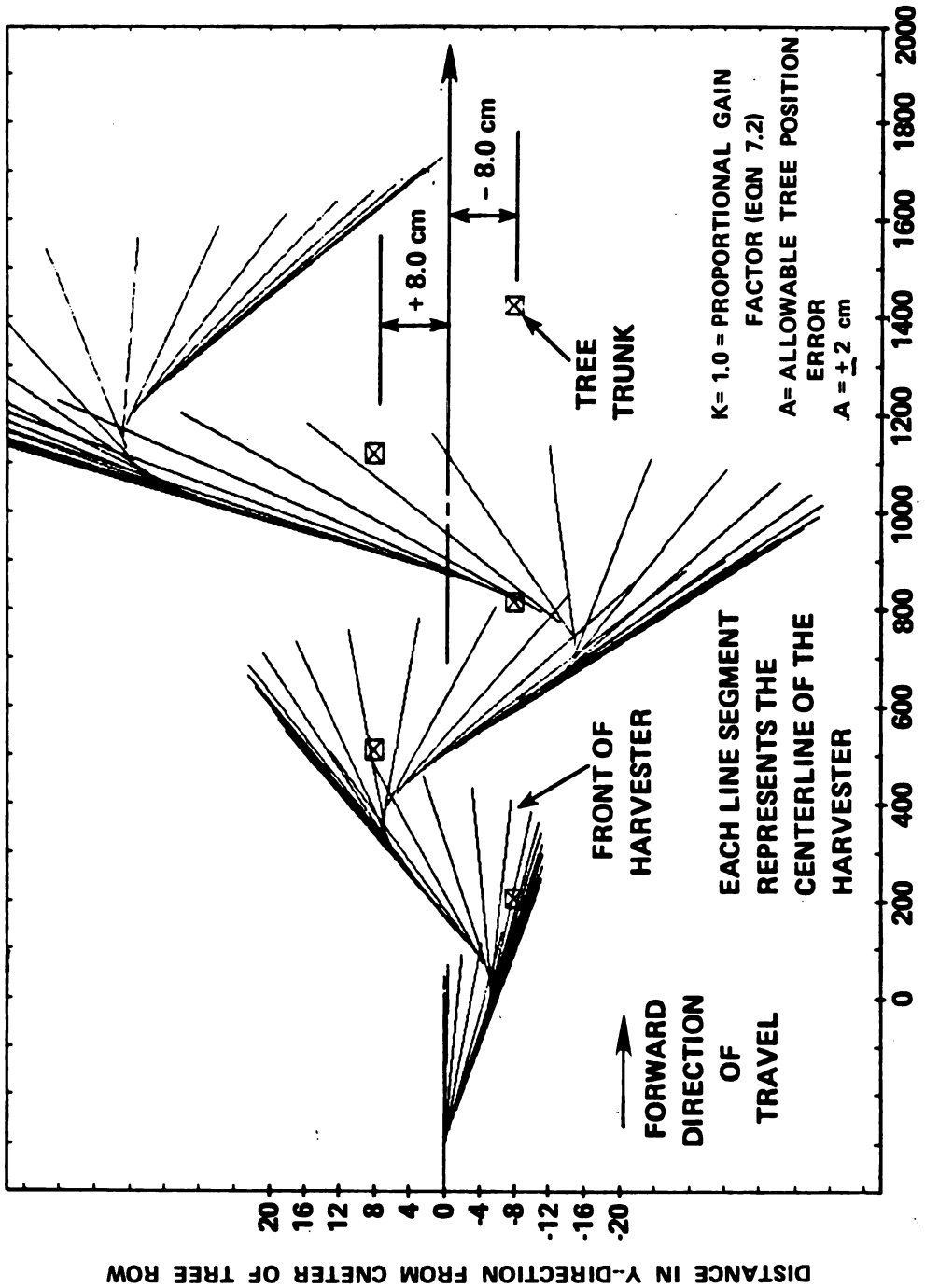

Figure 7.2 Mode 2 Graphical Output from the Simulation with K = 1.0

These line segments represent the harvester centerline as the harvester moved along the tree row.

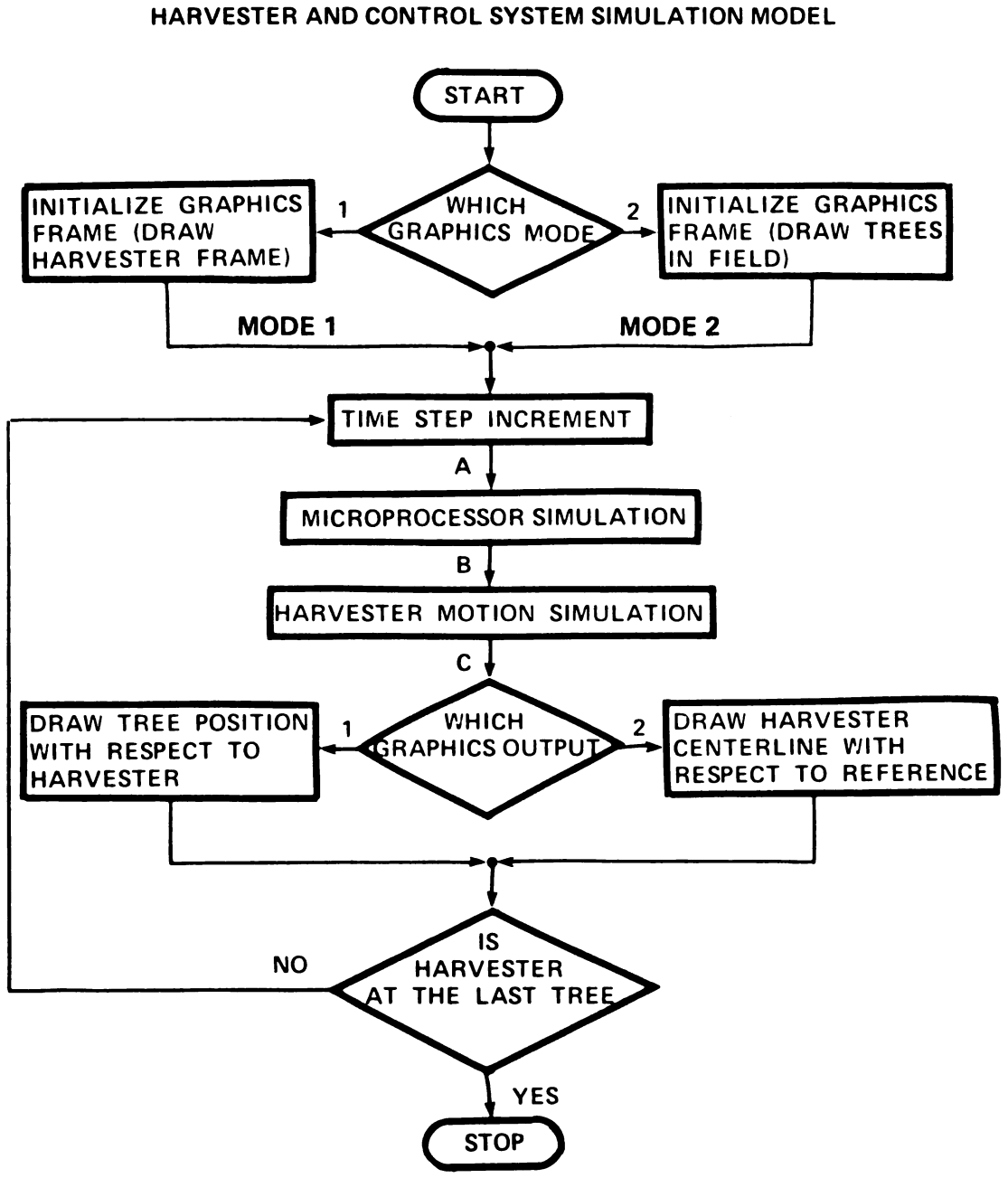

Figure 7.3 Flow Chart of Harvester Steering Control System Simulation

the simulation program first selects either Mode 1 or Mode 2 graphic display routines. The variable that determines Mode 1 or Mode 2 was contained in a computer data file. Thus, before a simulation was executed, the appropriate values were placed in this data file. This allowed the program to run without having to recompile. Also, by using a data file for all the major system parameters, time was not needed to reload all the values of the parameters for each run of the simulation. After the graphics mode was selected, the next step in the flow chart was the algorithm for the microprocessor which was the controller for the harvester steering system. Then the harvester motion equations were used to determine the position of the harvester at a particular time. The model used a time step increment of 0.01 second, therefore, the harvester's coordinate position was computed every 0.01 second. The simulation used numerical integration to solve the modeling equations and the time step size of 0.01 s was selected to keep the integration error small and to keep the actual computer run-time small. As the time step size became smaller the computer run time became larger. A check was made to determine the amount of change in the harvester's X - Y coordinates when the time step size was changed from 0.01 s to 0.001 s. The simulation results showed that when the time step size was changed, the Y-coordinate value changed by 0.7 cm and the X-coordinate value changed by 2.0 cm. The changes in the coordinate values were computed at the end of a simulation when the harvester had moved past five trees. These changes in the coordinate values basically represented integration error which decreases as the time step size decreases. Since there was only a small change in the coordinate values when the time step size was changed from 0.01 s to 0.001 s it was concluded that the time step size

was adequate for analyzing the apple harvester motion. Also, the accuracy of the modeling equations was checked (Section 7.2.2) and this check of the modeling equation accuracy was done with a time step size of 0.01 s. The results indicated that the modeling equations were valid and thus these results indicated that the time step was adequate because the simulation accurately predicted the harvester motion. Typically, the simulation used a row of five trees, although the number of trees was a variable. Appendix B contains a copy of the simulation program which included the program for computer graphics output.

7.2.1 Microprocessor Simulation Model

The control functions of a microprocessor (also called steering controller) were simulated and a flow chart of the computer program is shown in Figure 7.4. The operation of the steering control system is described in Chapter Five. The major task of the microprocessor is the computation of the desired wheel position code (D) such that it is proportional to the magnitude of the position error. The position error of the harvester is actually the amount the tree trunk is offset from the harvester centerline. This tree offset (also called tree position error) is equal to:

$$E = 78 - S \tag{7.1}$$

where E = tree position error (cm)

S = sonar measurement (cm)

The value for D is computed using the equation:

$$D = K\,(78-S) + 32 \tag{7.2}$$

where K = proportional gain factor

D = desired wheel position

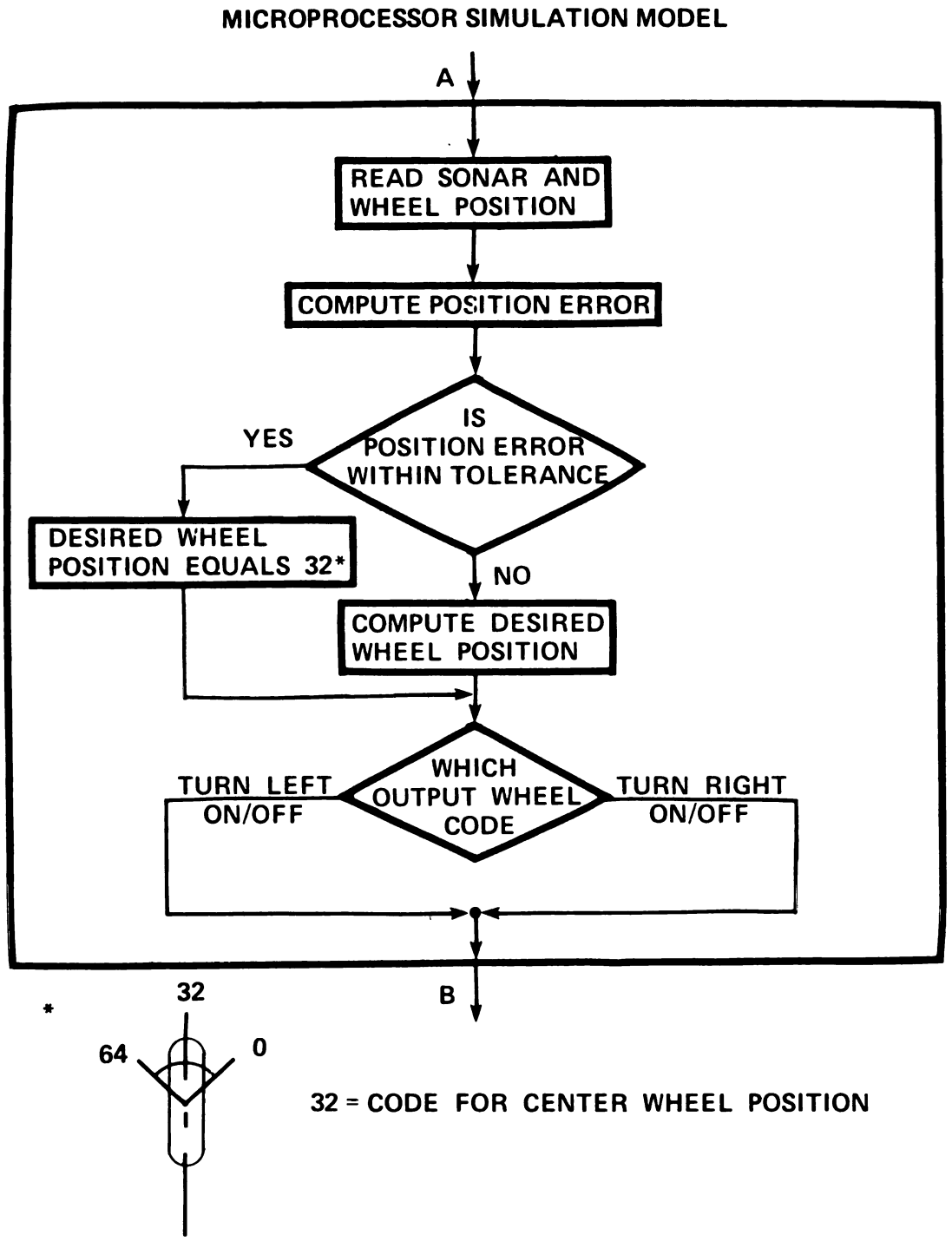

Figure 7.4 Flow Chart of the Simulation Model for the Harvester's Microprocessor Functions

The value D is scaled such that it can be compared directly with the value from the shaft encoder. Therefore, when the steering controller determines that the value from the wheel shaft encoder equals the value of D, then the wheels are at the correct position.

7.2.2 Harvester Motion Simulation Model

The simulation model of the harvester motion was based on kinematic equations which assumed that there was no wheel slip. It was believed that this assumption of no wheel slippage was valid since during actual operation of the harvester there was no wheel slippage observed. Also during tests with the harvester driving on a campus lawn, the harvester followed a curved row (121.9 m radius) effectively and this indicated that there was not a wheel slippage problem. To investigate the effects of inertia on the harvester motion, a preliminary study was done using a vehicle dynamic model that was developed by Ellis (1969). In this preliminary study (shown in Appendix C) it was concluded that there were negligible inertial effects on the motion of the apple harvester for speeds less than 6.4 km/h (4.0 mph). Therefore, kinematic equations should accurately predict the motion of the apple harvester. The kinematic equations that were used to simulate the harvester motion were developed by Shukla et al. (1970). They developed a set of kinematic differential equations which described the kinematic motion of a vehicle with front and rear wheel steer. Only front wheel steering was used on the apple harvester. It appeared that these equations by Shukla et al. had inconsistencies in the sign convention. This resulted in a vehicle response that was erroneous. Effective results were achieved by changing some of the arithmetic signs in these differential equations of

motion. The following equations were used to describe the harvester motion:

$$\dot{XA} = V1 \cos(SIGF + DELT) + \left[\sqrt{\left(\frac{Y12}{2}\right)^2 + (X17)^2} \cos\left(DELT - \arctan\left(2 * \frac{X17}{Y12}\right)\right) \right] (|DELT|) \tag{7.3}$$

$$\dot{YA} = -V1 \sin(SIGF + DELT) - \left[\sqrt{\left(\frac{Y12}{2}\right)^2 + (X17)^2} \sin\left(DELT - \arctan\left(2 * \frac{X17}{Y12}\right)\right) \right] (|DELT|) \tag{7.4}$$

$$\dot{DELT} = \frac{V1 \sin(SIGF)}{X13} \tag{7.5}$$

where

$\dot{XA}$ = X-component of velocity of point A (Figure 7.6) (cm/s)
$\dot{YA}$ = Y-component of velocity of point A (cm/s)
SIGF = front wheel steering angle (radians)
DELT = angle between the harvester centerline and the X-AXIS (radians)

Y12 = distance between the front wheel centerlines (cm)
X17 = distance that defines the position of point A (X17 was equal to zero) (cm)

X13 = distance between the front and rear wheel centerlines (cm)

These equations were integrated to determine the harvester's position relative to a fixed X - Y coordinate system. At the beginning of each

simulation the harvester was oriented such that the centerline of the harvester was parallel to the X-axis. The sign convention for the equations are defined in Figure 7.5.

Effective performance of these kinematic equations was checked by verifying that the predicted path of the harvester was a circle when the steering angle was held constant. The radius of the circular path was defined by the ideal steering geometry which was the basis for the development of the kinematic equations of motion. For a four wheel vehicle with front wheel steering Durstine (1966) explained that ideal steering geometry is defined as a condition where all four tires are oriented during a turn such that all four tires experience pure rollng about a point which is the vehicle's turning center. This condition is satisfied when the axes of rotation for the two front wheels meet at a common point on the line that is the axes of rotation for the rear wheels. Figure 7.5 shows that this common point is the vehicle's turning center. Note, Durstine (1965) explained that ideal steering geometry is often called Akermann Geometry. Figure 7.5 also shows the turning center for a vehicle turn assuming ideal steering geometry. The steering geometry as shown in Figure 7.5 conformed to the dimensions of the apple harvester. The vehicle turning radius was computed using a steering angle of 10 degrees. The computed radius of the circular path of point A which was on the harvester centerline was 2534 cm. The radius of the circular path as predicted by the differential equations of motion was 2532 cm. The computed radius for the path of point B at the rear of the harvester was 2501 cm and the predicted radius was

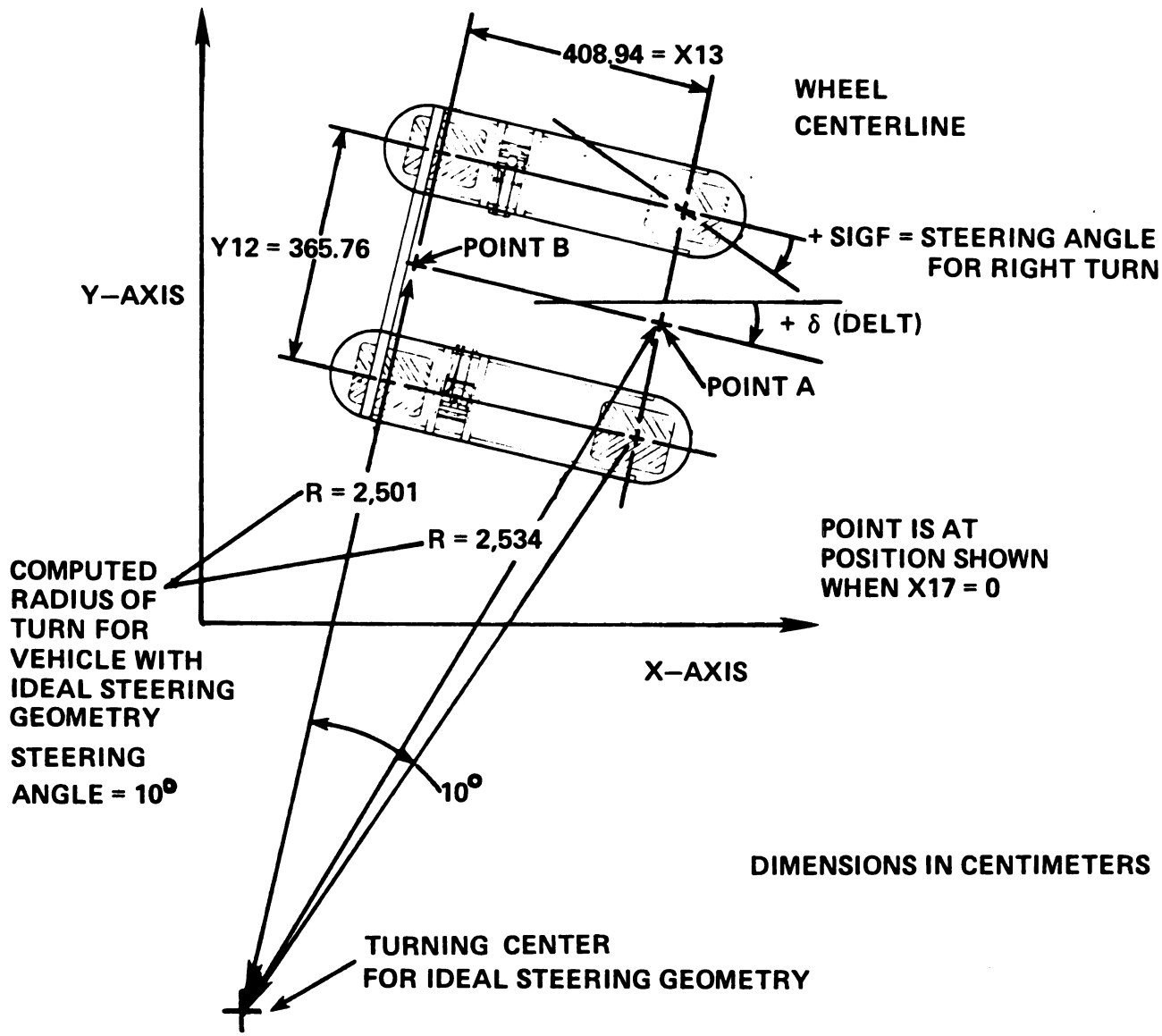

Figure 7.5 Diagram of the Harvester Steering Geometry

2497 cm. Note that the simulation program computed the X and Y coordinates of point B on the harvester centerline using the following geometrical equations:

$$XB = XA - X13\ COS(DELT) \tag{7.6}$$

$$YB = YA + X13\ SIN(DELT) \tag{7.7}$$

These results from the simulation indicated that the equations accurately described the harvester's kinematic motion.

7.2.3 Model Verification and Validation

The next phase of developing the harvester simulation model was verification that the model reasonably predicted the actual harvester motion. In order to accomplish this, data was collected during a test where the harveter was steered under computer control. The sensing system for this test was a sonar unit that was used to detect the position of a wooden fence. Figure 7.6 shows the position of the sonar on the harvester and it shows the position of the fence. For this test sonar and wheel position data were collected by the same computer that was controlling the steering. The data collection rate was 50 samples per second. This sampling rate was used because it was approximately twice as fast as the sonar measurement rate (21.7 Hz) and by using this sampling rate all the sonar values were recorded close to the time that the sonar value became valid. The steering controller was programmed to make any needed steering correction so that the harvester was kept centered over the fence while moving forward. The data from a typical test was plotted by a CalComp plotter and is shown in Figure 7.7.

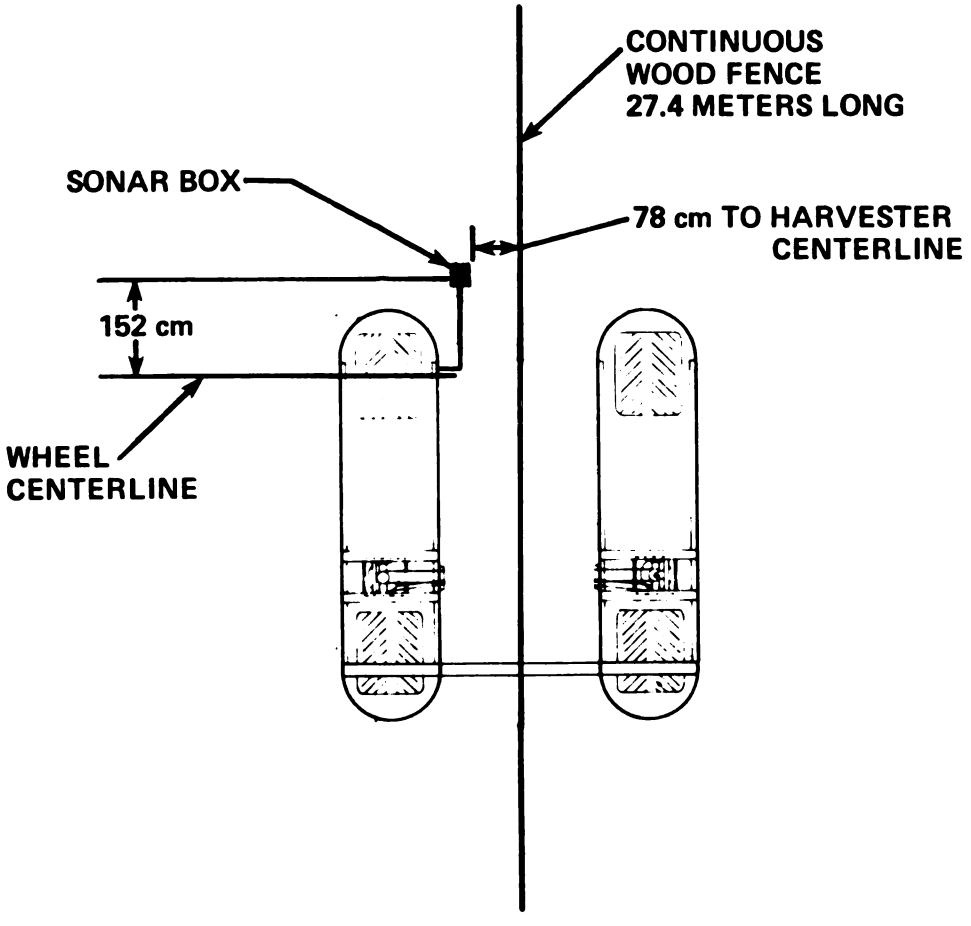

Figure 7.6 Diagram of Harvester for Data Collection Test

Figure 7.7 shows the data plotted with respect to time. Note that the data were plotted with the plotter pen held down so that the pen was continuously drawing as it moved to each data point. The wheel position in the data plot is the front wheel steering angle and a positive angle indicates the wheel was turned to the right. The sonar value in the data plot represents the sonar measurements (in centimeters) from the sonar unit to the wooden fence that was used in the test.

Notice in the data plot (Figure 7.7) that the sonar value slowly decreased and then a wheel turn was made under computer control. For this test the lower allowable sonar value of 78 was used by the steering controller. When the sonar value was lower than 78, a steering correction was made as shown in the data plot. The upper allowed sonar value was 83. It was observed during several test runs that the harvester slowly moved to the right while the wheels were held in the centered position. This was probably caused by misalignment of the front and rear wheels. Some adjustments were made to better align the wheels but the problem was not totally corrected. Next, a preliminary simulation model using the differential equations of motion was used to determine if the equations of motion simulated the motion observed in the test. The preliminary model was written to simulate the steering control system which used only one sonar unit as shown in Figure 7.6. Next, a check was made to determine if the simulation predicted the same harvester response as shown in the measured test data of Figure 7.7. To accomplish this, the model included the same control algorithm as was used by the harvester steering controller during the test. The control algorithm was written so that the harvester would follow the wooden fence. The algorithm for the controller also executed any necessary

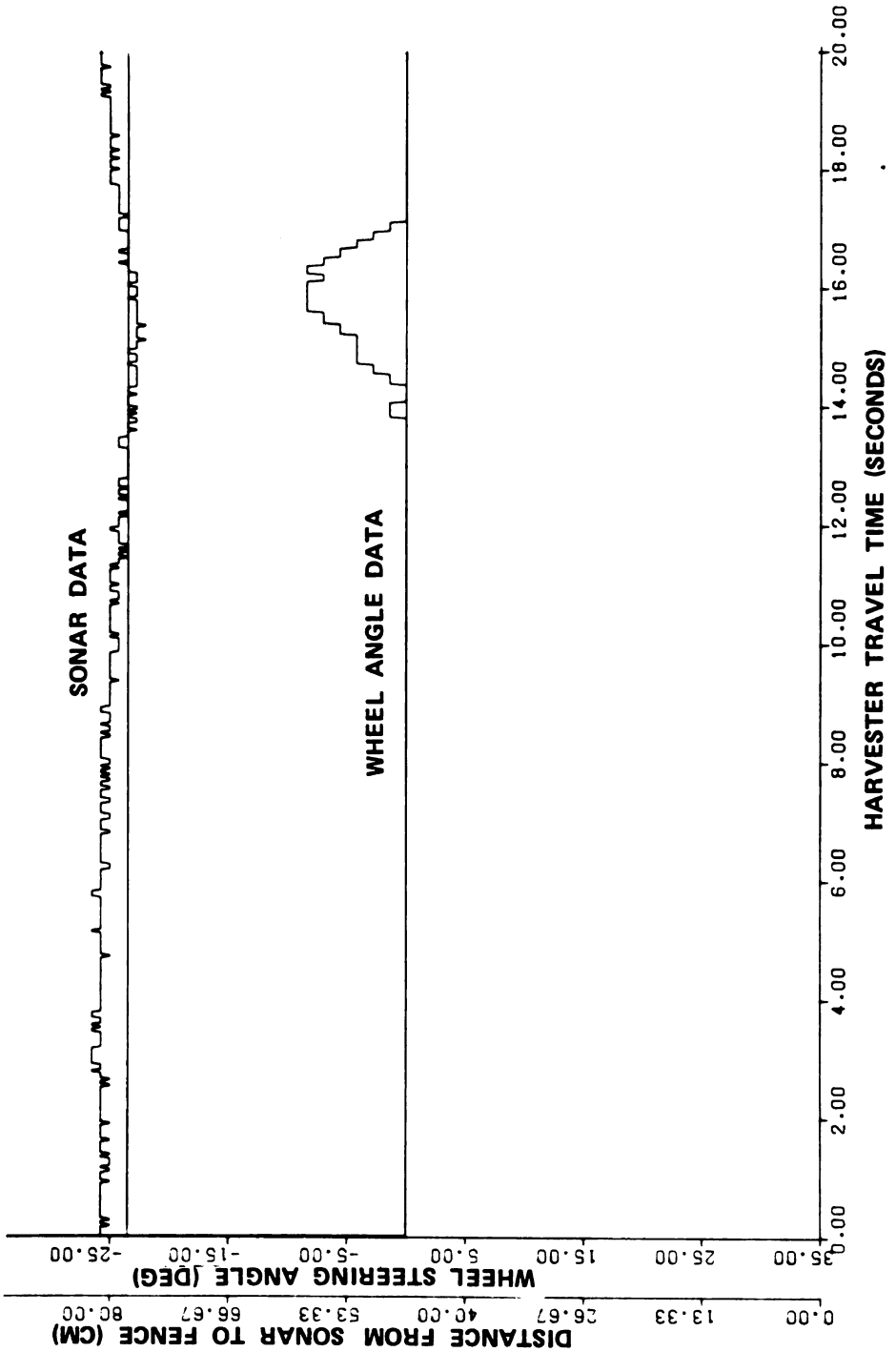

Figure 7.7 Sonar Data and Wheel Position from System Test at 0.8 km/hr using a continuous wooden fence

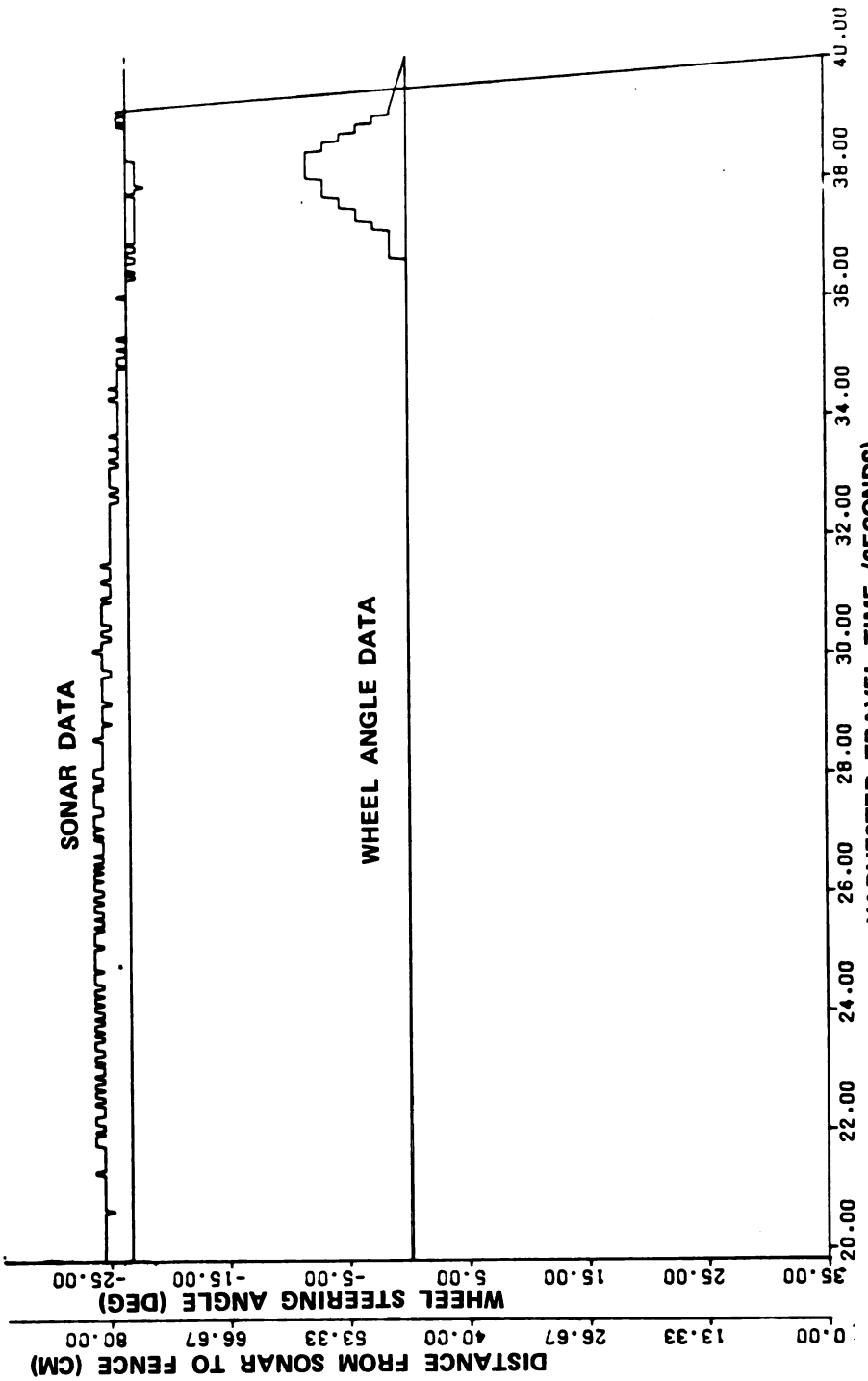

Figure 7.7 (continued)

steering correction to keep the harvester centered over the wooden fence. To approximate the harvester's wheel misalignment the model was programmed to use an initial harvester position offset. The offset coordinates for the harvester were; X = 0, Y = 3 cm and DELT = $+1^{o}$. This initial offset was necessary so the harvester during the simulation would move toward the fence and then over-shoot the fence. This over-shoot caused a steering correction so that the harvester could restore correct alignment with the fence.

The results of the simulation showed that the harvester very quickly became aligned with the fence and that very small steering correction was required. The test data as shown in Figure 7.7 shows that a significant wheel turn was executed during the test and the harvester responded slowly as seen by the slow change of the measured sonar values. The simulation showed that the sonar values changed very quickly when the steering correction was executed. Therefore, it was believed that due to the tire characteristics on the harvester, there was a delay in the response of the harvester. Also, any "play" in the mechanical steering linkage may delay the wheels steering to the full steering angle as measured by the wheel shaft encoder. To slow down the steering responsiveness of the model, a first order delay of the front wheel steering angle was incorporated into the model.

In order to delay the steering response of the harvester for the model, a first order differential equation was used to delay the change of the front wheel steering angle during the simulation.

The model was programmed with the equation:

$$T \dot{Q}_o + Q_o = Q_i \tag{7.8}$$

where Q_o = delayed steering angle (rad)

Q_i = steering angle (input) (rad)

T = time constant (seconds)

The value for Q_i was the value for the steering angle that resulted from the microprocessor routine when it directed a wheel turn. The microprocessor routine was programmed so that the wheels turned at 7.0 degrees per second. The value of Q_o was the delayed steering angle and this steering angle was the input to the differential equations of motion for the harvester. The solution of Equation 7.8 was programmed in the model as a difference equation which is also called the solution equation for a discrete-time system. This type of equation is explained by Bibbero (1977) and by Swisher (1976). The difference equation for the solution of Equation 7.8 is:

$$Q_o(n) = Q_o(n-1) + \frac{Ts}{T_s+T} \left(Q_i - Q_o(n-1)\right) \tag{7.9}$$

where T_s = time step interval = 0.01 seconds

T = time constant (seconds)

$Q_o(n)$ = current value for Q_o

$Q_o(n-1)$ = previous value for Q_o

The delayed value for steering angle, Q_o, was usually a smaller value than Q_i. Therefore, when this smaller value for Q_o was used in the equations of motion, the instantaneous velocity in the Y-direction was smaller for point A on the harvester (Figure 7.5). The results of the simulation showed a good match with the measured data of Figure 7.7 when the time constant for Equations 7.8 and 7.9 was 2.0 seconds. Therefore, based on these results it was believed that the simulation was a reasonable approximation of the harvester motion with an automatic steering control system. Also, this first order delay of the front wheel steering angle was selected as a means to make the harvester motion program a valid model. A time constant value of 2.0 seconds was selected for the completed simulation model.

The following is a description of the completed model to simulate the harvester motion. The harvester motion routine also simulated the sonar sensing system which was mounted on the harvester as shown in Figure 5.1. The sensing system measured the distance to the trees. Information on the coordinate positions of the trees was stored in a data file. Figure 7.8 shows a flow chart of the main functions of the harvester motion simulation model. Note that in this flow chart, the computer model was also developed to simulate the complete sonar sensing system which included five sonar units as shown in Figure 5.1. The main function of the sensing system was to measure the distance to the tree trunk. The X-Y coordinates for each tree trunk were used to compute the distance from the sonar unit to the tree. The first step of the flow chart (Figure 7.8) was to increment or decrement the front wheel position (steering angle) by 0.07 degree when the simulation directed the wheels to turn to a new position. This value of 0.07 degree was

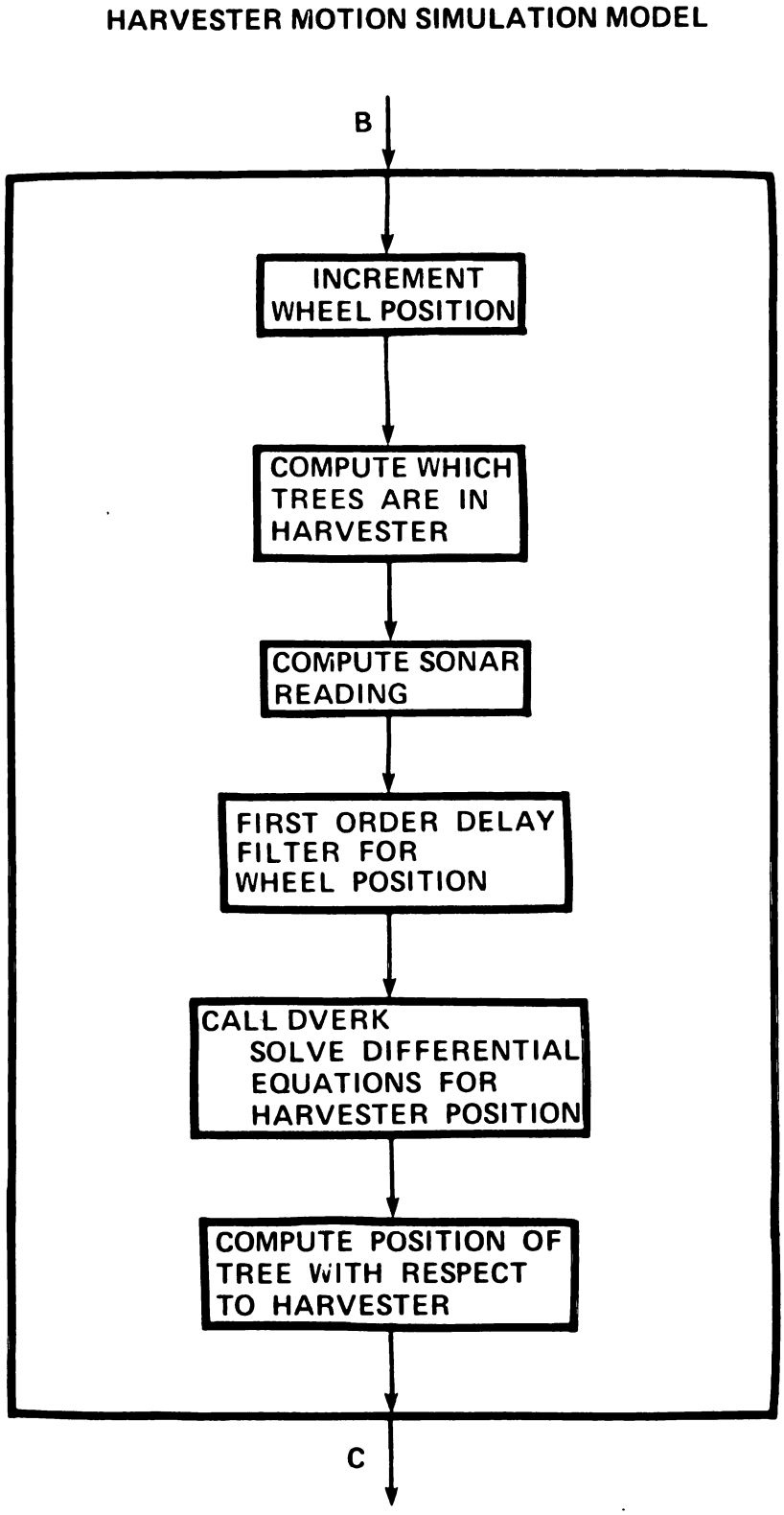

Figure 7.8 Flow Chart of Harvester Motion Simulation

used because the wheel turn rate was 7.0 degree per second and the wheel steering angle can only change by 0.07 degree during a single time step in the simulation. The time step was equal to 0.01 second. Next, the program determined which tree and which sonar unit would be used to compute the sonar measurement. The program then computed the sonar measurement. Geometrical equations were used to compute the sonar measurement. This computation for sonar measurements was based on the current position of the harvester and the position of the tree trunk. Since the actual sensing system made sonar measurements every 0.046 second, the program only computed the sonar value every 0.04 second. The next function of the simulation model was the computation of the first order delay of the front wheel steering angle using equation 7.9. The output of the first order delays was a delayed wheel steering angle and it was used as the input to the harvester's differential equations of motion. The final function of this routine was the computation of the tree trunk positon relative to the harvester. This relative tree position was used to plot the location of the tree trunks for a Mode 2 graphical output. The harvester velocity was 0.8 km/h (0.5 mph) during simulation.

7.3 Simulation Results

The simulation was used to determine the value for the parameters of the steering control algorithm which was described by Equation 7.2. The simulation was used to determine values for the parameters K and A. The parameter K is the proportional gain factor and A is the value of the allowable tree position error as discussed in Chapter 5. Other major parameters of the steering control system could be changed if needed for effective control, but for this study the simulation used a

wheel turn rate of 7.0 degrees per second and used sonar configuration as defined in Figure 5.1. The harvester velocity was kept fixed at 0.8 km/h. The tree trunks for this simulation were positioned in an alternating pattern with Y-coordinate position of either Y = +8cm or Y = -8 cm. The value of $\pm$8 cm of tree offset from the X-axis (which was the tree centerline) was selected to test the harvester's steering control system stability during simulation. The value of $\pm$8 cm was used because this 8 cm of tree offset was close to the maximum amount of allowable tree offset that was described in the design requirements (Chapter 3). Although, this alternating pattern of tree positions with $\pm$8 cm offset represented a tree row with tree offset that was more severe than was specified by the design requirements. The trees were spaced in the X-direction with 305 cm of space between trees which was the spacing specified by the design requirement. The results from the simulation showed that the control system was unstable and the output is shown in Figure 7.1 and 7.2. Inspection of these figures shows that the control system was <u>not</u> effective in keeping the harvester centered on each tree trunk.

Next, in order to make the control system stable, the variable K was changed to K = 0.5 and all other variables remained unchanged. The simulation results are shown in Figures 7.9 and 7.10. In these two figures it can be seen that the steering control system was effective at maintaining the proper alignment on each tree. Figure 7.10 shows that each tree moved through the center portion of the harvester's allowable zone and the maximum offset of the tree centerline from the harvester centerline was 8 cm. Based on these results the values of A = 2.0 and K = 0.5 for the steering control algorithm should cause the apple

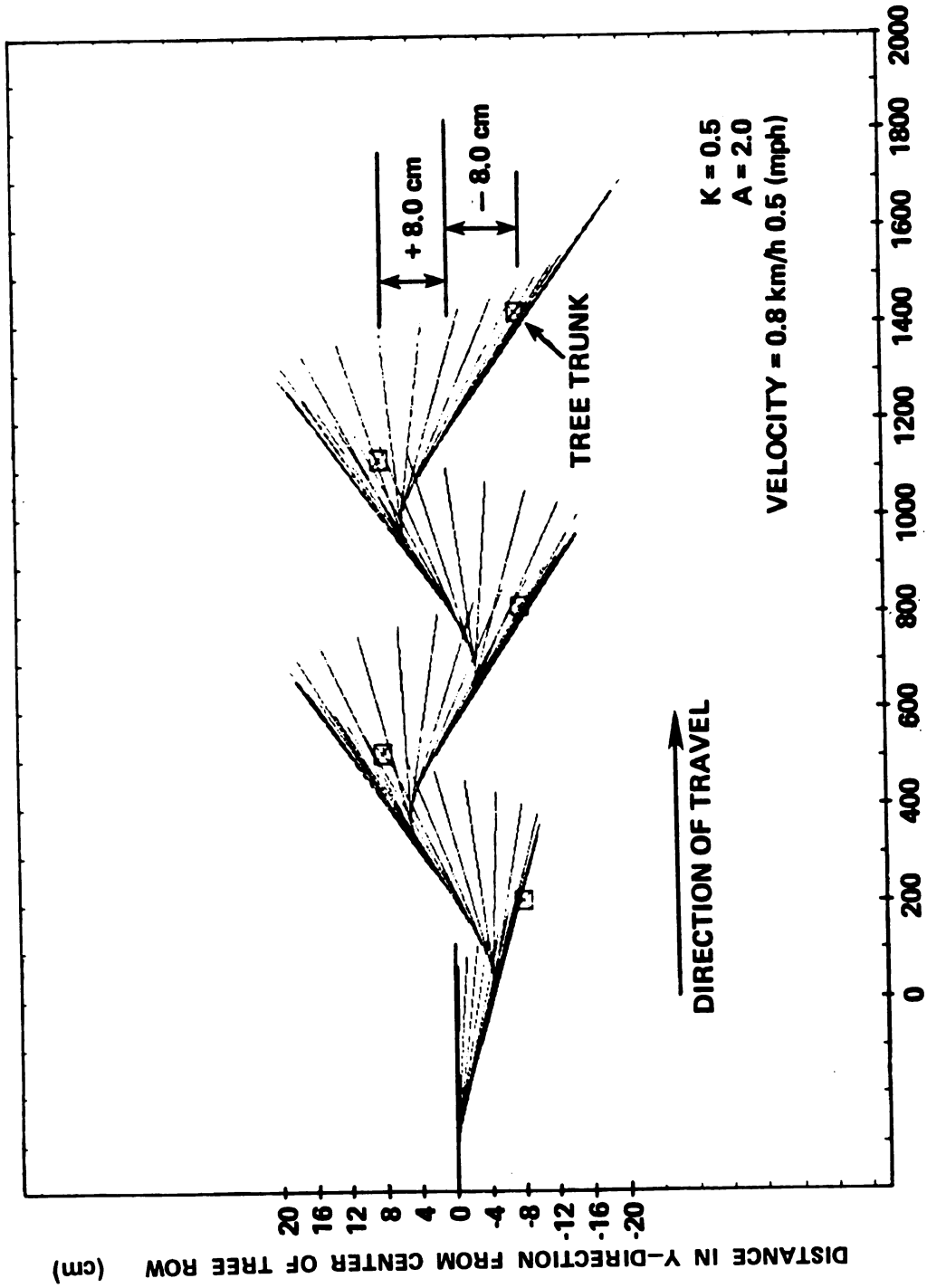

Figure 7.9 Graphical Output of Simulation-Mode 2 with K = 0.5

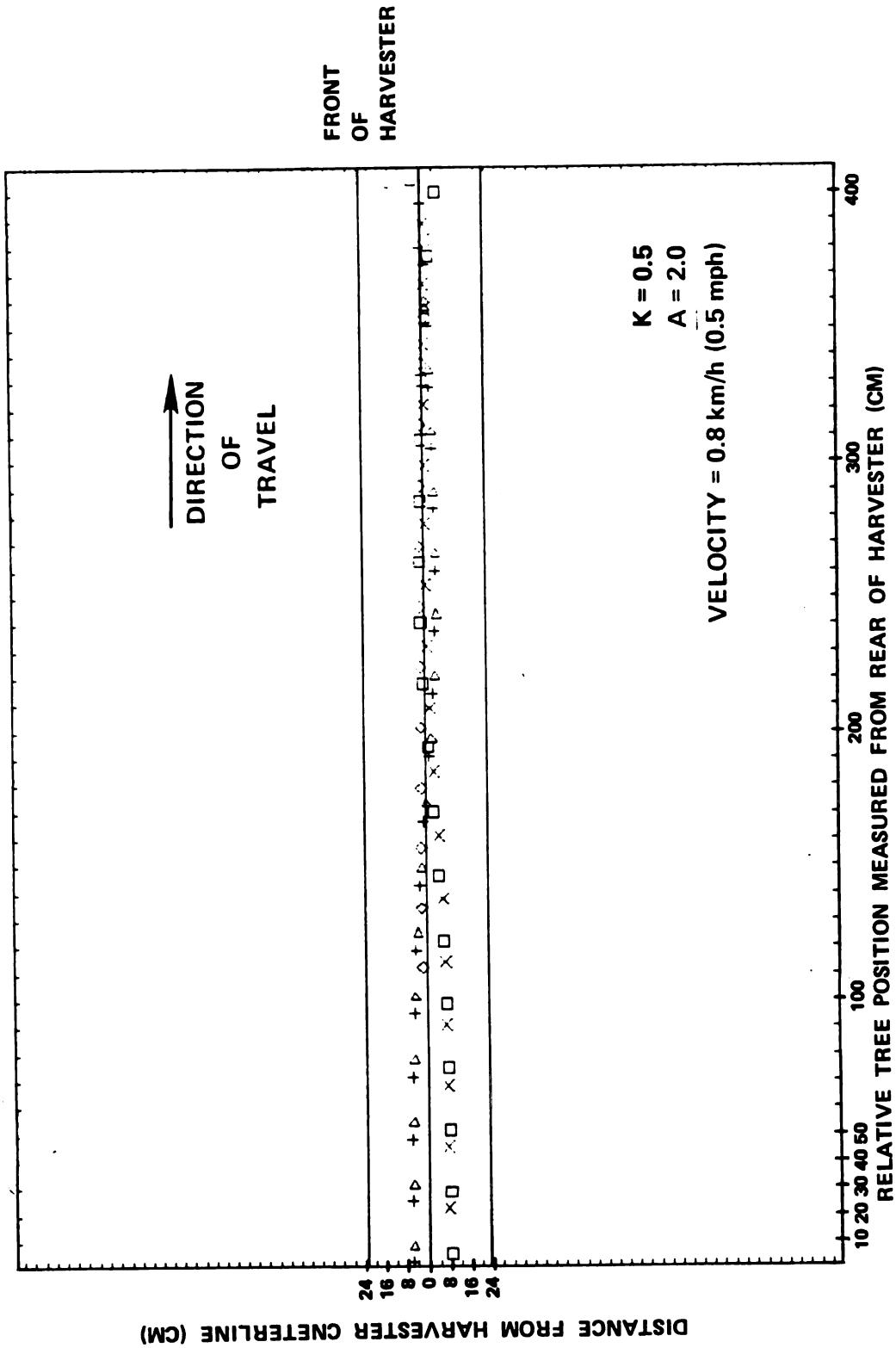

Figure 7.10 Graphical Output of Simulation - Mode 1 with K = 0.5

harvester to steer effectively at a ground speed of 0.8 km/h (0.5 mph). These values of A and K were selected for use in the controller for the actual harvester steering control system.

Another performance requirement for the harvester steering control system was that the harvester must follow a curved tree row. The minimum radius of curvature for the tree row was 121.9 m (400 ft). The simulation was run for a curved row with radius of curvature of 60.9 m. Figures 7.11 and 7.12 showed that the harvester during simulation followed the curved tree row effectively. The values of K = 0.5 and A = 2.0 cm were used in this simulation. Figure 7.12 shows the maximum offset of the harvester centerline from the tree trunk centerline is 13 cm. This maximum offset ocurred when the tree was leaving the back of the harvester. Figure 7.11 shows that this maximum offset occurred because the harvester was turning to align with the next tree in the row. Note that the sensing system was mounted in front of the harvester's front wheels and therefore steering corrections were executed before the tree entered the allowable zone of the harvester. This maximum tree offset was acceptable because the tree trunk stayed in the allowable tree zone. The simulation was also run for a row curvature of 121.9 m and the simulation showed that the harvester effectively followed the tree row.

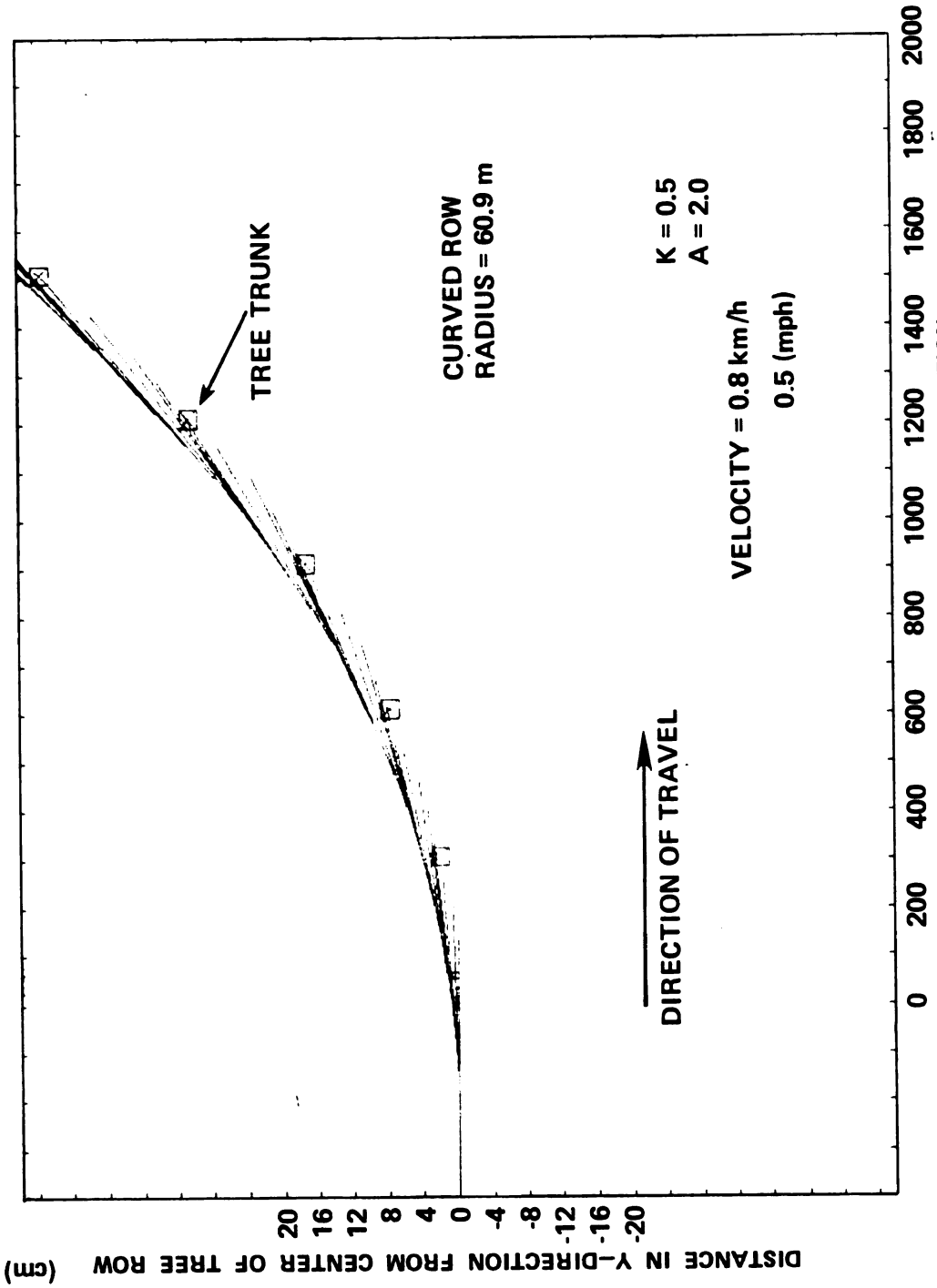

Figure 7.11 Graphical Output of Simulation - Mode 2 with K = 0.5

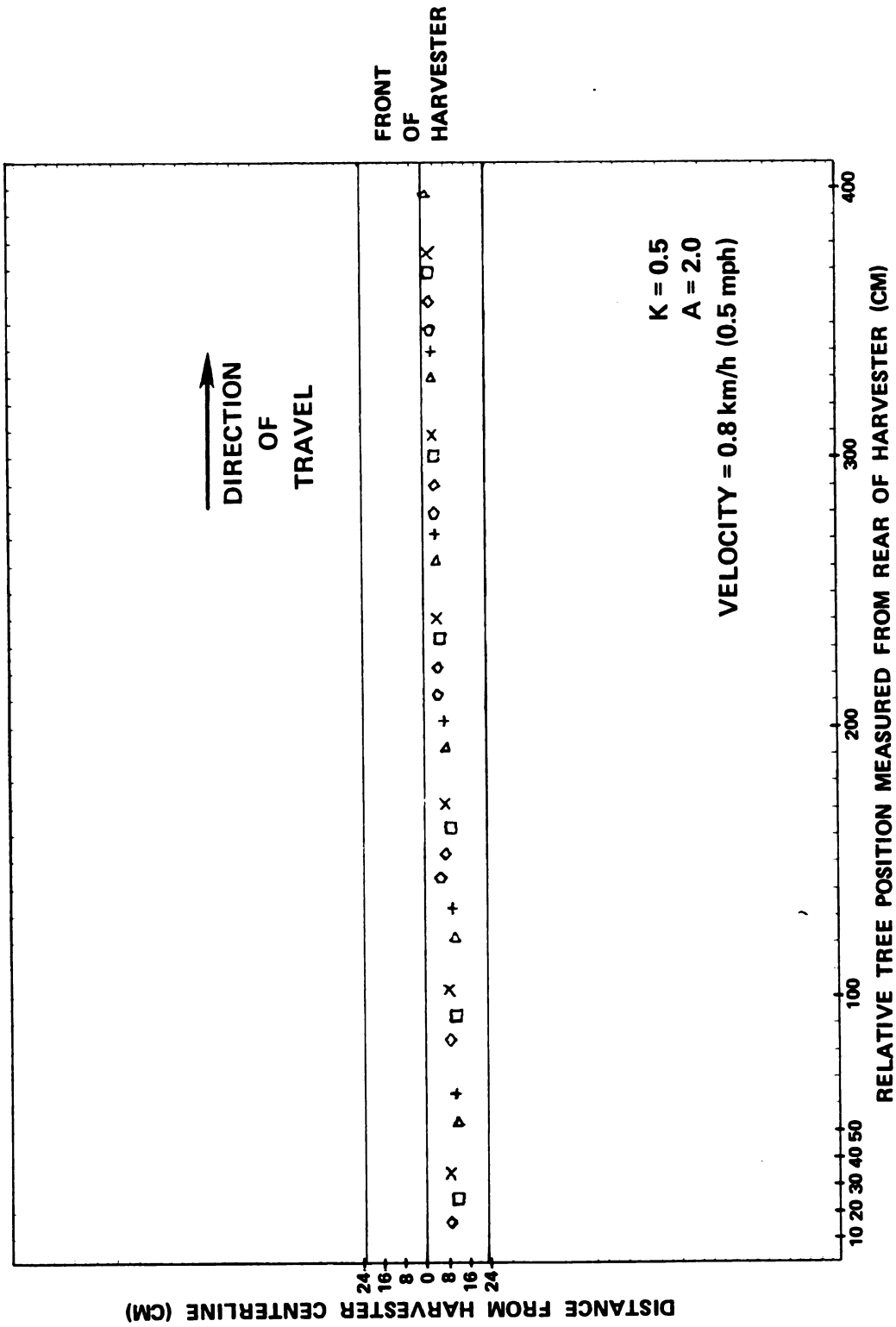

Figure 7.12 Graphical Output of Simulation - Mode 1 with K = 0.5

8. CONTROL SYSTEM SOFTWARE

The steering control system for the apple harvester used a microprocessor-based computer (model CDP18S694 by RCA) which contained an 1802 microprocessor. The software for the microprocessor was written in assembly language to perform the following functions:

1. Read the sonar distance measurement from the interface circuit. The measured value had dimensions in centimeters (Figure 5.2).
2. Read the front wheel angular position (a gray code number) from the shaft encoder.
3. Turn ON one of the five sonar units at the appropriate time.
4. Display on the video monitor the sonar measurement (cm), wheel position code (decimal number zero to 64), and sonar unit number for the sonar unit which made the sonar measurement.
5. Turn ON one of the two relays that cause the wheels to turn (steer) to a new position.
6. Compute tree position error according to Equation 5.1.
7. Compute the desired-wheel-position (D) according to Equation 5.2.

The software was written to perform these tasks using the control system which is shown in Figure 8.1. Figure 8.1 is a block diagram of the harvester's steering control system that was tested. Notice, that Figure 8.1 shows that the control system contains five solid state relays that were used to turn ON individually the 12 VDC power that was

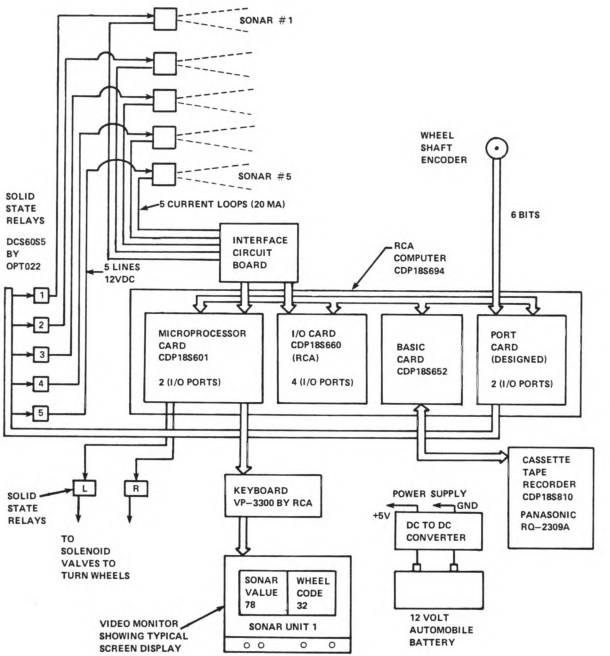

BLOCK DIAGRAM OF THE STEERING CONTROL SYSTEM

Figure 8.1 Block Diagram of the Steering Control System

required for each sonar unit. These relays were added to the original design of the control system (Figure 5.1) after the control system was tested. These relays were added because when all five of the sonar units were ON, then each sonar unit received sound pulses from the adjacent sonar units and this caused the sonar units to make false measurements. Thus, by activating the sonar units individually this problem was eliminated.

Often in developing microprocessor software for the control of machinery the "timing" is the most critical factor. The software must be developed to insure that each task or function is executed at the proper time. For the apple harvester's steering control system an important timing consideration was developing the software for controlling the steering of the front wheels. When the wheels were directed to turn, the program had to check the value of the current wheel position so that the wheels could be stopped at the correct position. When the program was running, the wheel position was checked about every 3 ms. Although during the operation of some portions of the program, the wheel position was checked more frequently. The developed software used a subroutine that read the wheel position and controlled the wheel turning by activating or deactivating two solid state relays that control wheel turning. This subroutine (Figure 8.2) was used in many places in the control program so there would not be any long time intervals between the execution of this subroutine because a long delay would cause the wheels to over-shoot the correct positon and then the wheels would have to be turned back to the other direction.

Another timing consideration for the software involved the display of information on the video monitor. A subroutine was written to

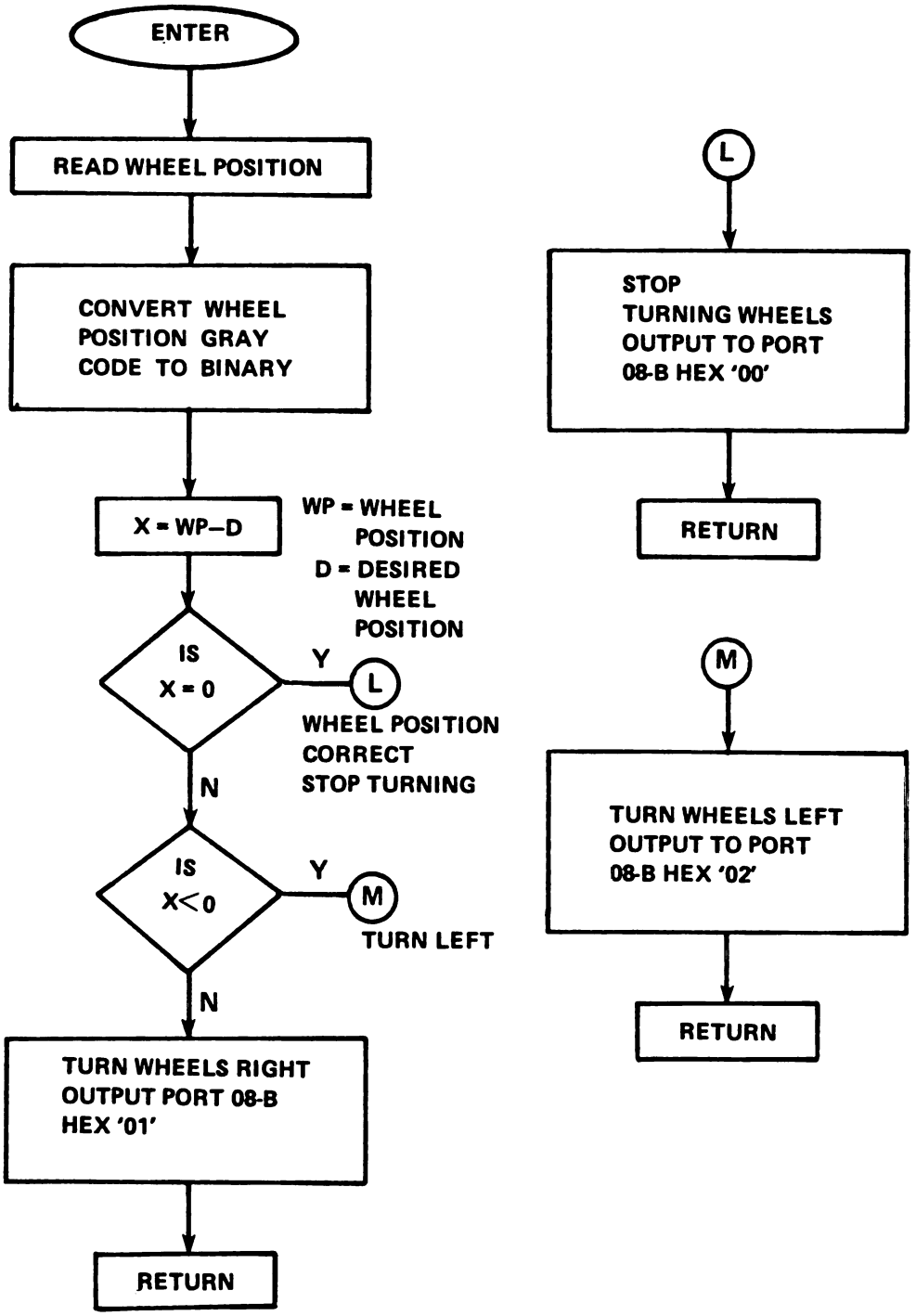

Figure 8.2 Flow Chart of the Computer Subroutine Used to Turn the Harvester Front Wheels

display three numbers on the video monitor. These three numbers were the measured sonar value, sonar unit number, and front wheel position code. These numbers were transmitted by the computer as serial data, at 1200 baud, to the keyboard and the keyboard transmitted this information to the video monitor. The time required to send these three numbers was about 0.2 second. The reason that this much time was used to display the data was that each number required five bytes of control information that was used to position the cursor on the video screen. Since the computer used 0.2 s to send the number to the video monitor, this subroutine for displaying the data was not called during the time the microprocessor was sampling the sonar data. This was done so that the executing of the display subroutine did not interfere with the sampling of the sonar data. If the display routine was called during the sampling of the sonar data, then some of the sonar data would not have been received because a new sonar value was transmitted to the computer about every 0.04 second. Figure 8.1 shows the format of the video monitor display.

Another timing consideration for the software development was the reading of the sonar measurement by the microprocessor. The program was written to read the sonar value from the interface circuit when the sonar data was received by the computer's input port. The interface circuit was designed to send a strobe pulse to the computer input port. The strobe pulse caused the sonar data (8 bits) to be latched into the port and caused one of the microprocessor's EF lines to change from HIGH to LOW. The computer used line EF1 and EF2 as sense lines and these lines were controlled by the six I/O ports on two computer cards, CDP 18S601 and CDP 18S660, shown in Figure 8.1. But, only one of these

six ports was enabled at any given time. A group number was used to enable one of these six ports.[6] Therefore before a sonar value was read a check was made to determine if the appropriate EF Line was low. If the EF line was low, the data was read by the microprocessor. When the data was read by the microprocessor, the input port integrated circuit (IC), CDP 1851, caused the EF signal to change from LOW to HIGH. In order to determine if a sonar value had been received, the EF line was checked to determine its logic state. The EF line was checked about 300 times per second. Thus, the sonar values were read into the microprocessor within approximately 0.003 second after the sonar value had been received by the computer input port.

Microprocessor timing considerations were not a problem when reading the value of the wheel position code. This wheel position code was a gray code number and thus the gray code value was only inaccurate by a value of one. This occurred because only one bit changed for each new gray code value and this change caused the gray code value to either increase or decrease by a value of one.

The flow chart of Figure 8.3 shows the major steps of the software that was developed for the harvester's steering control system. It can be seen in this flow chart that the subroutine for turning the wheels was called at several places in the program to insure that the turning of the wheels was done at the proper time. This computer program used the subroutie technique designated "Standard Call and Return" which was developed by the RCA Corporation for use with the 1802 microprocessor.

---

[6]The use of the group number is defined by the specification sheets for the computer card CDP 18S601 made by RCA.

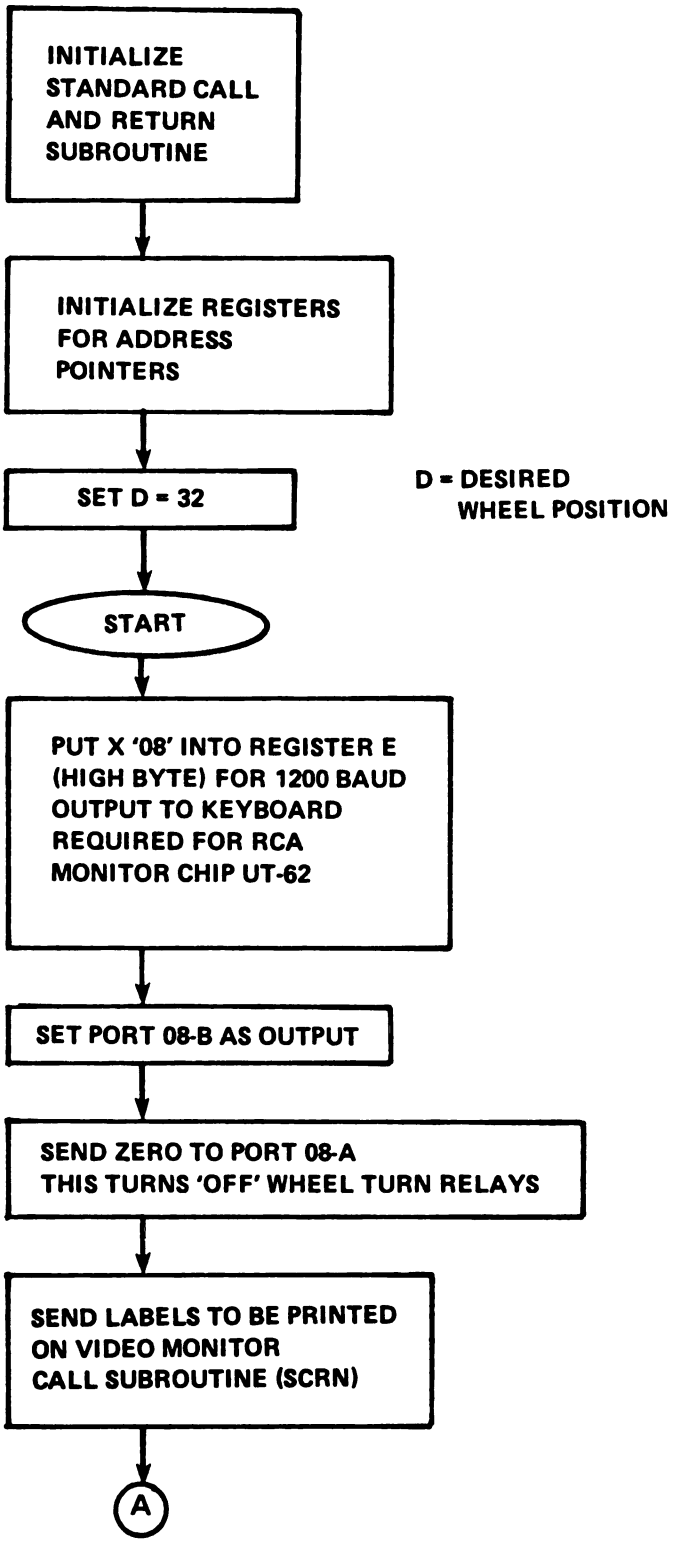

Figure 8.3 Flow Chart of the Steering Control Program for the 1802 Microprocessor

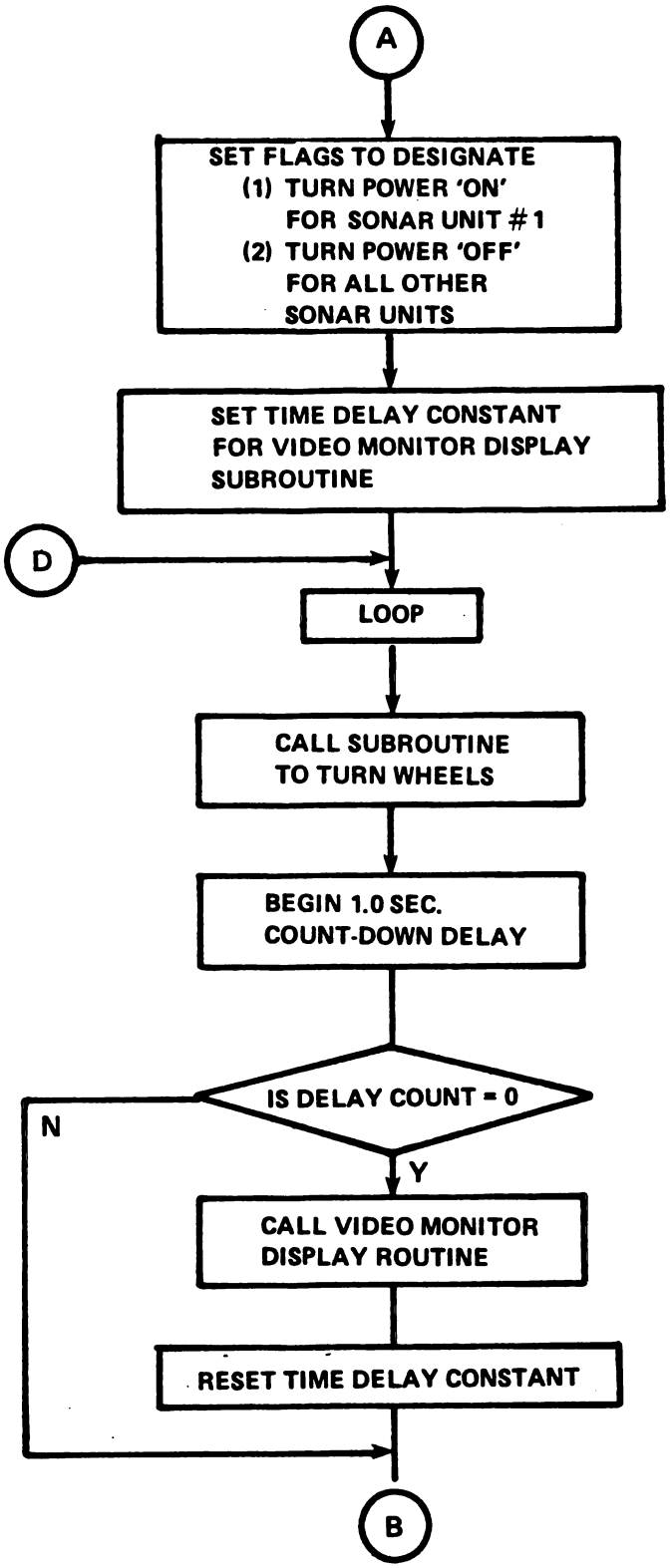

Figure 8.3 (Continued)

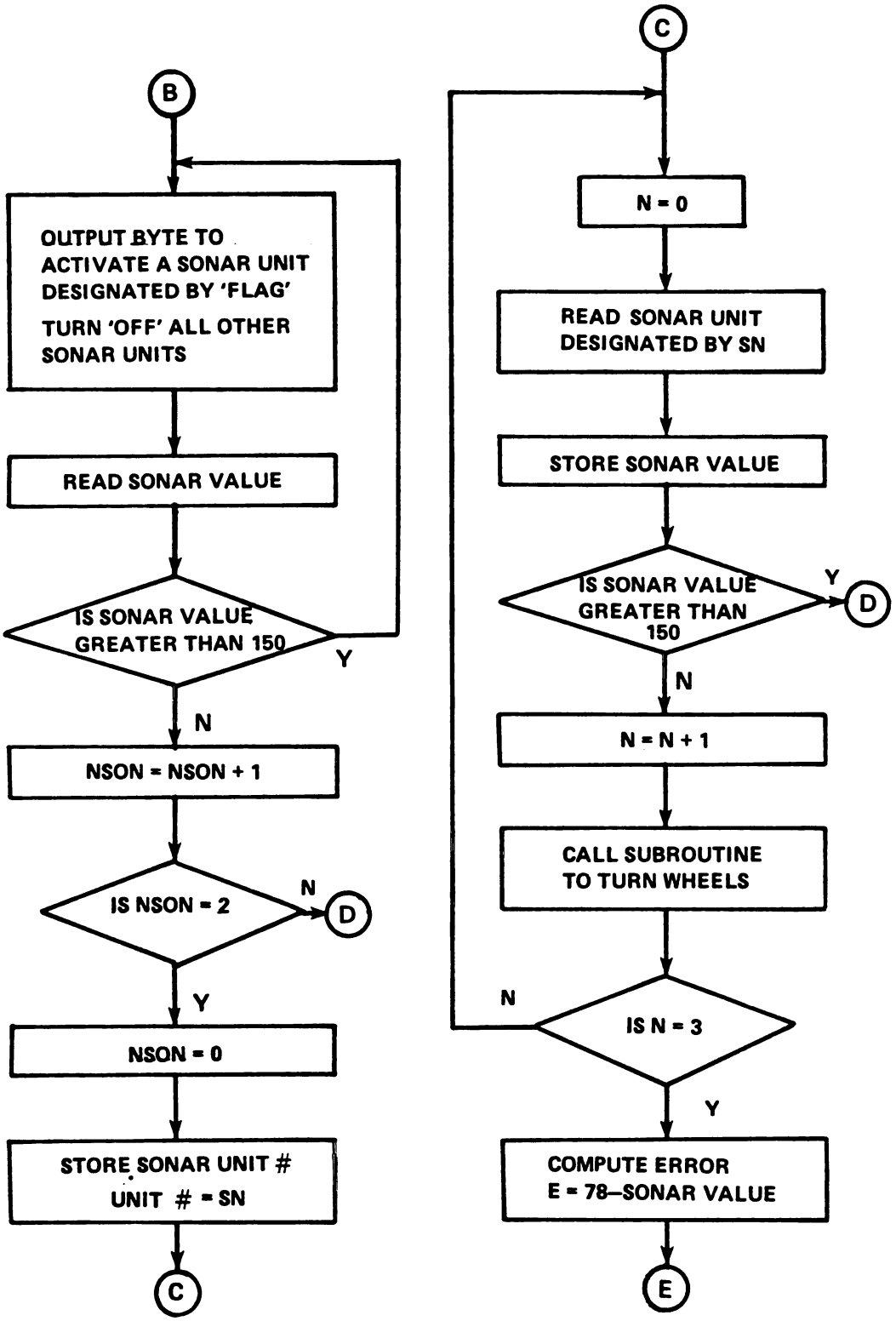

Figure 8.3 (Continued)

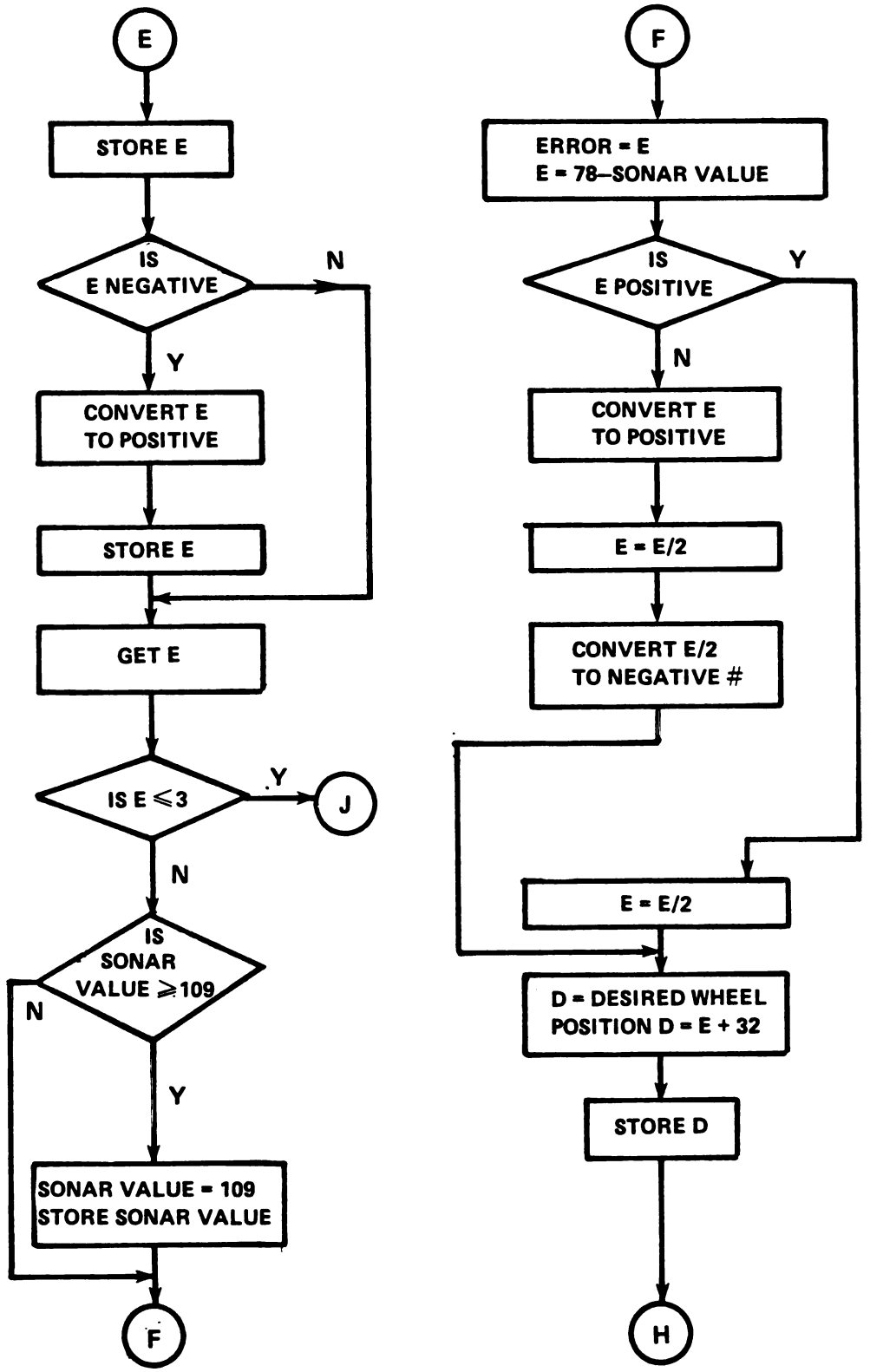

Figure 8.3 (Continued)

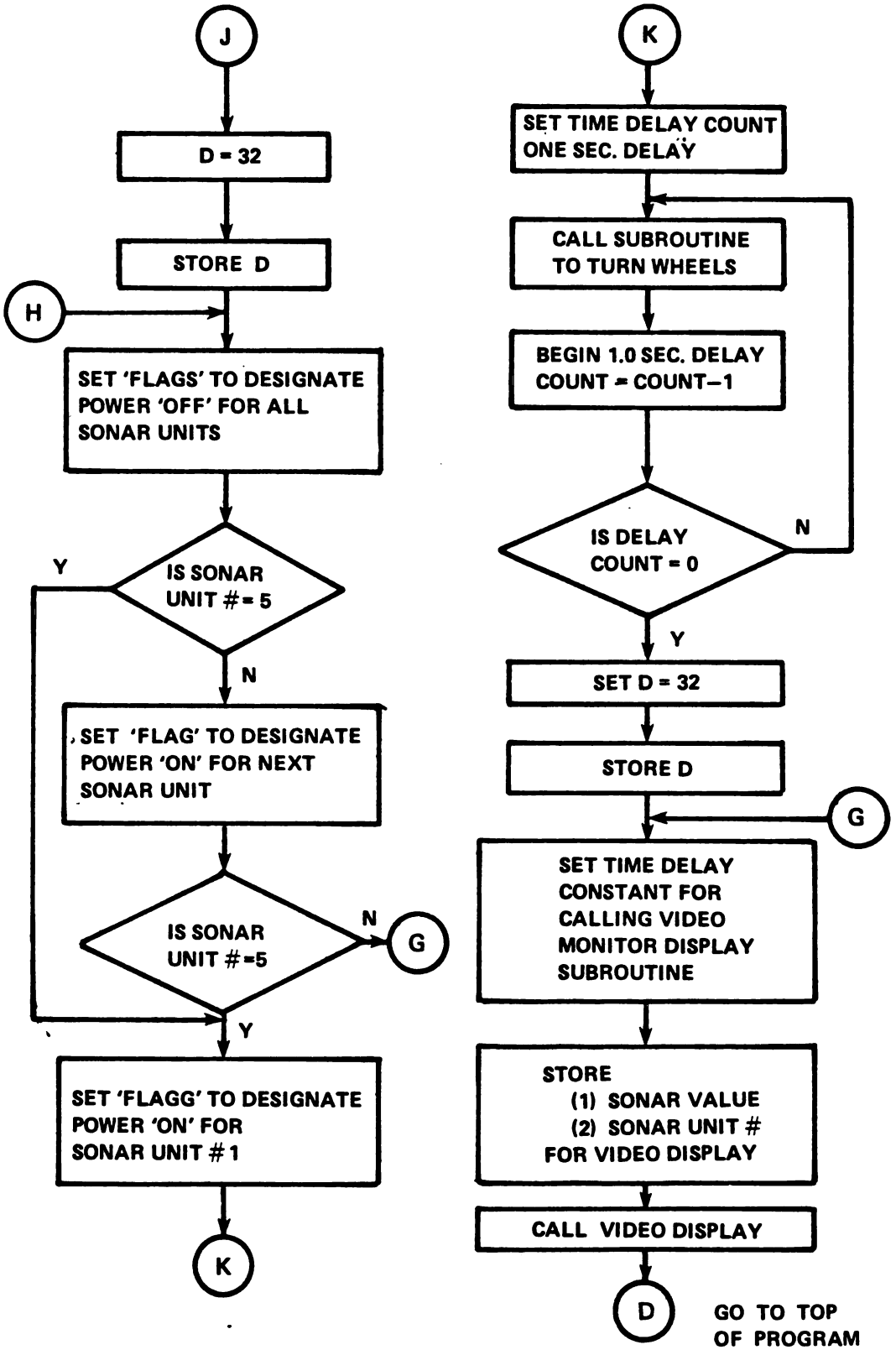

Figure 8.3 (Continued)

This program for the 1802 microprocessor was written to use the I/O ports on the computer cards CDP18S601 and CDP18S660. These two computer cards used six I/O ports, (CDP1851 made by RCA) and these ports required group numbers to be sent out to the port so that a specific port was enabled. Two additional ports were designed on a port card shown in the block diagram of Figure 8.1. This port card was designed to connect to the bus of the computer CDP18S694. These two ports that were designed on the port card shown in Figure 8.1 were designed so that they did not require a group number. The ports were used to receive wheel position code, and to send data for selecting a sonar unit. A sonar unit was selected by using one of the five lines from the port to turn ON one of five solid state relays. With a relay ON, 12 VDC power was sent to the sonar unit that was selected. Note, that a "dummy" group number must be sent before using the ports on the port card. This "dummy" group number was used to disable the other ports (CDP1851) on the other computer cards and this allowed I/O instructions to be executed to use the port card without affecting any of the ports using the CDP1851. A "dummy" group number was any allowable group number that did <u>not</u> activate a CDP1851. The port card used two port IC's (8212). Table 8.1 lists the function of each I/O port and the required group number for each port. Note that each port CDP1851 contains two 8 bit ports.

The computer program was also used to control the length of the time delay that was needed to obtain a valid sonar measurement. A time delay was used so that during the operation of the steering control system, time would be provided so that the tree trunk would be at a position well inside the sonar beam angle (Figure 6.12). This was done

to avoid the erroneous sonar mesurement that occurred when the object being measured was near the edge of the sonar sensing zone. Further investigation was done to determine the cause for these erroneous sonar measurements and the cause was related to inaccurate triggering of the Polaroid ultrasonic circuit due to a weak echo signal. The echo signal was weak when the object was near the edges of the sonar beam angle. This was determined by examining the Amplified Echo signal on the Polaroid ultrasonic circuit board. The signal was observed using an

Table 8.1 List of the Microprocessor I/O Ports

Port Function	Group Number Hexadecimal	Computer Card Designation	Operation Code Hexidecimal
Input Sonar I	20	CDP18S660	6E
Input Sonar 2	20	CDP18S660	6C
Input Sonar 3	10	CDP18S660	6E
Input Sonar 4	10	CDP18S660	6C
Input Sonar 5	08[1]	CDP18S601	6C
Output relays	08[1]	CDP18S601	6F
Input Wheel Code	None[2]	Port Card[3]	6F
Output Sonar Unit Selector	None[2]	Port Card[3]	63

[1]This port card was built and inserted into the bus on the computer CDP18S69A by RCA.

[2]To use these ports a "dummy" group number must be used to disable the other I/O ports.

[3]The port card used port IC's 8212 and the other computer cards used port IC's CDP1851 by RCA.

osciloscope as the object was moved from side to side across the sonar sensing zone perpendicular to the sonar beam centerline. Thus, the program was written to delay use of the measured sonar value until the tree trunk was inside the sonar sensing zone (away from the edge of the sonar beam).

The computer program was written to delay computation of the tree position until five sonar measurements which were less than 150 cm were read by the computer. This was done to allow more time for the tree trunk to move further into the sonar sensing zone. The first step in obtaining a valid sonar value was the sampling of sonar values until a value less than 150 cm was obtained. Sonar values less than 150 cm were used to indicate that the tree had entered the sonar beam angle. After two sonar values (less than 150 cm) were read, the computer program then required that three sonar measurements in sucession be made and the third value was used to compute tree position. If one of these values was larger than 150 then the program would not compute the tree position. If one of these three sonar values was greater than 150, then the computer stopped executing this portion of the program and returned back to the top of the program and started the sequence again to obtain a valid sonar measurement. This program sequence was used to avoid getting false sonar values, because a sonar value greater than 150 cm indicated that a tree trunk was not in the sensing zone. If all five sonar values were less than 150 cm then there was a time delay from the first sonar reading to the fifth sonar reading of approximately 0.18 second. If the harvester had a ground speed of 22.3 cm/s (0.8 km/h), the tree trunk would move into the sonar sensing zone a distance of 4.1 cm which is approximately 27 percent of the distance from the edge of

sonar beam to beam centerline. Also, by using this small time delay the harvester ground speed could be increased and a valid sonar value could be obtained while a tree is still inside the beam angle. Note that if the sonar is 78 cm from the tree trunk and the sonar beam angle is 22^{o} then the width of the sonar beam is 30.3 cm at a distance 78 cm from the sonar unit. If the harvester is moving at 134 cm/sec (3 mph) then the tree moves across the sensng zone in 0.22 seconds. Since the sonar measurements are made every $0.046 \pm .004$ second then there would only be time to obtain four sonar values while the tree trunk moved across the sonar sensing zone. The speed of 134 cm/s is the speed used by the harvester during the spraying operation. Thus, software must be developed to process the sonar readings when the harvester speed is higher than 22.3 cm/s.

The software for the steering control system was developed to read the sonar unit, compute tree position error, and compute the desired wheel position code (D). The sonar units were read in successive order beginning with sonar unit number one (Figure 5.1). During the operation of the steering control system, a tree trunk entered the sensing zone of sonar unit number one and a valid sonar value was obtained. Next the tree position error was computed and the value of D was computed. The front wheels were then directed to turn to the wheel position code that was equal to the value of D. The wheels stayed at this position until the next value of D was computed. After the tree position error and the value for D was computed for sonar unit one, then sonar unit one was turned OFF and sonar unit two was turned ON. This was done by turning ON one of the five solid state relays which supplied 12 VDC power to the proper sonar unit. Sonar unit two stayed ON until the tree position

error and a value for D was computed. This process continued for sonar units three and four. When sonar unit four was turned OFF, sonar unit five was turned ON. Next, using the sonar value from unit 5, the tree position error was computed and the value for D was computed. Since sonar unit five was the last sonar unit in the set of five units, a different program sequence was then executed. This program sequence allowed 1 second of time for the wheels to move to the desired wheel position. Since the wheels usually did not require a full second of time to get to the desired wheel position, the wheels stopped at the desired wheel position and stayed at that position until the 1 second time interval had elapsed. Next at the end of this time interval the wheels were directed to turn back to the centered position (zero steering angle). This was followed by turning OFF sonar unit five and turning ON sonar unit 1.

This method of reading the sonar units in succession was based on the assumption that a position measurement will always be obtained by each sonar unit for every tree. This assumption was based on preliminary tests in the lab where sonar readings were recorded as an object was moved across the sensing zone. These tests indicated that the sonar circuit was reliable when the object was inside the sensing zone. Also during tests described in Chapter 9, all sonar units always gave enough values to the microprocessor so that the tree position was computed. There were problems with the accuracy of some of the sonar readings and this will be discussed in Chapter 9.

After the controller had obtained a valid sonar value, this value was used to compute the tree position error. This was done for each sonar unit. The flow chart of Figure 8.2 shows the steps that were used

to compute the tree position error. Before the desired wheel position was computed a check was made to determine if the tree position error was greater than 2 cm. This value of 2 cm was the value for allowable tree position error (A) that was described in Chapter 7. This value of A = $\pm$2 cm was selected for use in the microprocessor control algorithm based on satisfactory results from the simulation model. In the microprocessor control program, if the absolute value of the position error was greater than 2 cm, then the program proceeded to compute D, and if the absolute error was two or less then D was set equal to the value 32. The value of D was used by the wheel-turn subroutine to turn the wheels to the straight-ahead position (zero steering angle). The program computed the tree position error acording to Equation 5.1. After the error was computed then the program computed the value for D according to Equation 5.2. Note, in the flow chart (Figure 8.3) the program checked the magnitude of the sonar value and if it was greater than 109 cm then the sonar value was changed to 109 cm. This was done to prevent addition-overflow when the value for D was computed. Note, that the program stored sonar values up to this value of 109 cm. Thus, if the measured sonar value was greater than 109 then the video monitor displayed the value 109 instead of the actual sonar measured value.

The software and hardware were debugged using several methods. First the interactive software simulator (developed by RCA) was used to simulate the assembly language program and this simulator provided a printed output of the operations of the program. The simulator was a FORTRAN program which was run on the Michigan State University's main computer (CDC Cyber 750). This simulator was effective for debugging a large portion of the program. Next an electronic simulator was used to

run the program in the real-time mode. This electronic simulator contained all of the electronic components that were used on the harvester's control system. To simulate the harvester's wheel motion, the simulator used a small electric motor to turn a wheel position shaft encoder. The microprocessor-based controller activated the motor so that the motor's shaft turned in the proper direction and this caused the shaft encoder to be turned in the same manner that occurred on the actual harvester. With this electronic simulator the control lines were observed on an oscilloscope while the microprocessor was running and this helped to find errors in the program. Also, a "single-stepper" computer board (Model CDP18S640 by RCA) was used to single-step the microprocessor through critical portions of the program and this helped to find errors in the program. The video monitor also was helpful in debugging the program and the hardware. The video monitor displayed the values for the sonar measurement, wheel position and sonar unit number. The information on the video display was useful in determining if the control system was operating effectively. If the video display showed any numbers which were out of the normal range then this indicated there was a problem with the operation of the control system. Many times there were problems with the connectors for the signal lines and the video display monitor was very helpful in solving those problems. This video monitor was useful for debugging the circuits and software for the electronic simulator that was tested in the laboratory. During operation of the control system on the harvester the video display of data was very useful for debugging and for monitoring the performance of the control system.

9.0 PERFORMANCE TESTS AND RESULTS

The steering control system was tested to determine its performance by examining the alignment of the harvester as it moved over the row. To facilitate the testing procedure, the performance tests were done on a concrete driveway and on a campus lawn. In order to simulate the tree trunks for a tree row, a simulated "tree stand" was made and these tree stands were used for all control system performance tests. Figure 9.1 shows the dimensions of the tree stand. Tests were done on the campus lawn in order to determine the control system performance on a surface that had a lower coefficient of friction than the concrete driveway. The grass in the lawn had a height of 6 cm. The tests were done on a straight row of tree stands and on a curved row at a ground speed of 0.8 km/hr (0.5 mph). These test conditions were the design requirements for the steering control system. Another test was done to evaluate the response of the steering control system to a step-change in the tree row.

9.1 Configuration of the Steering Control System

The steering control system as described by Figure 5.1 and Figure 8.1 was tested using the computer program that was described in Chapter 8. After some preliminary tests were done, the harvester's front wheels were found to be turning to an angle larger than necessary for effective control. Thus a change was made to the electronic control system so that the wheels would turn to a smaller angle for a given

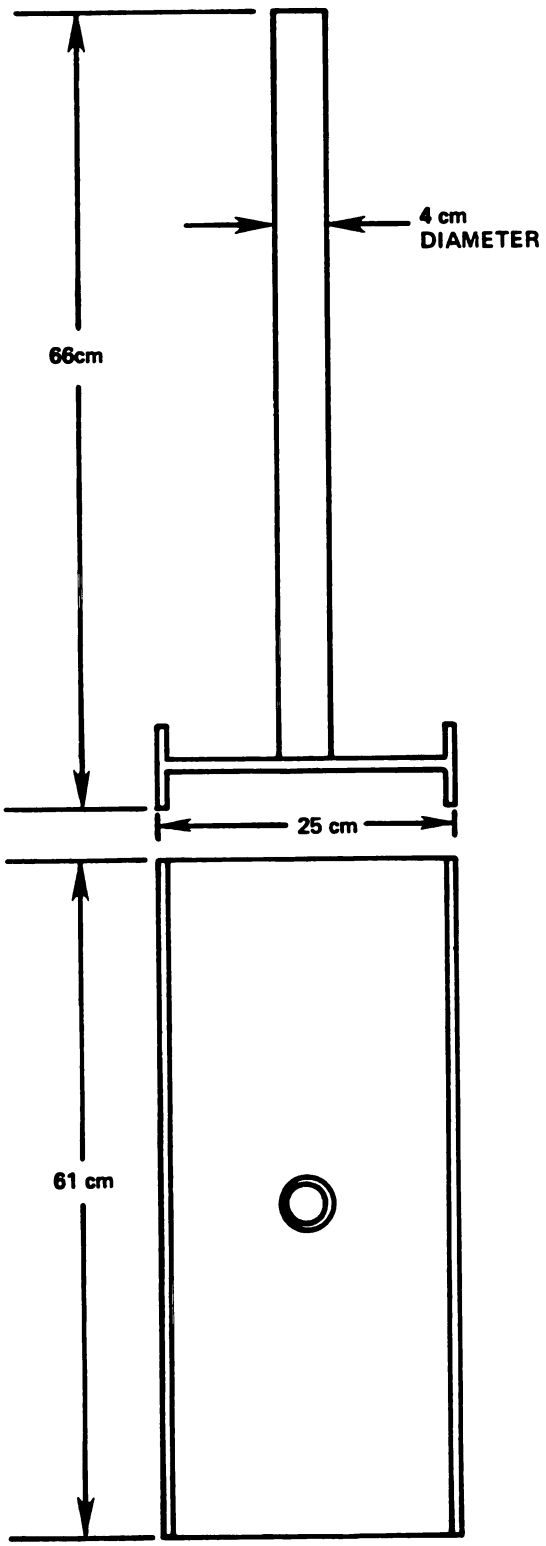

Figure 9.1 Diagram of Simulated Tree Stand Used in Steering Control System Tests

value of tree position error. This reduced the amplitude of oscilation of the front of the harvester. The change was made in the circuit where the wheel position data lines are connected to the wheel shaft encoder. The data lines were disconnected and then reconnected in a different order. Of the ten data lines available from the shaft encoder, lines numbered 2 through 7 were used as data inputs to the steering controller. Line number 1 represented the shaft encoder's least significant data bit. By making this change, the shaft on the shaft encoder rotated approximately 0.7 degree for each change in the value of the encoder's output number. Before this change was made the shaft rotated approximately 1.4 degrees for each change of the encoder's output code. Note, that the control algorithm was written to turn the wheel by one wheel position code for each 2 cm of tree position error. Thus, after the modification was completed the wheel rotated about 0.7 degree for each 2 cm of tree position error that was computed by the steering controller.

Another change was made to improve the reliability of making valid sonar measurements. A change was made to the software which provided a longer time delay for the microprocessor's measurement sequence for each sonar unit. This longer delay was used to allow sufficient time so that the tree stand would be more near the center of the sensing zone when the last sonar measurement in the program sequence was made. The computer program achieved a time delay initially by waiting until three sonar values were read in successive order. To make a longer time delay the progam was changed so that the microprocessor read six sonar values in successive order. The last sonar reading in this sequence was used to compute the tree position error. This change was made because a

sonar value of 109 cm was measured intermittently during the tests with a straight row. These sonar values of 109 cm were erroneous and they caused deviations from the typical path travel by the harvester. This software change was used for all tests except the straight row tests. Also, when the alternator was disconnected so that it was not charging the harvester's battery, the sonar measurements appeared to be more reliable. The alternator was disconnected during all of the curved row tests.

9.2 Test Procedure

To evaluate the alignment of the harvester with each tree stand as the harvester moved over the row, data was needed that described the path traveled by the harvester. This data was obtained by attaching felt-tip pens to the harvester's frame and these pens drew lines on a long paper strip to record the path of the harvester. These pens were attached using a mechanical linkage as shown in Figure 9.2. This linkage used a hinge so that as the harvester frame moved up or down the pen would stay in contact with the paper. A small caster wheel was used to support the weight of the linkage arm. Each pen was supported in a steel tube and a small spring pressed on the top of the pen so that there was a small force downward on the pen to keep the pen in contact with the paper. Two pens were attached to the frame of the harvester so that data could be obtained for the path of the front and rear of the harvester. Figure 9.3 shows a plan view of the harvester and shows that the pens were located at each of the wheel centerlines. The pens were positioned so that they were offset 60 cm from the harvester's centerline to provide clearance so the tree stands could pass through the center space of the harvester.

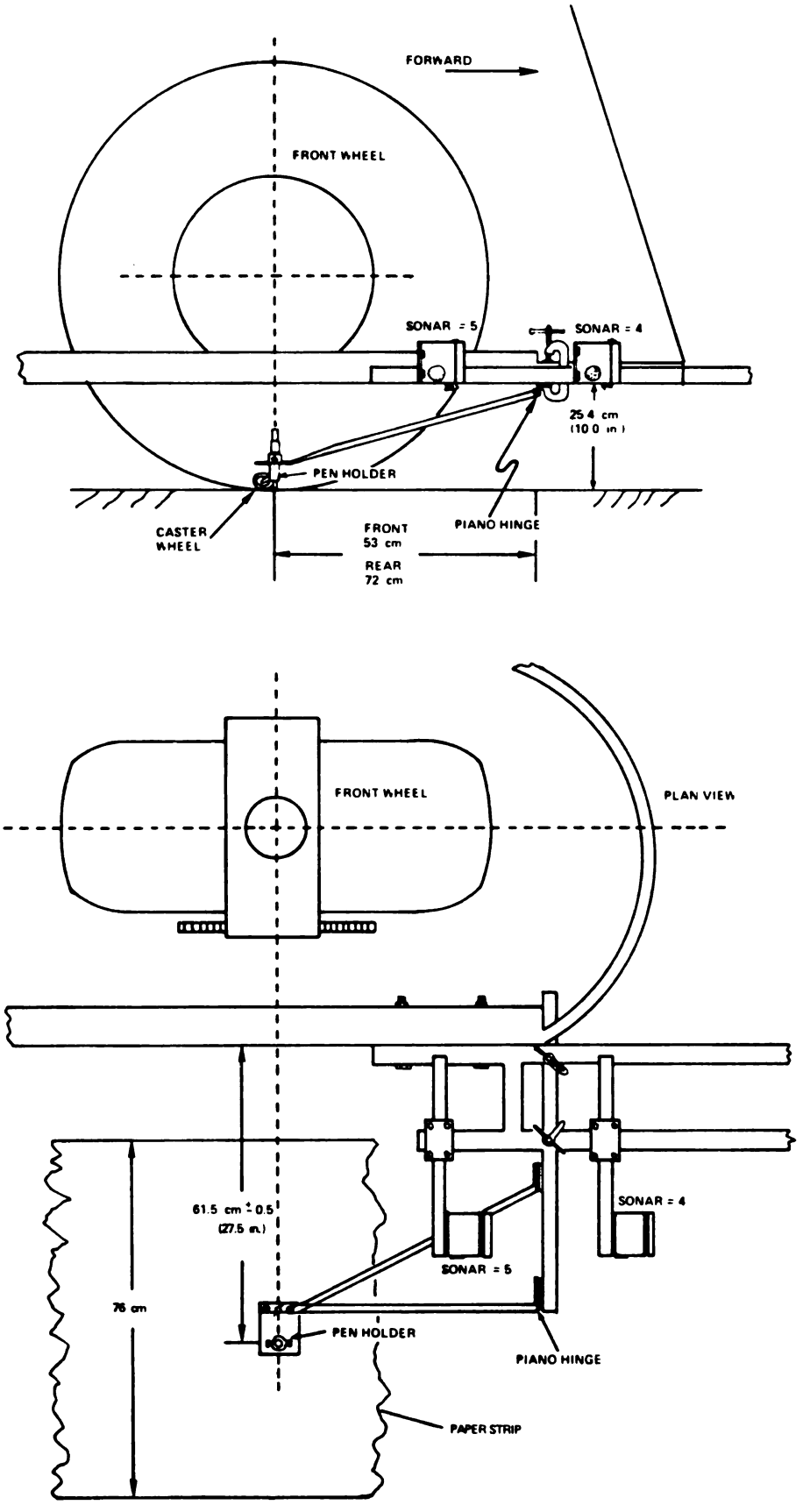

Figure 9.2 Diagram of Linkage that Supports the Front Pen

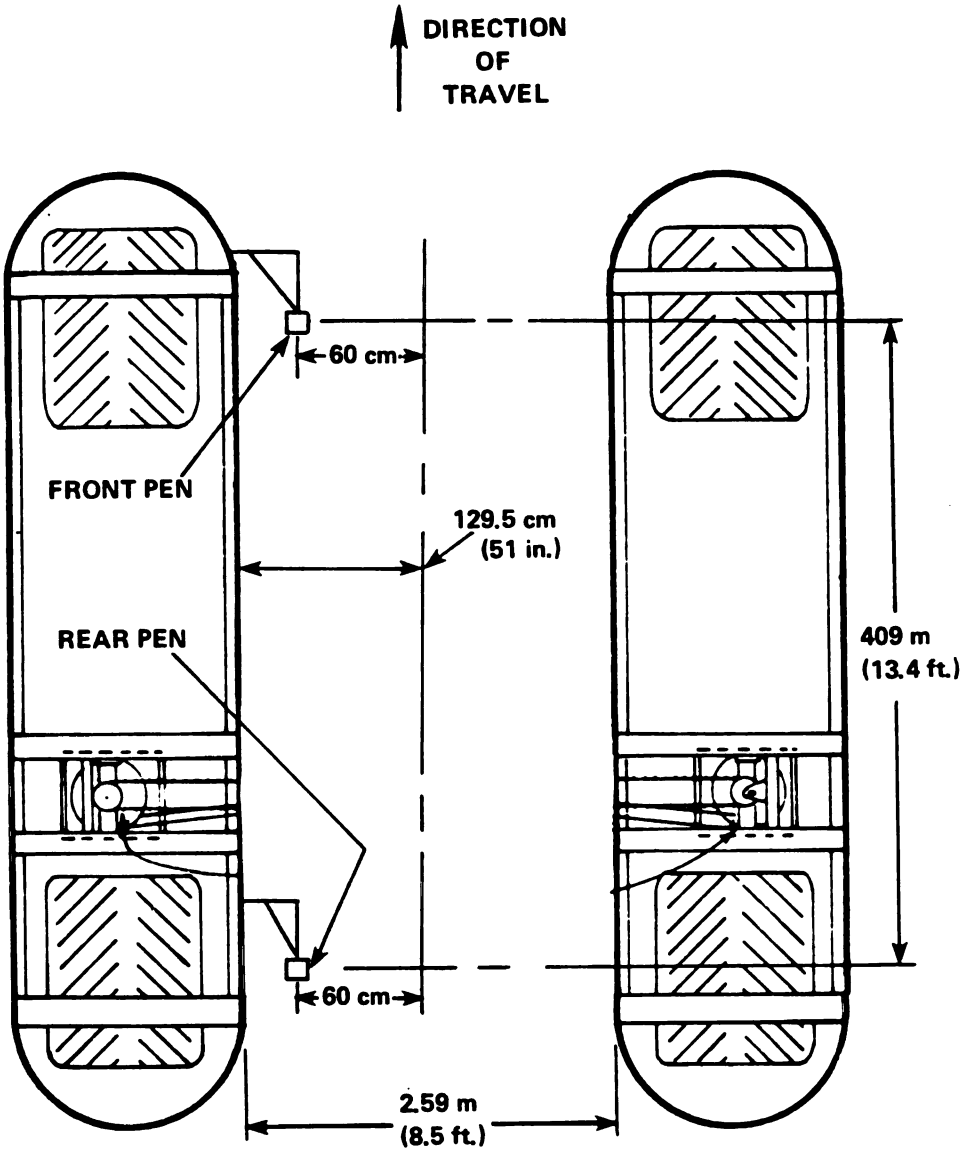

PENS WERE USED TO DRAW LINES ON A STRIP OF PAPER TO RECORD THE PATH TRAVELED BY THE HARVESTER

Figure 9.3 Plan View of Harvester Showing Pen Locations for Performance Tests

The harvester was tested on a straight row as shown in Figure 9.4. A wooden fence 15.2 m (50.0 ft) in length was used at the beginning of each test to get the harvester into alignment with the row. Since the fence was a continuous surface, the sonar system was able to bring the harvester into accurate alignment with the fence in a short amount of travel. Thus, the fence was used to obtain consistency in the procedure. The data from the three test runs using a straight row of tree stands were evaluated to determine if the control system performance was consistent.

A straight row test was done using tree stands that were set on a concrete driveway. A straight seam in the concrete was used as a line that represented the X-axis. The tree stands were positioned in the Y-direction by measuring from this straight line in the concrete. The paper was rolled along the row so that the pens were approximately centered on the paper. The paper was held down by laying strips of steel on both edges of the paper along the whole length of the row to prevent the paper from blowing away. Each pen on the harvester drew a continuous line as the harvester traveled along the row.

Data to describe the path of the harvester were obtained from the paper which had a set of two lines for each run. The two pens on the harvester were different colors so that the path of the front and rear could be easily analyzed. Data points consisting of X-Y coordinate values were obtained by manually measuring to specific points on the line drawn by the front pen on the harvester. The distance along the X-axis between the measured points varied when the path curvature varied. A total of approximately seventy data points were measured for each test run and approximately 4 hours were required to measure and

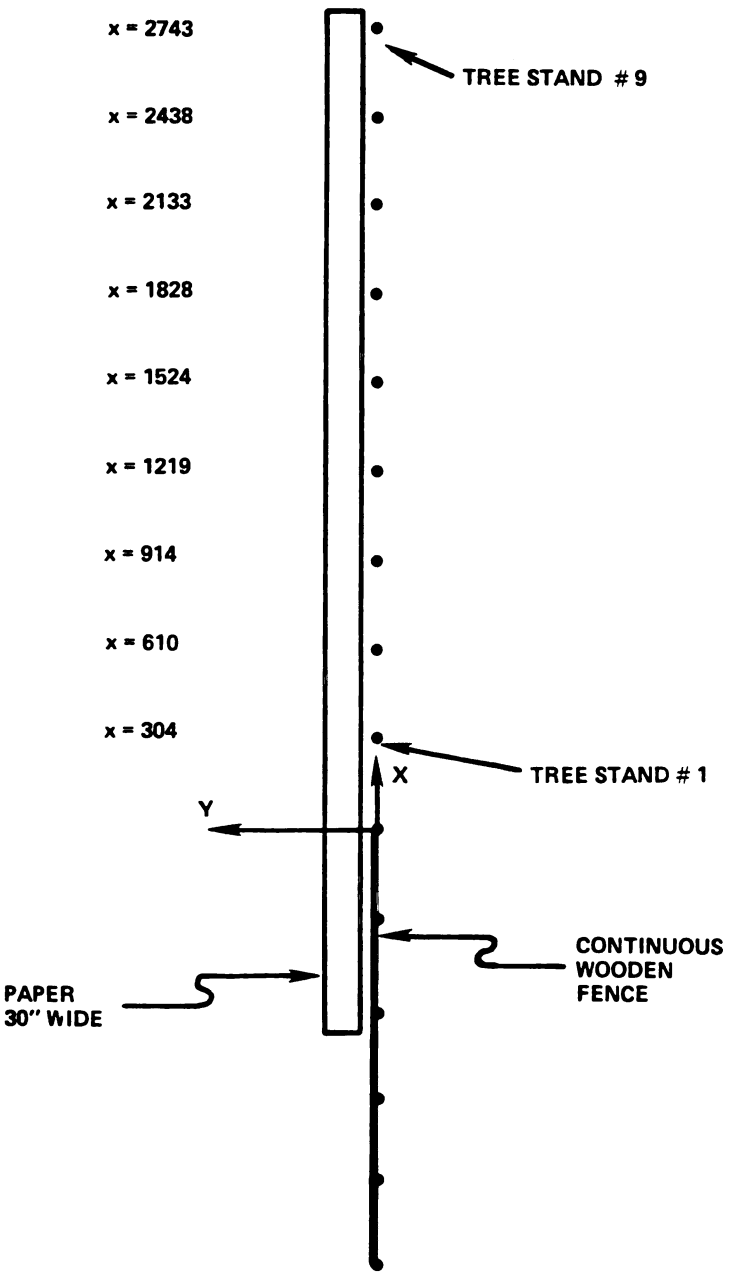

Figure 9.4 Plan View of Test Configuration Used For Straight Row Test

record the data points for a group of three test runs. The specific data points were selected such that a straight line drawn through two adjacent data points approximated the actual line drawn by the pen on the front of the harvester. The felt tip pens drew lines which were about 0.5 cm wide and the coordinates of each data point were measured to the approximate center of the lines drawn by the pens. For each front data point a specific point was marked on the test paper that represented the position of the rear pen. This was done by using a long straight stick that had a length of 409 cm which was the distance between the harvester's two pens. One end of the stick was placed on the front data point and the other end was placed so that it was on the line drawn by the rear pen. The back end of the stick thus indicated the position of the rear pen that corresponds to the front data point which was made by the front pen. Thus, these two data points define the position of the harvester. For the rear data point, the Y coordinate was measured and the X coordinate was computed by subtracting 409 cm from the front data point X-coordinate. Three test runs were made with a straight row and data were recorded.

The harvester was also tested using a curved row on the same concrete driveway and the same procedure was used to obtain the data points. For the test on a curved path the X-coordinate for the harvester's rear-pen data point was computed. The curved row for this test had a radius of curvature of 121.9 m (400 ft) which was the design requirement for the harvester. For this test the wooden fence was used in the same way as the test for the straight row. The trees were positioned so that they curved to the right and the X-Y coordinates for these trees are shown in Table 9.1.

Table 9.1 The X-Y Coordinate Position of Tree Stands For The Curved Row Tests

Tree Stand Number	X (cm)	Y (cm)
1	304	-0
2	609	0
3	914	-4
4	1218	-15
5	1523	-34
6	1826	-61
7	2129	-95
8	2431	-137
9	2732	-186

Another test was done on a campus lawn with the harvester traveling over a curved row. A string was used to make a straight reference line and the tree stands were positioned by measuring from this reference line. The procedure for obtaining data points was the same as described for the other tests. The tree stands for this test were positioned at the coordinates of Table 9.1. The wooden fence was also used as described in the straight row test.

The last test was done with a course that had a step change in the position of the tree stands. The row consisted of the wooden fence (as was used in other tests) and nine tree stands. The first three tree stands were on the X-axis and thus their Y-coordinate value was zero. The other six tree stands in the row had a Y-coordinate value of 8 cm. The X-coordinate values for the tree stands were the same as used in the straight row test.

9.3 Results of Straight Row Tests

In order to determine the alignment of the harvester during the straight row tests, the data from each test were used to plot two lines as shown in Figures 9.5, 9.6, and 9.7. In each figure one of the lines represents the path traveled by a point on the harvester's centerline at the position between the front wheels (point A, Figure 7.5) and the other line represents the path traveled by a point on the harvester's centerline at the position between the rear wheels (point B, Figure 7.5). For each test the paths traveled by points A and B were plotted by the Calcomp plotter. A computer program was used to compute the X-Y coordinates for points A and B using test data and these coordinates were used to plot the two lines that represent the paths traveled by the front and the rear of the harvester. To verify that the computer program computed the coordinates correctly, a full scale drawing was drawn manually using a set of X-Y coordinates for one harvester position using data from a curved row test. This drawing demonstrated that the computed position coordinates were within 1 cm of the positions of points A and B which were determined graphically. This indicated that the computer program was correct.

Inspection of Figure 9.5 shows that the harvester deviated at most 5 cm to the right of the row centerline and 0.5 cm to the left. Due to inaccuracy in collecting the test data and due to round-off error in the computations, the plotted data has a tolerance on the accuracy of ± 1 cm in the X and Y direction. This data was also plotted with unequal scale factors in the X and Y direction so that the harvester's travel in the Y direction could be easily seen in the data plot. Notice that since the scaling factors for the data plot are unequal, the paths shown in the

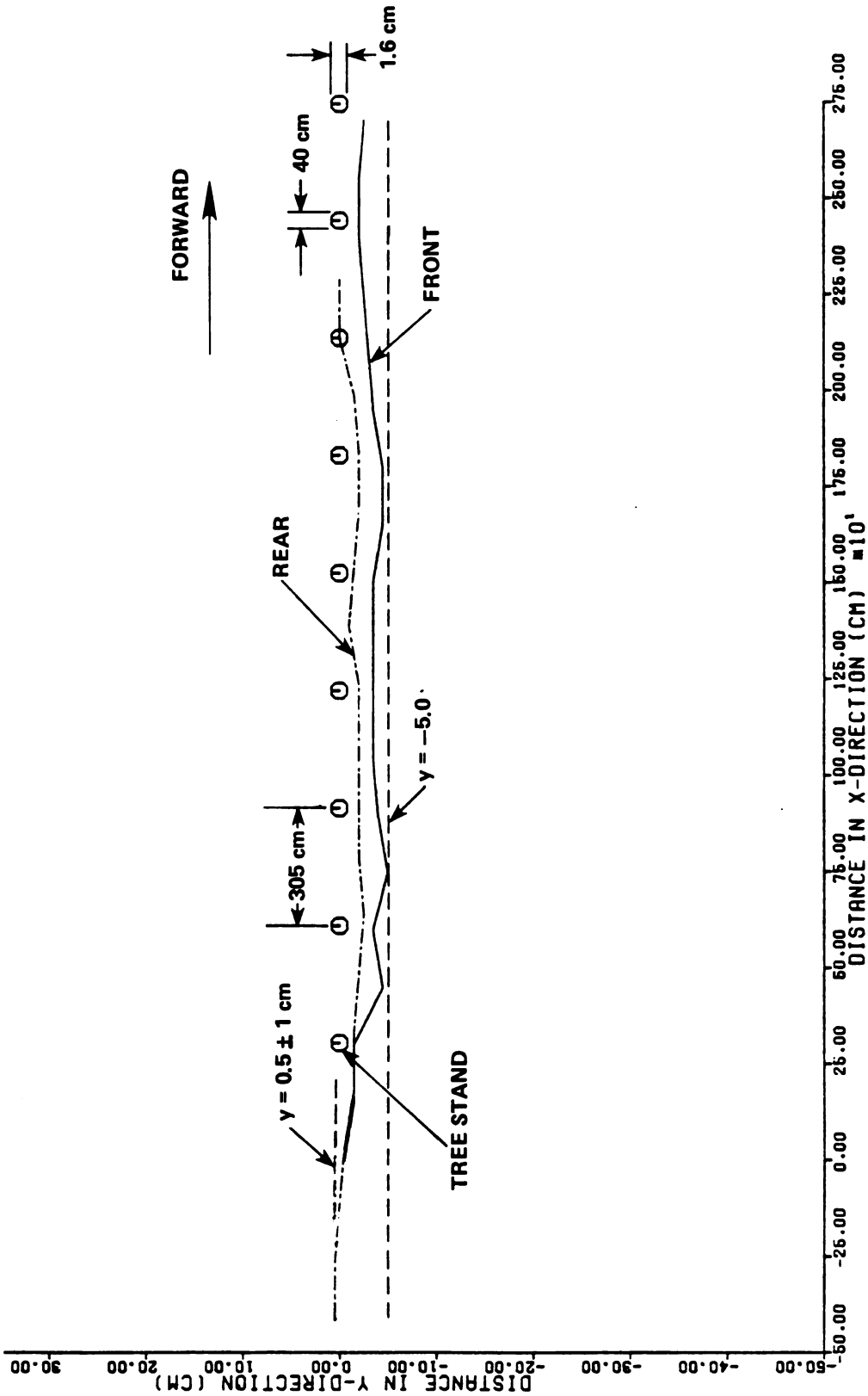

Figure 9.5 Path of the Harvester for Straight-Row Test Number 1

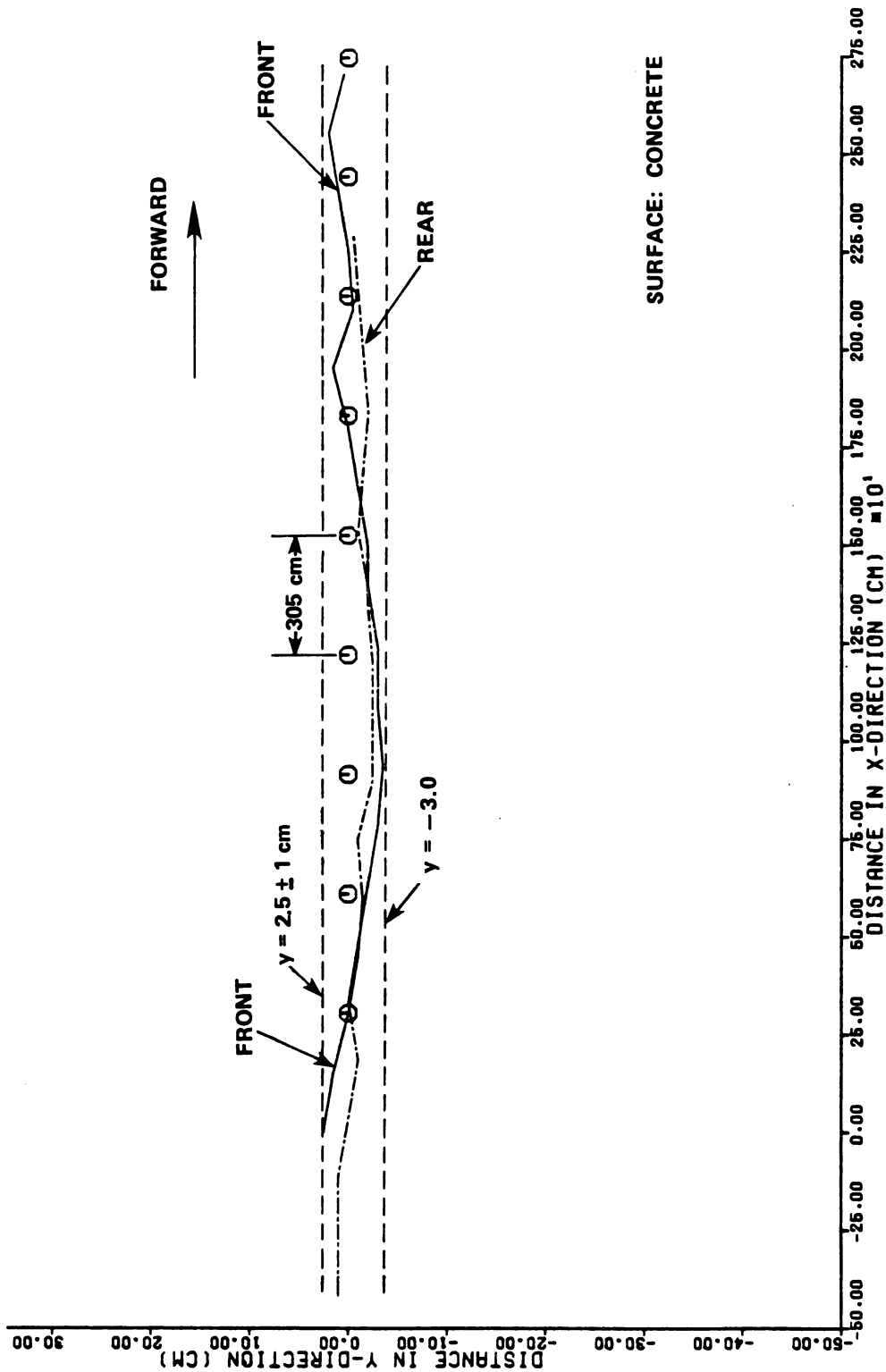

Figure 9.6 Path of the Harvester for Straight-Row Test Number 2

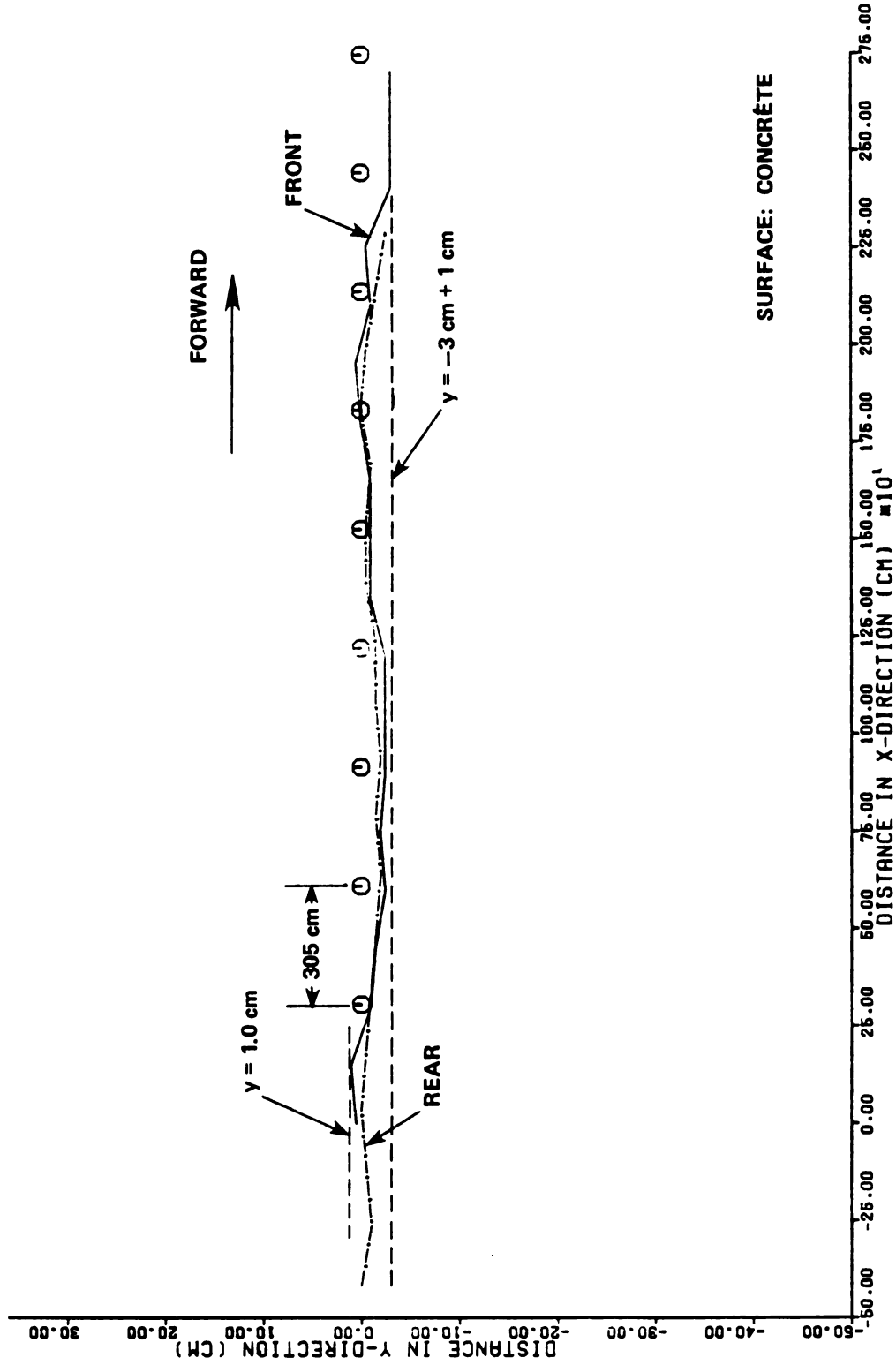

Figure 9.7 Path of the Harvester for Straight-Row Test Number 3

plot are distorted and do not represent the true shape of the lines for the actual paths for points A and B. To visualize the scaling factors used in these data plots, notice that the round symbols shown in the data plot (Figure 9.5) have dimensions of 1.6 cm in the Y-direction and 40 cm in the X-direction. Figure 9.6 shows the harvester's path for the second straight row test and the paths traveled by the front and the rear of the harvester did not exceed y=2.5 cm and y=-3cm. For the third straight row test, Figure 9.7 shows that the front and rear points of the harvester did not exceed y=1.0 cm and y=-3.0 cm. The data from these three tests shows that the automatic steering control system was effective at keeping the harvester aligned with the row centerline within the tolerance specified by the design requirements of Chapter 3. The required tolerance for alignment was $\pm$20 cm.

9.4 Results of the Curved Row Tests

The alignment of the harvester for the curved row tests was analyzed by plotting the data using the same methods as described for the straight row tests. The paths of the front and the rear of the harvester are plotted for each of the three tests and these plots are shown in Figure 9.8, 9.9 and 9.10. These tests were done on a concrete driveway. Notice in these plots that the X and Y scaling factors are not equal. The round symbols in these plots have a dimension of 6.4 cm in the Y-direction and 40 cm in the X-direction.

The data plot of Figure 9.8 is the first test with the curved row and this plot shows the front of the harvester had a maximum deviation in the Y direction from the center of a tree stand of 7.5 cm. This value of 7.5 cm was obtained by measuring the data plot. Note that due to the distortion in this plotted data, the value measured on the data

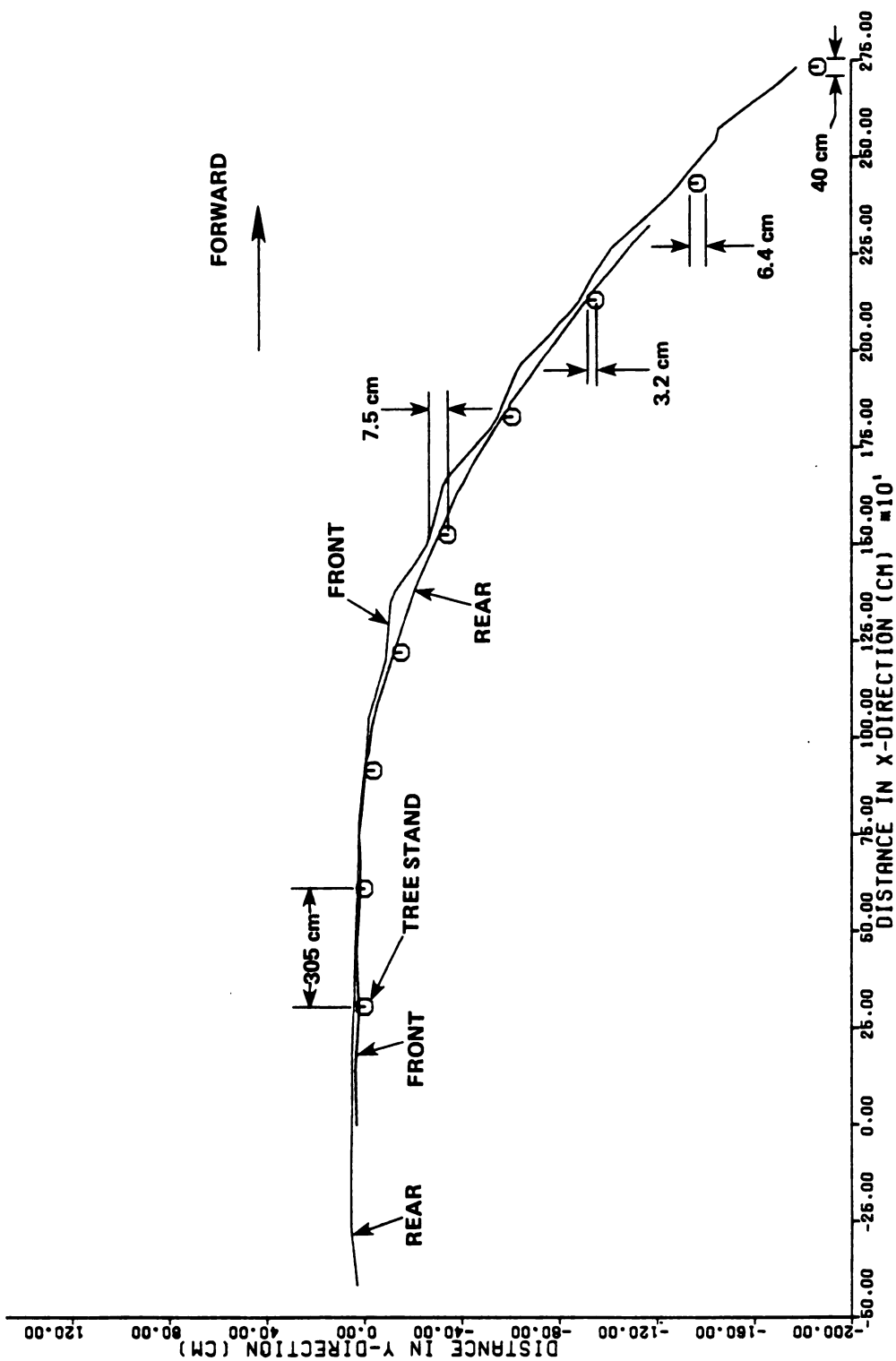

Figure 9.8 Path of the Harvester for Curved Row Test Number 1 on a Concrete Driveway

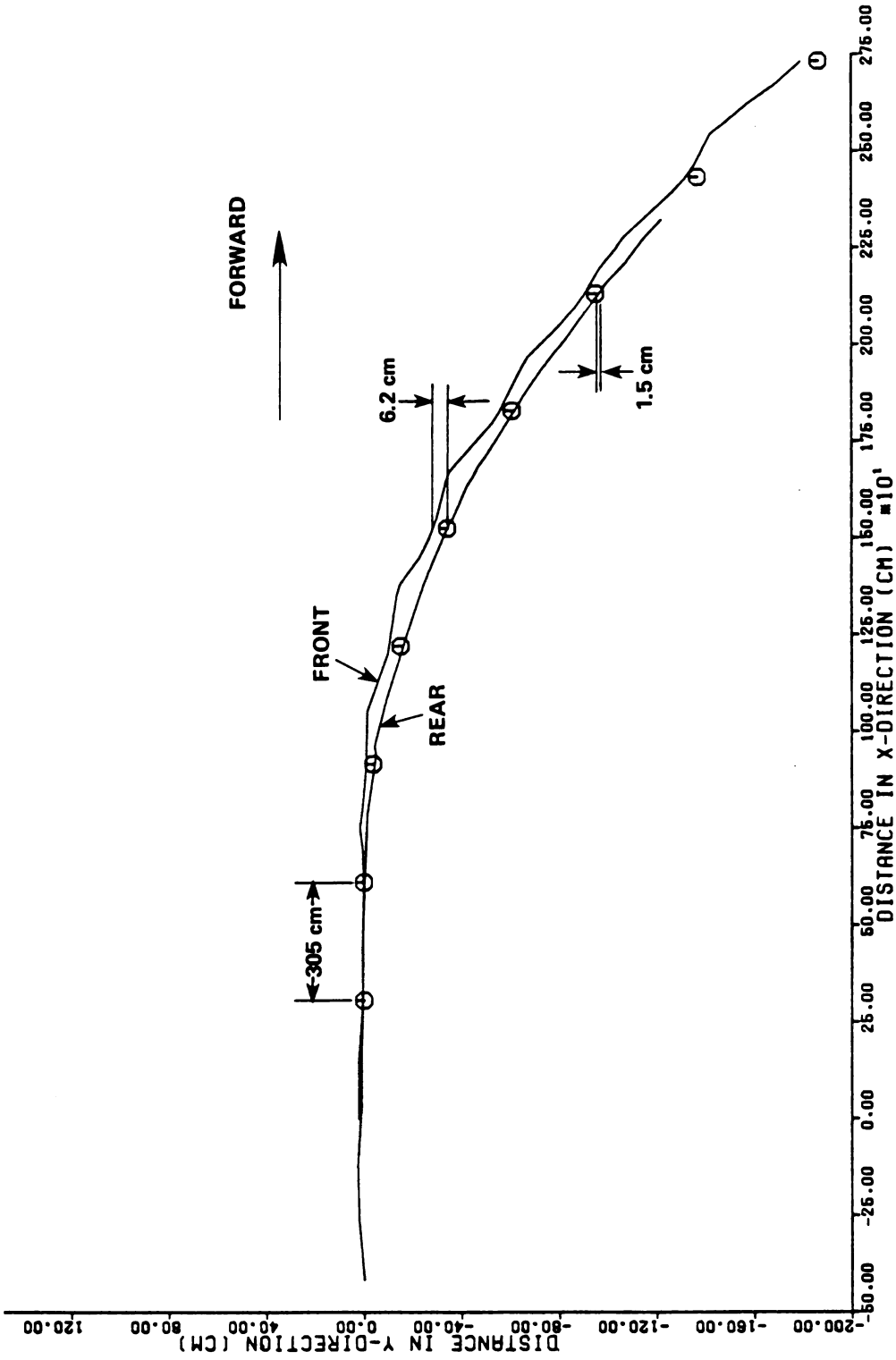

Figure 9.9 Path of the Harvester for Curved Row Test Number 2 on a Concrete Driveway

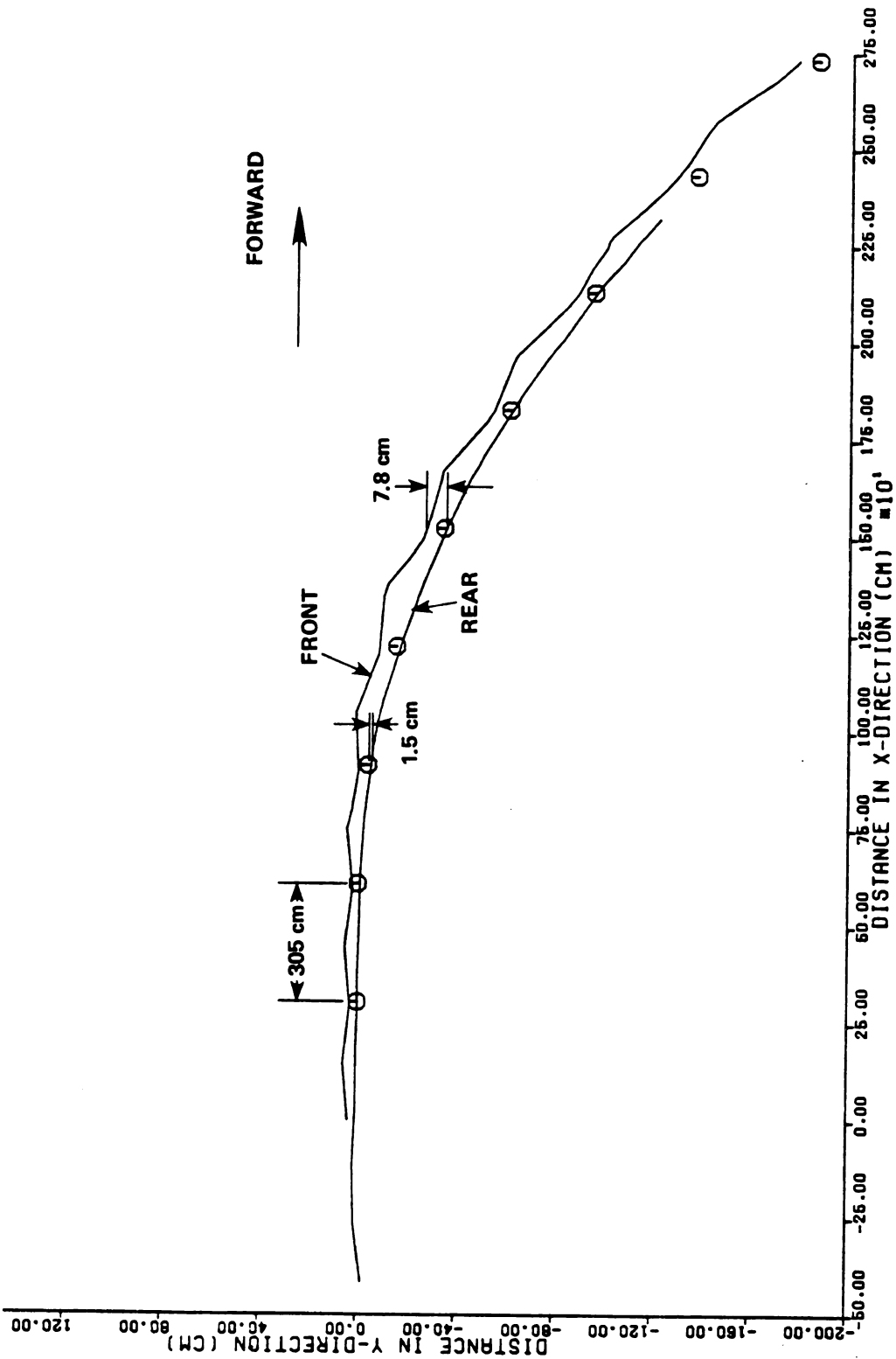

Figure 9.10 Path of the Harvester for Curved Row Test Number 3 on a Concrete Driveway

plot in the Y-direction is within one centimeter of being the perpendicular distance from the machine centerline to the center of the tree as the harvester's front point passes the tree. This value of 7.5 cm has a tolerance on the accuracy of $\pm$2 cm. This value for the tolerance considered inaccuracies in the data collection process and also inaccuracy in measuring the harvester's position from the data plot. Note that the deviation of 7.5 cm of the front point on the harvester, occurred at the time the front of the harvester was moving past the tree stand. Figure 9.8 also shows that the path of the rear coordinate had a maximum deviation from the center of a tree stand of 3.2 cm as the rear of the harvester was moving past the tree stand. Figure 9.9 and 9.10 shows the data plotted for the second and third curved-row tests. For the second and third tests the maximum deviation of the front of the harvester was 6.2 cm and 7.8 cm from the center of a tree stand respectively and the rear paths for the second and third tests each had a maximum deviation from the tree stand of 1.5 cm.

The curved row test was also done three times on a campus lawn. The plots of the path traveled by the harvester for these three tests are shown in Figure 9.11, 9.12 and 9.13. From these figures the maximum deviation of the path of the front of the harvester from the tree stands (in the Y-direction) for tests numbered 1, 2 and 3 are 6.2 cm, 7.0 cm and 8.7 cm, respectively and the maximum deviation of the rear path for these three tests are 1.5 cm, 3.2 cm and 1.5 cm, respectively. Combining data from all six-tests with the curved row shows that the front of the harvester centerline was within 8.7 cm from the center of the tree stand when it moved past a tree stand and the rear of the harvester was within 3.2 cm of the tree stand when it moved past a tree

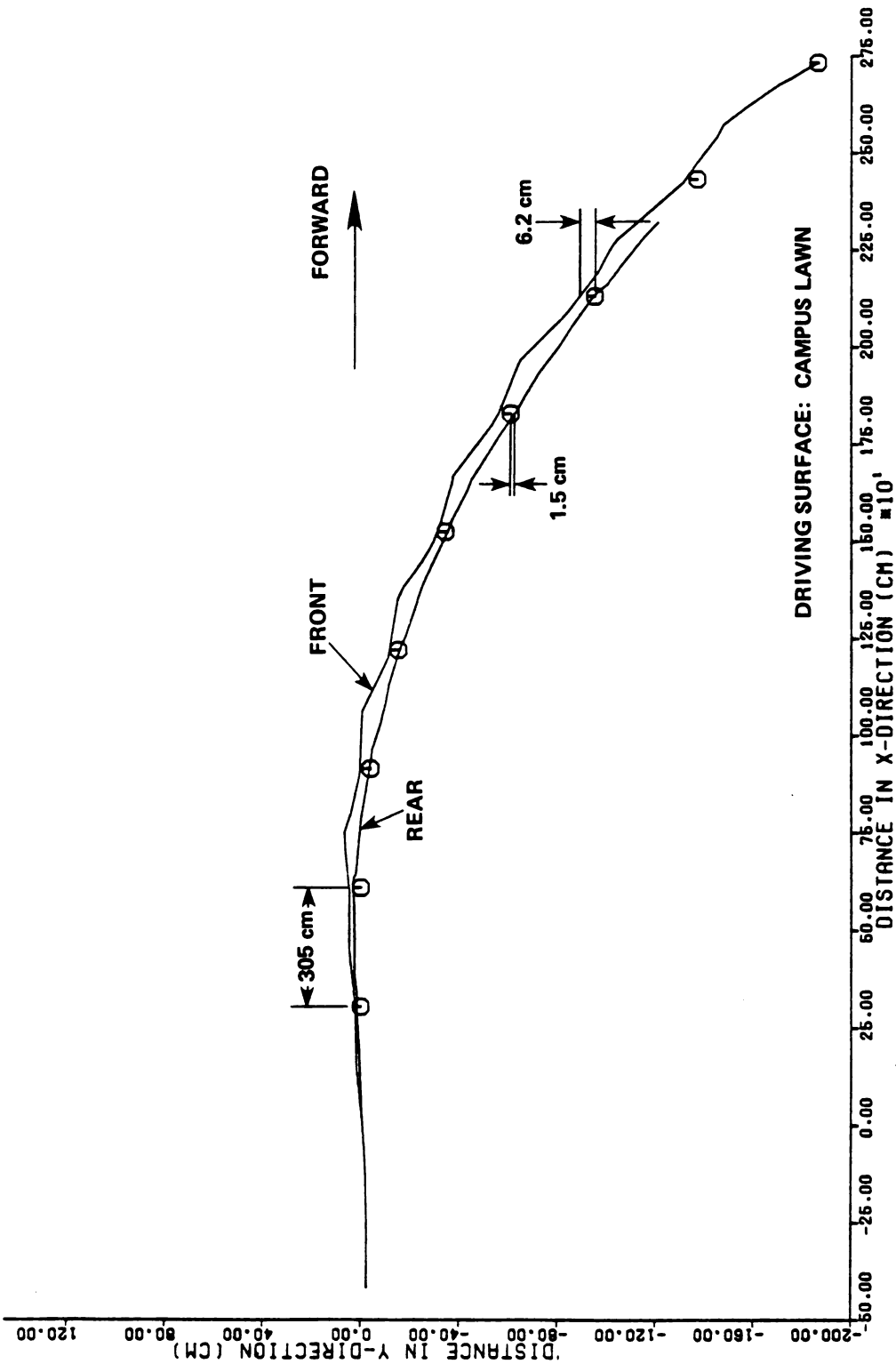

Figure 9.11 Path of the Harvester for Curved Row Test Number 1 on a Campus Lawn

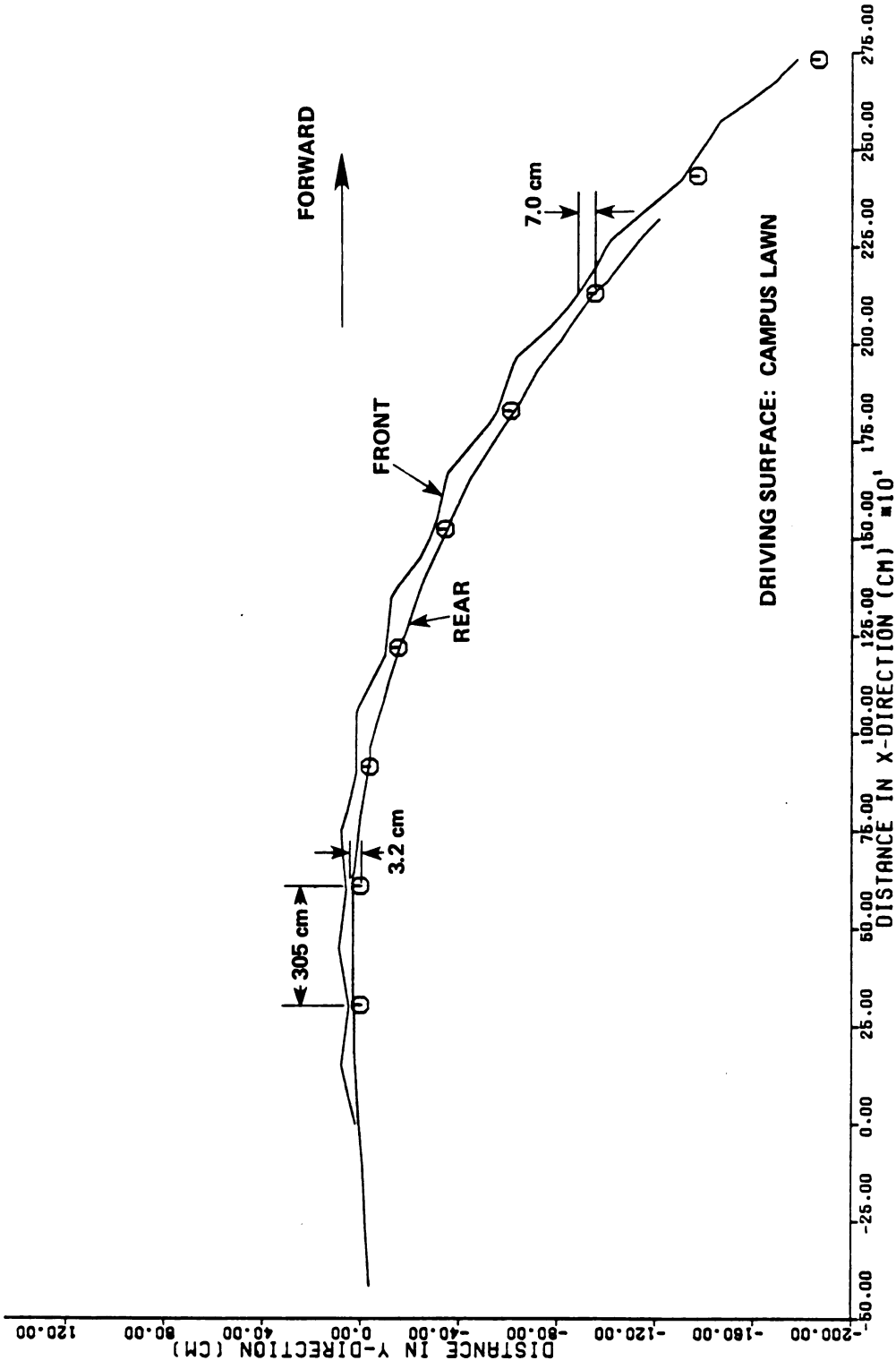

Figure 9.12 Path of the Harvester for Curved Row Test Number 2 on a Campus Lawn

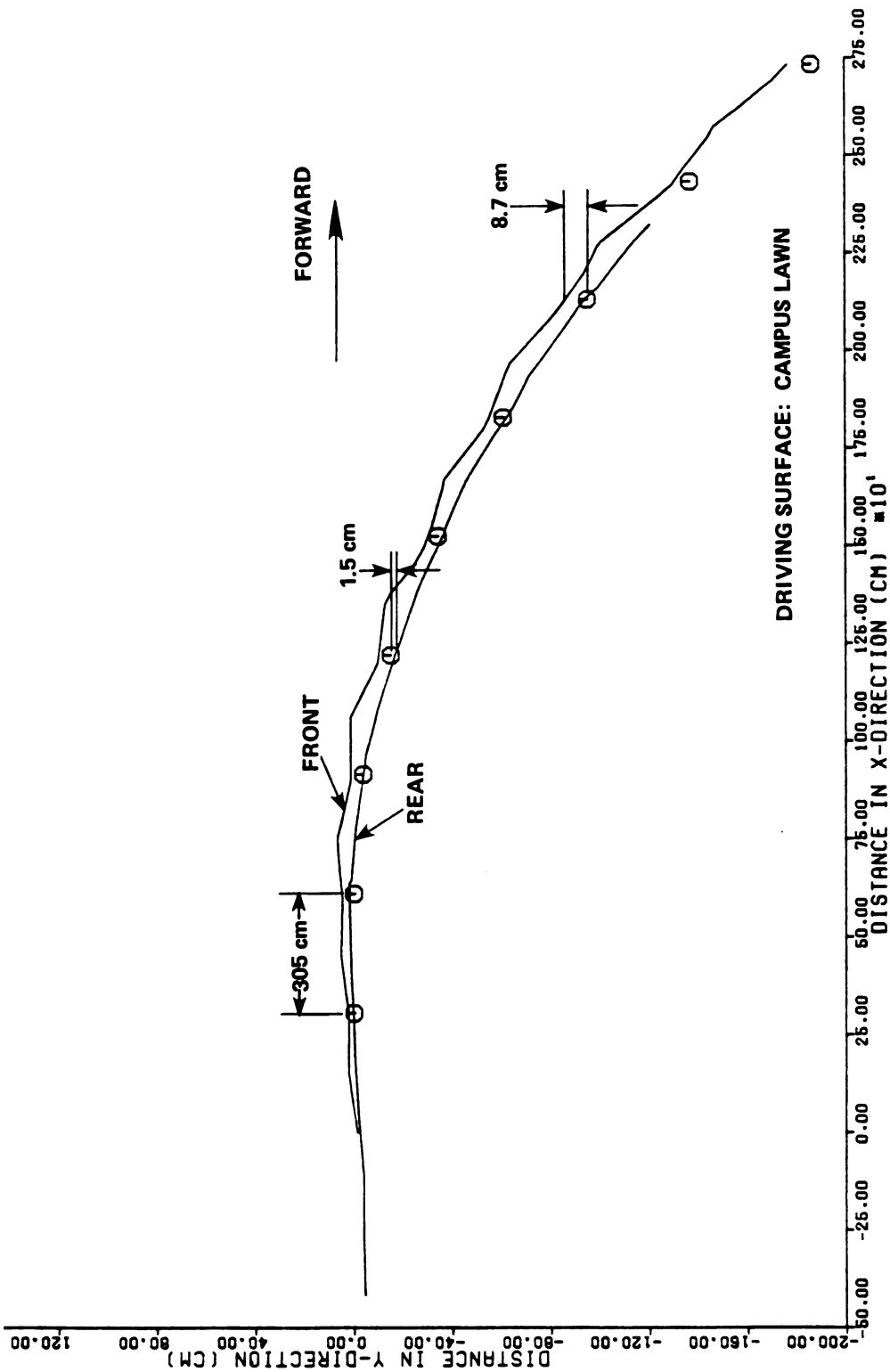

Figure 9.13 Path of the Harvester for Curved Row Test Number 3 on a Campus Lawn

stand. Thus, these data along with the descriptions of the paths (in the six data plots) show that each tree stand stayed well within the allowable zone as defined by the design requirements (Figure 3.1). Several preliminary tests were done on a curved row with radius of curvature of 60.9 m (200 ft) and the harvester drove over this row at speeds of 1.6 (1.0), 2.4 (1.5), 3.2 (2.0) and 4.0 km/h (2.5 mph). For tests at speeds up to 3.2 km/h (2.0 mph) the harvester was able to move over the row and keep the tree stands within the allowable tree zone. For the test with speed of 4.0 km/h one of the sonar units did not make a tree position measurement and this caused the harvester to move far to the left of the curved row because the steering controller had stopped controlling the steering of the wheels. The controller's program was written such that a desired wheel position code was computed for each sonar unit in successive order. Thus once a particular sonar unit was turned ON, the controller waits until that sonar unit provides values to compute the desired wheel position. This problem of a sonar unit's not sensing the tree position appears to be a problem at the higher speeds.

In order to determine if the simulation model (Chapter 7) predicts the path as observed during the curved row tests, the simulation model was modified to incorporate the change to the shaft encoder configuration as described in Section 9.1. The path of the harvester's front and rear center point as predcted by the simulation model is shown in Figure 9.14. This simulation data was plotted in this form so that it could be compared with the plots of the test data. This simulation shows that the path of the front point had a maximum deviation of 2 cm from the tree stand and the rear point had a maximum deviation of 3.2 cm from the tree stand. Thus the model predicts that the front of the

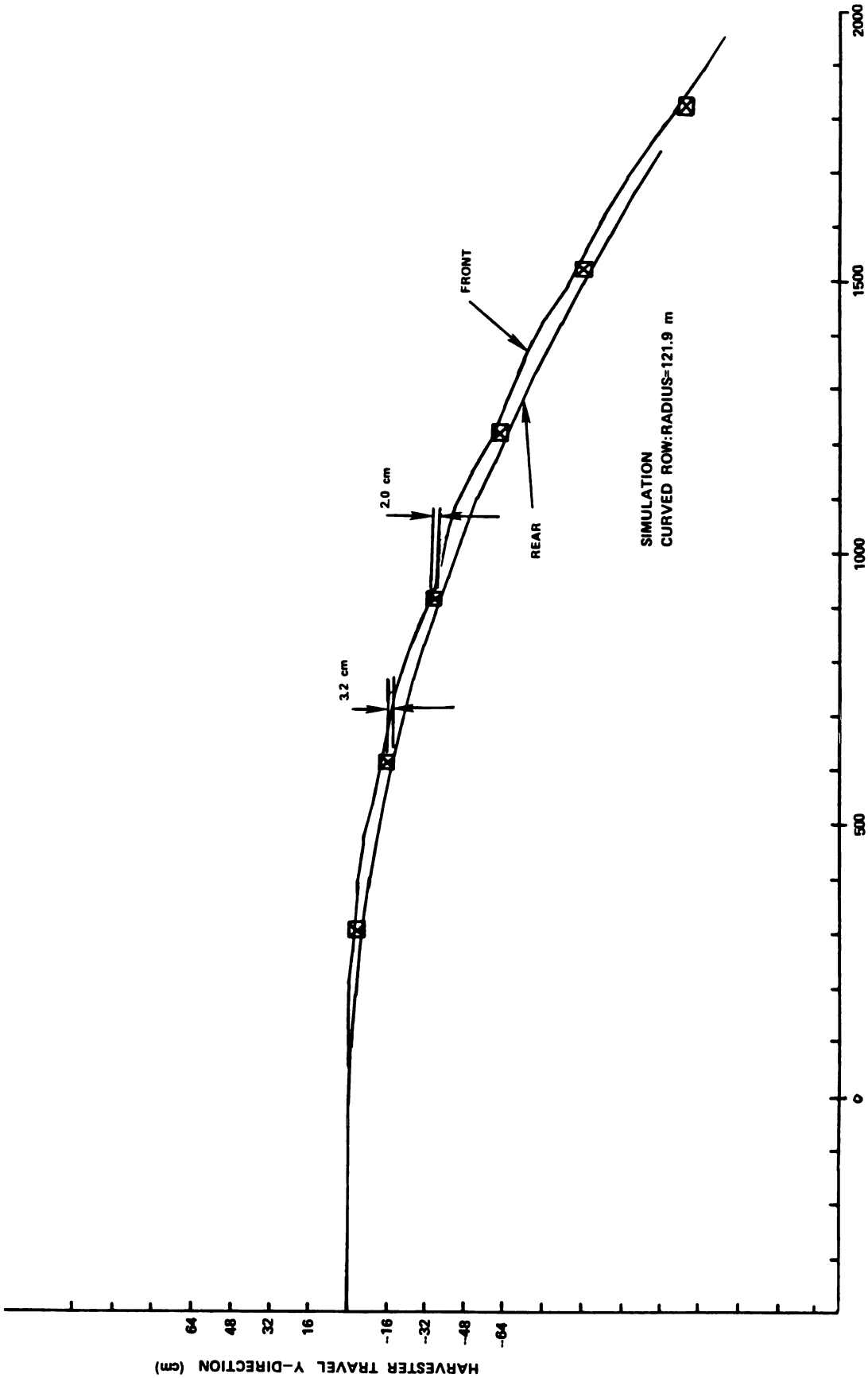

Figure 9.14 Path of the Harvester Predicted by the Simulation Model for Curved Row

harvester is closer to the tree than the actual test data shows. Note, the simulation predicts that the trees move through the harvester near the harvester's centerline and the maximum deviation of the tree from the harvester centerline occurs when the tree enters the front of the harvester's allowable tree zone and when the tree exists the rear of the allowable tree zone.

9.5 Tests Results - Row with Step-Change

A test was done to determine how the steering control system responds to a step-change in the row. Figure 9.15 shows the path of the front and the rear of the harvester as it traveled over the row of tree stands. This plot of Figure 9.15 shows that the position of the harvester changed gradually as the harvester responded to the step-change in the row. Also, the plot shows that after the front of the harvester had moved past the step in the row, the maximum deviation of the front of the harvester from the row centerline was 4 cm. The front of the harvester was within 1 cm of the row centerline as it moved past the step change in the row. The rear of the harvester was within 3 cm of the row centerline as it moved past the step in the row. Also notice in Figure 9.15 that as the front of the harvester was moving past the first three trees in the row, the front of the harvester was oscilating. This oscilation may have caused the front of the harvester to be moving towards the left as the harvester was approaching the step change in the row. Thus, the sonar units detected a smaller sonar measurement value and this would have caused the wheels to steer to a smaller angle than for the condition where the sonar measurement was a larger value. Thus, if the wheel angle was smaller (due to the smaller sonar value), then this would cause the front of the harvester to move slower in the

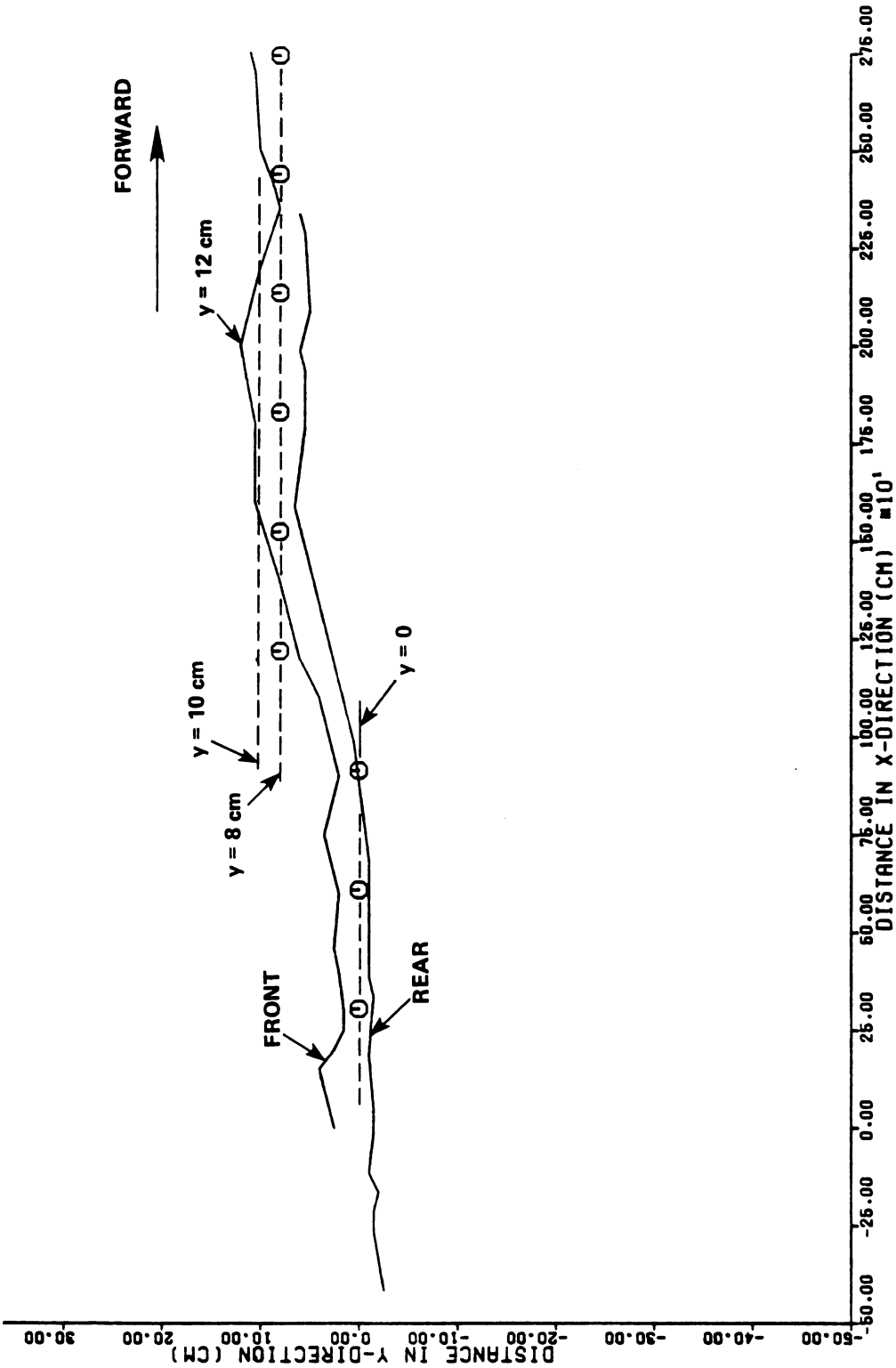

Figure 9.15 Path of the Harvester for Row with Step-Change--Test Number 3

Y-direction. This data of Figure 9.15 shows that the steering control system was able to drive over the tree row with an 8 cm step change while maintaining the proper alignment as specified by the design requirement.

The results from the simulation model for a row with a step change were compared with the harvester's actual performance. Figure 9.16 shows the path of the harvester as predicted by the simulation model with a time constant of 2.0 seconds as described in Chapter 7. Figure 9.16 shows that the motion of the harvester in the Y direction has a faster response than the harvester's actual response shown in Figure 9.15. The simulation model showed that as the front of the harvester moved past the step in the row that the maximum deviation of the front of the harvester from the row centerline was 3 cm and then the front of the harvester oscilated between y=10 cm and y=4 cm. After the simulation had run for 8 trees past the step-change, the simulation shows that the oscilation continued. This amplitude of oscilation predicted by the simulation model varied between 2 cm and 3 cm. Figure 9.16 shows that the rear of the harvester stayed within 2 cm of the row centerline as the rear point of the harvester moved past the step change in the row. Figure 9.16 shows that the response of the front and the rear of the harvester as predicted by the simulation mode, was faster than the response of the actual harvester. The actual harvester may have responded slower due to misalignment between the front and rear wheels. If the front and rear wheels were perfectly aligned then the centerlines through the left front and left rear wheels would lie in a single plane and the same would occur for the wheels on the right side.

The simulation model assumes that when the front wheel steering angle is zero, then the wheels are perfectly aligned and thus the paths of the front and rear points on the harvester centerline would lie on the same straight line.

For the actual harvester, the task of aligning both the front and the rear wheels was difficult. The technique used to align the wheel was to allow the steering control system to follow the wooden fence described previously. The harvester's pens were used to observe the path of the front and rear points on the harvester. Adjustments were made to change the specified zero position of either the front or the rear wheels. For the front wheels the shaft encoder connection to the front wheel shaft was used to change the centered position of the wheels. For the rear wheels a limit switch assembly was used to keep the wheels at the centered position and wheel position was changed by moving the limit switch assembly. After a wheel position change was made, the harvester was tested to determine if the harvester traveled along the fence such that the lines drawn by the two pens were close together. Also, it was observed if the steering controller needed to turn the front wheels in order to follow the fence. If the two lines drawn by the harvester pens were not close together (within 6 cm) then the process was repeated. Also, if the steering controller had to consistently turn the front wheels to keep the front centered on the fence then the front wheel center position was adjusted.

The factors that may contribute to the harvester's not responding as fast as the model are deformation of the tires when turning; looseness or "play" in the steering linkage; and misalignment between the front and rear wheels. Note that the steering linkage was a well

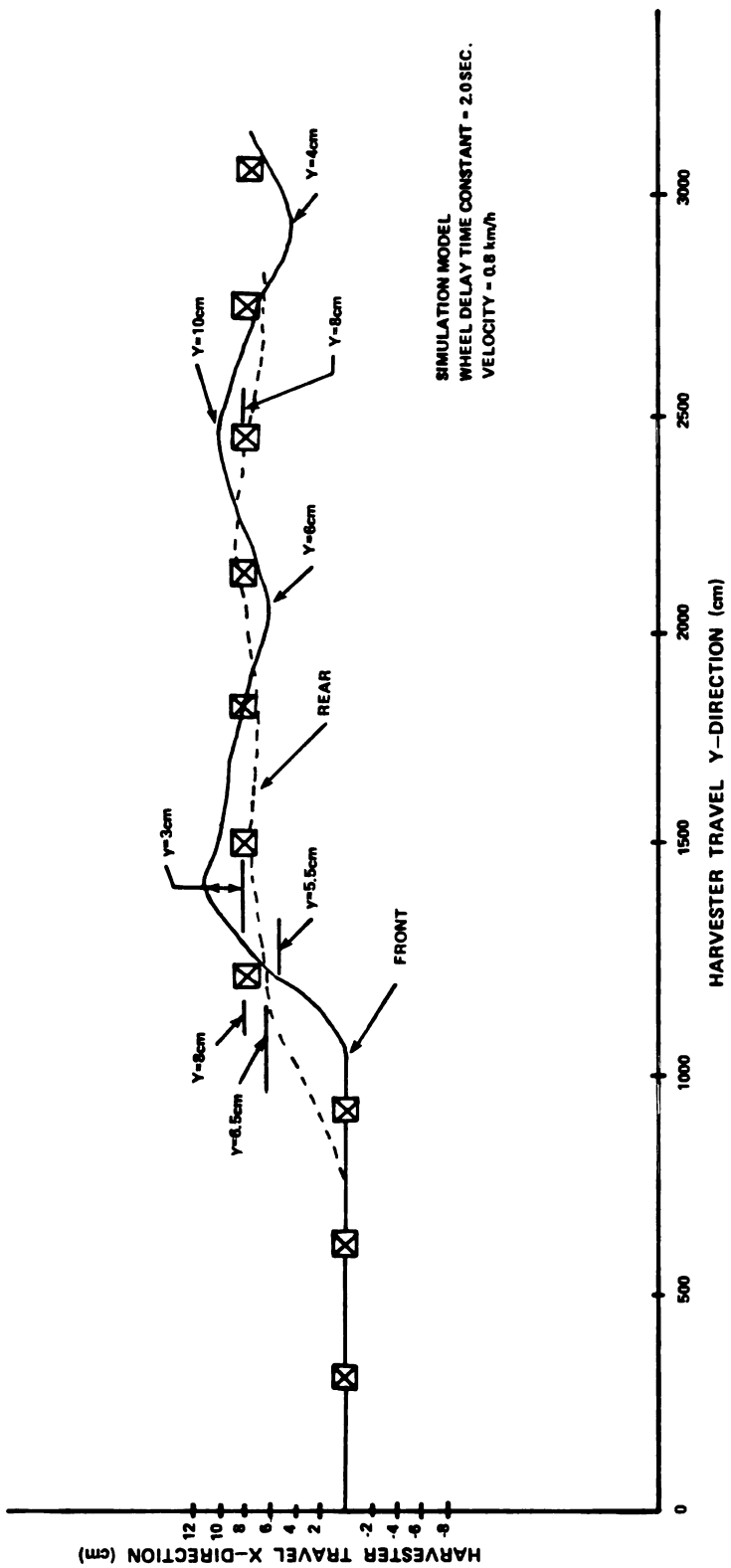

Figure 9.16 Path of the Harvester Predicted by the Simulation Model for Row with Step-Change with Time Constant Equal to 2.0 seconds

designed system and little improvement would be obtained by redesigning the steering linkage. Thus the model was modified so that it would show a slower response for the harvester's motion in the Y-direction. The simulation model was modified such that the model used a steering angle which was about 50 percent less than the actual harvester steering angle. For the modification the first order time constant was not used because it only decreased the steering angle by 10 percent. The actual harvester turns the wheels 0.7 degree for each 2 cm of tree position error computed. The model before it was modified was programmed to turn the wheels 0.7 degree for each 2 cm of error computed. To modify the model this value of 0.7 was changed to 0.4. This value was selected because the simulation showed a harvester motion response similar to the actual harvester response for the row with a step change. Figure 9.17 shows the results from the modified simulation model for the row with a step change. From this figure it can be seen that the model predicts that the front of the harvester is 2.5 cm from the row centerline as the front of the harvester moves past the step change in the row. The rear is 4 cm from the row centerline as it moves past the step change in the row. For the actual harvester performance for the step row (Figure 9.15) the front was within 1 cm and the rear was within 3 cm as these points on the harvester moved past the step in the row. The modified model was also used to simulate the harvester's travel over a curved row with radius of curvature of 121.9 cm (400 ft.) and the simulation results are shown in Figure 9.18. The simulation model predicted that the front of the harvester is within 9 cm as it passes by the tree and the actual harvester was within 8.7 cm as shown in Figure 9.13. The simulation model predicted the rear of the harvester is within 4 cm as

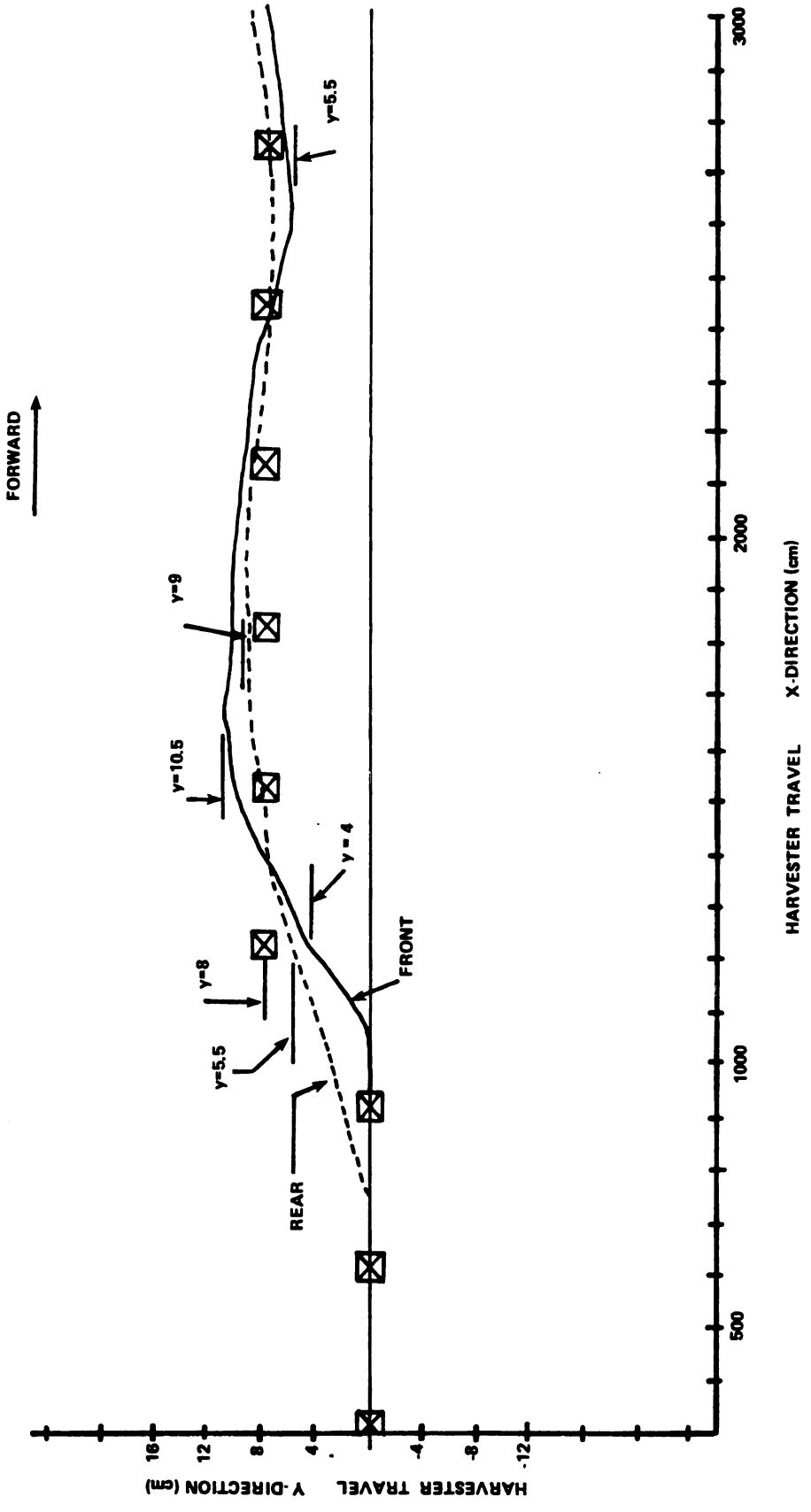

Figure 9.17 Path of the Harvester Predicted by the Simulation Model for Row with Step Change and Model Modified to Turn the Wheel 0.40 for Each 2 cm of Tree Position Error

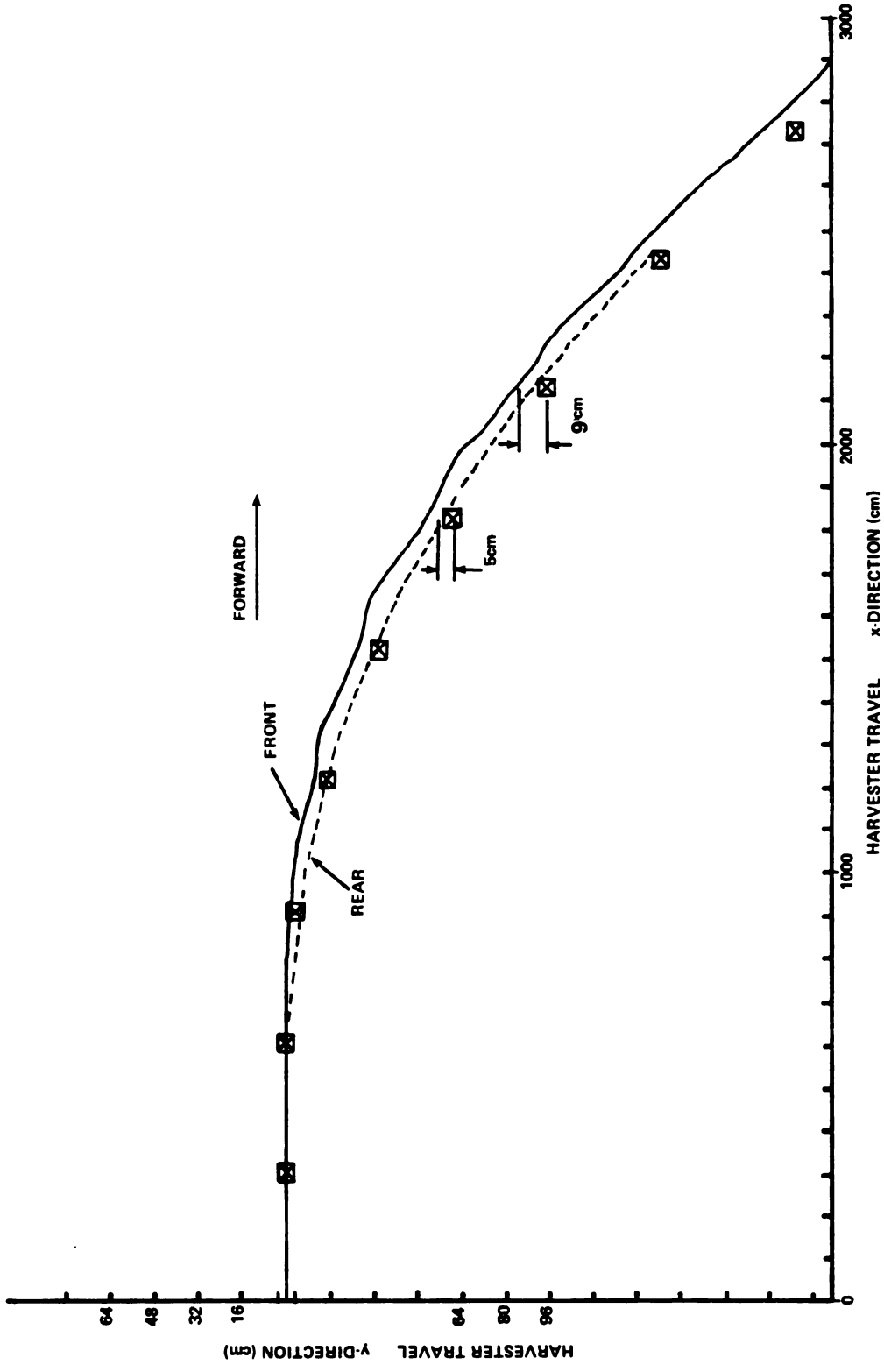

Figure 9.18 Path of the Harvester Predicted by the Simulation Model for Curved Row with Model Modified to Turn the Wheels 0.4° for Each 2 cm of Tree Position Error

it passes by the tree and the actual harvester was within 3.2 cm as shown in Figure 9.8. Thus, these results indicate the model reasonably predicts the motion of the harvester when the model is modified to decrease the magnitude of the steering angle.

9.5.1 Reliability Problems During Test

During the two successive tests with the step-change row, sonar unit 1 read a value of 109 cm for the first tree stand in the row, and this value was erroneous. The sonar value of 109 was observed on the video monitor and actual sonar value may have been larger than 109 as explained in Chapter 8. This tree was observed to be leaning slightly in the positive Y direction (about 3^{o}). The path of the harvester for these two tests is shown in Figure 9.19 and 9.20. The test was repeated after the tree stand was straightened and the erroneous sonar value was not obtained. These results show that the front of the harvester deviated from the row centerline by 15.5 cm. Another test was run with tree stand leaning 12^{o} in the positive Y direction and both sonar 1 and sonar 2 read a value of 109 cm when these sonar units moved past this leaning tree stand. Tests were done in the laboratory to investigate the cause of the sonar units making a measurement with a large error. A test was done with a tree stand and a large apple tree limb. The limb diameter varied between 3 cm and 7 cm and the limb length was 70 cm. For this test, an oscilloscope was connected to the PROCESSED ECHO signal on the Polaroid ultrasonic circuit (Figure 6.1) which was a component of a sonar circuit (Figure 6.5). The amplitude of this signal was observed on the oscilloscope as the tree stand was tilted from the vertical toward the sonar transducer which was transmitting sound pulses toward the tree stand. The tree stand was 78 cm from the sonar

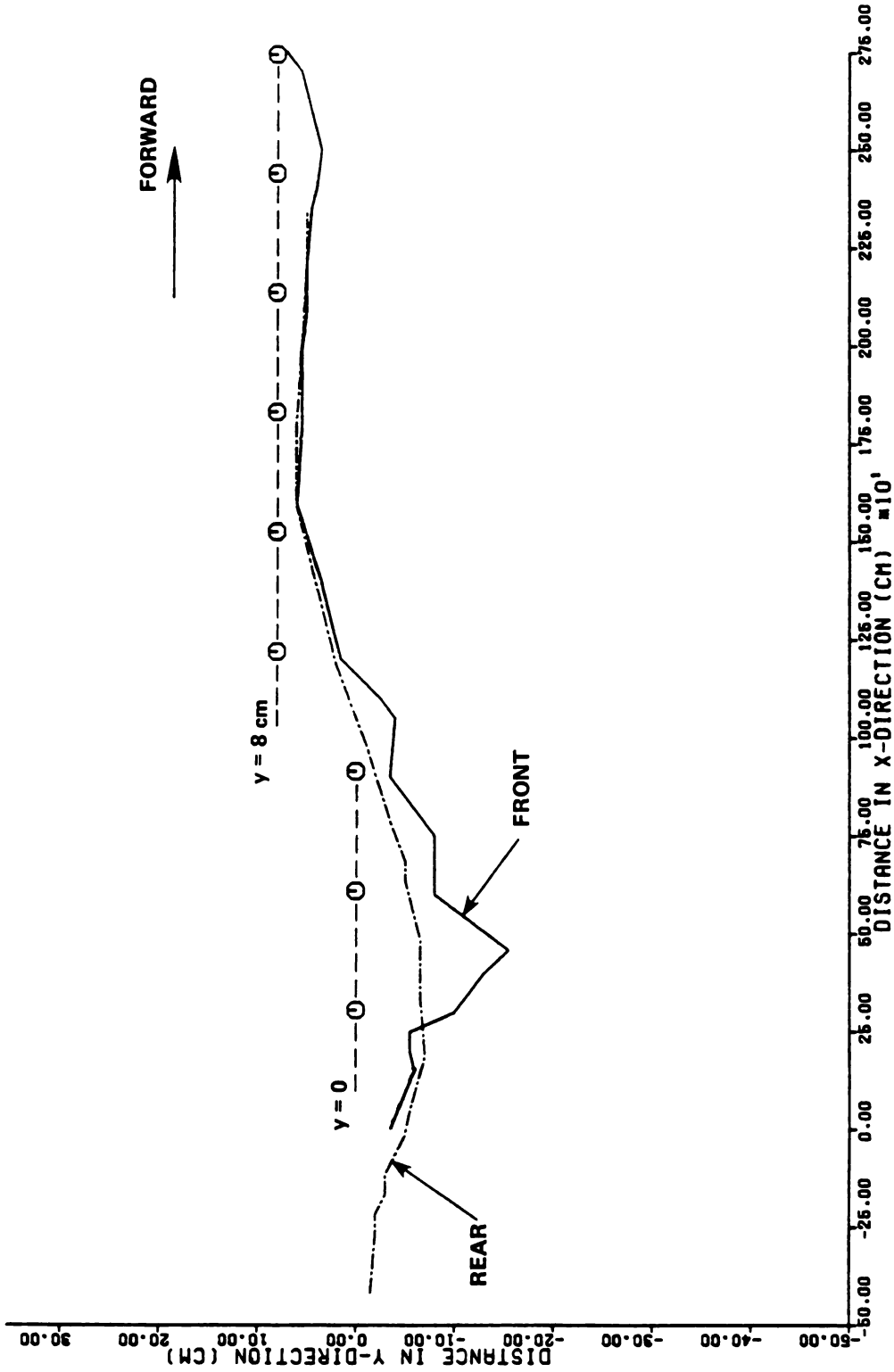

Figure 9.19 Path of the Harvester for Row with Step-Change--Test Number 1

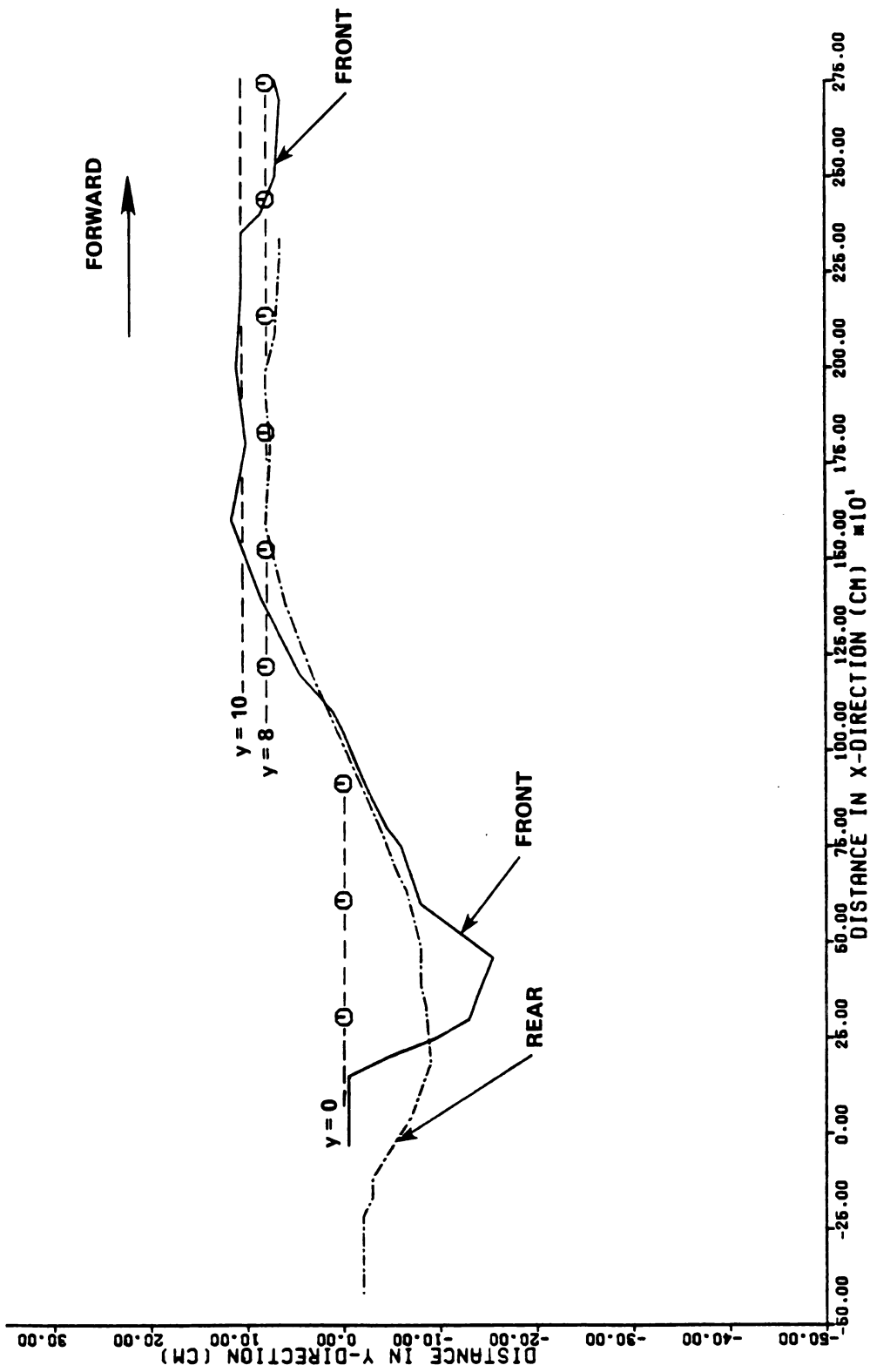

Figure 9.20 Path of the Harvester for Row with Step-Change--Test Number 2

transducer and positioned on the transducer's centerline. When the tree stand was tilted about 10^{o} from the vertical, the amplitude of the PROCESSED ECHO signal decreased to about 10 percent of its maximum value and the timing signals indicated a sonar distance measurement which had an error of about 16 cm. When the tree stand was tilted about 15^{o} from the vertical toward the sonar transducer, the PROCESSED ECHO signal had an amplitude less than 5 percent of its full value and the timing signals on the Polaroid circuit indicated that the echo from the tree stand was not detected. This low amplitude of the PROCESSED ECHO signal was probably caused by the sound pulse being reflected downward by the tree stand and the sound pulse passes below the sonar transducer. Thus only a portion of the sound pulse is detected by the sonar transducer. This same test was done with the apple tree limb. The apple tree limb was tilted about 40^{o} from the vertical and the PROCESSED ECHO signal was about 20 percent of its full value and the timing signals from the Polaroid ultrasonic circuit indicated that the sonar distance measurement has an error of about 5 cm. This information indicated that a tree trunk was more effective than a tree stand at reflecting the ultrasonic sound pulse back to the sonar unit. Therefore the erroneous sonar measurements that were made during the harvester's performance tests with tree stands tilted from the vertical should not occur when the harvester is operating in an apple orchard if the tree trunks are tilted less than 40^{o} from the vertical.

10. SUMMARY

An automatic steering control system is needed for the USDA-over-the-row apple harvester because the operator is positioned on the harvester such that the operator is above the top of the tree row and thus manual steering is difficult because the operator's view of the tree trunk is blocked by tree foliage. Also, the task of steering is very monotonous and the operator often becomes fatigued within a few hours. Typically, if an operator becomes bored or fatigued then his ability to steer accurately is reduced and this could result in the harvester colliding with trees which could damage the trees and the harvester. An operator which is fatigued will often decrease the forward velocity of the vehicle so that he can accurately steer the vehicle, and decreasing the velocity will decrease the machine's productivity. Also, when an automatic steering system is used; the operator could direct his attention at performing other tasks which could increase the machine's productivity.

A main component of an automatic steering control system is the sensing system. Sensing systems can generally be divided into two categories, contact and non-contact sensing. The contact sensors have the problem of requiring a large amount of maintenance time because they often fail due to excessive wear of moving parts, due to damage by collision and due to fouling by debris. A non-contact sensing system can typically be designed with no moving parts and the non-contact sensors can be mounted in a remote location where they can be protected

from collision or fouling by debris. Also, a non-contact sensor may have a faster response time and be able to detect objects which are moving past the non-contact sensor at a high speed.

The objectives of this research were to develop a non-contact sensing system and an automatic steering control system for the USDA over-the-row apple harvester. The automatic steering control system was required to accurately steer the apple harvester's front wheels such that each tree stayed within the harvester's allowable zone. This zone was 45 cm wide, 409 cm long and centered on the harvester's centerline. The zone extended from the harvester's front wheels to the rear wheels (Figure 3.1). The tree row was required to be either straight or a smooth continuous curve with radius of curvature of 121.9 cm (400 ft) or greater. To put limits on this research effort performance tests of the steering control system were done under simulated conditions. To simulate a row of trees, metal stands were used for the performance tests. Each tree stand had a 4 cm diameter post which simulated a tree trunk.

From the literature review information was found for two non-contact sensors that appeared to be feasible as a non-contact sensor for use with the apple harvester's automatic steering system. One of the sensors was an infrared photodetector which could be used to detect the presence of an object in a sensing zone. The sensor transmitted a light beam to an object equipped with a reflector. When the light beam ws reflected back to the sensor, an output signal indicated that an object was in the sensor's sensing zone. The second non-contact sensor was the Polaroid sonar system which included a transducer and circuit board which were manufactured by the Polaroid Corporation. The sonar system could measure the distance to an object. This could be accomplished by

measuring the time required for the ultrasonic sound pulse to travel out to the object and reflect back to the sonar system. The distance to the object can be computed if the travel time of the sound pulse to the object and the speed of sound are known. Six concepts for the apple harvester's non-contact sensing system were developed using these two non-contact sensors.

One of the six concepts was selected for development and a prototype non-contact sensing system was built. This developed concept contained an array of five sonar units (Figure 5.1) which were used to measure the distance from each sonar unit to the tree trunk as the harvester drove over each apple tree at 0.8 km/h (0.5 mph). The five sonar units were positioned on the left side of the harvester in an array which was parallel to the harvester's centerline. The sonar units were 80 cm from the harvester's centerline. The sonar units were positioned ahead of the harvester's front wheels so that the distance to each tree could be measured, and if the tree trunk was offset more than 2 cm from the harvester's centerline, a steering correction could be made before the tree trunk entered the front of the harvester's allowable zone. As the harvester traveled over a tree, the tree trunk moved past each of the five sonar units. One valid tree position measurement was made by each sonar unit. These sonar measurements were sent to the steering controller, and this microprocessor-based steering controller computed a tree position error which was the distance of offset of the tree trunk centerline from the harvester's centerline. If the tree position error was within ± 2 cm then a steering correction was not needed and the front wheels remained in the straight-ahead position (zero steering angle). After the tree position error was computed then

the value for desired wheel position was computed. If the tree position error exceeded the limit of ± 2 cm, then the steering controller activated one of two hydraulic solenoid valves to turn the harvester's front wheels either right or left. The controller turned (steered) the wheels to the computed wheel position. Once the wheels were turned to the desired wheel position, the wheels were held at that position until the next sonar unit in the array made a tree position measurement. Once the next sonar unit made a tree position measurement, a new value for the desired wheel position was computed and the wheels were turned to the new desired wheel position. This process was used for the first four of the five sonar units. For the fifth sonar unit, the wheels were turned to the computed desired wheel position and held at that position for about one second. Next, the wheels were turned to the straight-ahead position. The wheels stayed at the straight-ahead position until the next tree trunk moved past the first sonar unit in the array of five sonar units.

The steering control system used a microprocessor to perform a proportional control algorithm. For this algorithm the microprocessor directed the wheels to turn to a steering angle that was proportional to the harvester's position error. This steering control system was a closed-loop control system with one feedback signal which was the sonar measurement. This sonar measurement was used by the control system to compute the distance from the harvester's centerline to the tree trunk's centerline and this value represented the error signal. The sonar units were positioned on the harvester so that the sonar measurement was 78 cm when the tree was centered on the harvester's centerline. Thus, this control system may be classified as a regulator because the reference

signal for the control system is a fixed value of 78 cm. Figure 5.3 is a block diagram of the steering control system. The complete steering control system was built using electronic components with total cost of $2,205 which was $205 over the cost objective. Some of the components used could have been replaced by components which were less expensive and then the total cost would have been $1,430. This total cost was less than the $2,000 which was the maximum cost set by the cost objective. The components used in the actual control system had features that allowed it to be used for debugging hardware and software and these features caused the actual cost to exceed the cost objective.

The sonar system was tested for distance measurement accuracy. For these tests the sonar system was used to measure the distance to a target. The target was a flat metal plate with length and width of 12.7 cm. All five sonar units (Figure 6.5) were tested individually with one interface circuit (Figure 6.8) and the sonar measurements which had the units of centimeters were recorded for a target which was at a distance of 30 to 150 cm from the sonar units. These data indicated that each sonar unit had nearly identical accuracy and that the maximum sonar measurement error was 4 cm at an actual target distance of 150 cm. The air temperature was 25.5^{o}. The sonar measurement error decreased as the target distance decreased. At a target distance of 70 cm the sonar measurement error was only 1 cm. This same accuracy test was done with two sonar units at an air temperature of -1.0^{o}C. This sonar measurement error was 3 to 4 cm for a target distance between 30 and 150 cm. This same result was observed for both sonar units tested. Thus, the sonar sensing system which was designed can make distance measurements with an accuracy of ± 4 cm or less when the distance from the sonar unit to the

target is between 30 and 150 cm, and when the air temperature is in the range of $-1^{o}C$ to $25.5^{o}C$. The sonar unit was also tested to determine its sensing zone. This sensing zone is described as the zone in front of the sonar unit where an object can be detected. Tests were done using a steel cylinder as a target. The test results showed that the sonar transducer has a triangular shaped sensing zone in the horizontal plane and the included angle which is at the sonar unit is 22^{o} (Figure 6.12). Test data also showed that there was about a 10 percent increase in the sonar measurement error when the target was at the outer edges of the sonar sensing zone. This indicated that a target must be well inside the sonar sensing zone to avoid this increase in sonar measurement error.

Tests were also done in the laboratory with tree stands to determine if tilting the tree stand from the vertical affects the accuracy of the sonar measurement. Each tree stand is basically a round steel post with 4 cm diameter and a length of about 60 cm. These tree stands were used in all of the performance tests of the steering control system. The tests in the laboratory showed that as the tree stand was tilted from the vertical, the signal strength of the returning sound pulse was low and the sonar unit was making intermittent measurements which had an error of about 16 cm. For these tests the tree stand was at a distance of 78 cm from the sonar unit. This same test was done with an apple tree limb to determine if the accuracy of the sonar unit was affected by tilting the tree limb from the vertical. The tests showed that the tree limb could be tilted as much as 40^{o} from the vertical and the sonar unit made a measurement which has an error of

about 5 cm. Note that the error due to temperature during these tests with the tree stand and the tree limb was about 1 cm.

A simulation model was developed to simulate the complete closed-loop steering control system. The major elements of the steering control system that affect the dynamic response of the steering control system are the microprocessor-based steering controller; the hydraulic system for steering the front wheels; the kinematic motion of the harvester; and the non-contact sensing system (sonar system). The sonar measurement was the feedback signal and this sonar measurement represented the distance from the sonar unit to the tree trunk. The microprocessor was used to execute a proportional control function. The microprocessor computed a desired wheel position (D) which was a desired wheel steering angle. The microprocessor computed D using D=KE where K is the proportional gain factor and E is the tree position error. The simulation model's response was compared with the actual response of a simplified steering control system which had only one sonar unit. This system was mounted on the harvester and some performance data were collected and the actual harvester's steering control system responded slower than the response predicted by the simulation model. To make the simulation response slower, a first-order delay was used to slow the rate of change of the front wheel steering angle. This delayed front wheel steering angle was used as the input to the harvester's kinematic equations of motion. By using a delayed steering angle as the input, the simulation showed that the harvester's simulated response in the Y-direction was slower and more closely predicted the harvester's actual response. Factors that contribute to the harvester having a slower response than the simulation model are deformation of the tires during a

turn, misalignment between the harvester's front and rear wheels, and looseness in the steering linkage.

The model was used to check the sensitivity of the proportional gain factor (K) and also the simulation model was used to determine a value for K which was used in the actual controller for the apple harvester's steering control system. The simulation showed an unstable response for K=1.0 and a stable response for K=0.5. The simulation model was useful in designing the control algorithm for the harvester's steering controller. Data from the performance tests of the final design of the steering control system showed that the simulation, with first-order delay on the steering angle, had a faster response than the actual harvester's response. A comparison was made between the harvester's actual motion (Figure 9.15) and the motion predicted by the model using a row which has an 8 cm step change (Figure 9.16). The model used the first order delay to delay the steering angle. These data showed that during the simulation the harvester's motion in the Y-direction was faster than the actual harvester. Thus, this showed that the first order delay in the simulation was not completely effective at slowing down the harvester's reponse so that the model could accurately predict the motion of the actual harvester. When the simulation was run with a larger time constant for the first order delay, the simulation showed a harvester motion with oscillations in the Y-direction that were larger than those observed during tests. Based on this information, the first order delay was taken out of the simulation model and the simulation model was modified to reduce the steering angle by a proportional scale factor. The model was programmed to turn the wheels 0.4 degree for each 2 cm of tree position error, and the harvester

actually turned the wheels 0.7 degree for each 2 cm of tree position error. The model was modified in this manner so that it more accurately predicted the motion of the harvester during the test for a row with a step change. Next, the modified simulation model was run for a curved row (Figure 9.18) and the modified simulation model was found to accurately predict the actual motion observed by the harvester during tests with a curved row (Figure 9.8 to 9.13). The row radius of curvature was 121.9 m (400 ft). Thus the model reasonably predicted the motion of the harvester for a row with a step change and for a curved row.

Performance tests were done for the harvester's automatic steering control system to determine if the control system was able to control the steering of the harvester's front wheels and keep each tree stand within the harvester's allowable tree zone. Tests were done using simulated conditions on either a concrete driveway or on a campus lawn. Pens were attached to the harvester to draw lines on a strip of paper to record the path of the harvester. Tree stands were used to simulate a row of apple tree trunks for each of the performance tests of the steering control system. Three tests were done on a concrete driveway with a straight row. Six tests were done using a curved row with radius of curvature of 121.9 m (400 ft). Three of these six tests were done on a concrete driveway and the other three tests were done on a campus lawn. For each test a plot was made of the path of two points on the harvester. One of these points was on the harvester's centerline at the intersection of the front wheel centerline and the other point was on the harvester centerline at the intersection with the rear wheel centerline. The path of these two points were used to plot the motion

for all of the harvester's performance tests of the steering control system. For the three straight row tests there was a 5 cm maximum deviation of the front point and rear point on the harvester from the row centerline (Figure 9.5 to 9.3). For the six curved row tests, there was a maximum deviation of 8.7 cm of the harvester's front point from a tree stand and a maximum deviation of 3.2 cm of the harvester's rear point from a tree stand. These data showed that for the straight and curved row tests the steering control system was effective at keeping each tree stand within the harvester's allowable zone which had a width of 45 cm and each edge of the allowable zone was 22.5 cm from the harvester's centerline.

Performance tests of the steering control system were also done using a row with a step change. The step in the row was made by offsetting a portion of the straight row by 8 cm. The response of the motion of the harvester (Figure 9.15) was similar to the response of a first order system. Two other tests were done with a row which contained a step change. During both of these tests sonar unit one made an erroneous distance measurement for the first tree stand in the row. This erroneous reading caused the front of the harvester to have a maximum deviation of 15.5 cm from the center of the tree stand. The first tree stand in the row was observed to be tilted by 4^{o} from the vertical and this probably caused the sonar unit to make the erroneous reading. Another test was done with the first tree stand positioned so that it was closer to the vertical and then none of the sonar units made erroneous measurements. This problem of erroneous measurements should not occur in an apple orchard when the tree trunks are tilted from the vertical because tests have shown that a tree trunk which is tilted from

the vertical is more effective at reflecting an ultrasonic sound pulse back to the sonar unit so that accurate sonar measurements can be made by the sonar unit.

11. CONCLUSIONS

This study has led to the following conclusions:

1. An automatic steering control system and a non-contact sensing system were designed for the USDA over-the-row apple harvester.

2. This steering control system with a non-contact sensing system was tested using metal posts of 4 cm diameter to simulate a row of tree trunks. The tests were done using a straight row on a concrete surface. Also, tests were done using a curved row with radius of curvature of 121.9 m (400 ft) on a concrete surface and on a campus lawn. These tests were done to verify that the steering control system could control the steering of the harvester's front wheels such that each simulated tree stayed within the harvester's allowable zone as the harvester traveled over the row at 0.8 km/h (0.5 mph). This allowable zone was 45 cm wide and 409 centimeters long. The zone was centered on the harvester's longitudinal centerline such that the left and right edges of the allowable zone were 22.5 cm from the harvester's centerline. The allowable zone extends from the front wheel centerline to the rear wheel centerline. The results of the tests showed that for the straight and curved row the steering control system was effective at keeping each tree within the harveter's allowable zone.

3. The steering control system can be designed such that the total cost of the electronic components is $1,430. A cost of less than $2,000 for the electronic components was an objective for the control system.

4. A simulation model was developed to simulate the harvester's closed-loop automatic steering control system. The model reasonably predicted the motion of the apple harvester for curved tree row with radius of curvature of 121.9 m (400 ft) and for a row with an 8 cm step change in the row.

12. SUGGESTIONS FOR FURTHER RESEARCH

It is suggested that this study can be expanded in the following ways:

1. The steering control system that was developed should be tested in one or more commercial apple orchards. This type of testing is needed to determine if there are any deficiencies in the performance of the steering control system when the harvester is tested in an orchard instead of testing with a simulated environment.

2. An investigation should be done for changing the design of the steering control system so that the array of sonar units extends a shorter distance from the front wheel centerline. This will reduce the probability of damaging the sonar units due to objects colliding with the sonar units. Also a study should be done for the development of a connecting arm which supports the sonar unit. This connecting arm should have a hinge-joint and a return-spring so that if an object does collide with the sonar unit, then the connecting arm will be deflected by pivoting at the hinge-joint and thus help prevent damage to the sonar unit and the support structure. The return-spring would be used to hold the connecting arm in the normal position and to return the connecting arm to the normal position after it is deflected.

3. During the testing of the steering control system at a ground speed of 0.8 km/h (0.5 mph), the sonar units made occasional erroneous sonar measurements. These erroneous measurements may have occurred because the tree was not well inside the sensing zone of the sonar unit.

Also, the erroneous measurements were probably caused by a simulated tree trunk being tilted from the vertical. Tests have shown that a sonar unit can make erroneous sonar measurements when a simulated tree trunk is tilted from the vertical. Thus, tests should be done to determine how the sonar measurements change with respect to time as a tree trunk moves through a sonar unit's sensing zone. This information could then be used to develop an averaging technique which could eliminate the problem of the erroneous sonar measurements which occured during the apple harvester's performance tests.

4. Since the apple harvester power frame can be used for tree spraying at speeds up to 9.7 km/h (6.0 mph), the steering control system needs to be modified so that the control system operates effectively at speeds up to 9.7 km/h. The steering control system as designed, used a software sampling technique. This sampling technique was used to execute a time delay which allowed the tree trunk to get well inside the sonar unit's sensing zone before a sonar measurement was made. This software sampling technique was developed for a harvester ground speed of 0.8 km/h (0.5 mph). Thus, the hardware and the software should be modified so that the harvester's steering control system operates effectively at speeds up to 9.7 km/h. The new control system should be modified so that the steering control system operates effectively at specific ground speeds which are selected by the operator with a selector switch. Instead of using a selector switch, the steering control system could use a sensor to detect the actual ground speed, and automatically modify the operation of the steering control system for changes in ground speed. Another useful system for the harveter would be an automatic speed controller.

5. The harvester motion should be investigated to determine whether it can be accurately defined as the kinematic motion of a vehicle with ideal steering geometry and based on the results, modify the simulation model to improve the accuracy of the model.

APPENDICES

APPENDIX A

DATA FROM SONAR ACCURACY TESTS

APPENDIX A

DATA FROM SONAR ACCURACY TESTS

This appendix contains data that were collected to determine the accuracy of the five sonar units using a procedure that is described in Section 6.2.1. Sonar distance data were collected at an air temperature of 25.5^{o}C for sonar units 1 to 5. These data are shown in Tables 6.1, and A.1 to A.4 and a plot of these data is shown in Figures 6.10, and A.1 to A.4. Sonar distance data were also collected for sonar units 1 and 2 at an air temperature of -1.0^{o}C. These data are shown in Tables 6.2 and A.5 and are plotted in Figures 6.11 and A.5.

Table A.1 Sonar Distance Data from Accuracy Test for Sonar Unit - 2 at Air Temperature of 25.5°C.

SONAR DATA FROM ACURACY TEST

SONAR UNIT # 2 AT 25.5 DEG. C.

ACTUAL DISTANCE (CM)	DISTANCES READ BY SONAR UNIT (CM)				AVERAGE READ DISTANCE (CM)
30	31	31	31	31	31.00
40	41	40	41	41	40.75
50	50	50	50	50	50.00
60	60	60	60	60	60.00
70	69	69	69	70	69.25
75	75	74	74	74	74.25
76	76	75	75	75	75.25
77	76	76	77	76	76.25
78	77	77	78	77	77.25
79	79	78	79	78	78.50
80	79	79	79	79	79.00
81	80	80	80	80	80.00
82	81	81	81	81	81.00
83	82	82	82	82	82.00
84	83	83	83	83	83.00
85	84	84	84	84	84.00
90	89	89	89	89	89.00
100	99	98	99	98	98.50
110	108	108	108	108	108.00
120	118	117	117	118	117.50
130	127	127	127	127	127.00
140	137	137	137	137	137.00
150	147	146	147	146	146.50

Table A.2 Sonar Distance Data from Accuracy Test for Sonar Unit - 3 at Air Temperature of 25.5°C.

SONAR DATA FROM ACURACY TEST

SONAR UNIT # 3 AT 25.5 DEG. C.

ACTUAL DISTANCE (CM)	DISTANCES READ BY SONAR UNIT (CM)				AVERAGE READ DISTANCE (CM)
30	31	30	31	31	30.75
40	40	40	40	41	40.25
50	50	50	50	50	50.00
60	60	59	59	60	59.50
70	70	69	70	70	69.75
75	74	74	74	74	74.00
76	75	75	75	76	75.25
77	76	76	76	77	76.25
78	77	77	77	77	77.00
79	78	78	78	78	78.00
80	79	79	79	79	79.00
81	79	80	80	80	79.75
82	81	81	81	81	81.00
83	81	82	82	82	81.75
84	83	83	83	83	83.00
85	84	84	84	84	84.00
90	88	89	89	89	88.75
100	99	98	99	99	98.75
110	108	107	108	108	107.75
120	117	118	117	118	117.50
130	127	127	127	127	127.00
140	137	136	137	137	136.75
150	146	146	147	147	146.50

Table A.3 Sonar Distance Data from Accuracy Test for Sonar Unit - 4 at Air Temperature of 25.5°C.

SONAR DATA FROM ACURACY TEST

SONAR UNIT # 4 AT 25.5 DEG. C.

ACTUAL DISTANCE (CM)	DISTANCES READ BY SONAR UNIT (CM)				AVERAGE READ DISTANCE (CM)
30	31	30	30	31	30.50
40	41	40	41	41	40.75
50	50	50	50	50	50.00
60	60	59	59	60	59.50
70	69	70	69	70	69.50
75	74	74	74	74	74.00
76	75	75	75	75	75.00
77	76	76	76	76	76.00
78	77	77	77	77	77.00
79	78	78	78	78	78.00
80	79	79	79	79	79.00
81	80	80	80	80	80.00
82	81	80	81	81	80.75
83	82	82	81	82	81.75
84	83	83	82	83	82.75
85	84	84	84	84	84.00
90	89	89	88	89	88.75
100	98	98	98	98	98.00
110	108	108	108	108	108.00
120	118	117	118	117	117.50
130	127	127	128	127	127.25
140	137	137	137	137	137.00
150	146	147	147	147	146.75

Table A.4 Sonar Distance Data from Accuracy Tests for Sonar Unit - 5 at Air Temperature of 25.5°C.

SONAR DATA FROM ACURACY TEST

SONAR UNIT # 5 AT 25.5 DEG. C.

ACTUAL DISTANCE (CM)	DISTANCES READ BY SONAR UNIT (CM)				AVERAGE READ DISTANCE (CM)
30	31	31	30	31	30.75
40	41	41	41	41	41.00
50	50	50	50	51	50.25
60	60	60	60	60	60.00
70	69	70	70	70	69.75
75	75	74	74	75	74.50
76	75	75	76	75	75.25
77	76	76	77	76	76.25
78	77	77	77	77	77.00
80	79	79	79	79	79.00
79	79	78	78	78	78.25
81	80	80	80	80	80.00
82	81	81	81	81	81.00
83	82	82	82	82	82.00
84	83	83	83	83	83.00
85	84	84	84	84	84.00
90	88	89	89	88	88.50
100	98	98	98	98	98.00
110	108	108	109	108	108.25
120	117	118	118	118	117.75
130	127	128	127	128	127.50
140	137	137	137	137	137.00
150	147	146	146	147	146.50

Table A.5 Sonar Distance Data from Accuracy Test for Sonar Unit - 2 at Air Temperature of -1.0°C.

SONAR DATA FROM ACURACY TEST

SONAR UNIT # 2 AT -1.0 DEG. C.

ACTUAL DISTANCE (CM)	DISTANCES READ BY SONAR UNIT (CM)				AVERAGE READ DISTANCE (CM)
30	32	32	33	32	32.25
40	42	42	42	42	42.00
50	53	52	52	52	52.25
60	63	63	63	63	63.00
70	73	73	73	73	73.00
75	78	78	78	78	78.00
76	79	79	79	79	79.00
77	80	80	80	80	80.00
78	81	80	81	81	80.75
79	82	82	82	82	82.00
80	83	83	82	83	82.75
81	84	84	84	84	84.00
82	84	85	85	85	84.75
83	86	86	86	86	86.00
84	87	87	87	87	87.00
85	88	88	88	88	88.00
90	93	93	93	93	93.00
100	104	103	103	104	103.50
110	113	114	113	114	113.50
120	123	124	123	124	123.50
130	133	134	134	133	133.50
140	144	144	144	144	144.00
150	154	154	154	154	154.00

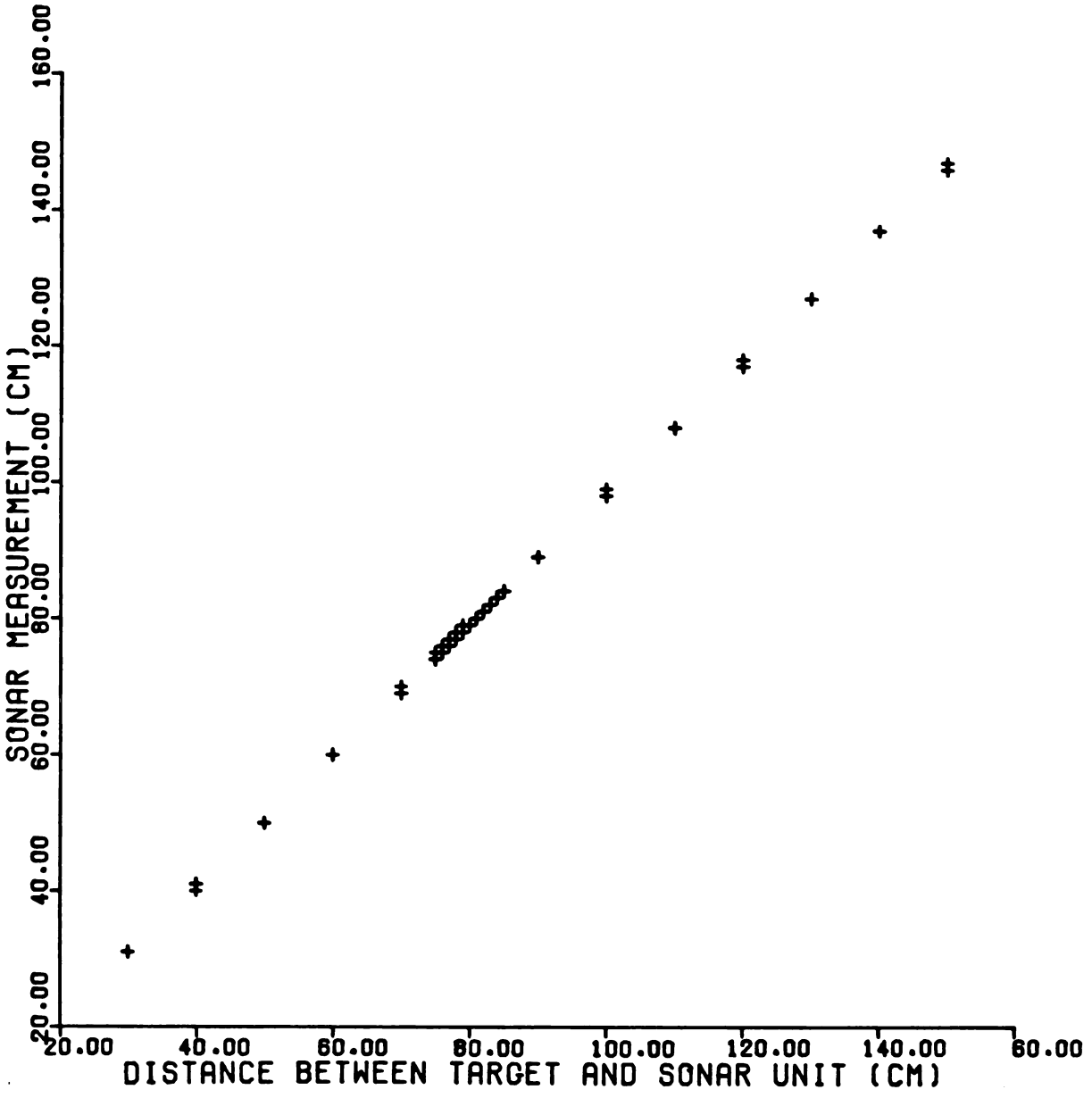

Figure A.1. Distance Data from Sonar Unit-2 At Air Temperature Of 25.5^{o}C.

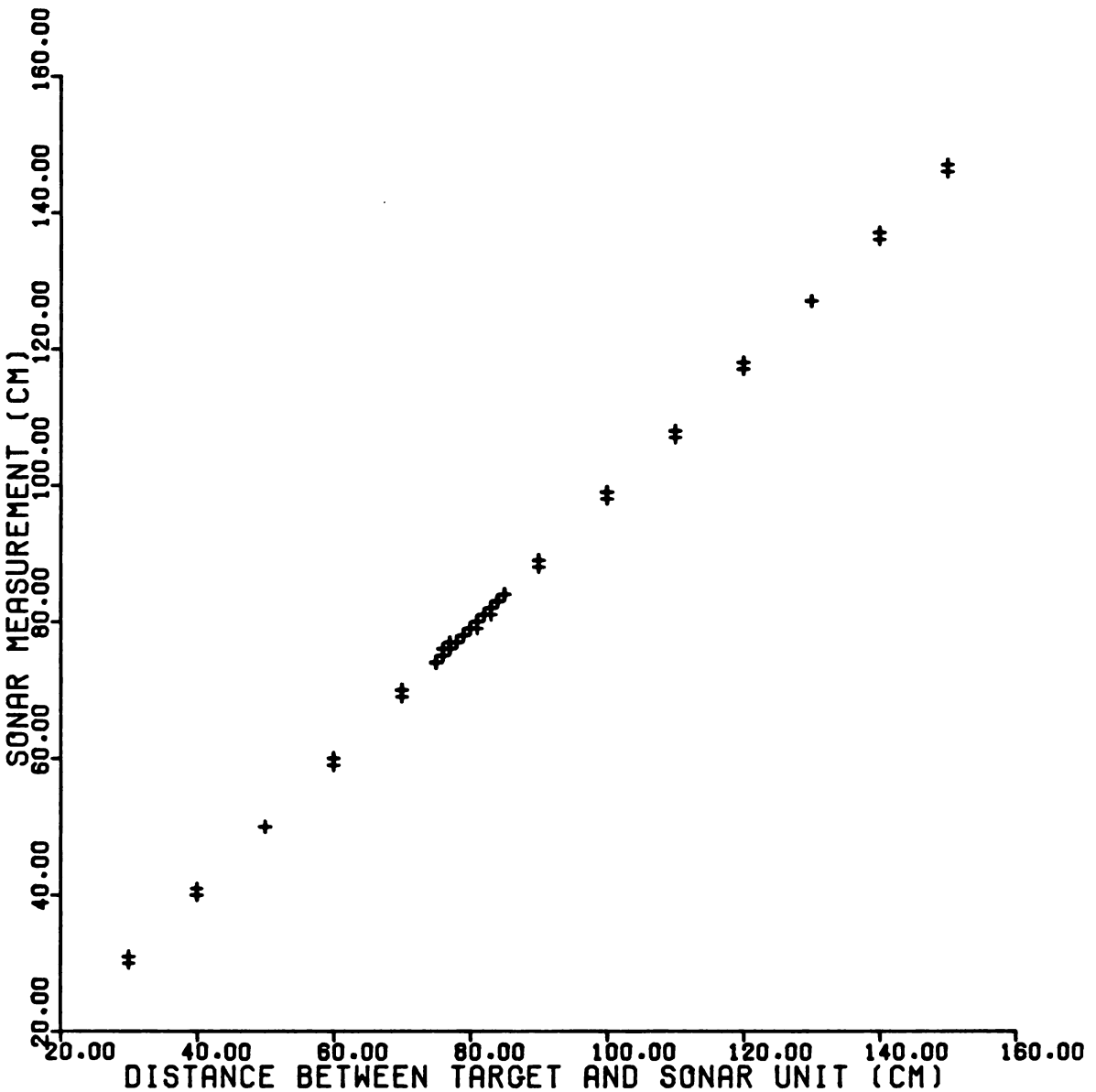

Figure A.2. Distance Data from Sonar Unit-3 At Air Temperature Of 25.5^{o}C.

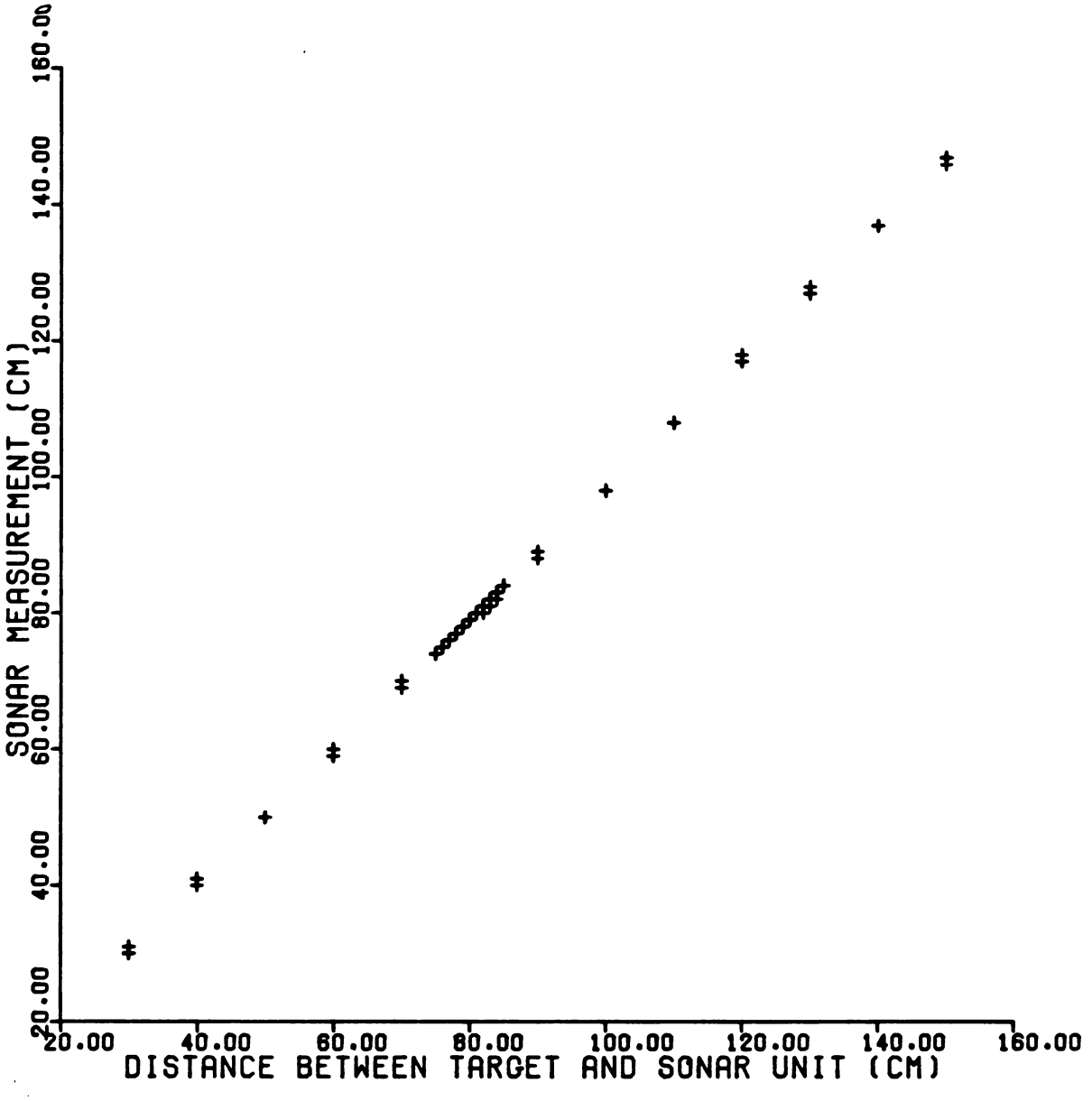

Figure A.3. Distance Data From Sonar Unit-4 At Air Temperature of 25.5°C.

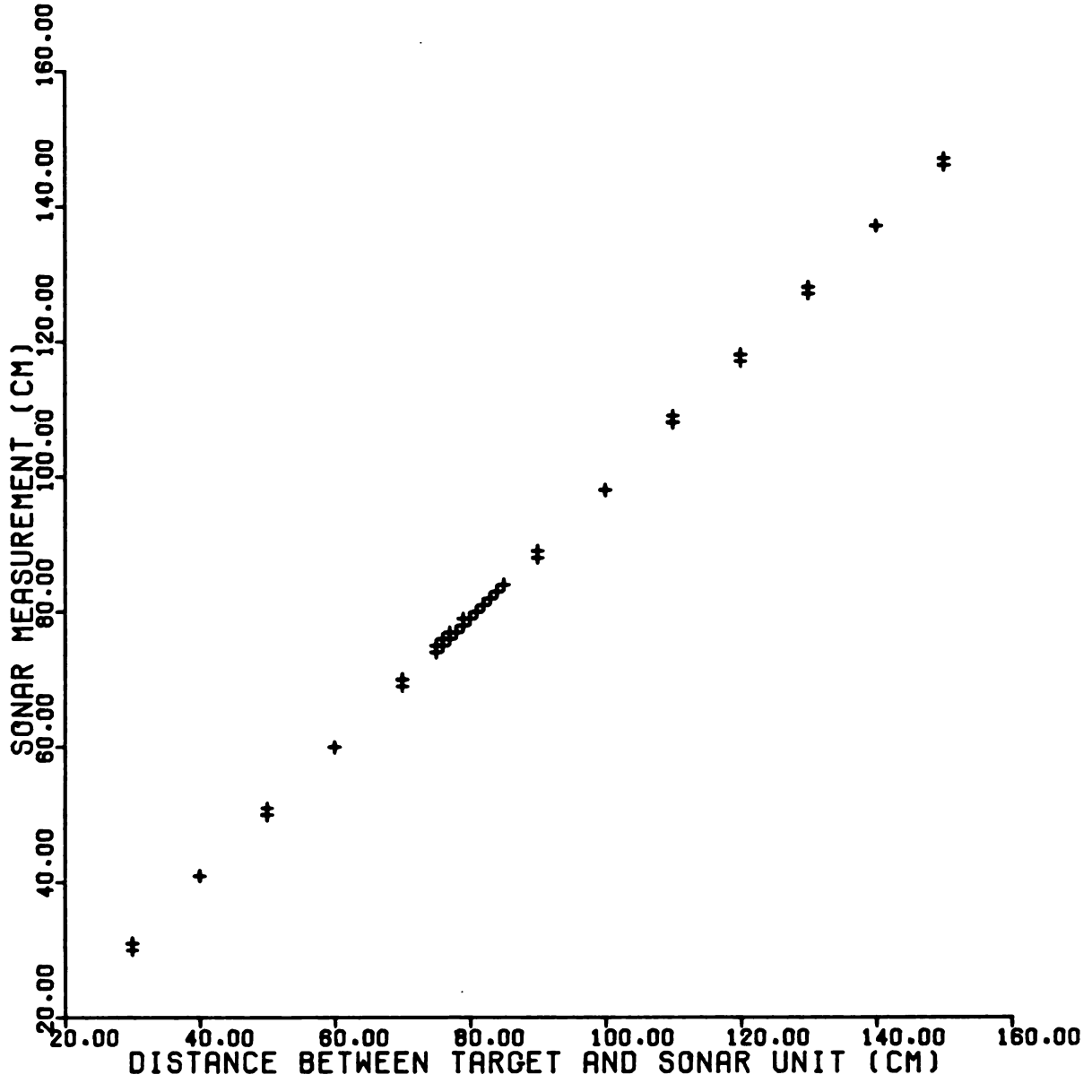

Figure A.4. Distance Data From Sonar Unit-5 At Air Temperature Of 25.5^{o}C.

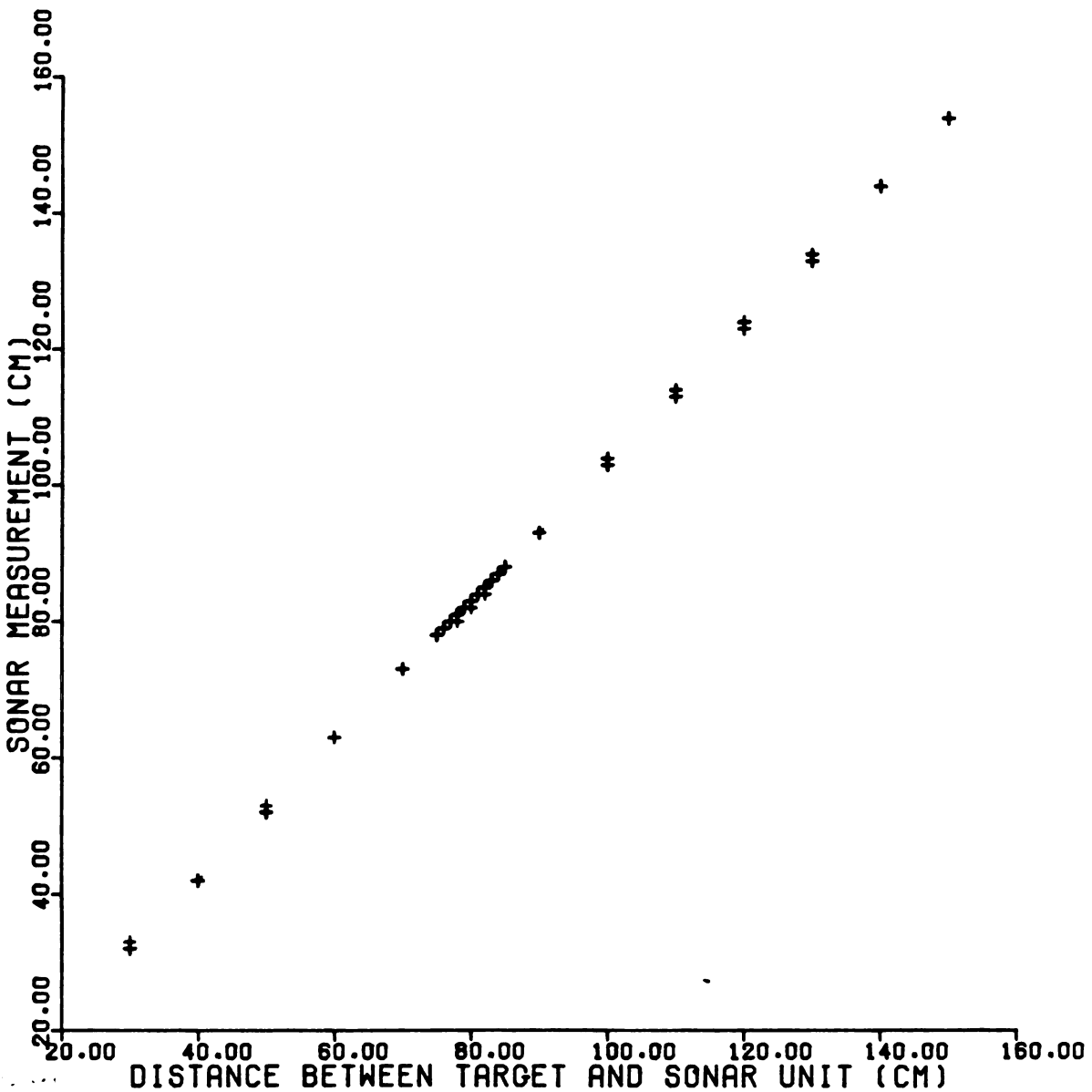

Figure A.5. Distance Data From Sonar Unit-2 At Air Temperature Of -1.0^{0}C.

APPENDIX B

COMPUTER PROGRAM FOR HARVESTER SIMULATION MODEL

APPENDIX B

COMPUTER PROGRAM FOR HARVESTER SIMULATION MODEL

This appendix contains a listing (Figure B.1) of the computer program that was developed to simulate the complete closed-loop steering control system which was developed for the USDA apple harvester. The steering control was developed so that the harvester automatically followed a tree row. Figure 5.3 is a block diagram of the major elements in the control system which affect the dynamics of the steering control system. These major elements are the microprocessor steering controller, the harvester's kinematic motion; the hydraulic system for turning the wheels, and the sonar sensing system which produced a feedback signal. The feedback signal represented the harvester's position from the tree trunk. This simulation model was also developed to graphically show the motion of the harvester as the harvester traveled over a tree row as described in Section 7.0.

Figure B.1. Listing of the Program for the Harvester's Steering Control System Simulation Model.

```
C*************************************************************************
C*************************************************************************
C******** GRAPHICAL DISPLAY OF HARVESTOR MOTION => GDISP ******************
C*************************************************************************
C*************************************************************************
C      PROGRAM GDISP SIMULATES THE MACHINE REACTION OF A NON-CONTACT
C AUTOMATIC STEERING SYSTEM TO BE USED ON AN EXPERIMENTAL APPLE
C HARVESTER.  THE APPLE HARVESTER IS A U.S.D.A. RESEARCH PROJECT AT
C MICHIGAN STATE UNIVERSITY.  THE COMPUTER PROGRAM SIMULATES THE
C DESIGNED STEERING RESPONSE USING FRONT WHEEL STEERING WHICH IS
C COMPUTED BY A MICROPROCESSOR.
C      THE PROGRAM COMPUTES THE POSITION AND ORIENTATION OF THE HAR-
C VESTER USING THE SUBROUTINE DVERK FROM THE IMSL COMPUTER PACKAGE,
C SOLVING THREE DIFERENTIAL EQUATIONS WHICH ARE IN THE SUBROUTINE
C FCN.  IT THEN DETERMINES IF ANY 'TREES' ARE WITHIN THE FIELD OF
C VISION FOR ANY OF FIVE SONAR UNITS, AND IF SO THE DISTANCE BETWEEN
C THAT UNIT AND THE TREE.  THIS DISTANCE IS USED TO CALCULATE THE ERROR
C IN MACHINE POSITION.  THIS ERROR IS CONVERTED INTO 1.4 DEGREE INCRE-
C MENTS OF THE DESIRED WHEEL POSITION (THE 1.4 DEGREE INCREMENTS
C ARE THE INCREMENTS OF TURNING USED BY THE ENCODERS ON THE APPLE
C HARVESTER).  THE ACTUAL WHEEL POSITION IS COMPARED TO THE DESIRED
C WHEEL POSITION.  THE DIFFERENCE BETWEEN THEM, IF ANY, DETERMINES THE
C WHEEL CODE (LEFT, RIGHT, OR NONE).  THE WHEEL CODE IS USED
C TO CALCULATE THE AMOUNT OF CHANGE IN WHEEL POSITION.  IT IS CAL-
C CULATED OVER A .01 SECOND INTERVAL WITH THE FRONT WHEELS ROTATING
C 7.0 DEGREES PER SECOND.  THE CHANGE IN POSITION IS ADDED TO THE
C PRIOR WHEEL POSITION TO FIND THE ACTUAL WHEEL POSITION.  THE ACTUAL
C WHEEL POSITION AND THE VELOCITY OF THE MACHINE ARE THEN USED TO
C CALCULATE A NEW MACHINE POSTION.
C
C      THE PROGRAM OUTPUT IS IN ONE OF TWO GRAPHIC MODES:
C
C      IN THE FIRST MODE, THE TREE POSITIONS ARE DRAWN WITH RESPECT TO THE
C HARVESTER.  THE OUTLINE OF THE HARVESTER IS DRAWN FIRST, ALONG WITH
C REFERENCE LINES SHOWING THE AREA WHICH THE TREE SHOULD REMAIN WITHIN.
C THIS AREA IS THE ALLOWABLE TREE ZONE.  RELATIVE TREE POSITIONS ARE THEN
C DRAWN AS THE HARVESTER MOVES DURING SIMULATION.
C
C      THE SECOND MODE OF OUTPUT IS DRAWING THE HARVESTER POSITION
C WITH RESPECT TO THE ROW OF TREES.  THE FRONT AND BACK COORDINATES
C OF THE HARVESTER ARE USED TO DRAW THE POSITION OF THE CENTER LINE AS
C THE HARVESTER ADVANCES.
C
C      TO RUN GDISP THE DATA FILE 'PAULDF' CONTAINS DATA FOR TREE POSI-
C TIONS AND VARIABLES FOR HARVESTOR CONTROL.
C      THE FOLLOWING IS AN EXAMPLE OF 'PAULDF'.  ONLY THE NUMBERS ARE
C IN THE FILE 'PAULDF'.
C 6                    <= NTREES
C ***************************
C 304.7 7.6
C 608.6 30.45
C 911.0 68.4           <= TREELO
C 1211.1 121.5
C 1508.2 189.9
C 1828.8 272.26
C ***************************
C .171.379 .472520
C 140.450 .988792
C 112.666 .764686 <= SNR
C 90.402 1.040811
C 78.664 1.440765
C ***************************
C .1745329             <= ANG
C 0.01                 <= TINCR
C 75000                <= NLOOP
C 7.0                  <= AWPINC
C 2.0                  <= INCALC
C 44.8                 <= AWP
C 10                   <= IPR
C 2.0                  <= EALWNC
C 22.35                <= V
C 300                  <= ICOUNT
C 4                    <= ICK
C 1                    <= Q
C 2.0                  <= SCAL
C 2.0                  <= T1
C 2000                 <= LENGTH
C 4                    <= SIZE
C 200                  <= WID
C 2                    <= POINT
C
C      WHERE:
C
C      NTREES => THE NUMBER OF TREES BEING USED IN THE SIMULATION.
C
C      TREELO => AN ARRAY CONTAINING THE X AND Y COORDINATES OF
C                EACH TREE
C
C      SNR => AN ARRAY CONTAINING THE DISTANCE TO EACH OF FIVE SONAR
C             UNITS FROM THE POINT CENTERED BETWEEN THE FRONT WHEELS (CM)
C             AND THE ANGLE BETWEEN THE LINE FROM CENTER POINT TO
C             THE CORESPONDING SONAR AND THE CENTER LINE OF THE HAR-
C             VESTER (RADIANS).
C
C      ANG => HALF THE CONE ANGLE OF THE SONAR UNITS (RADIANS)
C
C      TINCR=> TIME INCREMENT FOR ITERATION OF HARVESTER MOTION SIMULATION.
C
C      NLOOP => NUMBER OF TIMES THRU MAIN LOOP. CAUSES PROGRAM TO STOP
C               WHEN COMPLETED.
C
```

Figure B.1. (continued)

```
102)  C      AWPINC => WHEEL TURN RATE (DEG/SEC)
103)  C
104)  C      INCALC => SCALE FACTOR FOR ERROR USED TO OBTAIN DWP: INCALC = 1/K
105)  C                K = PROPORTIONAL GAIN
106)  C
107)  C      AWP => INITIAL ACTUAL WHEEL POSTIION
108)  C
109)  C      IPR => COUNTER FOR PRINTING IN VALUE DUMP MODE (G=0) : IE. IT DET-
110)  C             ERMINES THE AMOUNT OF DATA PRINTED.
111)  C
112)  C       EALWNC => ALLOWED ERROR IN SONAR READING (CM) BEFORE TURNING WHEELS
113)  C
114)  C       V => VELOCITY (CM/SEC)
115)  C
116)  C      ICOUNT => COUNTER FOR DRAWING HARVESTER CENTER LINE OR TREES IN
117)  C                GRAPHICS MODE: IE. DETERMINES THE NUMBER OF ITEMS DRAWN.
118)  C
119)  C      ICK => THE NUMBER OF TIME STEPS BETWEEN SONAR READINGS
120)  C
121)  C      G => MODE DETERMINING VARIABLE.
122)  C           G = 1 FIRST GRAPHICS MODE, DRAWS TREES WITH RESPECT TO THE
123)  C                 HARVESTRER INTERIOR.
124)  C           G = 2 SECOND GRAPHICS MODE, DRAWS HARVESTER CENTER LINE WITH
125)  C                 RESPECT TO TREES.
126)  C           G = 0 PRINTS VALUES OF SELECTED VARIABLES EVERY IPR TIMES THRU
127)  C                 THE MAIN LOOP.
128)  C
129)  C      SCAL => SIZE FOR SYMBOLS REPRESENTING TREES WITH RESPECT TO HARVESTER
130)  C
131)  C      T1 => TIME DELAY CONSTANT FOR FIRST ORDER DELAY IN DISCRETE FORM
132)  C
133)  C      LENGTH => LENGTH OF THE FIELD IN SECOND GRAPHICS MODE (CM)
134)  C
135)  C      SIZE => SCALING FACTOR FOR TREES IN GRAPHICS MODE 1
136)  C
137)  C      WID => WIDTH OF THE FIELD IN SECOND GRAPHICS MODE (CM)
138)  C
139)  C*************************************************************************
140)  C*************************************************************************
141)  C************************VARIABLE DEFINITIONS*****************************
142)  C*************************************************************************
143)  C ANG = ONE HALF THE ANGLE OF VISION FOR SONAR UNITS (RADIANS)
144)  C AWP = ACTUAL WHEEL POSITION ( IN 1.4 DEGREE INCREMENTS)
145)  C AWPINC = THE RATE OF CHANGE FOR ACTUAL WHEEL POSITION (DEG/SEC)
146)  C COUNT = LOOP COUNTER FOR GRAPHICS OUTPUT
147)  C DELT = HARVESTER ANGLE OFF OF THE HORIZONTAL REFERENCE
148)  C DELTD = DERIVATIVE OF HARVESTER ANGLE FUNCTION
149)  C DIF = ABSOLUTE VALUE OF ERROR
150)  C DIS = DISTANCE FROM FIRST TREE WITHIN HARVESTER TO CENTER POINT
151)  C DIST = DISTANCE FROM THE TREE, WITHIN A SONAR FIELD OF VISION, TO THE
152)  C         SONAR UNIT
153)  C DISTIN = DISTANCE FROM THE FIRST TREE WITHIN HARVESTER TO THE
154)  C           FRONT OF THE HARVESTER
155)  C DISTI2 = DISTANCE FROM SECOND TREE WITHIN HARVESTER TO FRONT
156)  C           OF HARVESTER.
157)  C DIS2 = DISTANCE FROM SECOND TREE WITHIN HARVESTER TO CENTER POINT
158)  C DWP = DESIRED WHEEL POSITION (IN 1.4 DEGREE INCREMENTS)
159)  C EALWNC = ALLOWED ERROR WITH RESPECT TO IDEAL HARVESTER POSITION
160)  C ERROR = HARVESTOR POSTION ERROR
161)  C G = MODE OF OUTPUT WHERE:  IF G = 0 THE PROGRAM DUMPS VARIABLE
162)  C     VALUES, IF G = 2 THE PROGRAM DRAWS POSITION OF HARVESTER WITH
163)  C     RESPECT TO A ROW OF TREES, IF G = 1 THE PROGRAM DRAWS THE
164)  C     POSITION OF THE TREES WITH RESPECT TO THE HARVESTER
165)  C IAWP = ACTUAL WHEEL POSITION IN 1.4 DEGREE INCREMENTS WHERE 32 IS
166)  C         CENTER AND 32+ IS TURNING LEFT
167)  C ICK = THE NUMBER OF TIME STEPS BETWEEN SONAR READINGS
168)  C ICOUNT = INCREMENT FOR DRAWING HARVESTER OR TREE POSITIONS
169)  C IER = ERROR PARAMETER FOR DVERK
170)  C IERR = ERROR PARAMETER FOR OPEN$G
171)  C INC = AMOUNT OF CHANGE FOR DESIRED WHEEL POSITION
172)  C INCALC = SCALE FACTOR FOR ERROR TO OBTAIN THE CHANGE IN DWP
173)  C          IE. INCALC = 1/K, K = PROPORTIONAL GAIN FACTOR
174)  C IND = INDICATOR (INPUT AND OUTPUT) FOR DVERK
175)  C IPR = SPECIFIES WHEN TO PRINT IN PRINT MODE
176)  C ITLAP = TIME DELAY BEFORE WHEELS RETURN TO CENTER AFTER LAST
177)  C          SONAR READING
178)  C ITR = THE TREE LAST SEEN BY A SONAR UNIT
179)  C ITREE = TREE PRESENTLY BEING VIEWED BY A SONAR UNIT
180)  C JINX = CONTROL PARAMETER FOR DRAWING TREE POSITIONS WITH RESPECT
181)  C         TO HARVESTER
182)  C KOUNT = LOOP COUNTER FOR READING FROM THE SONAR UNITS
183)  C LAB(6) = WORKSPACE MATRIX FOR LABELING GRAPH
184)  C LENGTH = HORIZONTAL LENGTH OF FIELD VISIBLE WITHIN GRAPHICS FRAME
185)  C LINED$ = DISTANCE FROM FIRST TREE WITHIN THE HARVESTER
186)  C          TO CENTER LINE
187)  C LINED2 = DISTANCE FROM SECOND TREE WITHIN THE HARVESTER
188)  C          TO CENTER LINE
189)  C N = NUMBER OF DIFFERENTIAL EQUATIONS TO BE SOLVED BY DVERK
190)  C NLOOP = NUMBER OF TIMES THROUGH MAIN LOOP
191)  C NTREES = THE NUMBER OF TREES BEING USED IN THE SIMULATION.
192)  C NW = ROW DIMENSION OF THE MATRIX W EXACTLY AS SPECIFIED IN THE
193)  C       DIMENSION STATEMENT
194)  C N1 = FILE TYPE RETURNED FROM SRCH$$
195)  C N2 = ERROR CODE RETURNED FROM SRCH$$
196)  C PRESIG = SIGF USED IN DVERK OVER THE LAST TIME INCREMMENT
197)  C OLDSIG = POSITION OF ENCODER (RADIANS)
198)  C SCAL = RADIUS OF TREES DRAWN RELATIVE TO THE HARVESTER
199)  C SIGF = FRONT WHEEL ANGLE (RADIANS)
200)  C SIZE = SCALING FACTOR FOR TREES IN GRAPHICS MODE 1
201)  C SNR(5,3) = LOCATION OF SONAR
202)  C SONAR = TRUNCATED DISTANCE FROM THE TREE, WITHIN A SONAR FIELD OF
```

Figure B.1. (continued)

```
C            VISION, TO THE SONAR UNIT
C  THETA = ANGLE BETWEEN CENTER LINE OF HARVESTER AND LINE FROM
C            FIRST TREE TO CENTER POINT
C  THET2 = ANGLE BETWEEN CENTER LINE OF HARVESTER AND LINE FROM
C            SECOND TREE TO CENTER POINT
C  TINCR = TIME INCREMENT FOR ITERATION OF HARVESTER MOTION SIMULATION
C  TOL = TOLERANCE FOR ERROR CONTROL IN DVERK
C  TR = NUMBER OF THE TREE WITHIN HARVESTER CLOSEST TO THE FRONT
C  TREELO = LOCATION OF TREE IN FIELD FRAME OF REFERENCE
C  TR2 = LAST TREE SEEN BY SONAR UNITS
C  TWHICH = LAST SONAR UNIT TO HAVE A TREE WITHIN ITS FIELD OF VISION
C  T1 = TIME DELAY CONSTANT FOR FIRST ORDER DELAY IN DISCRETE FORM
C  V = FORWARD VELOCITY (CM/SEC)
C  V1 = FRONT WHEEL VELOCITY (CM/SEC)
C  W(3,9) = WORKSPACE MATRIX FOR DVERK
C  WHICH = IDENTIFIES THE SONAR UNIT PRESENTLY READING TREE POSITION
C  WID = VERTICAL WIDTH OF FIELD VISIBLE IN GRAPHICS FRAME
C  WPDEG = WHEEL POSITION IN DEGREES
C  X = INDEPENDENT VARIABLE FOR DVERK
C  XDATA7 = X-COORDINATE OF FRONT POINT TO BE PLOTTED
C  XDATA8 = X-COORDINATE OF REAR POINT TO BE PLOTTED
C  XDIF = DIFFERENCE BETWEEN X-COORDINATES OF HARVESTER AND FIRST TREE
C            WITHIN HARVESTER
C  XD2 = DIFFERENCE BETWEEN X-COORDINATES OF HARVESTER AND SECOND TREE
C            WITHIN HARVESTER
C  XEND = THE END POINT OF EACH TIME INCREMENT
C  XMAX = MAXIMUM X-VALUE IN GRAPHICS FRAME
C  XMIN = MINIMUM X-VALUE IN GRAPHICS FRAME
C  X1 = FRONT X-COORDINATE SAVED AND PLOTTED FROM FOR EACH TIME INCREMENT
C  X13 = WHEEL BASE (CM)
C  X17 = DISTANCE BETWEEN FRONT AXLE AND FRONT POINT BEING TRACED (CM)
C  X2 = REAR X-COORDINATE SAVED AND PLOTTED FROM FOR EACH TIME INCREMENT
C  Y(3) = MATRIX FOR DEPENDENT VARIABLES IN DVERK
C  YDATA7 = Y-COORDINATE OF FRONT POINT TO BE PLOTTED
C  YDATA8 = Y-COORDINATE OF REAR POINT TO BE PLOTTED
C  YDIF = DIFFERENCE BETWEEN Y-COORDINATES OF HARVESTER AND FIRST
C            TREE WITHIN HARVESTER
C  YD2 = DIFFERENCE BETWEEN Y-COORDINATES OF HARVESTER AND SECOND
C           TREE WITHIN HARVESTER
C  YIDEAL = SONAR VALUE OF CENTERED TREE (=78 CM)
C  YMAX = MAXIMUM Y-VALUE IN GRAPHICS FRAME
C  YMIN = MINIMUM Y-VALUE IN GRAPHICS FRAME
C  Y1 = FRONT Y-COORDINATE SAVED AND PLOTTED FROM FOR EACH TIME INCREMENT
C  Y12 = DISTANCE BETWEEN FRONT WHEELS (CM)
C  Y2 = REAR Y-COORDINATE SAVED AND PLOTTED FROM FOR EACH TIME INCREMENT
C*************************************************************
C*************************************************************
C   FCN=SUBROUTINE CONTAINING DIFFERENTIAL EQUATIONS TO BE SOLVED
C   C IS NOT BEING USED IN THIS CASE
C   YPRIME(N)=DIFFERENTIAL EQUATION TO BE SOLVED
C*************************************************************
C*************************************************************
C*************************************************************
C***************BEGINNING OF PROGRAM QDISP********************
C*************************************************************
C
C
      INTEGER IER, IND, K, N, NW, SAMPLT, INC, COUNT, SONAR
     %, IAMP, I, ITLAP, NLOOP, IPR, WHICH, NTREES, ICOUNT, C2, POINT
     %, TR, ITR, ITREE, ICK, KOUNT, IERR, Q, TR2, JINX
      REAL C(24), TOL, W(3,9), X, XEND, Y(3), SIGF, V,
     %DELT, DELTD, YIDEAL, LAB(6), AMP, DMP, ERROR, AMPINC, TINCR, EALWNC,
     %V1, X17, Y12, X13, XMIN, XMAX, YMIN, YMAX, X1, Y1, Y2, XDIF, YDIF
     %, TREELO(2,20), SNR(5,3), ANG, DIST, DIS, THETA, LINEDS, SIZE
     %, XD2, YD2, DIS2, THET2, LINED2, DISTIN, DISTI2, LENGTH, INCALC
      EXTERNAL FCN, SNRDST, TREE
       EXTERNAL TEST17
      COMMON/BLOCK/XEND, SIGF, DELT, DELTD, V1, Y12, X17, X13
     %, TREELO, SNR
$INSERT SYSCOM>KEYS.F
      CALL SRCHS$(K$READ, 'PAULDF', 6, 5, N, N1)
C
C
C********INITIAL CONDITIONS FOR DIFFERENTIAL EQUATIONS********
C
C
      SIGF=0.0
      X17=0.0
      Y12=365.76
      X13=408.94
      DELT=0.0
      DELTD=0.0
      XMIN=0.0
C
C
C********INITIAL CONDITIONS FOR DVERK SUBROUTINE********
C
C
C        (N AND NW MUST BE SET TO THE NUMBER OF
C          DIFFERENTIAL EQUATIONS BEING SOLVED)
      N=3
      NW=3
      X=0.0
      IND=1
      Y(1)=0.0
      Y(2)=0.0
      Y(3)=0.0
      X1=0.0
      X2=-408.94
      Y1=0.0
      Y2=0.0
```

Figure B.1. (continued)

```
      TOL=0.01
C
C
C********INITIAL CONDITIONS ********
C
C
      IAWP=32
      COUNT=0
      C2=0
      XDIF=0
      YDIF=0
      TWPDEG=0.0
      PI=3.1415927
      ERROR=0.0
      SAMPLT=0
      DELTAT=0.01
      WPT=0.
      WTO=0.0
      DWP=32.
      FWP=0.0
       WPDEG=0.0
      R2=.04
      YIDEAL=78.0
      TR=1
       ITREE=1
       ITR=1
      DIS=78.
       LINEDS=78.0
       TR2=1
       LINED2=0.0
       DIS2=0.0
       XD2=0.0
       YD2=0.0
      JINX=1
      XDATA7=0.0
       YDATA7=0.0
      WHICH=0
      SONAR=78
       KOUNT=0
C
C
C******* READ VALUES FOR SNRDST CONSTANTS *****
C
C
      DO 1126 I=1,20
         TREELO(1,I)=-1
         TREELO(2,I)=0
 1126   CONTINUE
C READ DATA FROM 'PAULDF'
      READ(9,*) NTREES
      DO 1127 I=1,NTREES
         READ (9,*) TREELO(1,I),TREELO(2,I)
 1127   CONTINUE
      DO 1128 I=1,5
         READ(9,*) SNR(I,1),SNR(I,2)
 1128   CONTINUE
      READ (9,*) ANG
C
C
C****** READ IN CONSTANTS FOR PROGRAM CONTROL *****
C
C
      READ (9,*) TINCR,NLOOP,AWPINC,INCALC,AWP,IPR,EALWNC,V
     %,ICOUNT,ICK,G,SCAL,T1,LENGTH,SIZE,WID,POINT
       PRESIG=0.0
       YMIN=(-1*WID)
       YMAX=WID
       J=IPR
       V1=V
          XMAX=LENGTH
C
C
C*************************************************************
C SET UP FRAMES FOR GRAPHICS
C*************************************************************
C
C
C*DRAW FRAME AND LABEL FOR HAVESTOR WITH RESPECT TO TREE ROW**
        IF (G.NE.1) GOTO 1151
C      CALL CLOSE(5)
       CALL SRCH$$(K$CLOS,0,0,5,N1,N2)
       CALL INITT(120)
       CALL OPEN$Q('G_DATAG',7,IERR)
       CALL DWINDO(-400.0,LENGTH,(-1*WID),WID)
       CALL FRAME(100.0,(WID/12.5),5)
  300  FORMAT(F7.1)
  311  FORMAT(F3.1)
  312  FORMAT(F6.1)
  303  FORMAT(F6.1)
       CALL MOVEA(0.2,0.1)
       ENCODE(3,311,LAB)XMIN
       CALL ANPLOT(LAB,4,0.8)
       CALL MOVEA(0.1,(0.0-(WID-(WID/50.0))))
       ENCODE(6,312,LAB)YMIN
       CALL ANPLOT(LAB,4,0.8)
       CALL MOVEA((LENGTH-200),00.0)
       ENCODE(7,300,LAB)XMAX
       CALL ANPLOT(LAB,5,0.8)
       CALL MOVEA(0.1,(0.0+(WID-(WID/25.0))))
       ENCODE(7,303,LAB)YMAX
       CALL ANPLOT(LAB,4,0.8)
```

Figure B.1. (continued)

```
405)        CALL MOVEA(0.0,0.0)
406)  C
407)  C
408)  C***** DRAW TREES IN FIELD*****
409)        DO 1135 J=1,NTREES
410)        CALL TRESL(TREELO(1,J),TREELO(2,J),(LENGTH+500),(2*WID),SIZE)
411)   1135 CONTINUE
412)   1151 CONTINUE
413)  C
414)  C
415)  C***** DRAW ALLOWABLE TREE ZONE **********
416)  C
417)  C
418)        IF(Q.NE.2) GOTO 1122
419)        CALL SRCH88(KSCLOS,0,0,5,N1,N2)
420)        CALL INITT(120)
421)        CALL OPEN88('Q_DATA',6,IERR)
422)        CALL DWINDO(-409.0,0.0,-155.5,155.5)
423)        CALL FRAME(10.0,4.0,5)
424)        CALL MOVEA(-409.0,22.86)
425)        CALL DRAWA(0.0,22.86)
426)        CALL MOVEA(0.0,-22.86)
427)        CALL DRAWA(-409.0,-22.86)
428)        CALL MOVEA(0.0,0.0)
429)        CALL DRAWA(-409.0,0.0)
430)  C
431)        CALL SNRDST(XDATA7,YDATA7,DELT,WHICH,DIST,ANG,ITREE)
432)        IF (WHICH .NE. 0 ) GOTO 1231
433)        GOTO 1216
434)   1231 CONTINUE
435)        SONAR=INT(DIST)
436)        ITLAP=1/TINCR
437)   1216 CONTINUE
438)  C
439)  C BEGINNING OF MAIN LOOP FOR HARVESTOR MOTION IN TREE ROW
440)  C*****!*****************************************************************
441)  C*****************************************************************
442)  C
443)  C
444)   1122   CONTINUE
445)        DO 12 K=1,NLOOP
446)        COUNT=COUNT+1
447)         C2=C2+1
448)        XEND=FLOAT(K)*TINCR
449)         KOUNT=KOUNT+1
450)  C
451)  C
452)  C
453)  C*****************************************************************
454)  C     MICROPROCESSOR SIMULATION
455)  C*****************************************************************
456)  C
457)  C
458)  C
459)  C
460)  C*******************DETERMINE ERROR*******************
461)  C
462)  C
463)          ERROR=YIDEAL - SONAR
464)          DIF=ABS(ERROR)
465)          IF(DIF.GT.EALWNC) GO TO 1013
466)          ERROR = 0.0
467)   1013   CONTINUE
468)  C
469)  C
470)  C ** CALCULATE INCREMENTS OF ERROR & DESIRED WHEEL POSTION**
471)  C
472)  C
473)        INC=AINT(ERROR/INCALC)
474)        DWP=FLOAT(32+INC)
475)        ITLAP=ITLAP-1
476)        IF (TWHICH.EQ.5) GOTO 1132
477)        GOTO 1134
478)   1132 CONTINUE
479)        IF (ITLAP.LE.0) DWP=32
480)   1134 CONTINUE
481)  C
482)  C
483)  C** TURN WHEEL ACCORDING TO DESIRED WHEEL POSTION **
484)  C
485)  C
486)   333  IAWP=AINT(AWP/1.4)
487)        IF(IAWP.GT.DWP) GO TO 301
488)        IF(IAWP.EQ.DWP) GO TO 302
489)  C
490)  C TURN LEFT
491)  C
492)        AWP=AWP+(AWPINC*TINCR)
493)        GO TO 302
494)  C
495)  C TURN RIGHT
496)  C
497)   301  AWP=AWP-(AWPINC*TINCR)
498)        GO TO 302
499)  C CONVERT AWP TO SIGF
500)   302  WPDEG=(44.8-AWP)
501)        OLDSIG=WPDEG*(PI/180.0)
502)  C COMPUTE FIRST ORDER DELAY OF FRONT WHEEL POSITION
503)        SIGF=PRESIG+(TINCR/(TINCR+T1))*(OLDSIG-PRESIG)
504)        PRESIG=SIGF
505)  C
```

Figure B.1. (continued)

```
C
C
C*************************************************************************
C GRAPHICS OUTOUT
C*************************************************************************
C
C
C*****************************************
C IF DRAWING POSITION OF TREE WITH RESPECT TO
C THE HARVESTOR, CALCULATE POSITION AND DRAW
C A SYMBOL AT PROPER TIME INCREMENT
C*****************************************
C
C
C** CALCULATE DISTANCE FROM TREES WITHIN HARVESTOR TO CENTER LINE **
C
C
      IF (WHICH .NE. 0 ) GOTO 1131
      GOTO 1016
 1131 CONTINUE
      SONAR=INT(DIST)
      ITLAP=1/TINCR
      TWHICH=WHICH
      ITR=ITREE
      IF (WHICH.EQ. 5) JINX=0
      GOTO 1136
 1016  CONTINUE
      IF(TWHICH.EQ.5) GOTO 1144
      JINX=0
      GOTO 1136
 1144 IF(JINX.EQ.1) GOTO 1136
      JINX=1
      TR2=TR
      TR = ITR
 1136 CONTINUE
C
C
C*** DETERMINE NEW READING FROM SONAR ***
C
C
       IF (KOUNT.NE.ICK) GOTO 201
       KOUNT=0
      CALL SNRDST(XDATA7,YDATA7,DELT,WHICH,DIST,ANG,ITREE)
      IF (WHICH .NE. 0 ) GOTO 200
      GOTO 201
 200  CONTINUE
      SONAR=INT(DIST)
      ITLAP=1/TINCR
 201  CONTINUE
C
C
C** CALCULATE NEW HARVESTER POSITION***
C
C
      CALL DVERK(N,FCN,X,Y,XEND,TOL,IND,C,NW,W,IER)
      XDATA8=Y(1)-X13*COS(Y(3))
      YDATA8=Y(2)+X13*SIN(Y(3))
      XDATA7=Y(1)
      YDATA7=Y(2)
      DELT=Y(3)
      DELTD=V1*SIN(SIGF)/X13
      XDIF=XDATA7-TREELO(1,TR)
      YDIF=YDATA7-TREELO(2,TR)
      DIS=(XDIF**2+YDIF**2)**.5
      IF (XDIF.EQ.0.0) GOTO 1137
      THETA=ATAN(YDIF/XDIF)+DELT
      GOTO 1139
 1137 THETA = (PI/2)+DELT
 1139 LINEDS= DIS*SIN(THETA)*(-1)
      DISTIN= DIS*COS(THETA)*(-1)
       IF( DISTIN.LT.(-1*X13)) LINEDS=99.9
      XD2=XDATA7-TREELO(1,TR2)
      YD2=YDATA7-TREELO(2,TR2)
      DIS2=(XD2**2+YD2**2)**.5
      IF(XD2.EQ.0.0) GOTO 1147
      THET2=ATAN(YD2/XD2)+DELT
      GOTO 1149
 1147 THET2=(PI/2)+DELT
 1149 LINED2=DIS2*SIN(THET2)*(-1)
      DISTI2=DIS2*COS(THET2)*(-1)
      IF (DISTI2.LT.(-1*X13)) LINED2=99.9
C
C
C**** DRAW TREES AS THEY PASS THROUGH THE ALLOWABLE ZONE ****
C
C
      IF (0.NE.2) GOTO 1153
      IF(COUNT.NE.ICOUNT) GOTO 1153
      COUNT=0
      IF(XDATA7.LE.TREELO(1,1)) GOTO 1153
      IF (LINEDS.EQ.99.9) GOTO 1150
       CALL TREE(DISTIN,LINEDS,SCAL,TR)
 1150 IF(LINED2.EQ.99.9) GOTO 1153
      CALL TREE(DISTI2,LINED2,SCAL,TR2)
C
C
C*****************************************************************
C IF DRAWING HARVESTER WITH RESPECT TO TREES
C DRAW ACTUAL POSITION OF HARVESTER
C
C
```

Figure B.1. (continued)

```
607)  1153  IF(G.NE.1) GOTO 530
608)       IF(COUNT.EQ.ICOUNT) GO TO 11
609)       IF(C2.EQ. IPR) GOTO 14
610)        GOTO 530
611)  14     CONTINUE
612)       C2=0
613)       CALL MOVEA(X2,Y2)
614)       CALL DRAWA(XDATA8,YDATA8)
615)       CALL MOVEA(X1,Y1)
616)       CALL DRAWA(XDATA7,YDATA7)
617)       GO TO 13
618)  11    COUNT=0
619)       CALL MOVEA(X1,Y1)
620)       CALL DRAWA(X2,Y2)
621)       GO TO 13
622)  13    X1=XDATA7
623)       X2=XDATA8
624)       Y1=YDATA7
625)       Y2=YDATA8
626)  530   CONTINUE
627)       J=J-1
628)       IF(G.NE.0) GOTO 12
629)        IF (J.NE.0) GOTO 12
630) C
631) C
632) C*************************************** PRINT RESULTS*******
633) C IF G = 0 , PRINT VALUES OF SELECTED VARIABLES PERIODICALLY ACCORDING
634) C TO VALUE IPR
635) C*********************************************************************
636) C
637) C
638)       PRINT 909,XEND,WHICH,ITR,SONAR,DIST,TWPDEG,WPDEG,IAWP,DWP
639)      %,TR,LINEDS,TR2,LINED2,XDATA7,YDATA7,XDATA8,YDATA8,DELT
640)  909  FORMAT(1X,F6.2,1X,I1,1X,I2,1X,I3,1X,F7.2,1X,F4.1,1X,F6.3
641)      %,1X,2(I4,1X),2(I2,1X,F7.2,1X),4(F8.2,1X),F9.6)
642)       J=IPR
643) C BOTTOM OF MAIN LOOP
644)  12    CONTINUE
645) C CLOSE GRAPHICS FILES AND STOP
646)        CALL CLOSGO(IERR)
647)       CALL ANMODE
648)       CALL EXIT
649)  66      CONTINUE
650)       STOP
651)       END
652) C*********************************************************
653) C*******SUBROUTINE FCN IS USED BY SUBROUTINE DVERK*******
654) C****                              ***********
655) C****  *****  ***  *   *          ***********
656) C****  *      *    **  *          ***********
657) C****  ***    *    * * *          ***********
658) C****  *      *    *  **          ***********
659) C****  *       **** *   *          ***********
660) C****                              ***********
661) C*********************************************************
662)       SUBROUTINE FCN(N,X,Y,YPRIME)
663)       INTEGER N
664)       REAL X,Y(N),YPRIME(N),M,XEND,DELT,DELTD,SIGF,
665)      %V1,X13
666)       COMMON/BLOCK/XEND,SIGF,DELT,DELTD,V1,Y12,X17,X13
667)      %,TREELO,SNR
668) C*****X-COORDINATE FOR FRONT POINT*****
669)       YPRIME(1)=(V1*COS(SIGF+Y(3)))+(((((Y12/2.0)**2)+(X17**2))**0.5)
670)      %*COS(Y(3)-ATAN(2.0*X17/Y12)))*ABS(DELTD)
671) C*****Y-COORDINATE FOR FRONT POINT*****
672)       YPRIME(2)=(-V1*SIN(SIGF+Y(3)))-(((((Y12/2.0)**2)+(X17**2))**0.5)
673)      %*SIN(Y(3)-ATAN(2.0*X17/Y12)))*ABS(DELTD)
674) C*****  ANGLE OF ROTATION OF MACHINE*****
675)       YPRIME(3)=(V1*SIN(SIGF))/408.94
676)       M=X
677)       RETURN
678)       END
679) C*****************************************************************************
680) C****                                                        ********************
681) C****   ***   *   *  ****   ****    ***   *****  ********************
682) C****  *   *  **  *  *   *  *   *  *   *     *    ********************
683) C****   ***   * * *  ****   *   *  *  **     *    ********************
684) C****      *  *  **  *  *   *   *      *     *    ********************
685) C****   ***   *   *  *   *  ****    ***      *    ********************
686) C****                                                        ********************
687) C*****************************************************************************
688) C*****************************************************************************
689) C      SUBROUTINE SNRDST
690) C       SNRDST USES THE LOCATION OF THE HARVESTOR IN X & Y COORDINATES,
691) C AND THE ANGLE IN RADIANS THAT THE CENTER LINE OF THE MACHINE MAKES
692) C WITH THE HORIZONTAL REFERENCE FRAME.  IT DETERMINES WHICH IF ANY OF THE
693) C SONAR UNITS HAS A TREE WITHIN ITS FIELD OF VISION, AND THE DISTANCE TO
694) C THAT TREE
695) C
696) C GLOBAL VARIABLES
697) C   TREELO=> ARRAY 2 BY 20 THE FIRST ROW CONTAINS THE X DISTANCES OF UP TO 19 TREES
698) C   UP TO 19 TREES FROM THE ORIGIN, FOLLOWED BY A STOPPER VALUE
699) C   OF -1.  THE SECOND ROW CONTAINS THE Y DISTANCES FROM THE ORIGIN.
700) C
701) C   SNR=> 5 BY 2 ARRAY, CONTAINS THE DISTANCE FROM THE CANTER
702) C   POINT OF THE HARVESTOR TO EACH OF THE 5 SONAR UNITS IN CM
703) C   IN THE FIRST COLUMN, AND THE ANGLE BETWEEN THE CENTERLINE OF
704) C   THE HARVESTOR AND THE LINE FROM THE CENTER POINT TO THE SONAR UNIT
705) C   IN THE SECOND COLUMN.
706) C
707) C PARAMETERS
```

Figure B.1. (continued)

```
708) C    XBEAST => X COORDINATE OF THE HARVESTOR IN THE FIELD.
709) C
710) C    YBEAST => Y COORDINATE OF THE HARVESTOR IN THE FIELD.
711) C
712) C    DELTA => THE ANGLE THE CENTER LINE OF THE HARVESTOR MAKES WITH
713) C             THE X-AXIS IN THE NEGITIVE Y DIRECTION.  (RADIANS)
714) C
715) C*************************************************************************
716) C*************************************************************************
717)       SUBROUTINE SNRDST(XBEAST,YBEAST,DELTA,WHICH,DISTA,ANG,NEXTRE)
718)       REAL XTREE,YTREE,XBEAST,YBEAST,DISTA,TREELO,SNR,ANG
719)       REAL DELTA,XSNR,YSNR
720)       INTEGER SNRPO,TEST,NEXTRE,WHICH
721)       COMMON/BLOCK/XEND,SIOF,DELT,DELTD,V1,Y12,X17,X13
722)      %,TREELO,SNR
723) C SNRPO   =  POINTER FOR WHICH SONAR UNIT IS BEING TESTED
724) C TEST = IF TEST = 0 TREE IS IN FRONT OF SONAR FIELD OF VISION
725) C         IF TEST = 1  TREE IS IN SONAR VIEW
726) C         IF TEST = -1  TREE IS PAST SONARS FIELD OF VISION
727) C         TEST IS RETURNED FROM SUB.  AFIELD
728) C NEXTRE = POINTER TO NEXT TREE TO BE OR BEING TESTED FOR
729)       DIMENSION TREELO(2,20),SNR(5,2)
730)       NEXTRE=1
731)       XTREE=TREELO(1,NEXTRE)
732)       YTREE=TREELO(2,NEXTRE)
733)       SNRPO=1
734) 100   IF (XTREE .LT. 0) GOTO 99
735)        XSNR=XBEAST+SNR(SNRPO,1)*COS(SNR(SNRPO,2)-DELTA)
736)        YSNR=YBEAST+SNR(SNRPO,1)*SIN(SNR(SNRPO,2)-DELTA)
737)       CALL AFIELD(XTREE,YTREE,XSNR,YSNR,DELTA,TEST,ANG)
738)        IF (TEST .EQ. 0) GO TO 99
739)        IF (TEST .EQ. 1) GO TO 200
740)            SNRPO=SNRPO+1
741)            IF (SNRPO .LT. 6) GO TO 100
742)               NEXTRE=NEXTRE+1
743)               XTREE=TREELO(1,NEXTRE)
744)               YTREE=TREELO(2,NEXTRE)
745)               SNRPO=1
746)            GO TO 100
747) 200       CONTINUE
748)       WHICH=SNRPO
749)       DISTA=((XTREE-XSNR)**2+(YTREE-YSNR)**2)**.5
750)       RETURN
751) 99    DISTA=-999.00
752)       WHICH=0
753)       RETURN
754)       END
755) C*****************************************
756) C****                                  ****
757) C****  ***  ***** *** ***** *     ****  ****
758) C**** *   * *     *  *     *     *    * ****
759) C**** ***** ***    *  ***   *     *    * ****
760) C**** *   * *     *  *     *     *    * ****
761) C**** *   * *    *** ***** ***** ****  ****
762) C****                                  ****
763) C*****************************************
764) C**** SUBROUTINE AFIELD ********************
765) C GIVEN X&Y COORDINATES OF A TREE,  THE X&Y COORDINATES OF A SONAR UNIT
766) C THE ANGLE,  DELTA,  THE HARVESTER MAKES WITH THE HORIZONTAL REFERENCE AND
767) C THE ANGLE OF VISION OF THE SONAR UNIT,  AFIELD RETURNS A VALUE IN 'TEST'
768) C INDICATING THE POSITION OF THE TREE RELATIVE TO THE SONARS FIELD OF VISION
769) C
770) C XTREE=>  X COORD.  OF TREE
771) C
772) C YTREE=> Y COORD. OF TREE
773) C
774) C XSNR=> X COORD. OF SONAR UNIT
775) C
776) C YSNR=> Y COORD. OF SONAR UNIT
777) C
778) C DELTA=> ANGLE (IN RADIANS) BETWEEN CENTER LINE OF HARVESTER AND HORIZONTAL
779) C          REFERENCE.  WHERE NEG. DELTA IS IN POSITIVE Y DIRECTION.
780) C
781) C TEST=> TREE POSTION RELATIVE TO SONAR
782) C              TEST=0 => THE TREE IS AHEAD OF SONAR'S FIELD OF VISION
783) C              TEST=1 => THE TREE IS WITHIN THE SONAR'S FIELD OF VISION
784) C              TEST=-1 => THE TREE IS PAST THE SONAR'S FIELD OF VISION
785) C
786) C*************************************************************************
787) C
788)       SUBROUTINE AFIELD(XTREE,YTREE,XSNR,YSNR,DELTA,TEST,ANG)
789)       REAL XTREE,YTREE,XSNR,YSNR,DELTA,PHI,ANG
790)       INTEGER TEST
791)       TEST=0
792)       IF(YSNR.EQ.YTREE) GOTO 201
793)       PHI= ATAN((XTREE-XSNR)/(YSNR-YTREE))+DELTA
794)       GOTO 202
795)  201  PHI=1.570796
796)  202  CONTINUE
797)       IF(PHI .GT. ANG) RETURN
798)          TEST=1
799)           IF(PHI .GE. (-1*ANG)) RETURN
800)              TEST=-1
801)        RETURN
802)       END
```

Figure B.1. (continued)

```
C***** SUBROUTINE TREE****************************************
C*************************************************************
C****                                                    *****
C**** ***** ****  *****  *****                           *****
C****   *   *   * *      *                               *****
C****   *   ****  ****   ****                            *****
C****   *   *   * *      *                               *****
C****   *   *   * *****  *****                           *****
C***********************************************************
C SUBROUTINE TREE => GIVEN THE X & Y COORDINATES,THE RADIUS
C AND THE TYPE,FOR A SYMBOL, TREE DRAWS THAT SYMBOL CENTERED ABOUT X & Y.
C
C X=> X COORD.  OF THE SYMBOL
C
C
C Y=> Y COORD.  OF THE SYMBOL
C
C SC=> RADIUS OF THE SYMBOL
C
C TYPE=> SYMBOL TYPE, WHERE:
C              TYPE=1 => X
C              TYPE=2 => +
C              TYPE=3 => BOX
C              TYPE=4 TO N => POLYGON WITH N-1 SIDES
C
C*********************************************************
      SUBROUTINE TREE(X,Y,SC,TYPE)
      INTEGER TYPE,SIDES,J1
      REAL X,Y,SC,X1,Y1,RADS,PI
      PI=3.141592654
       SIDES = TYPE-1
      IF(TYPE.LE.0) GOTO 940
      IF(TYPE.GE.4) GOTO 990
      GOTO (960,970,980),TYPE
  960 CONTINUE
C DRAW AN X AT X,Y
      CALL MOVEA(X,Y)
      CALL MOVER((1.0*SC),(1.0*SC))
      CALL DRAWR((-2.0*SC),(-2.0*SC))
      CALL MOVER(0.0,(2.0*SC))
      CALL DRAWR((2.0*SC),(-2.0*SC))
      GOTO 940
  970 CONTINUE
C DRAW A PLUS SIGN AT X,Y
      CALL MOVEA(X,Y)
      CALL MOVER(SC,0.0)
      CALL DRAWR((-2.*SC),0.0)
      CALL MOVER((1.0*SC),(1.0*SC))
      CALL DRAWR(0.0,(-2.*SC))
      GOTO 940
  980 CONTINUE
C DRAW A BOX AT X,Y
      CALL MOVEA(X,Y)
      CALL MOVER(SC,SC)
      CALL DRAWR((-2.*SC),0.)
      CALL DRAWR(0.0,(-2.*SC))
      CALL DRAWR((2.*SC),0.0)
      CALL DRAWR(0.0,(2.*SC))
      GOTO 940
   990 CONTINUE
C DRAW A POLYGON WITH TYPE-1 SIDES
      CALL MOVEA(X,Y)
      CALL MOVER(SC,0.0)
      DO 1000 J1=1,SIDES
      RADS=J1*PI*2./SIDES
      X1=SC*COS(RADS)+X
      Y1=SC*SIN(RADS)+Y
      CALL DRAWA(X1,Y1)
 1000 CONTINUE
  940 RETURN
      END
C%%%%%%%%%%%%%%%%%%%%%%%%%%%%%%%%%%%%%%%%%%%%%%%%%%%%%%%%%%%%%%%
C%%%%                                %%%%%%%%%%%%%%%%%%%%%%%%%%%
C%%%% %%%%% %%%%  %%%%%  %%%% %      %%%%%%%%%%%%%%%%%%%%%%%%%%%
C%%%%   %   %   % %     %     %      %%%%%%%%%%%%%%%%%%%%%%%%%%%
C%%%%   %   %%%%  %%%%   %%%  %      %%%%%%%%%%%%%%%%%%%%%%%%%%%
C%%%%   %   %   % %         % %      %%%%%%%%%%%%%%%%%%%%%%%%%%%
C%%%%   %   %   % %%%%% %%%%  %%%%%  %%%%%%%%%%%%%%%%%%%%%%%%%%%
C%%%%                                %%%%%%%%%%%%%%%%%%%%%%%%%%%
C%%%%%%%%%%%%%%%%%%%%%%%%%%%%%%%%%%%%%%%%%%%%%%%%%%%%%%%%%%%%%%%
C%%% SUBROUTINE TRESL %%%%%%%%%%%%%%%%%%%%%%%%%%%%%%%%%%%%%%%%%%
C GIVEN X, AND Y COORDINATES, THE LENGTH,AND WIDTH OF THE
C AREA REPRESENTED BY A TEKTRONIX GRAPHICS SCREEN, AND THE SIZE
C WANTED, DRAWS A SQUARE (INDEPENDENT OF SCREEN SCALE) CONTAINING A X
C CENTERED AT X AND Y.
C
C X=> X COORD.  OF SQUARE
C Y=> Y COORD.  OF THE SQURE
C
C SCX=> TOTAL LENGTH OF WINDOW FOR PRIME GRAPHICS
C
C SCY=> TOTAL WIDTH OF WINDOW FOR PRIME GRAPHICS
C
C SIZE=> ONE-HALF THE WIDTH OF THE BOX
C
C*****************************************************************
      SUBROUTINE TRESL(X,Y,SCX,SCY,SIZE)
      REAL X,Y,SCX,SCY,SX,SY,SIZE
      SX=SCX/(SCY*1.312)*SIZE
      SY=SIZE
      CALL MOVEA(X,Y)
```

Figure B.1. (continued)

```
      CALL MOVER(SX,SY)
      CALL DRAWR((-2.0*SX),(-2.0*SY))
      CALL MOVER(0.0,(2.0*SY))
      CALL DRAWR((2.0*SX),(-2.0*SY))
      CALL DRAWR(0.0,(2.0*SY))
      CALL DRAWR((-2.0*SX),0.0)
      CALL DRAWR(0.0,(-2.0*SY))
      CALL DRAWR((2.0*SX),0.0)
      RETURN
      END
```

APPENDIX C

ANALYSIS OF THE HARVESTER'S INERTIAL EFFECTS DUE TO GROUND SPEED

APPENDIX C

ANALYSIS OF THE HARVESTER'S INERTIAL EFFECTS DUE TO GROUND SPEED

The following analysis was done to determine what harvester speed would cause the harvester to deviate from pure kinematic motion.

Model of Vehicle Motion

A model of vehicle motion must accurately predict the position of the vehicle for a specified input. The input to a dynamic model is wheel steering angle, δ, and the output is the vehicle position in X-Y coordinates. The variables X and Y vary with time. Figure C.1 shows a diagram of wheel steering angle and shows a simplified block diagram of the vehicle model.

Dynamic Model

A kinetic model of a vehicle, considers the inertial effects of the vehicle. The inertial effects on the vehicle result due to the mass of the vehicle and the mass moment of inertia of the vehicle. The equations of the kinetic model were used to describe the motion of the vehicle. Note, that when inertia effects are not significant then kinematic equations can be developed to describe the vehicle motion. Kinematic equations do not consider any effects from the system's inertia. The vehicle kinetic model has an input which is steering angle and the vehicle mass is moved by forces from the vehicle tires.

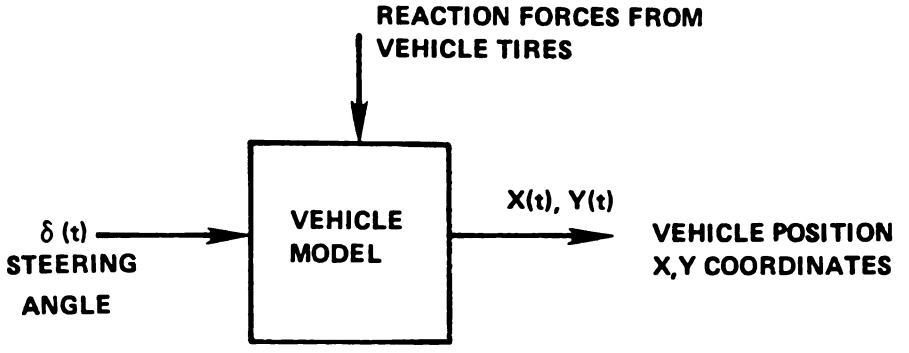

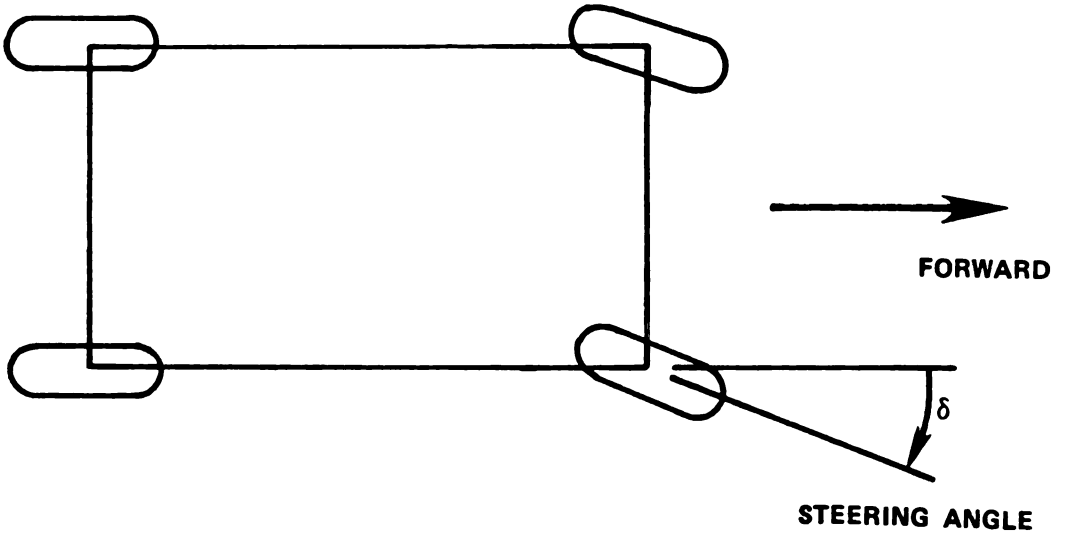

Figure C.1 Diagram of Steering Angle and Block Diagram of Vehicle Model

Tire Force Characteristics

According to Ellis (1969) tires generate a side force when the wheel is turned to an angle away from the direction of motion and this is shown in Figure C.2. The angle, , is called the side slip angle and the lateral side load is a function of the side slip angle. Figure C.3 shows a plot of the tire side load with respect to the side slip angle for a typical automobile tire. This data was obtained from Collins and Wong (1974). An accurate characterization of the side force is complex because it depends on tire size, construction, vertical load, air pressure speed, and tractive effort. Good results have been achieved by describing the side force as a coefficient, C_f, called the side force coefficient which is the initial slope of the plot of side force versus side slip angle as shown in Figure C.3. Note, that in Figure C.3, the slope is initially constant for slip angles as large as 6 degrees. Yet, C_f is reasonably accurate for side slip angles up to 10 degrees. Research by Ellis and by Collins and Wong have developed other techniques to model the tire side load for larger side slip angles and other special conditions. As reported by Ellis, an approximate value for C_f is 698 N/degree (157 lbf/degree) which is for a typical automobile tire with vertical load of 4,448 lbf (1000 lbf). This value was used as a conservative value for the tires on the harvester because specific data for the harvester's tires were not available.

Kinetic Equations of Motion

Kinetic equations of motion were developed for a vehicle model as shown in Figure C.4. These dimensions shown in Figure C.4 are for the apple harvester.

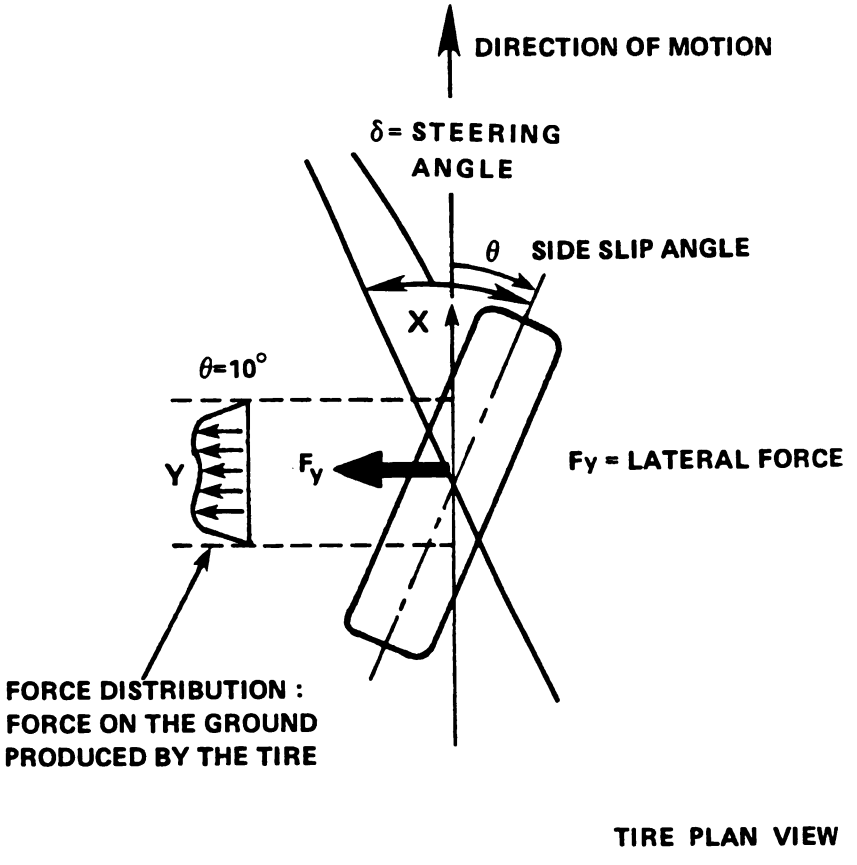

Figure C.2 Diagram of Tire Side Slip Angle

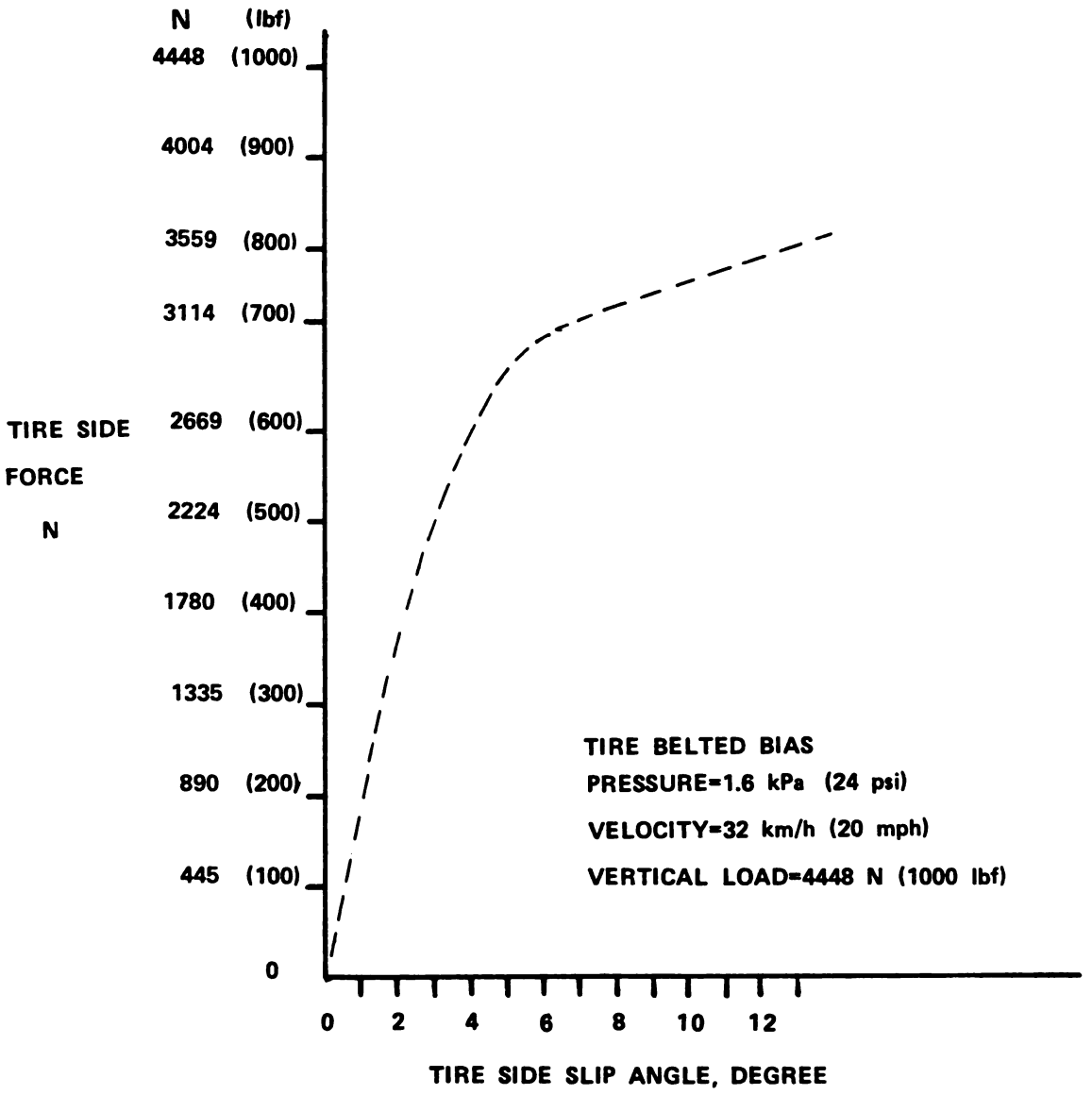

Figure C.3 Typical Tire Characteristic of Side Force with Respect to Side Slip Angle. This Data was Reported by Collins and Wong (1974).

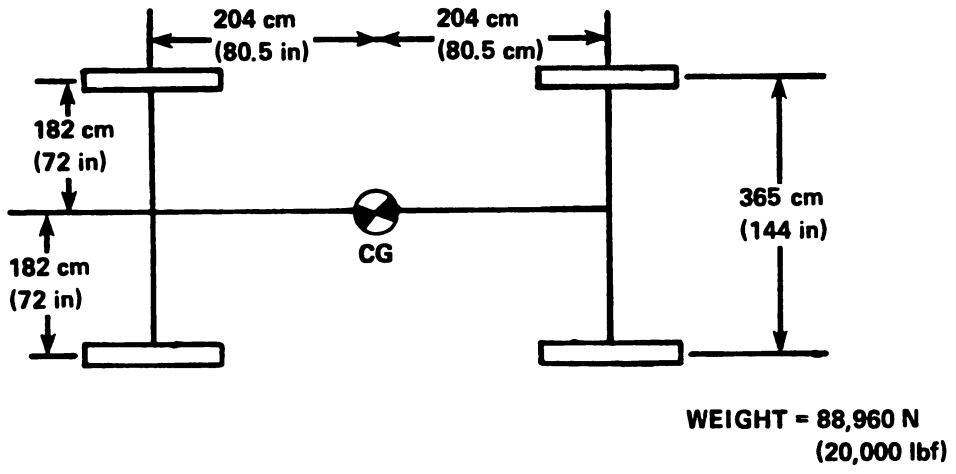

MODEL OF VEHICLE

Figure C.4 Dimension for Vehicle

Ellis (1969), developed equations of motion that describe a vehicle's motion for small steering angles and for the case of constant forward velocity. These equations were written with respect to axes on the vehicle at the center-of-gravity (CG) of the vehicle and these axes were moving with the vehicle. These kinetic equations of motion by Ellis are:

$$M(\dot{V} + Ur) = (C_f + C_r)(V/U) + (aC_f - bC_r)(r/U) - C_f\delta \quad (A.1)$$

$$I_z\dot{r} = (aC_f - bC_r)(V/U) + (a^2C_f + b^2C_r)(r/U) - aC_f\delta \quad (A.2)$$

$$\dot{\Psi} = r \quad (A.3)$$

$$\dot{y} = V\cos\Psi + U\sin\Psi \quad (A.4)$$

$$\dot{x} = U\cos\Psi - V\sin\Psi \quad (A.5)$$

C_f = effective side force coefficient for both front wheels (N/deg) or (lbf/deg)

C_r = effective side force coefficient for bother rear wheels (N/deg) or (lbf/deg)

I_z = mass moment of inertia of vehicle about the verical axis through the vehicle CG (cm-N-sec^2) or (in-lbf-sec^2)

a = location of CG (cm) or (in)

b = location of CG (cm) or (in)

M = vehicle mass $\frac{\text{N-sec}^2}{\text{cm}}$ or $\frac{\text{lbf-sec}^2}{\text{in}}$

V = lateral velocity of CG (cm/sec) or (in/sec)

U = forward velocity of CG (cm/sec) or (in/sec)

r = yaw rate about the CG (rad/sec)

Ψ = angular position of CG (rad)

X = position of CG (cm) or (in)

Y = position of CG (cm) or (in)

These equations developed by Ellis were derived in the following manner. First, a four wheel model was used to write two second order equations. These equations were (1) summation of forces in the Y-direction equals to the vehicle's mass times the acceleration in the Y-direction (the forces come from the tires) and (2) summation of moments about the vehicle's CG equals the vehicle's moment-of-inertia times the angular acceleration. The next step was to transform these equations to a form where the axes move with the CG of the vehicle. The last step, to simplify the equations, was to assume that the tire forces were symetrical and the vehicle equations could be written for a vehicle represented by one effective front wheel and one effective rear wheel as

shown in Figure C.5. Ellis stated that these Equations C.1 to C.5 are often used to study vehicle dynamics.

Effects of Tire Friction Force for Steady State Turning

If there is sufficient friction force, then during a steady state turn a vehicle will move in a circle according to the Ackermann geometry assuming the vehicle is designed to satisfy the requirements of the Ackermann geometry. Figure C.6 shows a diagram of the Ackermann geometry. Durstine (1965) explained that the Ackermann geometry is often referred to as "ideal" steering geometry because with this configuration the front wheels will roll without tire "scruff" or slipping. The vehicle turns about the turning center. If the centrifugal force or normal force, N, exceeds the tire friction force then the vehicle will slip and not track as described by the Ackermann geometry. The vehicle speed, that will produce a normal force equal to the tire friction force, can be calculated. Assume that, , the coefficient of friction can be as low as 0.1 for slippery conditions. The maximum friction force is calculated as

$$\frac{W}{4}\mu = F_{Friction} = 2{,}200 \text{ N } (500 \text{ lbf})$$

where W equals vehicle weight of 89,000 N. A free-body diagram is shown in Figure C.7 for equal 20 degrees. The necessary conditions for steady state turns are (1) the summation of the moments about the CG must equal zero and (2) the summation of forces in the X and Y direction must equal zero. A normal force is calculated to satisfy these conditions and is shown in Figures C.7. From the normal force, N, the

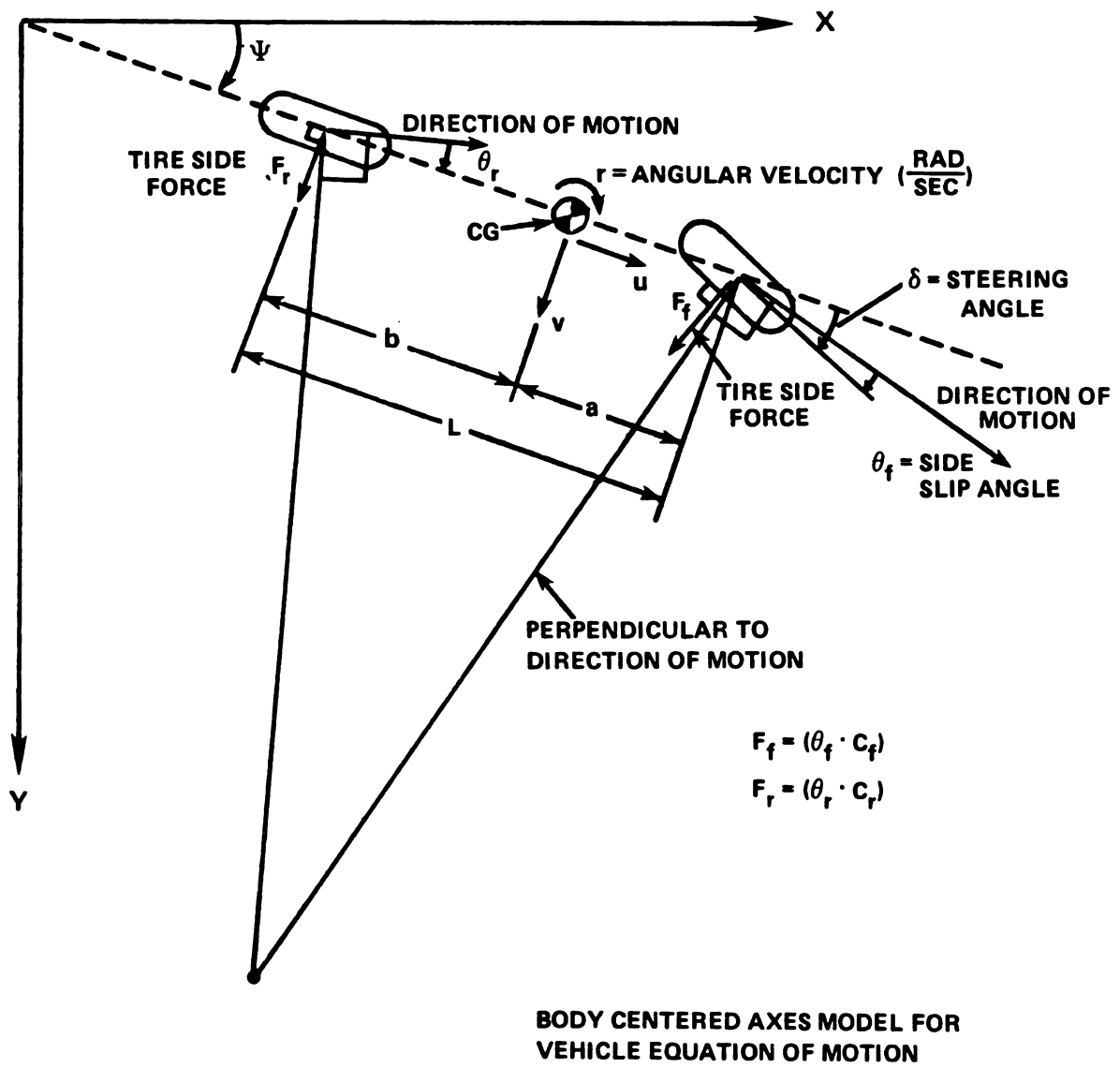

BODY CENTERED AXES MODEL FOR VEHICLE EQUATION OF MOTION

Figure C.5 Body Centered Axes Model for Vehicle Equation of Motion

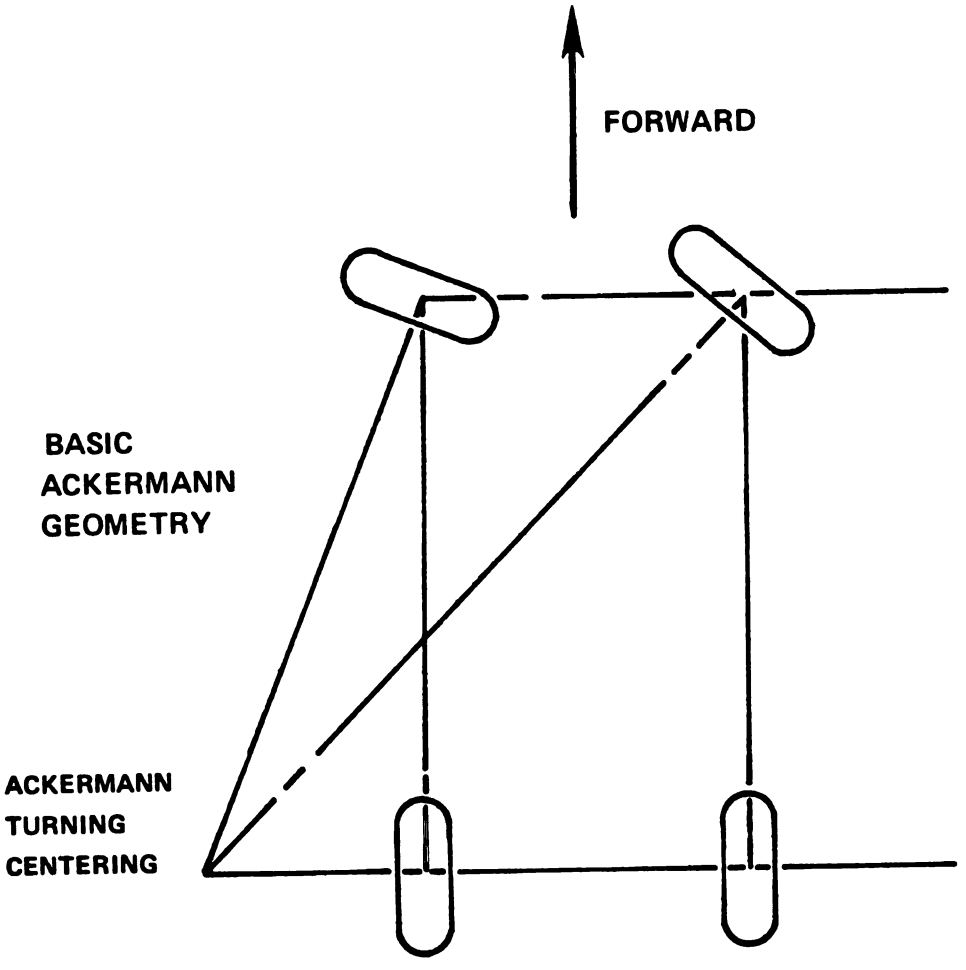

Figure C.6 Basic Ackermann Steering Geometry

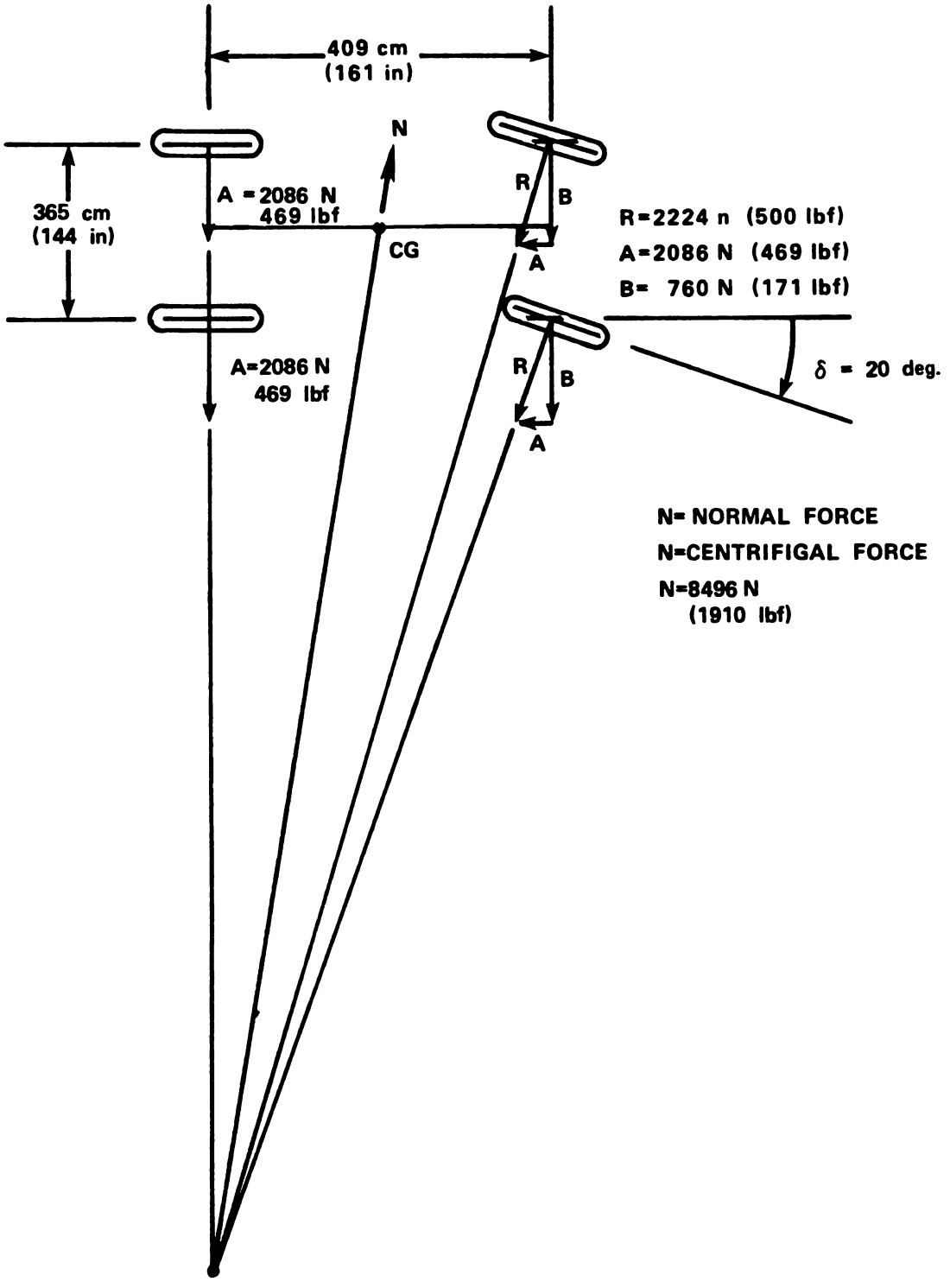

Figure C.7 Free-Body Diagram of Forces for Steady State Turn with Allowable Tire Friction Force Equal to 2,200 N (500 lbf)

speed that will cause the vehicle to slip can be calculated as follows:

$$W = 89{,}000 \text{ N } (20{,}000 \text{ lbf})$$

$$M = w/g$$

$$g = 980.6 \text{ cm/s}^2$$

$$N = M V^2/R$$

$$R = 1{,}120 \text{ cm } (442 \text{ in})$$

$$V = \sqrt{RN/M}$$

The calculated speed for steering angle equal to 20 degrees was 32 cm/s (7.25 mph). This same calculation was done for the case of vehicle weight equal to 22,200 N (5,000 lbf) and the same value for the vehicle speed was calculated.

Dynamic Considerations

The following values of the vehicle parameters were used in this study:

$$C_f = C_r = -80{,}000 \text{ N/rad } (-18\,000 \text{ lbf/rad})$$

$$a = b = 204.5 \text{ cm } (80.5 \text{ in})$$

$$I_z = \frac{1}{4} ML^2 \quad \text{N-s}^2/\text{cm } (\text{lbf-s}^2/\text{in})$$

$$L = a+b = 408.9 \text{ cm } (161.0 \text{ in})$$

for $W = 89{,}000$ N (20,000 lbf)

$$M = \frac{w}{g} = 90.7 \text{ N-s}^2/\text{cm } (51.7 \text{ lbf -s}^2/\text{in})$$

for $W = 22{,}200$ N (5000 lbf)

$$M = \frac{w}{g} = 22.7 \text{ N-s}^2/\text{cm } (12.9 \text{ lbf -s}^2/\text{in})$$

When the inertial effects on a system becomes significant, the mass is too large for the driving force (tire lateral force), and the system

will accelerate slower in the Y-direction when a turn is initiated. Therefore when the inertia or mass is large compared to the magnitude of the driving force, the vehicle response time is less than that described by kinematic motion. The response time for this study is defined as the time required by the system to reach a steady state condition beginning with the time of application of a specified input. The input selected for analysis was the truncated-ramp. The input is the steering angle and a plot of this input which changed with time is shown in Figure C.8. The slope of the initial portion of the curve corresponds to the vehicle's maximum wheel turning rate. The steady state value of the steering angle is 10^{o}.

Inertial Effects

For a given forward speed, increasing the weight of the vehicle to a large enough value will result in a significant increase of the system's response time. The dynamic or kinetic equations of motion are used to evaluate the response time of the vehicle for an input of steering angle as shown in Figure C.8. The steering angle increases at 15^{o}/s until it reaches 10^{o}; then the steering angle is held at that value. When the vehicle reaches a steady state condition it will move along a circular path. Also, the vehicle yaw rate, r, will reach a constant value at the steady state condition.

The equations of motion were integrated using a numerical method technique to determine the vehicle response to the specified input. The response was evaluated for a vehicle of weight 22,200 N (5,000 lbf) and 89,000 N (20,000 lbf) and a forward speed of 536 cm/s (12 mph). The response of the vehicle in terms of the yaw rate is shown in Figure C.8. A copy of the computer program for integrating the equations of motion

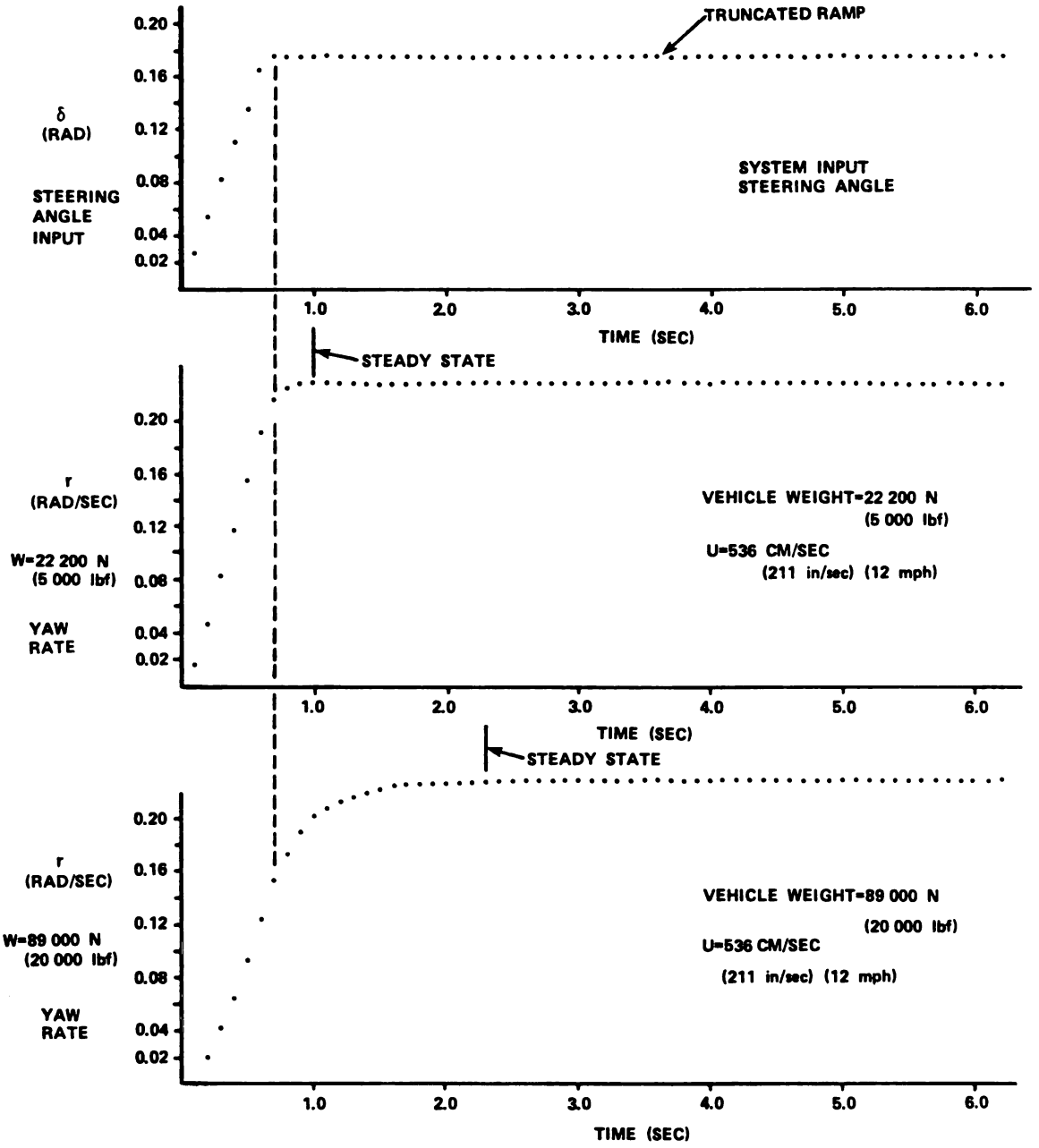

Figure C.8 Plot of Steering Angle and Yaw Rate

is shown in Figure C.9. It can be seen from Figure C.8 that the vehicle of weight 22,200 N has a smaller response time than the 89,000 N vehicle. This analysis assumes that there is enough friction force such that the wheels do not slip due to the centrifigal force. The vehicle of weight 22,200 N is assumed to react like a system of small mass because the response time is small.

Criteria for Vehicle Model Evaluation

During the operation of a vehicle guidance control system there must be periodic measurements of vehicle position so that the vehicle can correct for errors in position. It is expected that the actual position of a farm vehicle could be measured periodically at intervals of time represented by 304 cm (120 in) of travel. Thus, the estimated allowed position error for a farm vehicle with a steering control system is 2.5 cm 1.0 (in), therefore the following criteria were selected for use to evaluate the inertia effects on vehicle motion. For the vehicle to have negligible inertial effects the vehicle with large inertia must have the same position coordinates as the vehicle with small inertia within a tolerance of $\pm$2.5 cm ($\pm$1.0 in) when the vehicle had traveled 304 $\pm$10 cm (120 $\pm$4 in). The vehicle center of gravity is selected as the point used to specify vehicle position. This criterion was used to evaluate the effects on vehicle position due to the vehicle inertia.

Evaluation of the Kinetic Model

The dynamic model showed that the 89,000 N vehicle had a larger response time than the 22,200 N vehicle for the specified input. This larger response time will result in a different position with respect to time for these two vehicles with different weight and same forward

```
00006:        INTEGER K, IND, IER, J
00007:        REAL X, Y(5), I, M, CF, CR, U, T, B, CC, D, E, F, G, XEND, C(24), TOL, W(5, 9)
00008:       %, PI, WT
00009:        EXTERNAL FCN
00010:        COMMON/BLOCK/XEND, A, WP, I, M, CF, CR, U, V
00011: C
00012:        N=5
00013:        NW=5
00014:        X=0. 0
00015:        IND=1
00016:        Y(1)=0. 0
00017:        Y(2)=0. 0
00018:        Y(3)=0. 0
00019:        Y(4)=0. 0
00020:        Y(5)=0. 0
00021:        J=10
00022:        TOL=0. 0001
00023:        WT=100000. 0
00024:        I=(WT*161. *161. )/(32. 2*12. *4. )
00025:        M=WT*(1. /(32. 2*12. ))
00026:        CF=-18000.
00027:        CR=-18000. 0
00028:        U=17. 6
00029:        PRINT 200 WT, U
00030: 200    FORMAT (2F10. 3)
00031:        PI=3. 1415627
00032:        DO 50 K=1, 680
00033:        XEND=FLOAT(K)/100. 0
00034:        WP=XEND*(15. 75*PI)/180.
00035:        IF(WP. GT. 0. 17453) WP=0. 17453
00036: C
00037:        CALL DVERK (N, FCN, X, Y, XEND, TOL, IND, C, NW, W, IER)
00038:        J=J-1
00039:        IF(J. EQ. 0) GO TO 12
00040:        GO TO 50
00041: 12     F=Y(5)
00042:        G=Y(4)
00043:        A=Y(3)
00044:        CC=G+(80. 5*SIN(A) )
00045:        B=F+(80. 5*COS(A) )
00046:        D=F-(80. 5*COS(A) )
00047:        E=G-(80. 5*SIN(A) )
00048:        G=((F**2)+(G**2))**0. 5
00049:        PRINT 100 XEND, F, G, B, CC, D, E, WP, Y(1), Y(2), Y(3)
00050: 100    FORMAT(11F10. 3)
00051:        J=10
00052: 50     CONTINUE
00053:        STOP
00054:        END
00055:        SUBROUTINE FCN(N, X, Y, YPRIME)
00056:        INTEGER N
00057:        REAL X, Y(N), YPRIME(N), M, XEND, M, I, CR, CF, WP, A
00058:        COMMON/BLOCK/XEND, A, WP, I, M, CF, CR, U, V
00059:        YPRIME(1)=-(U*(Y(2)/M)) + ((1. /M)*(CF+CR)*(Y(1)/U))
00060:       %-((CF/M)*WP)


00061:        YPRIME(2)=(( (80. 5**2)*CF)+((80. 5**2)*CR))*(Y(2)/U)*(1. /I)
00062:       %-(80. 5*CF*WP*(1. /I))
00063:        YPRIME(3)=Y(2)
00064:        YPRIME(4)=(Y(1)*COS(A))+(U*SIN(A))
00065:        YPRIME(5)=(U*COS(A))-(Y(1)*SIN(A))
00066:        RETURN
00067:        END
BOTTOM
```

Figure C.9 Computer Program used to Compute the Vehicle Response Due to a Specified Steering Angle Input

velocity. The integration of the equations of motion was performed to determine the position of the vehicle CG with respect to time for forward speeds of 1.6, 3.2, 4.8, 6.4, 8.0 and 19.3 km/h (1,2,3,4,5 and 12 mph) for vehicle weight of 22,200 N and 89,000 N. Table C.1 shows the Y-coordinate position of the CG when the X-coordinate was approximately 304 cm (120 in). The Y-coordinate position for the 22,200 N vehicle was used as the reference for vehicle position without inertial effects. The difference in the Y-coordinate values of these two vehicles was considered the error in position that will result when the effects of inertia are not considered for computing vehicle motion. This error is tabulated in Table C.1.

Table C.1 Position Coordinates of CG from Dynamic Model for Vehicle of Weight 39,000 N and 22,200 N

FORWARD VELOCITY U		COORDINATE X		VEHICLE 89 000 N COORDINATE Y_1		VEHICLE 22 200 N COORDINATE Y_2		ERROR $(Y_2 - Y_1)$	
km/h	(mph)	cm	(in)	cm	(in)	cm	(in)	cm	(in)
19.3	12	321.795	126.691	7.579	2.984	14.150	5.571	6.57	2.58
8.0	5	311.887	122.790	28.042	11.040	31.651	12.461	3.60	1.42
6.4	4	302.743	119.190	30.726	12.097	33.155	13.053	2.42	0.95
4.8	3	306.822	120.796	35.720	14.063	37.211	14.650	11.49	0.59
3.2	2	310.810	122.366	40.704	16.025	41.394	16.297	0.69	0.27
1.6	1	301.727	118.790	42.669	16.799	42.812	16.855	0.14	0.05

These data show that at a forward speed of 6.4 km/h (4.0 mph) the difference in position of the two vehicles is 2.45 cm (0.95 in) and this difference gets larger as the forward speed increases.

Conclusions

It is calculated that for forward speeds less than 6.4 km/h (4 mph) the vehicle of weight 89,000 N (20,000 lbf) as described by the developed dynamic model can be modeled without inertial effects without causing excessive error in the calculated position. These results were based on motion equations developed for the apple harvester. The input of the motion equations was wheel steering angle. The wheel steering angle was set at zero and allowed to increase up to 20^{o} at a rate of 15 deg/s. For ground speeds less than 6.4 km/h (4 mph) the results show that the vehicle can be described by a kinematic model. This conclusion is based on the assumption that there is enough friction so that the tires will not slip. For steady state turns with steering angle of 20 degrees and coefficient of friction equal to 0.1 it is calculated that the 89,000 N vehicle will slip at speeds greater than 11.6 km/h (7.25 mph).

APPENDIX D

COMPUTER PROGRAM FOR HARVESTER'S MICROPROCESSOR-BASED STEERING CONTROLLERS

APPENDIX D

COMPUTER PROGRAM FOR THE HARVESTER'S MICROPROCESSOR-BASED STEERING CONTROL SYSTEM

Appendix D contains a list of the assembly language program (Figure D.1) that was developed for the 1802 microprocessor which was used in the steering control system. Also shown in Figure D.1 is the object code that was used by the microprocessor. This listing shown in Figure D.1 is the output from the Cross-Assembler (made by RCA) which is a FORTRAN proram on the Michigan State University's main computer (Cyber 750). The object code has a total of about 2,000 bytes. If the program is modified to delete the portions of the object code which pertain to displaying data on the video monitor, then the control system's object code has about 1,000 bytes.

Figure D.1. Assembly Language and Object Code Listing of the Program Used by the Steering Controller's Microprocessor

```
   PROGRAM NAME IS' ASMDELAY '

LIST.
100= FL LOC  COSMAC CODE      LNNO SOURCE LINE
110=     0000                    1 ....PROGRAM = RCATREE  MCMAHON/CLEMENS
120=     0000                    2 INT=R0
130=     0000                    3 ..R1
140=     0000                    4 SP=R2
150=     0000                    5 PC=R3
160=     0000                    6 CALL=R4
170=     0000                    7 RETN=R5
180=     0000                    8 LINK=R6
190=     0000                    9 DSWPR=R7
200=     0000                   10 TEMP=R8....COUNTER ACCUM
210=     0000                   11 VSONR=R9
220=     0000                   12 SNR=RA
230=     0000                   13 FLAGR=RB
240=     0000                   14 ..RC
250=     0000                   15 NSONR=RD
260=     0000                   16 BINR=RE
270=     0000                   17 ..RF..POINTS TO LARGE ADDRESS FOR INPUT
280=     0000                   18 ......ALSO FOR PRINTING
290=     0000                   19 ....**************
300=     0000                   20 TYPE=X'8198'
310=     0000                   21 OSTRG=X'83F0'
320=     0000                   22 ....**************
330=     0000                   23 ....********
340=     0000                   24 ....PORT ASSIGNMENT
350=     0000                   25 ....PORT  NO.     SONAR #     OP CODE
360=     0000                   26 ....GROUP #20-A      2        INP 4=6C
370=     0000                   27 ....       20-B      1        INP 6=6E
380=     0000                   28 ....       10-A      4        INP 4=6C
390=     0000                   29 ....       10-B      3        INP 6=6E
400=     0000                   30 ....       08-A      5        INP 4=6C
410=     0000                   31 ....       08-B  RELAYS      OUTPUT CODE .
420=     0000                   32 ....TURN RIGHT=OUT 6;DC X'01'
430=     0000                   33 ....TURN LEFT=OUT 6;DC X'02'
440=     0000                   34 ...SET DSWP=32 WHICH IS CENTER POSITION
450=     0000                   35 ....   DSWP=0  IS FULL RIGHT TURN
460=     0000                   36 ....   DSWP=64 IS FULL LEFT TURN
470=     0000                   37 ..........................................
480=     0000                   38 ....INPUT PORT
490=     0000                   39 ...********************
500=     0000                   40 ... REGISTER INITILIZATION
510=     1000                   41 ORG X'1000'
520=     1000 71                42 DIS
530=     1001 00                43 DC 0
540=     1002 C4                44 NOP
550= F   1003 F800A3            45 INIT:LDI A.0(START);PLO PC
560= F   1006 F800B3            46 LDI A.1(START);PHI PC
570= F   1009 C00000            47 LBR ENTER2
580= F   100C F800B4B5          48 ENTER2: LDI A.1(CALLR);PHI CALL;PHI RETN
590= F   1010 F800A4            49 LDI A.0(CALLR);PLO CALL
600= F   1013 F800A5            50 LDI A.0(RETR);PLO RETN
610= F   1016 F800B5            51 LDI A.1(RETR);PHI RETN
620= F   1019 F800A2            52 LDI A.0(TOPSTK);PLO SP
630= F   101C F800B2            53 LDI A.1(TOPSTK);PHI SP
640=     101F E2D3              54 SEX SP;SEP PC
650=     1021                   55 ...********************
660=     1021                   56 ... DESCRIPTION:
670=     1021                   57 ...STANDARD SEP CALL; A(SUBR.NAME)
680=     1021                   58 ...********************
690=     1021                   59 ...STANDARD CALL
700=     1021 D3                60 EXITC: SEP PC
710=     1022 E2                61 CALLR:SEX SP
```

Figure D.1. (continued)

```
720=     1023 8673                 62 GLO LINK;STXD
730=     1025 9673                 63 GHI LINK;STXD
740=     1027 93B6                 64 GHI PC;PHI LINK
750=     1029 83A6                 65 GLO PC; PLO LINK
760=     102B 46B3                 66 LDA LINK; PHI PC
770=     102D 46A3                 67 LDA LINK;PLO PC
780=     102F C01021               68 LBR EXITC
790=     1032                      69 ...******
800=     1032                      70 ...STANDARD RETURN
810=     1032 D3                   71 EXITR:SEP PC
820=     1033                      72 RETR:
830=     1033 96B3                 73 GHI LINK;PHI PC
840=     1035 86A3                 74 GLO LINK; PLO PC
850=     1037 E212                 75 SEX SP;INC SP
860=     1039 72B6                 76 LDXA; PHI LINK
870=     103B F0A6                 77 LDX; PLO LINK
880=     103D C01032               78 LBR EXITR
890=     1040 C4                   79 NOP
900=     1041                      80 ....********************
910=     1041                      81 ....    START
920=     1041                      82 ....********************
930=     1041 C4                   83 START:NOP
940=     1042 F808B8               84 LDI 8;PHI R8....FOR 1200 BAUD
950= F   1045 D40000               85 SEP CALL;,A(SCRN)
960=     1048 C4C4C4               86 NOP;NOP;NOP
970=     104B F83FAFBF             87 LDI X'3F';PLO RF;PHI RF
980=     104F                      88 ...******
990=     104F                      89 ...OUTPUT ZERO TO PORT 08-A
1000=     104F E36108               90 SEX PC;OUT1;DC 8
1010=     1052 6253                 91 OUT2;DCX'53'
1020=     1054                      92 ... OUTPUT ZERO
1030=     1054 6600                 93 OUT 6;DC 0
1040= F   1056 F800A7               94 LDI A.0(DSWP);PLO DSWPR
1050= F   1059 F800B7               95 LDI A.1(DSWP);PHI DSWPR
1060=     105C F82057               96 LDI 32;STR DSWPR
1070=     105F                      97 ... SET UP PTR TO VSON AND NSON
1080= F   105F F800A9               98 LDI A.0(VSON);PLO VSONR
1090= F   1062 F800B9               99 LDI A.1(VSON);PHI VSONR
1100= F   1065 F800AD              100 LDI A.0(NSON);PLO NSONR
1110= F   1068 F800BD              101 LDI A.1(NSON);PHI NSONR
1120=     106B ED                  102 SEX NSONR
1130=     106C                     103 ....PUT ZERO IN ALL NSONR
1140=     106C F8005D60            104 LDI 0;STR NSONR;IRX
1150=     1070 5D60                105 STR NSONR;IRX
1160=     1072 5D60                106 STR NSONR;IRX
1170=     1074 5D60                107 STR NSONR;IRX
1180=     1076 5D60                108 STR NSONR;IRX
1190=     1078 5D                  109 STR NSONR
1200=     1079                     110 ...SET UP SNR AS PTR TO SN
1210= F   1079 F800AA              111 LDI A.0(SN);PLO SNR
1220= F   107C F800BA              112 LDI A.1(SN);PHI SNR
1230=     107F                     113 ....INITIALIZE--READ ONLY SON(X)
1240=     107F                     114 ....              WHEN FLAG(X)=1
1250=     107F                     115 ....FLAG(0)=0
1260=     107F                     116 ....FLAG(1)=1
1270=     107F                     117 ....FLAG(2 THRU 5)=0
1280= F   107F F800AB              118 LDI A.0(FLAG);PLO FLAGR
1290= F   1082 F800BB              119 LDI A.1(FLAG);PHI FLAGR
1300=     1085 EB                  120 SEX FLAGR
1310=     1086 F8005B              121 LDI 0;STR FLAGR...0
1320=     1089 60F8015B            122 IRX;LDI 1;STR FLAGR...1
1330=     108D 60F8005B            123 IRX;LDI 0;STR FLAGR...2
1340=     1091 605B                124 IRX;STR FLAGR...3
1350=     1093 605B                125 IRX;STR FLAGR...4
1360=     1095 605B                126 IRX;STR FLAGR...5
1370=     1097                     127 ....INITIALIZE
```

Figure D.1. (continued)

```
1380=     1097                    128 ....DISPLAY DELAY
1390=     1097 F800A8             129 LDI 0;PLO R8
1400=     109A F804B8             130 LDI 4;PHI R8
1410=     109D                    131 ...*******************************
1420=     109D C4                 132 LOOP2:NOP
1430=     109E C4C4               133 LOOP1:NOP;NOP
1440=     10A0 C4C4C4C4C4         134 NOP;NOP;NOP;NOP;NOP
1450=     10A5 C4C4C4C4C4         135 NOP;NOP;NOP;NOP;NOP
1460=     10AA 2898               136 DEC R8;GHI R8
1470= F   10AC 3A00               137 BNZ BERT
1480= F   10AE D40000             138 SEP CALL;,A(DISPL)
1490=     10B1 F804B8             139 LDI 4;PHI R8
1500=     10B4 F800A8             140 LDI 0;PLO R8
1510=     10B7 C4C4C4             141 BERT:NOP;NOP;NOP
1520= F   10BA F800AD             142 LDI A.0(NSON);PLO NSONR
1530= F   10BD F800BD             143 LDI A.1(NSON);PHI NSONR
1540=     10C0                    144 ....SET PTR TO FLGR
1550=     10C0                    145 ....USED TO TURN OFF SONAR(X)
1560= F   10C0 F800AB             146 LDI A.0(FLAG);PLO FLAGR
1570= F   10C3 F800BB             147 LDI A.1(FLAG);PHI FLAGR
1580= F   10C6 D40000             148 SEP CALL; ,A(TURN)
1590=     10C9                    149 ...***READ SONAR1 IF READY
1600=     10C9                    150 ...***STORE VALUE IN VSONR
1610=     10C9                    151 ...***VALUE=X'FF' MEANS SONAR NOT READY
1620=     10C9                    152 ...*******
1630=     10C9                    153 ...SONAR 1
1640=     10C9                    154 ...******
1650=     10C9                    155 ....***IS SONAR(1) LT 150
1660=     10C9 C4C4C4             156 NOP;NOP;NOP
1670=     10CC 1D                 157 INC NSONR
1680=     10CD 1B                 158 INC FLAGR....FLG1
1690=     10CE 4B                 159 LDA FLAGR....PTR TO FLG2
1700= F   10CF C20000             160 LBZ CONT2
1710=     10D2 F8015A             161 LDI 1; STR SNR ... STORE '1' IN SN
1720=     10D5 E3                 162 SEX PC
1730=     10D6 6101               163 OUT 1;DC X'01'
1740=     10D8 6301               164 OUT 3;DC X'01'
1750= F   10DA D40000             165 SEP CALL ;,A(READ)
1760=     10DD C4                 166 NOP
1770=     10DE 09                 167 LDN VSONR
1780=     10DF FF96               168 SMI 150 ... D=S-150
1790= F   10E1 3300               169 BPZ CONT2
1800=     10E3                    170 ...VSONR IS LT 150
1810=     10E3 0DFC015D           171 LDN NSONR ; ADI 1 ; STR NSONR
1820=     10E7 C4                 172 CONT2: NOP
1830=     10E8                    173 ...********
1840=     10E8                    174 ...SONAR 2
1850=     10E8                    175 ...********
1860=     10E8                    176 ....***IS VSONAR(2) LT 150
1870=     10E8 1D                 177 INC NSONR
1880=     10E9 4B                 178 LDA FLAGR....PTR TO FLG3
1890= F   10EA C20000             179 LBZ CONT3
1900=     10ED F8025A             180 LDI 2 ; STR SNR  ...STORE '2' IN SN
1910=     10F0 E3                 181 SEX PC
1920=     10F1 6101               182 OUT 1;DC X'01'
1930=     10F3 6302               183 OUT 3;DC X'02'
1940= F   10F5 D40000             184 SEP CALL ; , A(READ)
1950=     10F8 C4                 185 NOP
1960=     10F9 09                 186 LDN VSONR
1970=     10FA FF96               187 SMI 150
1980= F   10FC 3300               188 BPZ CONT3
1990=     10FE 0DFC015D           189 LDN NSONR ; ADI 1 ; STR NSONR
2000=     1102 C4C4               190 CONT3: NOP; NOP
2010=     1104                    191 ...********
2020=     1104                    192 ...SONAR 3
2030=     1104                    193 ...********
```

Figure D.1. (continued)

```
2040=     1104                    194 ...IS VSONR3 LT 150
2050=     1104 1D                 195 INC NSONR
2060=     1105 4B                 196 LDA FLAGR...PTR TO FLAG4
2070= F   1106 C20000             197 LBZ CONT4
2080=     1109 F8035A             198 LDI 3; STR SNR
2090=     110C E3                 199 SEX PC
2100=     110D 6101               200 OUT 1;DC X'01'
2110=     110F 6304               201 OUT 3;DC X'04'
2120= F   1111 D40000             202 SEP CALL; ,A(READ)
2130=     1114 C4                 203 NOP
2140=     1115 09                 204 LDN VSONR
2150=     1116 FF96               205 SMI 150
2160= F   1118 C30000             206 LBDF CONT4
2170=     111B 0DFC015D           207 LDN NSONR ; ADI1 ; STR NSONR
2180=     111F C4C4               208 CONT4: NOP; NOP
2190=     1121                    209 ...********
2200=     1121                    210 ...SONAR 4
2210=     1121                    211 ...********
2220=     1121                    212 ...IS VSONR4 LT 150
2230=     1121 1D                 213 INC NSONR
2240=     1122 4B                 214 LDA FLAGR....PTR TO FLAG5
2250= F   1123 C20000             215 LBZ CONT5
2260=     1126 F8045A             216 LDI 4 ; STR SNR
2270=     1129 E3                 217 SEX PC
2280=     112A 6101               218 OUT 1;DC X'01'
2290=     112C 6308               219 OUT 3;DC X'08'
2300= F   112E D40000             220 SEP CALL ; ,A(READ)
2310=     1131 C4                 221 NOP
2320=     1132 09                 222 LDN VSONR
2330=     1133 FF96               223 SMI 150
2340= F   1135 3300               224 BPZ CONT5
2350=     1137 0DFC015D           225 LDN NSONR ; ADI 1 ; STR NSONR
2360=     113B C4C4               226 CONT5: NOP; NOP
2370=     113D                    227 ...********
2380=     113D                    228 ...SONAR 5
2390=     113D                    229 ...********
2400=     113D                    230 ...IS VSONR5 LT 150
2410=     113D 1D                 231 INC NSONR
2420=     113E 0B                 232 LDN FLAGR
2430= F   113F C20000             233 LBZ CONTND
2440=     1142 F8055A             234 LDI 5 ; STR SNR
2450=     1145 E3                 235 SEX PC
2460=     1146 6101               236 OUT 1;DC X'01'
2470=     1148 6310               237 OUT 3;DC X'10'
2480= F   114A D40000             238 SEP CALL ; ,A(READ)
2490=     114D C4                 239 NOP
2500=     114E 09                 240 LDN VSONR
2510=     114F FF96               241 SMI 150
2520= F   1151 3300               242 BPZ CONTND
2530=     1153 0DFC015D           243 LDN NSONR ; ADI 1 ; STR NSONR
2540= F   1157 C00000             244 CONTND:LBR CHKNSO....BRANCH TO CHKNSO
2550=     115A                    245 ....*********************************
2560=     115A                    246 ...SUBROUTINE:   READ
2570=     115A                    247 ....*********************************
2580=     115A                    248 ...READ SONAR WHEN READY
2590=     115A                    249 ...SNR=RC ... AND IT MUST CONTAIN #1-5
2600=     115A C4C4C4             250 READ: NOP;NOP;NOP
2610=     115D 0A                 251 LDN SNR
2620=     115E FF01               252 SMI 1 ... D=D-1
2630= F   1160 C20000             253 LBZ CALL1
2640= F   1163 C00000             254 LBR CON1
2650=     1166                    255 CALL1:
2660= F   1166 D40000             256 SEP CALL ;, A(READ1)
2670= F   1169 C00000             257 LBR CON5
2680=     116C                    258 CON1:
2690=     116C 0A                 259 LDN SNR
```

Figure D.1. (continued)

```
2700=     116D FF02            260 SMI 2
2710= F   116F C20000          261 LBZ CALL2
2720= F   1172 C00000          262 LBR CON2
2730= F   1175 D40000          263 CALL2: SEP CALL ; ,A(READ2)
2740= F   1178 C00000          264 LBR CON5
2750=     117B 0A              265 CON2: LDN SNR
2760=     117C FF03            266 SMI 3
2770= F   117E C20000          267 LBZ CALL3
2780= F   1181 C00000          268 LBR CON3
2790= F   1184 D40000          269 CALL3: SEP CALL ; ,A(READ3)
2800= F   1187 C00000          270 LBR CON5
2810=     118A 0A              271 CON3: LDN SNR
2820=     118B FF04            272 SMI 4
2830= F   118D C20000          273 LBZ CALL4
2840= F   1190 C00000          274 LBR CON4
2850= F   1193 D40000          275 CALL4: SEP CALL; ,A(READ4)
2860= F   1196 C00000          276 LBR CON5
2870=     1199 0A              277 CON4: LDN SNR
2880=     119A FF05            278 SMI 5
2890= F   119C C20000          279 LBZ CALL5
2900= F   119F C00000          280 LBR CON5
2910= F   11A2 D40000          281 CALL5: SEP  CALL; ,A(READ5)
2920=     11A5 D5              282 CON5: SEP RETN
2930=     11A6                 283 ....*************************************
2940=     11A6                 284 ....SUBROUTINES TO READ A  SET OF 5 SONAR
2950=     11A6                 285 ....*************************************
2960=     11A6                 286 ....SUBROUTINE TO READ SONAR1
2970=     11A6                 287 .... STORE VALUE INTO VSON
2980=     11A6                 288 .... SET NR=1
2990=     11A6                 289 .... CALL READ1 TO READ SONR1
3000=     11A6                 290 ....PUT FF INTO VSONR IF NOT READY
3010=     11A6                 291 ....********************
3020=     11A6 C4C4            292 READ1 : NOP; NOP
3030=     11A8 E36120          293 SEX PC; OUT 1 ; DC X'20'
3040=     11AB E9              294 SEX VSONR ...PTR TO VSON
3050= F   11AC 3500            295 B2 GETSD1
3060= F   11AE C00000          296 LBR CCONT1
3070=     11B1 C4              297 GETSD1 : NOP
3080=     11B2 C4              298 NOP
3090= F   11B3 6EC00000        299 INP6;LBR B1....STORE VSONR BY REGX
3100=     11B7 F8FF59          300 CCONT1 : LDI X'FF' ; STR VSONR
3110=     11BA D5              301 B1:SEP RETN
3120=     11BB                 302 ...*****************************
3130=     11BB C4C4            303 READ2 : NOP; NOP
3140=     11BD E36120          304 SEX PC ; OUT1 ;DC X'20'
3150=     11C0 E9              305 SEX VSONR ... PTR TO VSON
3160= F   11C1 3400            306 B1 GETSD2
3170= F   11C3 C00000          307 LBR CCONT2
3180=     11C6 C4C4C4          308 GETSD2: NOP; NOP;NOP
3190= F   11C9 6CC00000        309 INP 4;LBR B2 ...STORE BY REGX - VSON
3200=     11CD F8FF59          310 CCONT2: LDI  X'FF' ; STR VSONR
3210=     11D0 D5              311 B2:SEP RETN
3220=     11D1                 312 ...*****************************
3230=     11D1 C4C4C4          313 READ3 : NOP; NOP; NOP
3240=     11D4 E36110          314 SEX PC; OUT 1; DC X'10'
3250=     11D7 E9              315 SEX VSONR
3260= F   11D8 3500            316 B2 GETSD3
3270= F   11DA C00000          317 LBR CCONT3
3280=     11DD C4C4C4          318 GETSD3 : NOP; NOP; NOP
3290= F   11E0 6EC00000        319 INP 6;LBR B3
3300=     11E4 F8FF59          320 CCONT3 : LDI X'FF' ; STR VSONR
3310=     11E7 D5              321 B3:SEP RETN
3320=     11E8                 322 ...*****************************
3330=     11E8 C4C4C4          323 READ4 : NOP; NOP; NOP
3340=     11EB E36110          324 SEX PC; OUT 1;DC X'10'
3350=     11EE E9              325 SEX VSONR
```

Figure D.1. (continued)

```
3360= F  11EF 3400            326 B1 GETSD4
3370= F  11F1 C00000          327 LBR CCONT4
3380=    11F4 C4C4C4          328 GETSD4 : NOP; NOP; NOP
3390= F  11F7 6CC00000        329 INP 4;LBR B4 ... STORE BY REGX-VSON
3400=    11FB F8FF59          330 CCONT4: LDI X'FF' ; STR VSONR
3410=    11FE D5              331 B4:SEP RETN
3420=    11FF                 332 ...*****************************
3430=    11FF C4C4C4          333 READ5 : NOP; NOP; NOP
3440=    1202 E36108          334 SEX PC; OUT 1; DC X'08'
3450=    1205 E9              335 SEX VSONR
3460= F  1206 3400            336 B1 GETSD5
3470= F  1208 C00000          337 LBR CCONT5
3480=    120B C4C4C4          338 GETSD5 : NOP; NOP; NOP
3490= F  120E 6C3000          339 INP 4;BR B5
3500=    1211 F8FF59          340 CCONT5 : LDI X'FF';STR VSONR
3510=    1214 D5              341 B5:SEP RETN
3520=    1215                 342 ....****END OF SUBROUTINE********
3530=    1215                 343 ..******IS NSON(X),1-5,=2?
3540=    1215                 344 ....*****************************
3550=    1215                 345 ....****CHKNSO:
3560= F  1215 F800AD          346 CHKNSO:LDI A.0(NSON);PLO NSONR..RESTORE D
3570=    1218 C4              347 NOP
3580= F  1219 F800BD          348 LDI A.1(NSON);PHI NSONR
3590=    121C 1D              349 INC NSONR..TO  POINT TO POS. 1 NOT 0
3600=    121D F8015A          350 LDI 1;STR SNR....PUT UNIT # INTO SNR
3610=    1220 0D              351 LDN NSONR ..INTO D
3620=    1221 FF02            352 SMI 2..D=D-2
3630= F  1223 C30000          353 LBDF A5..JUMP IF D=0
3640=    1226 1D              354 A1:INC NSONR...POINT TO POS 2
3650=    1227 F8025A          355 LDI 2;STR SNR
3660=    122A 0D              356 LDN NSONR
3670=    122B FF02            357 SMI 2
3680= F  122D C30000          358 LBDF A5
3690=    1230 1D              359 A2:INC NSONR
3700=    1231 F8035A          360 LDI 3;STR SNR
3710=    1234 0D              361 LDN NSONR
3720=    1235 FF02            362 SMI 2
3730= F  1237 C30000          363 LBDF A5
3740=    123A 1D              364 A3:INC NSONR
3750=    123B F8045A          365 LDI 4;STR SNR
3760=    123E 0D              366 LDN NSONR
3770=    123F FF02            367 SMI 2
3780= F  1241 C30000          368 LBDF A5
3790=    1244 1D              369 A4:INC NSONR
3800=    1245 F8055A          370 LDI 5;STR SNR
3810=    1248 0D              371 LDN NSONR
3820=    1249 FF02            372 SMI 2
3830= F  124B C30000          373 LBDF A5
3840=    124E C0109E          374 LBR LOOP1..GO BACK IF NOT
3850= F  1251 F800AD          375 A5:LDI A.0(NSON);PLO NSONR
3860= F  1254 F800BD          376 LDI A.1(NSON);PHI NSONR
3870=    1257 F800            377 LDI 0..RESET UNIT ACCUMULATORS
3880=    1259 ED              378 SEX NSONR
3890=    125A 5D              379 STR NSONR
3900=    125B 60              380 IRX
3910=    125C 5D              381 STR NSONR
3920=    125D 60              382 IRX
3930=    125E 5D              383 STR NSONR
3940=    125F 60              384 IRX
3950=    1260 5D              385 STR NSONR
3960=    1261 60              386 IRX
3970=    1262 5D              387 STR NSONR
3980=    1263 605D            388 IRX;STR NSONR
3990= F  1265 F800AD          389 LDI A.0(NSON);PLO NSONR
4000= F  1268 F800BD          390 LDI A.1(NSON);PHI NSONR
4010=    126B                 391 ....END OF RESETTING
```

Figure D.1. (continued)

```
4020=     126B                    392 ..
4030=     126B                    393 ..
4040=     126B                    394 ..
4050=     126B                    395 ..********
4060=     126B                    396 ..********
4070=     126B C4C4C4             397 NOP;NOP;NOP
4080=     126E C4C4C4             398 NOP;NOP;NOP
4090= F   1271 F800AD             399 LDI A.0(NSON); PLO NSONR
4100= F   1274 F800BD             400 LDI A.1(NSON); PHI NSONR
4110=     1277 F8005D             401 LDI 0; STR NSONR
4120=     127A C4C4C4             402 NOP;NOP;NOP
4130=     127D                    403 ...SET N=0:LET N=M(NSONR)
4140=     127D C4C4C4             404 NOP;NOP;NOP;
4150=     1280 5D                 405 STR NSONR
4160=     1281                    406 ....READ SONAR VALUE @ SNR
4170=     1281 D4115A             407 REPEAT:SEP CALL;,A(READ)
4180=     1284 C4C4C4             408 NOP;NOP;NOP;
4190=     1287                    409 ....IS VSONR=FF
4200=     1287 09FFFF             410 LDN VSONR;SMI X'FF'
4210= F   128A C20000             411 LBZ TW...SKIP IF VSON=FF
4220=     128D 09                 412 LDN VSONR
4230=     128E FF96               413 SMI 150...D=S-150
4240= F   1290 C30000             414 LBDF JUM150...BRANCH IF (+)
4250=     1293                    415 ....IS SONAR.LT.150
4260=     1293                    416 ...N=N+1
4270=     1293 0DFC015D           417 LDN NSONR; ADI 1;STR NSONR
4280=     1297                    418 .....TURN WHEELS
4290= F   1297 D40000             419 TW:SEP CALL;,A(TURN)
4300=     129A C4                 420 NOP
4310=     129B 0D                 421 LDN NSONR
4320=     129C FF03               422 SMI 3....D=NSONR-3
4330=     129E CA1281             423 LBNZ REPEAT
4340=     12A1                    424 ....HERE 3 GOOD VALUES WERE READ
4350=     12A1                    425 ....CHECK ERROR ?-2<E>+2
4360=     12A1                    426 .... E=78-VSON
4370=     12A1 09                 427 LDN VSONR ...D=VSONR
4380=     12A2 C4C4C4             428 NOP;NOP;NOP
4390=     12A5 FD4E               429 SDI 78...D=78-VSON
4400=     12A7 A8                 430 PLO R8...TEMP STORE ERROR
4410= F   12A8 C30000             431 LBDF EPOS...BRANCH TO EPOS
4420=     12AB                    432 ...HERE VSON IS NEG
4430=     12AB                    433 ...CONVERT TO POSITIVE
4440=     12AB FBFFFC01           434 XRI X'FF';ADI 1...D=+E
4450=     12AF A8                 435 PLO R8...TEMP STORE ERROR
4460=     12B0                    436 ....IS ERROR GE 3
4470=     12B0 88FF03             437 EPOS:GLO R8;SMI 3..D-3
4480=     12B3                    438 ....BRANCH IF D=NEG
4490= F   12B3 CB0000             439 LBNF SETT32
4500=     12B6                    440 ....SET DSWP
4510=     12B6 09                 441 LDN VSONR
4520=     12B7 FF6D               442 SMI 109..E=VSON-109 MAGIC SAFETY NUMBER
4530=     12B9                    443 ....TO PREVENT ADDITION OVER FLOW
4540= F   12B9 CB0000             444 LBNF ERROR..BRANCH IF NEG
4550=     12BC                    445 ....VSON IS TO LARGE
4560=     12BC                    446 ....VSON IS 109
4570=     12BC F86D59             447 LDI 109;STR VSONR
4580=     12BF                    448 ....***COMPUTE DSWP
4590=     12BF 09                 449 ERROR:LDN VSONR
4600=     12C0 FD4E               450 SDI 78.. E=78-VSONR
4610= F   12C2 C30000             451 LBDF E2....JUMP IF E=(+)
4620=     12C5 FBFFFC01           452 XRI X'FF';ADI 1....E IS NOW (+)
4630=     12C9 F6                 453 SHR....E=E/2
4640=     12CA FBFFFC01           454 XRI X'FF';ADI 1....E/2 IS NOW (NEG)
4650= F   12CE C00000             455 LBR ADD32
4660=     12D1 F6                 456 E2: SHR.... SHIFT THE POS E
4670=     12D2 FC20               457 ADD32:ADI 32
```

Figure D.1. (continued)

```
4680=     12D4 57              458 STR DSWPR...DONE
4690= F   12D5 C00000          459 LBR AAA
4700=     12D8 F82057          460 SETT32:LDI 32;STR DSWPR
4710=     12DB                 461 ....(1) INITIALIZE FLAGR TO
4720=     12DB                 462 ....      TOP OF STACK
4730=     12DB                 463 ....(2) PUT ZERO IN ALL FLAG(X)
4740=     12DB                 464 ....(3) PUT '1' IN FLAG(X)
4750=     12DB                 465 ....    FOR X=SNR
4760= F   12DB F800AB          466 AAA:LDI A.0(FLAG);PLO FLAGR
4770= F   12DE F800BB          467 LDI A.1(FLAG);PHI FLAGR
4780=     12E1 F800            468 LDI 0
4790=     12E3 EB              469 SEX FLAGR
4800=     12E4 5B60            470 STR FLAGR;IRX
4810=     12E6 5B60            471 STR FLAGR;IRX
4820=     12E8 5B60            472 STR FLAGR;IRX
4830=     12EA 5B60            473 STR FLAGR;IRX
4840=     12EC 5B60            474 STR FLAGR;IRX
4850=     12EE 5B              475 STR FLAGR
4860=     12EF                 476 ....IS SNR=5
4870=     12EF 0A              477 LDN SNR
4880=     12F0 FF05            478 SMI 5
4890= F   12F2 C20000          479 LBZ SN5
4900=     12F5                 480 ....PUT A 1 IN
4910=     12F5                 481 ....NEXT SNR
4920=     12F5 0A              482 LDN SNR
4930= F   12F6 FC00            483 ADI A.0(FLAG)
4940=     12F8 FC01AB          484 ADI 1;PLO FLAGR...A.0(FLAGR)=FLAGR + 1
4950=     12FB F8015B          485 LDI 1;STR FLAGR
4960= F   12FE F800AB          486 LDI A.0(FLAG);PLO FLAGR
4970= F   1301 F800BB          487 LDI A.1(FLAG);PHI FLAGR
4980=     1304 C4C4C4          488 NOP;NOP;NOP
4990=     1307                 489 ....****************************************
5000=     1307                 490 ....****************************************
5010= F   1307 C00000          491 LBR A
5020=     130A C0109D          492 JUM150:LBR LOOP2
5030=     130D C4              493 A:NOP....CONTINUE
5040=     130E                 494 ....**************************
5050=     130E                 495 ....IS SNR=5
5060=     130E                 496 ....**********************
5070=     130E 0A              497 SN5:LDN SNR
5080=     130F C4C4C4          498 NOP;NOP;NOP
5090=     1312 FF05            499 SMI 5
5100= F   1314 CA0000          500 LBNZ BLOOP
5110=     1317                 501 ....BEGIN DELAY @2
5120=     1317                 502 ....PUT A 1 IN FLAG(1)
5130= F   1317 F800FC01AB      503 LDI A.0(FLAG);ADI 1;PLO FLAGR
5140=     131C F8015B          504 LDI 1;STR FLAGR....FLAG(1)=1
5150=     131F F805A8          505 LDI 5;PLO R8
5160=     1322 F800B8          506 LDI 0;PHI R8
5170= F   1325 D40000          507 DELAY 2:SEP CALL;,A(TURN)
5180=     1328 28              508 DEC R8
5190=     1329 88              509 GLO R8
5200=     132A CA1325          510 LBNZ DELAY 2
5210=     132D                 511 ....SET ALL FLAG(X)=0
5220=     132D C4C4C4          512 NOP;NOP;NOP;
5230=     1330 F82057          513 LDI 32;STR DSWPR
5240=     1333                 514 ....NOP;NOP;NOP
5250=     1333                 515 ....LOOP BACK TO TOP
5260=     1333 C4C4C4          516 BLOOP:NOP;NOP;NOP
5270= F   1336 F800AD          517 LDI A.0(SONNUM); PLO NSONR
5280= F   1339 F800BD          518 LDI A.1(SONNUM); PHI NSONR
5290=     133C 095D            519 LDN VSONR; STR NSONR
5300=     133E 1D              520 INC NSONR....PTR TO BOXNUN
5310=     133F 0A              521 LDN SNR...GET SN
5320=     1340 5D              522 STR NSONR... PUT AT BOXNUN
5330= F   1341 F800AD          523 LDI A.0(NSON); PLO NSONR
```

Figure D.1. (continued)

```
5340= F  1344 F800BD          524 LDI A.1(NSON)¦ PHI NSONR
5350= F  1347 D40000          525 SEP CALL¦,A(DISPL)
5360=    134A F804B8          526 LDI 4¦PHI R8
5370=    134D F800A8          527 LDI 0¦PLO R8
5380=    1350 C0109D          528 LBR LOOP2
5390=    1353                 529 ....HERE LOOP BACK
5400=    1353                 530 ....TO TOP OF PRG
5410=    1353                 531 ....****************************
5420=    1353                 532 ....****************************
5430=    1353                 533 ....SUBROUTINE TO TURN WHEELS
5440=    1353                 534 ....****************************
5450=    1353                 535 ....**** GET FW POS
5460=    1353                 536 ....****AND TURN WHLS
5470=    1353 C4C4C4          537 TURN¦NOP¦NOP¦NOP
5480=    1356 E36101          538 SEX PC¦OUT1¦DC 1
5490=    1359 EF6FAE          539 SEX RF¦INP 7¦PLO BINR
5500=    135C                 540 ...CONVERT TO BINARY
5510= F  135C F800BE          541 LDI A.1 (BIN)¦PHI BINR
5520=    135F 17              542 INC DSWPR ... PRT TO WPBIN
5530=    1360                 543 ...*********WPBIN IS ADR BELOW THE ADR FOR
5540=    1360 0E              544 LDN BINR ... GET BINARY CODE
5550=    1361 57              545 STR DSWPR ...
5560=    1362 27              546 DEC DSWPR ... POINT BACK TO DWSPR
5570=    1363                 547 ...***EXECUTE WHEEL TURN
5580=    1363 0E              548 LDN BINR ... D=BINARY CODE
5590=    1364 E7              549 SEX DSWPR
5600=    1365 F7              550 SM...D=D-DSWP
5610=    1366                 551 ...POS=TURN R
5620=    1366                 552 ...NEG=TURN L
5630=    1366                 553 ...ZERO=STOP
5640= F  1366 C20000          554 LBZ FOKAY
5650= F  1369 CB0000          555 LBNF TFL
5660=    136C                 556 ...HERE RESULT POS¦TURN R
5670=    136C E3              557 SEX PC
5680=    136D                 558 ...OUTPUT PORT 08-B
5690=    136D 6108            559 OUT 1¦DC 8...GROUP NO.
5700=    136F 6601            560 OUT 6¦DC 1
5710= F  1371 C00000          561 LBR DUNTRN
5720=    1374 E36108          562 TFL¦ SEX PC¦OUT 1¦DC 8
5730=    1377 6602            563 OUT 6¦DC2
5740= F  1379 C00000          564 LBR DUNTRN
5750=    137C E3              565 FOKAY¦SEX PC
5760=    137D 6108            566 OUT 1¦DC 8
5770=    137F 6600            567 OUT 6¦DC 0
5780=    1381 C4              568 DUNTRN¦NOP
5790=    1382 D5              569 SEP RETN
5800=    1383                 570 ....******************
5810=    1383                 571 ....SUBROUTINE
5820=    1383                 572 ....******************
5830=    1383                 573 ..CONVERT BINARY TO BCD
5840=    1383                 574 ..NUMBER IN TEMP. 1
5850=    1383                 575 ..INTO STALK POINTED BY SNR AT NUMB
5860=    1383                 576 ..
5870=    1383                 577 ..INITIALIZATION
5880= F  1383 F800AA          578 BIBCD¦LDI A.0(NUMB)¦PLO SNR
5890= F  1386 F800BA          579 LDI A.1(NUMB)¦PHI SNR
5900=    1389 F800            580 LDI 0
5910=    138B 5A1A            581 STR SNR¦INC SNR
5920=    138D 5A1A            582 STR SNR¦INC SNR
5930=    138F 5A              583 STR SNR
5940=    1390 2A              584 DEC SNR
5950=    1391 2A              585 DEC SNR
5960=    1392                 586 ..
5970=    1392 98              587 GHI TEMP..D
5980=    1393 FF64            588 D100¦SMI 100..D=D-100
5990= F  1395 CB0000          589 LBNF NEX10..IS D NEG?
```

Figure D.1. (continued)

```
6000=     1398 A8                590 PLO TEMP..D INTO TEMP.0
6010=     1399 0A                591 LDN SNR ..N(D)
6020=     139A FC01              592 ADI 1..N=N+1
6030=     139C 5A                593 STR SNR
6040=     139D 88                594 GLO TEMP..TEMP.0INTO D
6050=     139E C01393            595 LBR D100
6060=     13A1 1A                596 NEX10:INC SNR ..N1
6070=     13A2 FC64              597 ADI 100..D=D+100
6080=     13A4 FF0A              598 D10:SMI 10
6090= F   13A6 CB0000            599 LBNF NEX1
6100=     13A9 A8                600 PLO TEMP
6110=     13AA 0A                601 LDN SNR
6120=     13AB FC01              602 ADI 1..N1=N1+1
6130=     13AD 5A                603 STR SNR
6140=     13AE 88                604 GLO TEMP
6150=     13AF C013A4            605 LBR D10
6160=     13B2 1A                606 NEX1:INC SNR..N2
6170=     13B3 FC0A              607 ADI 10
6180=     13B5 5A                608 STR SNR..N2=D (ONES PLACE)
6190=     13B6 1A1A              609 INC SNR;INC SNR
6200=     13B8 D5                610 SEP RETN
6210=     13B9                   611 ..
6220=     13B9                   612 ..FINISHED
6230=     13B9                   613 ..*****************************
6240=     13B9                   614 ..
6250=     13B9                   615 ..  RCA DISPLAY
6260=     13B9                   616 ..
6270=     13B9                   617 ..*****************************
6280=     13B9                   618 ..
6290=     13B9 C4C4C4C4C4        619 DISPL:NOP;NOP;NOP;NOP;NOP
6300=     13BE F808BE            620 LDI 8;PHI RE
6310= F   13C1 F800AA            621 LDI A.0(NUMB);PLO SNR
6320= F   13C4 F800BA            622 LDI A.1(NUMB);PHI SNR
6330= F   13C7 F800A9            623 LDI A.0(SONNUM);PLO VSONR
6340= F   13CA F800B9            624 LDI A.1(SONNUM);PHI VSONR
6350= F   13CD F800A7            625 LDI A.0(DSWP);PLO DSWPR
6360= F   13D0 F800B7            626 LDI A.1(DSWP);PHI DSWPR
6370=     13D3                   627 ....TYPE=X'8198'
6380=     13D3                   628 ....OSTRG=X'83F0'
6390=     13D3 09                629 LDN VSONR
6400=     13D4 B8                630 PHI TEMP
6410= F   13D5 F800A9            631 LDI A.0(VSON);PLO VSONR
6420= F   13D8 F800B9            632 LDI A.1(VSON);PHI VSONR
6430=     13DB D41383            633 SEP CALL;,A(BIBCD)
6440=     13DE D483F0            634 SEP CALL;,A(OSTRG)
6450=     13E1 1B59262300        635 DC X'1B59262300'..PUTS CURSOR AT SPOT ON
6460= F   13E6 F800AA            636 LDI A.0(NUMB); PLO SNR
6470= F   13E9 F800BA            637 LDI A.1(NUMB); PHI SNR
6480=     13EC 4A                638 LDA SNR
6490= F   13ED CA0000            639 LBNZ NZERO
6500=     13F0 F820              640 LDI X'20'
6510=     13F2 BF                641 PHI RF
6520=     13F3 D48198            642 SEP CALL;,A(TYPE)
6530= F   13F6 C00000            643 LBR SEC
6540=     13F9 FC30              644 NZERO:ADI 48
6550=     13FB BF                645 PHI RF
6560=     13FC D48198            646 SEP CALL;,A(TYPE)
6570=     13FF 4A                647 SEC:LDA SNR
6580=     1400 FC30              648 ADI 48
6590=     1402 BF                649 PHI RF
6600=     1403 D48198            650 SEP CALL;,A(TYPE)
6610=     1406 0A                651 LDN SNR
6620=     1407 FC30              652 ADI 48
6630=     1409 BF                653 PHI RF
6640=     140A D48198            654 SEP CALL;,A(TYPE)
6650=     140D 2A2A              655 DEC SNR;DEC SNR
```

Figure D.1. (continued)

```
6660=     140F                    656 ..
6670=     140F                    657 ..
6680=     140F 17                 658 INC DSWPR
6690=     1410 07                 659 LDN DSWPR
6700=     1411 27                 660 DEC DSWPR
6710=     1412 B8                 661 PHI TEMP
6720=     1413 D41383             662 SEP CALL;,A(BIBCD)
6730=     1416 D483F0             663 SEP CALL;,A(OSTRG)
6740=     1419 1B59262C00         664 DC X'1B59262C00'....CURSOR TO NEW SPOT
6750= F   141E F800AA             665 LDI A.0(NUMB);PLO SNR
6760= F   1421 F800BA             666 LDI A.1(NUMB);PHI SNR
6770=     1424 4A                 667 LDA SNR
6780= F   1425 CA0000             668 LBNZ NZER1
6790=     1428 F820               669 LDI X'20'
6800=     142A BF                 670 PHI RF
6810=     142B D48198             671 SEP CALL;,A(TYPE)
6820= F   142E C00000             672 LBR SEC1
6830=     1431 FC30               673 NZER1:ADI 48
6840=     1433 BF                 674 PHI RF
6850=     1434 D48198             675 SEP CALL;,A(TYPE)
6860=     1437 4A                 676 SEC1:LDA SNR
6870=     1438 FC30               677 ADI 48
6880=     143A BF                 678 PHI RF
6890=     143B D48198             679 SEP CALL;,A(TYPE)
6900=     143E 0A                 680 LDN SNR
6910=     143F FC30               681 ADI 48
6920=     1441 BF                 682 PHI RF
6930=     1442 D48198             683 SEP CALL;,A(TYPE)
6940=     1445 2A2A               684 DEC SNR;DEC SNR
6950=     1447                    685 ..
6960=     1447                    686 ..
6970=     1447 D483F0             687 SEP CALL;,A(OSTRG)
6980=     144A 1B59282F00         688 DC X'1B59282F00'..PUTS CURSOR IN PLACE
6990= F   144F F800AA             689 LDI A.0(BOXNUM);PLO SNR
7000= F   1452 F800BA             690 LDI A.1(BOXNUM);PHI SNR
7010=     1455 0A                 691 LDN SNR
7020=     1456 FC30               692 ADI 48
7030=     1458 BF                 693 PHI RF
7040=     1459 D48198             694 SEP CALL;,A(TYPE)
7050=     145C F83F               695 LDI X'3F'
7060=     145E BF                 696 PHI RF
7070= F   145F F800AA             697 LDI A.0(SN);PLO SNR
7080= F   1462 F800BA             698 LDI A.1(SN);PHI SNR
7090=     1465 D5                 699 SEP R5
7100=     1466                    700 ....**************************
7110=     1466 D483F0             701 SCRN:SEP CALL;,A(OSTRG)
7120=     1469 1B1B5027           702 DC X'1B1B5027'
7130=     146D 3030303030463046   703 DC T'00000F0F'
7140=     1475 3043304330433043   704 DC T'0C0C0C0C'
7150=     147D 1B1B5022           705 DC X'1B1B5022'
7160=     1481 3030303033433343   706 DC T'00003C3C'
7170=     1489 3043304330433043   707 DC T'0C0C0C0C'
7180=     1491 1B1B5023           708 DC X'1B1B5023'
7190=     1495 3043304330433043   709 DC T'0C0C0C0C'
7200=     149D 3043304330433043   710 DC T'0C0C0C0C'
7210=     14A5 1B1B5024           711 DC X'1B1B5024'
7220=     14A9 3043304330433043   712 DC T'0C0C0C0C'
7230=     14B1 3343334330303030   713 DC T'3C3C0000'
7240=     14B9 1B1B502A           714 DC X'1B1B502A'
7250=     14BD 3043304330433043   715 DC T'0C0C0C0C'
7260=     14C5 3046304630303030   716 DC T'0F0F0000'
7270=     14CD 1B1B5026           717 DC X'1B1B5026'
7280=     14D1 3030303033463346   718 DC T'00003F3F'
7290=     14D9 3030303030303030   719 DC T'00000000'
7300=     14E1 1B1B503C           720 DC X'1B1B503C'
7310=     14E5 3030303030303030   721 DC T'00000000'
```

Figure D.1. (continued)

```
7320=     14ED 3346334630303030   722 DC T'3F3F0000'
7330=     14F5 1B1B5028           723 DC X'1B1B5028'
7340=     14F9 3030303033463346   724 DC T'00003F3F'
7350=     1501 3043304330433043   725 DC T'0C0C0C0C'
7360=     1509 1B1B5029           726 DC X'1B1B5029'
7370=     150D 3043304330433043   727 DC T'0C0C0C0C'
7380=     1515 3346334630303030   728 DC T'3F3F0000'
7390=     151D 1B1B43301B1B5230   729 DC X'1B1B43301B1B5230'
7400=     1525 0C0A0A             730 DC X'0C0A0A'
7410=     1528 2726262626262626   731 DC T'!&&&&&&&'
7420=     1530 2826262626262626   732 DC T'(&&&&&&&'
7430=     1538 26262622           733 DC T'&&&"'
7440=     153C 2320534F4E415220   734 DC X'2320534F4E415220'
7450=     1544 232020574845454C   735 DC X'232020574845454C'
7460=     154C 2020202323205641   736 DC X'2020202323205641'
7470=     1554 4C5545202320504F   737 DC X'4C5545202320504F'
7480=     155C 534954494F4E2023   738 DC X'534954494F4E2023'
7490=     1564 2309092309092020   739 DC X'2309092309092020'
7500=     156C 2023               740 DC X'2023'
7510=     156E 2309092309092020   741 DC X'2309092309092020'
7520=     1576 2023               742 DC X'2023'
7530=     1578 2A3C3C3C3C3C3C3C   743 DC T'*<<<<<<<'
7540=     1580 293C3C3C3C3C3C3C   744 DC T')<<<<<<<'
7550=     1588 3C3C3C24           745 DC T'<<<$'
7560=     158C 202020             746 DC X'202020'
7570=     158F 534F4E4152         747 DC T'SONAR'
7580=     1594 20                 748 DC X'20'
7590=     1595 554E49543A         749 DC T'UNIT:'
7600=     159A 00                 750 DC X'00'
7610=     159B D5                 751 SEP R5
7620=     159C                    752 ....**********************
7630=     159C                    753 ...DATA
7640=     159C                    754 ....*********
7650=     1700                    755       ORG X'1700'
7660=     1700 C4                 756 TOPSTK:NOP
7670=     1701                    757 ..............................
7680=     1701                    758 ....WHEELL POSITION LOOK-UP TABLE
7690=     1701                    759 ......CONVERT GREY CODE
7700=     1701                    760 ......TO BINARY
7710=     1701                    761 ..............................
7720=     1600                    762       ORG X'1600'
7730=     1600 0001030207060405   763 BIN:DC X'0001030207060405'
7740=     1608 0F0E0C0D08090B0A   764 DC X'0F0E0C0D08090B0A'
7750=     1610 1F1E1C1D1B191B1A   765 DC X'1F1E1C1D1B191B1A'
7760=     1618 1011131217161415   766 DC X'1011131217161415'
7770=     1620 3F3E3C3D38393B3A   767 DC X'3F3E3C3D38393B3A'
7780=     1628 3031333237363435   768 DC X'3031333237363435'
7790=     1630 2021232227262425   769 DC X'2021232227262425'
7800=     1638 2F2E2C2D28292B2A   770 DC X'2F2E2C2D28292B2A'
7810=     1650                    771       ORG X'1650'
7820=     1650 2000               772 DSWP:DC X'2000'
7830=     1652 FF                 773 VSON:DC X'FF'
7840=     1653 0000000000         774 NSON:DC X'0000000000'
7850=     1658 00                 775 DC 0
7860=     1659 000000             776 NUMB:DC X'000000'
7870=     165C 00                 777 SN:DC 0
7880=     165D 00                 778 FLAG:DC 0
7890=     165E 00                 779 DC0
7900=     165F 00                 780 DC0
7910=     1660 00                 781 DC0
7920=     1661 00                 782 DC0
7930=     1662 00                 783 DC0
7940=     1663 00                 784 SONNUM: DC0
7950=     1664 01                 785 BOXNUM:DC1
7960=     1750                    786 ORG X'1750'
7970= F   1750 C00000             787 OST: LBR MSGE
```

Figure D.1. (continued)

```
7980=     1753 F8EFAC          788 MSGE:  LDI X'EF'; PLO RC
7990=     1756 F880BC          789 LDI X'80'; PHI RC
8000=     1759 46BF            790 MSGE1: LDA LINK; PHI RF
8010= F   175B 3200            791 BZ EXITM
8020=     175D C4C4C4          792 NOP;NOP;NOP
8030=     1760 3059            793 BR MSGE1
8040=     1762 D5              794 EXITM: SEP R5
8050=     1763 D5              795 TYP: SEP R5
8060=     1764                 796 END
OK-
```

APPENDIX E

DATA FROM PERFORMANCE TESTS OF THE HARVESTER'S STEERING CONTROL SYSTEM

APPENDIX E

DATA FROM PERFORMANCE TESTS OF THE HARVESTER'S STEERING CONTROL SYSTEM

Appendix E contains the data that were collected during the performance tests of the harvester's steering control system as described in Sections 9.1 to 9.2. Tables E.1 to E.4 show the data that represents the harvester's position as the harvester moved over a simulated tree row during the performance tests. Performance tests were done with straight row, curved row, and a row with an 8 cm step-change. The data in these Tables E.1 to E.4 are the X-Y position coordinates of selected points on the lines drawn by two pens which were attached to the harvester's frame. One pen was attached at the front wheel and the other at the rear wheel (Figure 9.3). Note, that for each X-value in the tables for the front of the harvester, there is a corresponding set of rear X-Y coordinates. These coordinates for the front and the rear of the harvester completely define the position of the harvester at one particular instant of time during a performace test. Note that the X coordinate for the rear of the harvester was computed by triangulation.

The steering control ysstem was required to maintain the harvester's centerline within about 20 cm fro each tree's centerline as the harvester traveled over each tree. Thus, to determine the position of the harvester's centerline, the coordinate position of points A and B on the harveter were computed and are shown in Tables E.5 to E.8.

Points A and B were on the harvester's centerline (Figure 7.5). Point A was between the front wheels and point B was between the rear wheels. The data in Tables E.5 to E.8 was used to plot the path of the harvester observed during the performace tests and these plots are shown in Sections 9.4 to 9.5.1.

Table E.1. Harvester's Position Data Collected for Three Performance Tests with a Straight Row.

STRAIGHT RUN (R = 121.9 M) JULY 12 , 1982
SURFACE = CONCRETE DRIVEWAY

	RUN 1				RUN 2				RUN 3			
FRONT X	FRONT Y	REAR X	REAR Y		FRONT Y	REAR X	REAR Y		FRONT Y	REAR X	REAR Y	
0	59.5	-415.5	60.5		62.5	-415.5	61.0		60.5	-415.5	60.0	
150	58.5	-265.5	60.5		61.5	-265.5	61.0		61.0	-265.5	59.0	
300	58.5	-115.5	60.0		60.0	-115.4	51.0		59.0	-115.5	59.5	
450	55.5	34.5	59.5		59.0	34.5	60.0		58.5	34.5	60.0	
600	56.5	184.5	58.5		58.5	184.5	59.0		57.5	184.5	59.5	
750	55.0	334.5	58.5		59.0	334.5	60.0		58.0	334.5	59.0	
900	56.0	484.5	58.0		57.5	484.5	59.0		57.5	484.5	58.5	
1050	56.5	634.5	57.5		57.5	634.5	58.0		57.5	634.5	58.0	
1200	56.5	784.5	58.0		57.5	784.5	57.0		57.5	784.5	58.5	
1350	56.5	934.5	58.0		58.0	934.5	56.5		59.0	934.5	58.0	
1500	56.5	1084.5	58.0		58.0	1084.5	57.0		59.0	1084.5	58.5	
1650	55.5	1234.5	58.0		59.0	1234.5	57.0		59.0	1234.5	58.5	
1800	55.5	1384.5	59.0		60.0	1384.5	58.0		60.0	1384.5	59.5	
1950	56.5	1534.5	58.5		61.5	1534.5	59.0		60.5	1534.5	59.5	
2100	57.0	1684.5	58.0		59.5	1684.5	58.5		59.0	1684.5	59.0	
2250	57.5	1834.5	58.0		60.0	1834.5	58.0		59.5	1834.5	60.0	
2400	58.0	1984.5	58.5		61.0	1984.5	58.5		57.0	1984.5	59.5	
2550	58.0	2134.5	60.0		62.0	2134.5	59.0		57.0	2134.5	58.5	
2700	57.5	2284.5	60.0		60.5	2284.5	59.5		57.0	2284.5	57.5	
2850	56.5	2434.5	59.5		60.5	2434.5	60.0		57.5	2434.5	57.0	

Table E.2. Harvester's Position Data Collected for Three Performance Tests with a Row Containing a 8 cm Step-change.

STEPPED RUN (STEP SIZE = 8 CM) JULY 12 , 1982
SURFACE = CONCRETE DRIVEWAY
STEP BEGINS WITH TREE 4 AT (1219.2, 8.0 CM)

	RUN 1				RUN 2				RUN 3			
FRONT X	FRONT Y	REAR X	REAR Y		FRONT Y	REAR X	REAR Y		FRONT Y	REAR X	REAR Y	
0	56.5	-415.5	58.5		59.5	-415.5	58.0		62.5	-415.5	57.5	
150	54.0	-265.5	58.0		59.5	-265.5	58.0		64.0	-265.5	58.5	
200	54.5	-215.5	58.0		55.5	-215.5	58.0		62.5	-215.5	58.5	
250	54.5	-165.5	57.0		50.5	-165.4	57.0		61.5	-165.5	58.0	
300	50.0	-115.4	57.0		47.0	-115.4	57.0		61.5	-115.5	59.0	
400	47.0	-15.4	55.0		45.5	-15.4	54.5		62.0	-15.5	58.5	
460	44.5	44.6	54.5		44.5	44.6	53.0		62.5	44.5	58.5	
600	52.0	184.5	53.0		52.0	184.5	51.0		62.0	184.5	59.0	
750	52.0	334.5	53.5		54.0	334.5	51.5		63.5	334.5	58.5	
800	53.5	384.5	53.5		55.5	384.5	52.0		63.0	384.5	59.0	
900	56.5	484.5	53.5		57.5	484.5	52.0		62.0	484.5	59.0	
1050	56.0	634.5	55.0		60.0	634.6	53.5		63.5	634.5	59.0	
1100	57.5	684.5	55.0		61.0	684.6	54.5		64.0	684.5	59.0	
1200	61.5	784.5	56.5		64.5	784.6	56.0		66.0	784.6	59.5	
1400	63.5	984.5	59.0		68.5	984.6	59.5		68.0	984.6	60.5	
1600	66.0	1184.5	62.0		71.5	1184.6	63.0		70.5	1184.6	62.5	
1800	66.0	1384.5	64.0		70.0	1384.5	66.0		70.5	1384.5	64.5	
2000	65.5	1584.5	66.0		71.0	1584.5	68.0		72.0	1584.5	66.5	
2200	65.0	1784.5	65.5		70.5	1784.5	67.5		70.0	1784.5	65.5	
2350	64.5	1934.5	65.5		70.5	1934.5	68.0		68.0	1934.5	65.5	
2400	64.0	1984.5	65.5		68.5	1984.5	68.0		68.5	1984.5	66.0	
2500	63.5	2084.5	65.0		67.0	2084.5	67.0		70.0	2084.5	65.0	
2700	65.5	2284.5	65.0		66.5	2284.5	66.5		70.5	2284.5	65.5	
2750	67.0	2334.5	65.0		67.0	2334.5	66.5		71.0	2334.5	66.0	
2750	67.0	2334.5	65.0		67.0	2334.5	66.5		71.0	2334.5	66.0	

Table E.3. Harvester's Position Data Collected for Three Performance Tests with a Curved Row on a Campus Lawn.

CURVED RUN (R = 121.9 M) JULY 9 , 1982
SURFACE = LAWN

FRONT X	RUN 1 FRONT Y	REAR X	REAR Y	RUN 2 FRONT Y	REAR X	REAR Y	RUN 3 FRONT Y	REAR X	REAR Y
0	59.0	-415.5	57.5	62.0	-415.5	56.5	58.5	-415.5	55.5
150	61.5	-265.5	57.5	67.5	-265.4	58.0	62.0	-265.5	56.0
300	62.0	-115.5	58.0	64.5	-115.5	59.0	62.0	-115.5	56.0
450	64.5	34.5	59.5	68.5	34.6	61.0	65.0	34.6	58.0
600	64.5	184.5	60.5	65.5	184.5	62.5	64.5	184.5	59.5
700	66.0	284.5	61.5	67.0	284.5	62.5	66.0	284.5	60.0
750	66.5	334.5	61.5	67.5	334.5	63.0	66.5	334.5	60.5
800	64.0	384.5	62.5	65.0	384.5	63.0	64.5	384.5	61.0
900	60.5	484.5	62.5	61.5	484.5	63.0	61.0	484.5	61.5
1050	59.5	634.5	63.0	61.5	634.5	63.0	61.0	634.5	62.0
1060	59.5	644.5	62.0	61.0	644.5	62.5	61.0	644.5	61.0
1200	49.0	784.6	60.0	50.0	784.6	60.0	50.0	784.6	59.0
1350	45.0	934.6	56.0	47.5	934.6	56.0	47.0	934.6	55.5
1380	43.0	964.7	55.5	44.5	964.7	56.0	44.5	964.6	55.0
1450	35.0	1034.8	52.0	36.0	1034.8	53.0	35.5	1034.8	52.0
1500	30.5	1085.0	50.0	32.0	1084.9	50.5	31.0	1084.9	50.0
1550	27.5	1135.0	48.5	29.0	1135.0	48.5	28.0	1135.0	47.5
1650	23.0	1235.0	43.5	25.5	1234.9	43.5	23.5	1234.9	42.5
1670	22.5	1255.0	42.0	24.5	1254.9	42.0	23.0	1254.9	41.0
1800	7.0	1385.4	35.0	7.5	1385.4	35.0	7.0	1385.4	34.0
1830	4.0	1415.5	33.0	4.5	1415.5	33.0	4.5	1415.4	32.0
1950	-3.5	1535.4	24.0	-2.0	1535.3	24.0	-2.5	1535.3	23.0
1970	-5.0	1555.4	23.0	-3.5	1555.3	23.0	-4.0	1555.3	22.0
2050	-17.5	1635.9	16.5	-17.5	1635.9	17.0	-15.5	1635.7	16.5
2075	-21.5	1661.1	15.0	-21.0	1661.1	15.0	-19.0	1660.9	14.6
2100	-25.0	1686.2	12.5	-24.5	1686.2	12.5	-22.5	1686.0	12.5
2130	-28.5	1716.2	9.5	-28.0	1716.2	9.5	-26.0	1716.0	9.5
2200	-37.0	1786.4	2.5	-35.5	1786.2	2.5	-34.0	1786.1	2.5
2250	-41.0	1836.2	-3.0	-39.5	1836.1	-3.0	-38.0	1836.0	-3.0
2270	-43.0	1856.2	-5.0	-41.5	1856.1	-5.0	-39.5	1855.9	-5.0
2282	-44.5	1868.3	-6.0	-43.5	1868.2	-6.0	-41.0	1868.0	-6.0
2350	-57.0	1936.9	-12.5	-56.0	1936.8	-12.0	-54.5	1936.7	-11.5
2400	-66.0	1987.2	-18.5	-65.5	1987.2	-18.0	-64.5	1987.2	-17.5
2430	-71.5	2017.5	-22.0	-71.0	2017.4	-22.0	-70.0	2017.4	-21.0
2470	-76.0	2057.5	-26.0	-75.0	2057.4	-26.0	-74.5	2057.4	-25.5
2550	-85.5	2137.6	-35.0	-83.5	2137.3	-35.0	-84.5	2137.5	-34.5
2580	-88.0	2167.2	-40.5	-86.5	2167.1	-40.5	-87.0	2167.2	-40.0
2630	-98.5	2217.8	-46.5	-98.0	2217.7	-46.5	-97.5	2217.7	-46.0
2685	-111.0	2273.5	-53.5	-109.5	2273.3	-53.5	-108.0	2273.2	-53.0
2700	-115.5	2288.9	-55.5	-111.5	2288.3	-55.5	-111.0	2288.3	-55.0
2740	-126.0	2329.5	-61.5	-118.0	2328.4	-61.5	-117.0	2328.3	-61.0

Table E.4. Harvester's Position Data Collected for Three Performance Tests with a Curved Row on a Concrete Driveway.

CURVED RUN (R = 121.9 M) JULY 7 , 1982
SURFACE = CONCRETE DRIVEWAY

	RUN 1			RUN 2			RUN 3		
FRONT X	FRONT Y	REAR X	REAR Y	FRONT Y	REAR X	REAR Y	FRONT Y	REAR X	REAR Y
0	63.5	-415.5	58.0	62.0	-415.5	60.0	63.0	-415.5	63.0
150	65.5	-265.5	61.0	62.0	-265.5	62.0	63.5	-265.5	65.5
300	63.0	-115.5	61.5	60.5	-115.5	62.5	62.0	-115.5	65.5
450	65.0	34.5	60.5	60.5	34.5	61.0	63.0	34.5	65.0
600	62.0	184.5	60.5	60.0	184.5	61.0	61.5	184.5	65.0
700	63.5	284.5	60.0	60.5	284.5	60.5	61.5	284.5	64.5
750	64.5	334.5	60.0	61.5	334.5	60.5	62.0	334.5	64.0
800	62.5	384.5	60.0	60.5	384.5	60.5	61.0	384.5	64.0
900	60.0	484.5	59.5	59.0	484.5	60.5	59.5	484.5	63.5
1050	61.0	634.5	59.0	58.5	634.5	59.5	58.0	634.5	62.5
1200	52.0	784.5	57.5	50.0	784.6	58.5	51.0	784.6	62.0
1350	50.0	934.5	54.5	46.5	934.6	55.0	49.0	934.6	59.5
1380	48.5	964.5	54.0	45.0	964.6	55.5	47.0	964.6	58.0
1450	39.5	1034.7	52.0	37.0	1034.8	52.5	39.0	1034.9	56.5
1500	34.0	1084.8	50.0	33.0	1084.9	50.5	34.0	1085.0	54.5
1550	31.5	1134.8	47.5	30.0	1134.9	48.0	31.5	1135.0	52.0
1650	27.0	1234.8	42.5	26.0	1234.8	43.0	27.5	1235.0	47.0
1670	26.5	1254.8	41.5	25.0	1254.8	42.0	36.0	1254.6	46.0
1800	8.5	1385.3	34.0	7.0	1385.4	35.0	8.0	1385.7	39.0
1830	5.5	1415.3	32.0	4.0	1415.5	33.0	5.0	1415.7	37.0
1950	-2.0	1535.3	24.0	-5.5	1535.6	25.0	-3.0	1535.7	28.5
1970	-3.5	1555.3	22.5	-7.5	1555.6	23.0	-5.0	1555.7	27.0
2050	-16.5	1635.8	16.5	-20.0	1636.2	17.5	-17.5	1636.3	21.5
2075	-20.5	1661.0	14.5	-23.5	1661.3	15.0	-20.5	1661.4	19.0
2100	-24.5	1686.1	12.0	-27.0	1686.4	13.0	-24.5	1686.6	17.0
2130	-28.5	1716.2	9.5	-30.5	1716.4	9.5	-28.5	1716.7	14.5
2200	-34.5	1786.2	2.5	-37.0	1786.4	2.5	-34.5	1786.6	7.5
2250	-40.0	1836.2	-2.5	-43.5	1836.5	-2.5	-40.0	1836.7	2.5
2270	-41.0	1856.1	-4.5	-45.5	1856.5	-4.5	-42.0	1856.6	0.0
2282	-42.5	1868.2	-5.5	-47.0	1868.6	-5.5	-44.0	1868.8	-.5
2350	-55.0	1936.6	-13.0	-58.5	1937.0	-13.0	-56.0	1937.2	-8.5
2400	-63.5	1986.9	-19.0	-67.0	1987.3	-19.0	-64.5	1987.6	-14.0
2430	-68.0	2016.9	-23.0	-71.5	2017.3	-23.0	-69.0	2017.6	-18.0
2470	-73.0	2057.0	-27.5	-76.0	2057.3	-27.5	-74.0	2057.7	-22.5
2550	-81.0	2136.9	-36.5	-82.5	2137.0	-37.0	-85.0	2137.9	-32.0
2580	-84.5	2166.9	-40.0	-88.5	2167.3	-40.5	-86.0	2167.6	-35.5
2630	-95.5	2217.3	-47.5	-98.0	2217.5	-48.0	-96.0	2218.0	-42.5
2685	-108.5	2273.1	-54.0	-110.0	2273.2	-54.5	-108.0	2273.6	-49.5
2700	-111.5	2288.2	-56.5	-112.5	2288.3	-56.5	-111.0	2288.8	-51.5
2740	-118.5	2328.4	-62.0	-119.5	2328.4	-62.5	-118.0	2328.9	-57.5

Table E.5. Computed Position Coordinates of Front-Point A and Rear-Point B for Three Performance Tests with Straight Row.

STRAIGHT RUN JULY 1&2 , 1982
SURFACE = CONCRETE DRIVEWAY

RUN 1				RUN 2				RUN 3			
FRONT X	FRONT Y	REAR X	REAR Y	FRONT X	FRONT Y	REAR X	REAR Y	FRONT X	FRONT Y	REAR X	REAR Y
-.7	-.5	-416.2	.5	-.3	2.5	-415.8	1.0	-.4	.5	418.9	-.0
149.2	-1.5	-266.3	.5	149.6	1.5	-265.9	1.0	149.8	1.0	569.1	-1.0
299.3	-1.5	-116.2	.0	300.8	.0	-114.6	-9.0	299.4	-1.0	718.7	-.5
448.9	-4.5	33.4	-.5	449.3	-1.0	33.8	.0	449.3	-1.5	868.6	.0
599.2	-3.5	183.7	-1.5	599.4	-1.5	183.9	-1.0	599.2	-2.5	1018.5	-.5
749.0	-5.0	333.5	-1.5	749.3	-1.0	333.8	.0	749.3	-2.0	1168.6	-1.0
899.2	-4.0	483.7	-2.0	899.3	-2.5	483.8	-1.0	899.3	-2.5	1318.6	-1.5
1049.3	-3.5	633.8	-2.5	1049.4	-2.5	633.9	-2.0	1049.4	-2.5	1468.7	-2.0
1199.3	-3.5	783.8	-2.0	1199.6	-2.5	784.1	-3.0	1199.3	-2.5	1618.6	-1.5
1349.3	-3.5	933.8	-2.0	1349.7	-2.0	934.2	-3.5	1349.6	-1.0	1768.9	-2.0
1499.3	-3.5	1083.8	-2.0	1499.6	-2.0	1084.1	-3.0	1499.6	-1.0	1918.9	-1.5
1649.1	-4.5	1233.6	-2.0	1649.8	-1.0	1234.3	-3.0	1649.6	-1.0	2068.9	-1.5
1799.0	-4.5	1383.5	-1.0	1799.8	.0	1384.3	-2.0	1799.6	.0	2218.9	-.5
1949.2	-3.5	1533.7	-1.5	1949.8	1.5	1534.4	-1.0	1949.6	.5	2368.9	-.5
2099.3	-3.0	1683.8	-2.0	2099.6	-.5	1684.1	-1.5	2099.5	-1.0	2518.8	-1.0
2249.4	-2.5	1833.9	-2.0	2249.8	.0	1834.3	-2.0	2249.4	-.5	2668.7	.0
2399.4	-2.0	1983.9	-1.5	2399.8	1.0	1984.4	-1.5	2399.1	-3.0	2818.4	-.5
2549.2	-2.0	2133.7	.0	2549.9	2.0	2134.4	-1.0	2549.3	-3.0	2968.6	-1.5
2699.1	-2.5	2283.6	.0	2699.6	.5	2284.1	-.5	2699.4	-3.0	3118.7	-2.5
2849.1	-3.5	2433.6	-.5	2849.6	.5	2434.1	.0	2849.6	-2.5	3268.9	-3.0

Table E.6. Computed Position Coordinates of Front-Point A and Rear-Point B for Three Performance Tests with Curved Row on Campus Lawn.

CURVED RUN (R = 121.9 M) JULY 9 , 1982
SURFACE = LAWN

RUN 1				RUN 2				RUN 3			
FRONT X	FRONT Y	REAR X	REAR Y	FRONT X	FRONT Y	REAR X	REAR Y	FRONT X	FRONT Y	REAR X	REAR Y
-.3	-1.0	-415.8	-2.5	.3	2.0	-415.2	-3.5	-.1	-1.5	419.2	-4.5
150.1	1.5	-265.4	-2.5	150.9	7.5	-264.5	-2.0	150.4	2.0	569.6	-4.1
300.1	2.0	-115.4	-2.0	300.3	4.5	-115.2	-1.0	300.4	2.0	719.6	-4.1
450.2	4.5	34.7	-.5	450.6	8.5	35.1	1.0	450.5	5.0	869.7	-2.1
600.1	4.5	184.6	.5	599.9	5.5	184.4	2.5	600.2	4.5	1019.5	-.5
700.1	6.0	284.7	1.5	700.1	7.0	284.7	2.5	700.4	6.0	1119.6	-.1
750.2	6.5	334.7	1.5	750.1	7.5	334.7	3.0	750.4	6.5	1169.6	.4
799.7	4.0	384.2	2.5	799.8	5.0	384.3	3.0	800.0	4.5	1219.3	1.0
899.2	.5	483.7	2.5	899.3	1.5	483.8	3.0	899.4	1.0	1318.7	1.5
1049.0	-.5	633.5	3.0	1049.3	1.5	633.8	3.0	1049.3	1.0	1468.6	2.0
1059.1	-.5	643.6	2.0	1059.3	1.0	643.8	2.5	1059.5	1.0	1478.8	1.0
1197.9	-11.0	782.5	.0	1198.0	-10.0	782.7	.0	1198.2	-10.0	1617.4	-.9
1347.9	-15.0	932.5	-4.0	1348.3	-12.5	932.8	-4.0	1348.3	-13.0	1767.5	-4.4
1377.7	-17.0	962.4	-4.5	1377.8	-15.5	962.5	-4.0	1378.0	-15.5	1797.1	-4.9
1447.0	-24.9	1031.9	-7.9	1447.0	-23.9	1031.9	-6.9	1447.1	-24.4	1866.1	-7.8
1496.7	-29.4	1081.6	-9.9	1496.8	-27.9	1081.7	-9.4	1496.7	-28.9	1915.6	-9.7
1546.5	-32.4	1131.5	-11.4	1546.7	-30.9	1131.6	-11.4	1546.7	-31.9	1965.5	-12.2
1646.5	-36.9	1231.5	-16.4	1646.9	-34.4	1231.8	-16.4	1646.7	-36.4	2065.6	-17.2
1666.7	-37.4	1251.6	-17.9	1667.0	-35.4	1251.8	-17.9	1666.9	-36.9	2085.8	-18.8
1795.4	-52.8	1380.9	-24.8	1795.5	-52.3	1380.9	-24.8	1795.6	-52.8	2214.0	-25.6
1825.3	-55.8	1410.8	-26.8	1825.4	-55.3	1410.8	-26.8	1825.5	-55.3	2243.9	-27.6
1945.5	-63.3	1530.9	-35.8	1945.7	-61.8	1531.0	-35.8	1945.8	-62.4	2364.3	-36.6
1965.4	-64.8	1550.9	-36.8	1965.7	-63.3	1551.0	-36.8	1965.7	-63.8	2384.2	-37.6
2044.6	-77.3	1630.5	-43.3	2044.5	-77.2	1630.4	-42.7	2044.9	-75.3	2462.9	-43.0
2069.2	-81.2	1655.3	-44.7	2069.3	-80.7	1655.4	-44.7	2069.6	-78.8	2487.6	-44.9
2094.1	-84.7	1680.3	-47.2	2094.1	-84.2	1680.3	-47.2	2094.4	-82.2	2512.2	-46.9
2124.0	-88.2	1710.2	-50.2	2124.1	-87.7	1710.3	-50.2	2124.4	-85.7	2542.1	-49.9
2193.8	-96.7	1780.2	-57.2	2194.0	-95.2	1780.2	-57.2	2194.2	-93.7	2611.9	-56.9
2244.0	-100.7	1830.2	-62.7	2244.2	-99.2	1830.3	-62.7	2244.4	-97.7	2662.2	-62.4
2264.0	-102.7	1850.2	-64.7	2264.2	-101.2	1850.3	-64.7	2264.5	-99.2	2682.4	-64.4
2275.9	-104.2	1862.2	-65.7	2276.1	-103.2	1862.3	-65.7	2276.4	-100.7	2694.2	-65.4
2343.1	-116.6	1930.0	-72.1	2343.1	-115.6	1930.0	-71.6	2343.3	-114.1	2760.3	-70.7
2392.6	-125.5	1979.9	-78.0	2392.6	-125.0	1979.9	-77.5	2392.7	-124.1	2809.3	-76.6
2422.3	-131.0	2009.8	-81.5	2422.4	-130.5	2009.8	-81.5	2422.4	-129.5	2838.8	-80.1
2462.3	-135.5	2049.8	-85.5	2462.4	-134.5	2049.8	-85.5	2462.4	-134.0	2878.8	-84.6
2542.2	-145.0	2129.8	-94.5	2542.5	-143.0	2129.8	-94.5	2542.3	-144.0	2958.5	-93.5
2572.6	-147.5	2159.9	-100.0	2572.8	-146.1	2159.9	-100.1	2572.7	-146.6	2989.3	-99.1
2622.0	-158.0	2209.7	-106.0	2622.1	-157.5	2209.8	-106.0	2622.1	-157.0	3038.1	-105.0
2676.2	-170.3	2264.7	-112.8	2676.4	-168.9	2264.7	-112.9	2676.5	-167.4	3092.2	-111.9
2690.8	-174.8	2279.7	-114.8	2691.4	-170.9	2279.7	-114.9	2691.4	-170.4	3106.9	-113.9
2730.2	-185.2	2319.7	-120.7	2731.3	-177.4	2319.7	-120.9	2731.4	-176.4	3146.9	-119.9

Table E.7. Computed Position Coordinates of Front-Point A and Rear-Point B for Three Performance Tests with Curved Row on Concrete Driveway.

CURVED RUN (R = 121.9 M) JULY 7 , 1982
SURFACE = CONCRETE DRIVEWAY

RUN 1				RUN 2				RUN 3			
FRONT X	FRONT Y	REAR X	REAR Y	FRONT X	FRONT Y	REAR X	REAR Y	FRONT X	FRONT Y	REAR X	REAR Y
.3	3.5	-415.2	-2.0	-.2	2.0	-415.7	.0	-.5	3.0	418.8	3.0
150.1	5.5	-265.3	1.0	149.5	2.0	-266.0	2.0	149.2	3.5	568.5	5.5
299.7	3.0	-115.8	1.5	299.2	.5	-116.3	2.5	299.0	2.0	718.3	5.5
450.1	5.0	34.7	.5	449.4	.5	33.9	1.0	449.2	3.0	868.5	5.0
599.7	2.0	184.2	.5	599.3	.0	183.8	1.0	599.0	1.5	1018.3	5.0
700.0	3.5	284.5	-.0	699.5	.5	284.0	.5	699.1	1.5	1118.3	4.5
750.1	4.5	334.7	.0	749.6	1.5	334.1	.5	749.2	2.0	1168.5	4.0
799.8	2.5	384.4	.0	799.5	.5	384.0	.5	799.1	1.0	1218.3	4.0
899.6	.0	484.1	-.5	899.3	-1.0	483.8	.5	898.9	-.5	1318.2	3.5
1049.8	1.0	634.3	-1.0	1049.3	-1.5	633.8	-.5	1048.8	-2.0	1468.1	2.6
1198.7	-8.0	783.2	-2.5	1198.3	-10.0	782.8	-1.5	1197.9	-9.0	1617.1	2.1
1348.8	-10.0	933.4	-5.5	1348.3	-13.5	932.8	-5.0	1348.0	-11.0	1767.1	-.4
1378.7	-11.5	963.2	-6.0	1378.0	-15.0	962.6	-4.5	1377.9	-13.0	1797.1	-1.9
1447.7	-20.5	1032.4	-8.0	1447.2	-22.9	1032.0	-7.4	1447.0	-20.9	1865.9	-3.3
1497.2	-25.9	1082.0	-9.9	1497.0	-26.9	1081.8	-9.4	1496.5	-25.9	1915.3	-5.2
1547.2	-28.4	1132.0	-12.4	1546.9	-29.9	1131.8	-11.9	1546.5	-28.4	1965.3	-7.7
1647.2	-32.9	1232.0	-17.4	1647.0	-33.9	1231.9	-16.9	1646.7	-32.4	2065.5	-12.7
1667.3	-33.4	1252.1	-18.4	1667.0	-34.9	1251.9	-17.9	1668.0	-24.0	2087.2	-13.9
1795.8	-51.4	1381.1	-25.9	1795.4	-52.8	1380.9	-24.8	1795.0	-51.8	2213.1	-20.5
1825.7	-54.3	1411.0	-27.8	1825.3	-55.8	1410.8	-26.8	1824.9	-54.8	2242.9	-22.5
1945.7	-61.8	1531.0	-35.8	1945.1	-65.3	1530.7	-34.8	1944.9	-62.8	2363.0	-31.0
1965.7	-63.3	1551.0	-37.3	1965.1	-67.3	1550.7	-36.8	1964.9	-64.8	2382.9	-32.5
2044.7	-76.3	1630.5	-43.3	2044.1	-79.7	1630.3	-42.2	2043.9	-77.2	2461.3	-37.8
2069.4	-80.2	1655.4	-45.2	2068.9	-83.2	1655.2	-44.7	2068.8	-80.2	2486.2	-40.3
2094.2	-84.2	1680.3	-47.7	2093.7	-86.7	1680.1	-46.7	2093.5	-84.1	2510.7	-42.3
2124.0	-88.2	1710.2	-50.2	2123.7	-90.2	1710.1	-50.2	2123.3	-88.1	2540.3	-44.7
2194.1	-94.2	1780.3	-57.2	2193.8	-96.7	1780.2	-57.2	2193.4	-94.1	2610.6	-51.8
2244.1	-99.7	1830.3	-62.2	2243.6	-103.2	1830.1	-62.2	2243.4	-99.6	2660.5	-56.7
2264.2	-100.7	1850.3	-64.2	2263.6	-105.2	1850.1	-64.2	2263.4	-101.6	2680.6	-59.3
2276.1	-102.2	1862.3	-65.2	2275.5	-106.6	1862.1	-65.1	2275.2	-103.6	2692.2	-59.7
2343.4	-114.6	1930.1	-72.6	2342.9	-118.1	1929.9	-72.6	2342.6	-115.5	2759.2	-67.6
2393.1	-123.1	1980.0	-78.6	2392.6	-126.5	1979.8	-78.5	2392.2	-124.0	2808.4	-73.0
2423.0	-127.6	2009.9	-82.6	2422.5	-131.0	2009.8	-82.5	2422.1	-128.5	2838.3	-77.0
2462.9	-132.6	2049.9	-87.1	2462.5	-135.5	2049.8	-87.0	2462.1	-133.5	2878.1	-81.5
2543.1	-140.6	2130.0	-96.1	2542.9	-142.1	2129.9	-96.6	2541.8	-144.4	2957.7	-91.0
2573.1	-144.1	2160.0	-99.6	2572.6	-148.0	2159.8	-100.0	2572.2	-145.5	2988.4	-94.5
2622.6	-155.0	2209.8	-107.0	2622.3	-157.5	2209.8	-107.5	2621.8	-155.4	3037.6	-101.4
2676.6	-167.9	2264.7	-113.4	2676.5	-169.4	2264.7	-113.9	2676.0	-167.3	3091.2	-108.3
2691.5	-170.9	2279.7	-115.9	2691.4	-171.9	2279.7	-115.9	2690.9	-170.3	3105.9	-110.3
2731.3	-177.9	2319.7	-121.4	2731.3	-178.9	2319.7	-121.9	2730.8	-177.3	3145.6	-116.2

Table E.8. Computer Position Coordinates of Front-Point A and Rear-Point B for Three Performance Tests with Row Containing 8 cm Step-change.

STEPPED RUN (STEP SIZE = 8 CM) JULY 12, 1982
STEP BEGINS WITH TREE 4 AT (1219.2, 8.0 CM)
SURFACE = CONCRETE DRIVEWAY

RUN 1				RUN 2				RUN 3			
FRONT X	FRONT Y	REAR X	REAR Y	FRONT X	FRONT Y	REAR X	REAR Y	FRONT X	FRONT Y	REAR X	REAR Y
-.8	-3.5	-416.3	-1.5	-.3	-.5	-415.8	-2.0	.2	2.5	419.5	-2.5
148.9	-6.0	-266.6	-2.0	149.7	-.5	-265.8	-2.0	150.3	4.0	569.5	-1.5
199.0	-5.5	-216.5	-2.0	199.1	-4.5	-216.4	-2.0	200.1	2.5	619.3	-1.5
249.1	-5.5	-166.4	-3.0	248.5	-9.5	-166.9	-3.0	250.0	1.5	669.3	-2.0
298.5	-10.0	-117.0	-3.0	298.0	-13.0	-117.3	-3.0	299.8	1.5	719.1	-1.0
398.3	-13.0	-17.1	-5.0	398.2	-14.5	-17.2	-5.5	400.0	2.0	819.3	-1.5
458.0	-15.5	42.7	-5.5	458.3	-15.5	42.8	-7.0	460.1	2.5	879.3	-1.5
599.3	-8.0	183.8	-7.0	599.6	-8.0	184.1	-9.0	599.9	2.0	1019.2	-1.0
749.3	-8.0	333.8	-6.5	749.8	-6.0	334.4	-8.5	750.2	3.5	1169.5	-1.5
799.5	-6.5	384.0	-6.5	800.0	-4.5	384.5	-8.0	800.1	3.0	1219.3	-1.0
899.9	-3.5	484.4	-6.5	900.3	-2.5	484.8	-8.0	899.9	2.0	1319.2	-1.0
1049.6	-4.0	634.1	-5.0	1050.4	.0	635.0	-6.5	1050.1	3.5	1469.4	-1.0
1099.8	-2.5	684.4	-5.0	1100.4	1.0	685.0	-5.5	1100.2	4.0	1519.5	-1.0
1200.2	1.5	784.7	-3.5	1200.7	4.5	785.3	-4.0	1200.4	6.0	1619.7	-.6
1400.1	3.5	984.7	-1.0	1400.8	8.5	985.4	-.5	1400.6	8.0	1819.8	.4
1600.1	6.0	1184.6	2.0	1600.7	11.5	1185.3	3.0	1600.6	10.5	2019.9	2.4
1799.8	6.0	1384.3	4.0	1800.1	10.0	1384.6	6.0	1800.4	10.5	2219.6	4.4
1999.4	5.5	1583.9	6.0	1999.9	11.0	1584.4	8.0	2000.3	12.0	2419.5	6.5
2199.4	5.0	1783.9	5.5	2199.9	10.5	1784.4	7.5	2200.1	10.0	2619.4	5.5
2349.3	4.5	1933.8	5.5	2349.8	10.5	1934.4	8.0	2349.8	8.0	2769.1	5.5
2399.3	4.0	1983.8	5.5	2399.6	8.5	1984.1	8.0	2399.8	8.5	2819.1	6.0
2499.3	3.5	2083.8	5.0	2499.5	7.0	2084.0	7.0	2500.2	10.0	2919.5	5.0
2699.6	5.5	2284.1	5.0	2699.5	6.5	2284.0	6.5	2700.2	10.5	3119.5	5.5
2749.8	7.0	2334.3	5.0	2749.6	7.0	2334.1	6.5	2750.2	11.0	3169.5	6.0

LIST OF REFERENCES

LIST OF REFERENCES

Ambler, B., Harries, G. O. 1980. Optical Ranging for Tractor Guidance. ASAE Paper 80-1558. ASAE, St. Joseph, MI.

Bibbero, R. J., 1977. Microprocessors in Instruments and Control. John Wiley, New York.

Busse, W., Coenenberg. H., Feldmann, F., and Crusinberry, T. F. 1977. The First Serial Produced Automatic Steering System for Corn Combines and Forage Harvesters. Proceedings of the International Grain and Forage Harvesting Conference. September 1977. pp.43-47.

Ciarcia, S. C. 1980. Home in the Range -- an Ultrasonic Ranging System. Byte 5(11):32-58. November, 1980.

Coad, C. A. Ruff, J. H., Coble, C. G. 1979. Microprocessor-Based Ultrasonic Height Controller for Sugarcane Harvesters. ASAE Paper 79-1571. ASAE, St. Joseph, MI.

Collins, R.L., Wong, J.P. 1974. A Comparison of Tire Influences on Vehicle Handling. Proceeding of the third Conference on Vehicle System Dynamics, Held at Virginia Polytechnic Institute and State University. Blacksburg Virginia, August 12-15, 1974.

Durstine, J.W. 1965. The Truck Steering System from Hand Wheel to Road Wheel. SAE paper No. 730039 SAE Transaction, Booklet No. SP-374.

Ellis, J. R. 1969. Vehicle Dynamics. London Business Books Limited.

Gross, T. A. 1978. Controlling with Ultrasonics. Machine Design 5(5). March 3, 1978, pp. 90-96.

Grovum, M. A., Zoerb, G. C. 1970. An Automatic Guidance System for Farm Tractors. Transactions of ASAE 13(5):565-573, 576.

Kirk, T. G., Krause, A. E. 1975. Swather Edge Guide Steering Control System. ASAE Paper No. 75-1029, ASAE, St. Joseph, MI.

Shukla, L. N., Goering, E., and Day, C. 1970. Effects of Tractor Parameters of Automatic Steering. Transactions of ASAE 13(5):678-681.

Smith, D. E. 1980. Electronic Distance Measurement for Industrial and Scientific Applications. Hewlett-Packard Journal 31(6):3-10, 19, June 1980

Smith, L. A., Schafer, R. L. and Bailey, A. C. 1979. Verification and Testing of Guidance Algorithms. ASAE Paper 79-1618. ASAE, St. Joseph, MI.

Swisher, G. M., 1976. Introduction to Linear Systems Analysis. Matrix Publishers, Champaign, IL.

Tennes, B. R., Burton, C. L., Levin, J. H. 1976. Concepts for Merchandizing High Density Orchard Fruit Culture. Transactions of the ASAE 19(1):35, 36, 40.

Tennes, B. R., Burton, C. L. 1979. A Rapid Planting Method for Fruit Trees and Bushes. Transactions of the ASAE 22(4):699-701, ASAE, St. Joseph, MI.

Tennes, B. R., Brown, G. K. 1981. Design, Development and Testing of a Sway-Bar-Shaker for Horticulture Crops--A Progress Report. ASAE Paper No. 81-1059, ASAE, St. Joseph, MI.

Upchurch, B. L., Tennes, B. R., Surbrook. T. C. 1980. Development of a Microcomputer-Based Controller for an Over-the-Row Apple Harvester, ASE paper 80-1556, ASAE, St. Joseph, MI.

Young. S. C. Schafer, R. L., Johnsn, C. E. 1980. A Microcomputer-Based Vehicle Guidance Controller. ASE Paper 80-1557. ASAE St. Joseph, eph.